

UC Berkeley

UC Berkeley Electronic Theses and Dissertations

Title

Making and Breaking C–F Bonds via Palladium-Catalysis

Permalink

<https://escholarship.org/uc/item/60h323qp>

Author

Thornbury, Richard

Publication Date

2018

Peer reviewed|Thesis/dissertation

Making and Breaking C–F Bonds *via* Palladium-Catalysis

By

Richard Tresslar Thornbury

A dissertation submitted in partial satisfaction of the requirements for the degree of

Doctor of Philosophy

in

Chemistry

in the

Graduate Division

of the

University of California, Berkeley

Committee in charge:

Professor F. Dean Toste, Chair

Professor Thomas J. Maimone

Professor Markita Landry

Spring 2018

Abstract

Making and Breaking C–F Bonds *via* Palladium-Catalysis

By

Richard Tresslar Thornbury

Doctor of Philosophy in Chemistry

University of California, Berkeley

Professor F. Dean Toste, Chair

Chapter 1 – A ligand controlled, palladium-catalyzed, enantioselective 1,3-arylfuorination of [2*H*]-chromenes was developed. The products were obtained in high enantioselectivity and with a *syn*- relationship of the introduced substituents. The pyranyl fluoride products were further derivatized to demonstrate the utility of the products. A ligand dependent divergent formation of 1,3- and 2,1- alkene difunctionalization products was also observed. This bifurcation in reactivity was investigated with a combination of experimental, computational, and statistical analysis tools. Ultimately, the site selectivity was found to be dependent on the ligand denticity and metal electrophilicity, the electronics of the boronic acid, and the donor ability of the directing group in the substrate.

Chapter 2 – A palladium-catalyzed defluorinative coupling of 1-aryl-2,2-difluoroalkenes with boronic acids was developed. Broad functional tolerance arises from a redox-neutral process in which a palladium(II) active species which is proposed to undergo a β -fluoride elimination to afford the products. The monofluorostilbene products were formed with excellent diastereoselectivity ($\geq 50:1$) in all cases. As a demonstration of this method's unique combination of reactivity and functional group tolerance, a Gleevec® analogue, using a monofluorostilbene as an amide isostere, was synthesized in 4 steps from commercially available materials.

Acknowledgements

As I look back on my time at Berkeley, I can't help but think about how fortunate I am to be here. I feel fortunate to have had people from every step of my life that have been there to support me. I am forever indebted to them for the opportunities that I have had and the great enjoyment I have gotten from my time here at Berkeley.

I first want to thank my family for their love and support. I have always been able to count on my mom, my sister Caroline, and my brother Stephen for encouragement. I also want to thank my Uncle Lou, my Aunt Maria, and my cousin Steve, my California family, for their support as I took the leap and moved out west.

I certainly would not have made it here to Berkeley without the support I had during my undergraduate studies at the University of Illinois. I want to thank Professor Scott Denmark for giving me the opportunity to work and learn as a neophyte in his lab. I also want to thank the Denmark group as a whole for their support in my early growth as a scientist. I particularly want to thank Dr. Lindsey Cullen and Dr. Jeremy Henle for their mentorship, but more importantly, their friendship.

I feel very fortunate to have had Dean as my Ph.D. advisor. His ability to guide students to success in so many different areas of research has always inspired me. Dean has cultivated a group culture that is creative, collaborative, and supportive. Consequently, it has been a great environment to do chemistry. Dean has always been supportive of my goals, and I know he always has his student's best interests in mind.

Contributing to the great group atmosphere in the Toste group are all of my fellow students. Not only are they great scientists, but they are also great people. There have been far too many to mention everyone, but I wanted to give a few a shout-out here. In addition to being great friends, the older graduate students and postdocs were also a great resource for helping navigate my graduate career. In particular I want to thank the two classes above mine, Mark Levin, Dave Kaphan, Rebecca Triano, Drew Samant, Andrew Neel, Willie Wolf, Jigar Patel, Dillon Miles, and Dimitri Khrakovsky, for their help and friendship. I also want to thank some of our postdocs, namely, Steve Jacob, John Brantley, Matt Winston, David Nagib, Takahiro Horibe, Hiroyuki Kawai, and Gabriel Schäfer for their advice and friendship. I have also learned so much from the students in the classes after mine and enjoyed friendships with them. You are all great people and brilliant scientists, and I hope you will enjoy the rest of your time in the Toste group as much as I did. Finally, I want to thank Cindy Hong. As classmates, you were the only person in the Toste group with me from start to finish. I couldn't have asked for a better friend in the journey.

During my time in the Toste group I have had the privilege of collaborating with a lot of great scientists. I want to thank Dr. Jeff McKenna, Dr. Talita Fernandes, Dr. Vaneet Saini, Dr. Celine Santiago, and Professor Matt Sigman for all of their work on our arylfluorination chemistry. I want to thank Dr. Miles Johnson for his mentorship and friendship during the hydroazidation project. I also want to thank Dr. Gabriel Schäfer for working with me on our enantioselective fluorination book chapter.

Perhaps the most fun I had in graduate school was during the chemistry league softball season. It was an honor to coach the team to our second and third consecutive championships. We have had so many talented players over the years, and I want to thank you all for your blood, sweat, and beers in pursuit of our goal of winning championships. I hope the group can carry on the Toste softball dynasty. It's in your hands now, Coach Alec. I'm thinking minimum 8-peat.

Finally, Aya. I want to thank you for all of your love and support. You make me smile every day. I am so proud of everything you do. I am so lucky to have you, and I am so excited for our life ahead.

Dedicated to James Richard Thornbury

Making and Breaking C–F Bonds *via* Palladium-Catalysis

Table of Contents

Chapter 1. The Development and Mechanistic Investigations of a Palladium-Catalyzed 1,3-Arylfluorination Reaction of Chromenes

1.1. Introduction	2
1.2. Results and Discussion.....	4
1.2.1. Discovery and Development of 1,3-Arylfluorination.....	4
1.2.2. Ligand Effects on Regioselectivity.....	9
1.2.3. Aryl Coupling Partner Effects on Regioselectivity	10
1.2.4. Directing Group Effects on Regioselectivity.....	11
1.2.5. Deuterium Labeling Experiments	12
1.2.6. Mechanistic Proposal.....	13
1.3. Conclusion.....	17
1.4. Supporting Information	18
1.4.1. General Information.....	18
1.4.2. Preparation and Characterization of Chromene Substrates	19
1.4.3. Optimization, Preparation, and Characterization of Arylfluorination Products	25
1.4.4. Preparation and Characterization of Deuterated Substrate	35
1.4.5. Preparation and Characterization of Derivatization Products.....	36

1.4.6. Experimental Data for Statistical Analysis	38
1.4.7. Spectral Data.....	41
1.4.8. Chiral HPLC/SFC Analysis	77
1.4.9. X-ray Chrystallographic Data for <i>rac</i> -2d.....	89
1.4.10. DFT Calculations	97
1.5. References	119
Chapter 2. Palladium-Catalyzed Functionalizations of Fluoroalkenes: A Defluorinative Coupling of 1-Aryl-2,2'-Dfluoroalkenes and Boronic Acids and the Enantioselective Aminofluorination 1-Aryl-2-Fluoroalkenes	
2.1. Introduction	125
2.2. Results and Discussion.....	126
2.2.1. Defluorinative Coupling of Difluorostyrenes	126
2.2.2. Aminofluorination of Fluoroalkenes.....	131
2.3. Conclusion.....	132
2.4. Supporting Information	133
2.4.1. General Information.....	133
2.4.2. Preparation and Characterization of Difluoroalkene Substrates	134
2.4.3. Optimization, Preparation, and Characterization of Defluoro-Coupling Products...	136
2.4.4. Mechanistic Experiments.....	143

2.4.5. Synthesis of Gleevec Derivative.....	146
2.4.6. Data for Aminofluorination of Monofluorostyrenes.....	148
2.4.7. Spectral Data.....	151
2.5. References	201

Chapter 1

The Development and Mechanistic Investigations of a Palladium-Catalyzed 1,3-Arylfluorination Reaction of Chromenes

Portions of this chapter have previously appeared in:

Thornbury, R. T.; Saini, V.; Fernandes, T. A.; Santiago, C. B.; Talbot, E. P. A.; Sigman, M. S.; McKenna, J. M.; Toste, F. D. *Chem. Sci.* **2017**, *8*, 2890-2897.

1.1. Introduction

In recent years, there has been significant interest in developing methods for the incorporation of fluorine into organic molecules. This can, in part, be attributed to desirable properties conferred by organofluorine compounds relative to their non-fluorinated analogues.¹⁻² Some of these properties include enhanced lipophilicity, increased metabolic stability, the ability to modulate pKa's of nearby functional groups, and conformational perturbations *via* the gauche effect.¹ It is thus not surprising that fluorine containing organic molecules have found widespread use in the pharmaceutical, agrochemical, and advanced materials industries. It has been estimated that as many as 20% of pharmaceuticals and 35% of agrochemicals contain fluorine in their structures.³⁻⁴

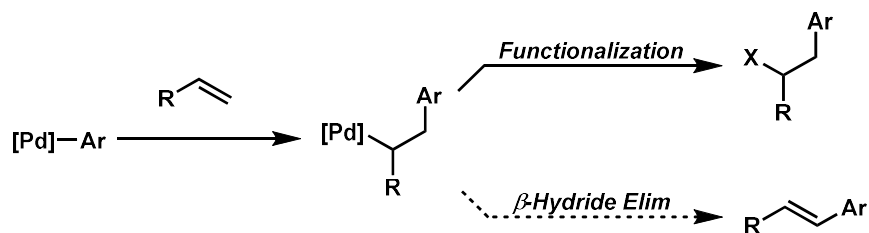
The widespread use of organofluorine compounds in these industries is particularly notable because naturally occurring organofluorine compounds are exceedingly rare. Only a single enzyme that incorporates fluorine into organic molecules has been identified,⁵ and as few as 12 naturally occurring organofluorine compounds are known to exist.⁶⁻⁷ In contrast, natural products containing the other halogens number in excess of 3,200.⁸ Two factors contributing to the scarcity of these molecules in nature are the high oxidation potential and high solvation energy of fluoride. The high oxidation potential precludes the existence of fluoroperoxidases, while the high solvation energy significantly attenuates the nucleophilicity of fluoride ions in aqueous solution.

The scarcity of chiral pool organofluorine compounds thus necessitates the development of stereoselective methodologies to introduce fluorine into organic molecules. Consequently, synthetic chemists have devoted substantial effort to the development of enantioselective C–F bond forming reactions, including our research group.⁹⁻¹⁶ The same properties that make fluorination rare in nature, namely the high oxidizing strength of electrophilic fluorinating reagents and the low nucleophilicity of fluoride, present a challenge to synthetic chemists. As a result, relatively few strategies have been successfully employed.

The first methods developed, and most robust methods, for installing C–F bonds in an enantioselective fashion involve α -fluorination reactions of carbonyl compounds.⁹⁻¹⁶ High yields and enantiomeric excess can be obtained for a great variety of carbonyl and pseudo-carbonyl compounds with many different catalysts. Despite these advances, it is inherently limiting to use a single substrate class as the lynchpin to install C–F stereogenic centers. Only in recent years have new strategies begun to emerge that exploit other substrate classes such as alkenes, allylic electrophiles, epoxides, and aziridines.⁹⁻¹⁶ With this in mind, we set out to develop new strategies to incorporate fluorine into organic molecules in an enantioselective fashion.

Oxidative difunctionalization of alkenes *via* multi-component reactions is an attractive strategy to rapidly introduce complexity and diversity.¹⁷ As such, intercepting Mizoroki-Heck intermediates has recently garnered attention as a means to achieve this type of transformation.¹⁸⁻²⁸ In this approach, the σ -alkyl palladium intermediate formed *via* insertion of an olefin into a Pd-aryl intermediate is functionalized rather than undergoing

β -hydride elimination and alkene dissociation typical of the Heck reaction (Scheme 1.1). Although some of the earliest reports on the Heck reaction described the formation of alkene difunctionalization products, presumably formed via a similar mechanistic scenario, the outlined strategy had been applied sparingly to the development of new synthetic methods.²⁹⁻³²



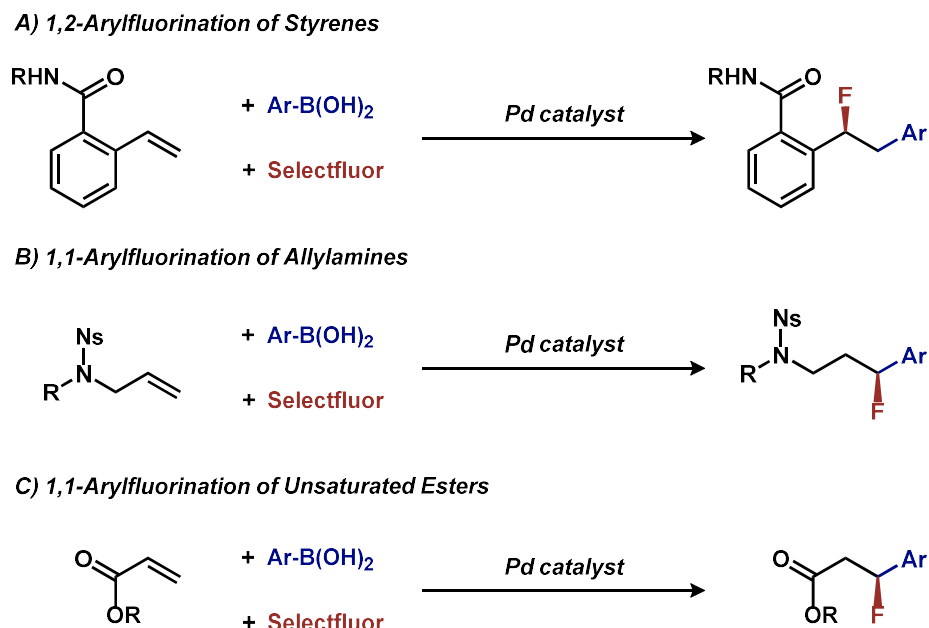
Scheme 1.1. Palladium-catalyzed difunctionalization *via* an interrupted Mizoroki-Heck reaction

In particular, this strategy was recently revived in the development of palladium-catalyzed protocols for the 1,2- and 1,1-arychlorination and bromination of unactivated α -olefins.^{18, 20} In addition, the Sigman group applied this strategy to the palladium catalyzed 1,2-diarylation of alkenes utilizing arylstannanes as the coupling partner and oxygen as the terminal oxidant.¹⁹ This technology was further extended to mixed diarylation reactions utilizing aryldiazonium salts and aryl boronic acids for the 1,1-diarylation of terminal alkenes and the 1,2-diarylations of dienes.^{21, 23} The 1,4-divinylation of isoprene was achieved using vinyl triflates and boronic acids.²⁶ The variety of coupling partners used to generate and intercept Mizoroki-Heck intermediates in these reports encouraged us to continue to explore the generality of this 3-component coupling platform.

The question we initially considered was that of oxidative fluorination of the σ -alkyl palladium intermediate on the basis of multiple studies describing sp^3 -C-F reductive elimination from high-valent metal intermediates, including palladium.³³⁻³⁶ Specifically in this regard, our group first demonstrated this could be applied to the enantioselective construction of sp^3 -C-F bonds,^{11, 13-14, 37-42} in our reported Pd-catalyzed directed enantioselective 1,2-arylfuorination of styrenes (Scheme 1.2A).²² This initial report was followed by the development of methods for enantioselective 1,1-arylfuorination of protected allylamines²⁵ and β,β -arylfuorination of α,β -unsaturated carbonyls (Scheme 1.2B and 1.2C).²⁷

Although these reactions apply similar conceptual strategies, the regiochemical outcome of the transformations is dependent on substrate and conditions. The ultimate outcome of these reactions is determined by both the regioselectivity of the initial migratory insertion event, and the propensity of the palladium to migrate *via* successive β -hydride elimination and insertion events prior to oxidative functionalization. The latter suggests that oxidative alkene difunctionalization beyond the reported 1,1- and 1,2- regioselectivity should be accessible through pathways analogous to those proposed for the redox-relay Heck reaction reported by the Sigman group.⁴³⁻⁴⁵ Herein, we present the development of the first Pd-catalyzed 1,3-arylfuorination reaction, including a catalytic enantioselective variant, as well as an integrated experimental, computational, and statistical analysis of the site selectivity as a function of substrate and ligand. The results of these studies shed light

on the factors that govern site selectivity in the migratory insertion step, which should inform future applications of the strategies described.⁴⁶

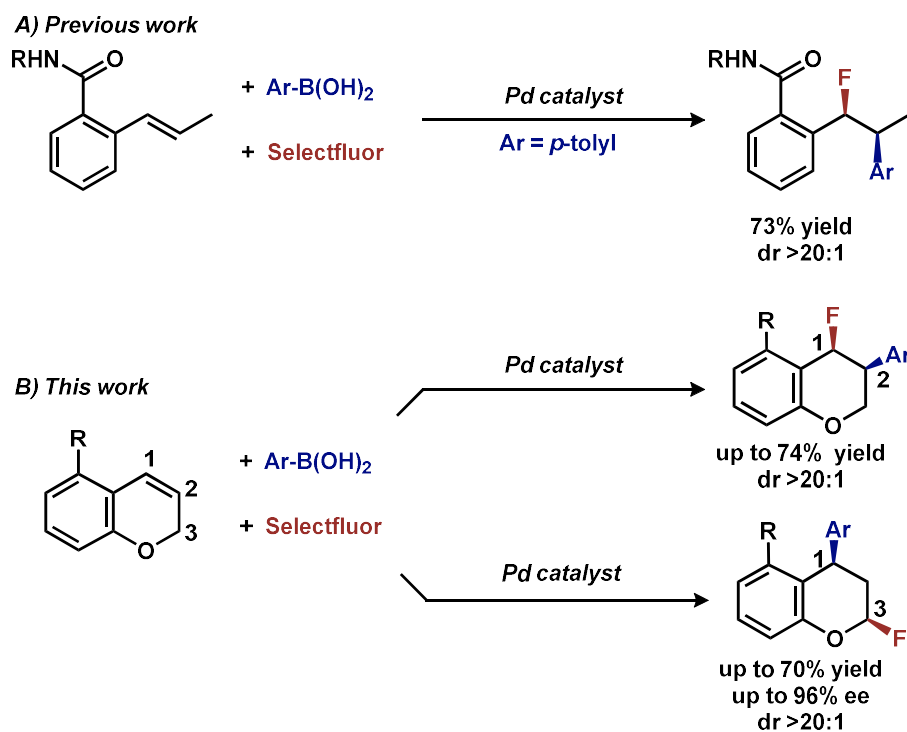


Scheme 1.2. Palladium-catalyzed arylfluorination reactions. A) Arylfluorination of styrenes. B) Arylfluorination of aminoalkenes. C) Arylfluorination of Michael acceptors

1.2. Results and Discussion

1.2.1. Discovery and Development of 1,3-Arylfluorination

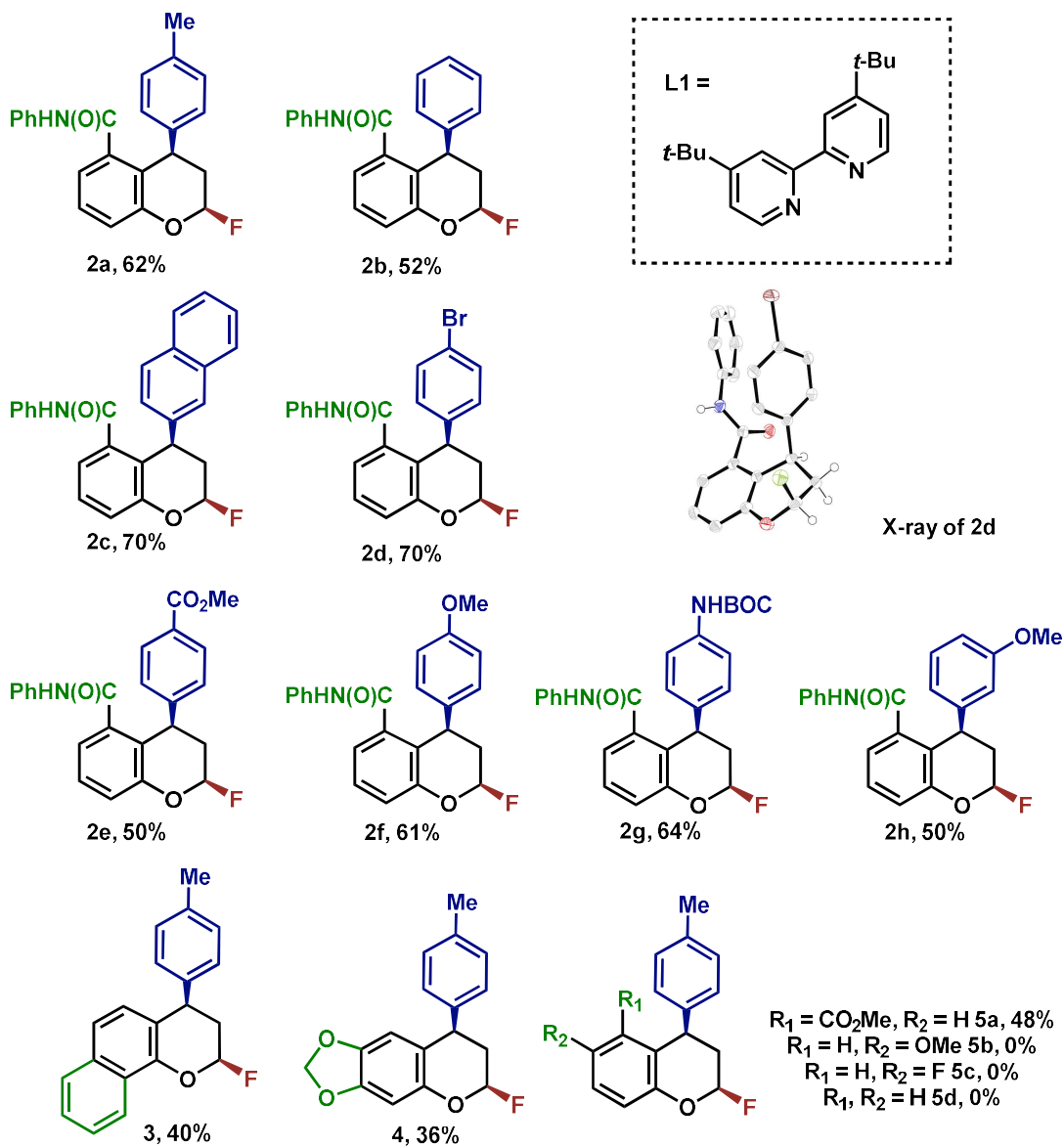
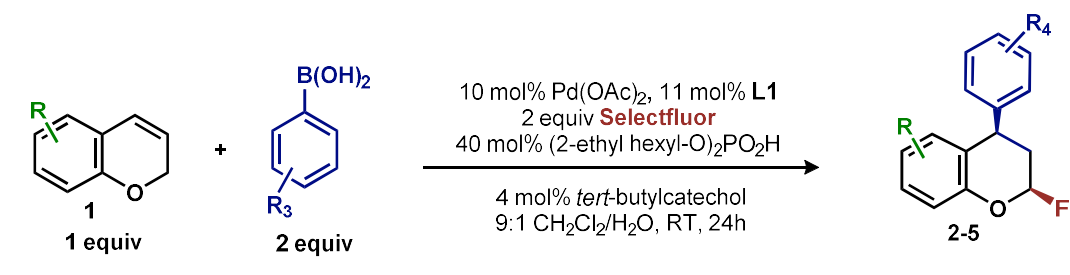
In our previous studies, we noted that the alkene was arylated at a single site resulting in a 2,1-arylfuorination of a *trans*-di-substituted styrene (Scheme 1.3A). In light of this result, the degree of substitution and geometry of alkenes that were competent to participate in this reaction was further examined. During these studies, our attention turned to the *ortho*-carboxamide of [2*H*]-chromene (Scheme 1.3B, R = CONHPh) as a substrate. Under the previously optimal conditions to achieve a directed 2,1-arylfuorination process, the resulting product was observed only in a trace amount. Surprisingly, the 1,3-arylfuorination product was the major product (Scheme 1.3B), thereby overcoming the expected directing group bias.^{22, 47} Given this unprecedented site selectivity of the initial migratory insertion event and the impact of ligand on such selectivity (*vide infra*), we posited that this transformation would be an ideal platform to investigate the subtle factors that contribute to regioselectivity in migratory insertion step of interrupted Mizoroki-Heck reactions.



Scheme 1.3. Palladium-catalyzed aryfluorination reactions. A) Reported 2,1-arylfuorination. B) 1,3-arylfuorination from this work

Intrigued by the 1,3-disposition of the introduced substituents, we sought to initially probe the scope of this transformation (Table 1.1). Using 4,4'-di-*tert*-butyl-2,2'-bipyridine, **L1**, as the ligand, a wide variety of boronic acids (bearing electron withdrawing and donating groups) were evaluated. Under these conditions, the 1,3-substitution pattern of the introduced functional groups was conserved with a range boronic acids (**2a-h**). Interestingly, [2*H*]-chromenes bearing different substitution patterns were either less efficient (**3-5a**) or ineffective (**5b-5d**) under these reaction conditions.

Having already achieved an enantioselective 2,1-arylfuorination utilizing a styrene as a substrate,²² we anticipated that the novel 1,3-arylfuorination manifold could also be rendered enantioselective. Several commercially available and readily accessible chiral *N,N* ligands were evaluated (see supporting information); however, only trace amounts of the target product were observed in nearly all cases. In a similar fashion to our previous study, the most promising class of ligand for this transformation were the PyrOx class, of which (*S*)-4-*tert*-butyl-2-(2-pyridyl)oxazoline led to the formation of **2a** with the highest enantioselectivity (see supporting information). After extensive optimization (see supporting information), we identified that the addition of 1.5 equivalents of sodium fluoride and a DCE/H₂O solvent mixture rendered the reaction selective for the 1,3-product (5:1 relative to the 2,1-arylfuorination product), while also maintaining a high enantioselectivity. Although the role of the sodium fluoride is not certain, some possible roles include serving as a base for the phosphate or as a ligand on palladium to block coordination of the directing group. The role of the directing group is discussed later in further detail.

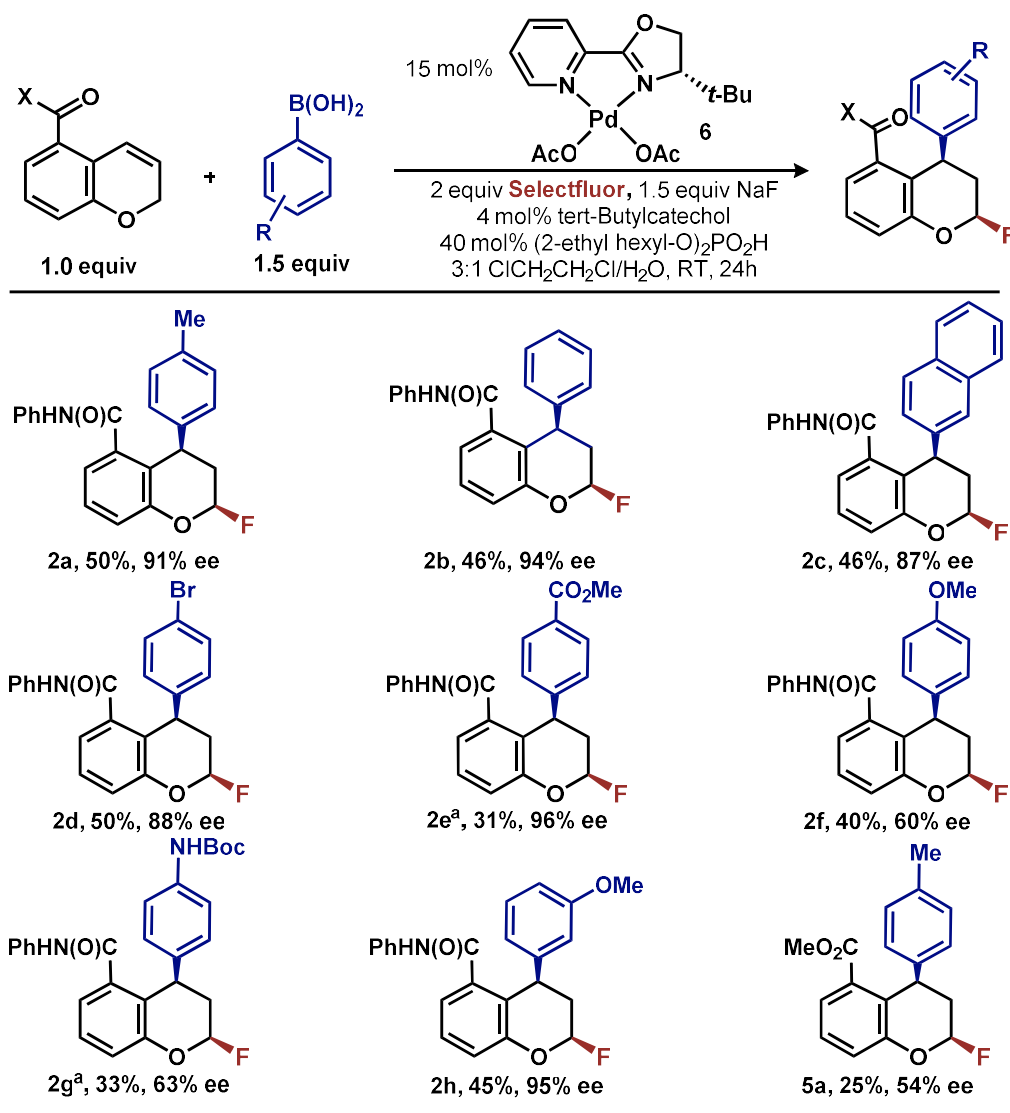


Reactions performed on 0.1 mmol scale and 2.0 mL total volume of solvent. a.) Yields refer to isolated yields.

b.) All samples are racemic

Table 1.1. 1,3-Arylfuorination of chromenes^{a,b}

Using these modified reaction conditions, the scope of the enantioselective reaction was explored (Table 1.2). It should be noted that the preformed palladium(II) complex **6** was utilized in this investigation as this aided the reproducibility.⁴⁸ The 1,3-difunctionalized products were obtained in moderate yields and high enantiomeric excess (Table 1.2, 2a-2h), when chromenes with an *ortho*-amide substituent were employed. When the corresponding ester substituent was employed in the *ortho*- position, the product **5a** was formed in both lower yield and reduced enantiomeric excess.

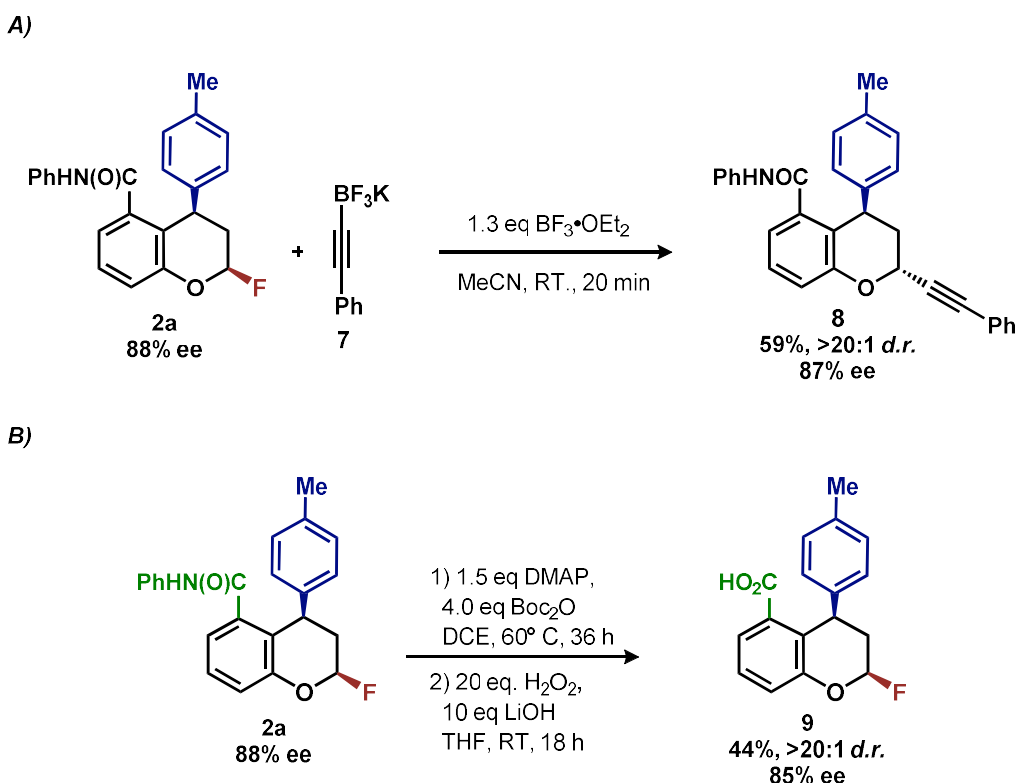


Reactions performed on 0.1 mmol scale and 2.0 mL total volume of solvent. a.) Yields refer to isolated yields. b.) Enantiomeric excess determined by chiral HPLC

Table 1.2. Asymmetric 1,3-arylation of chromenes

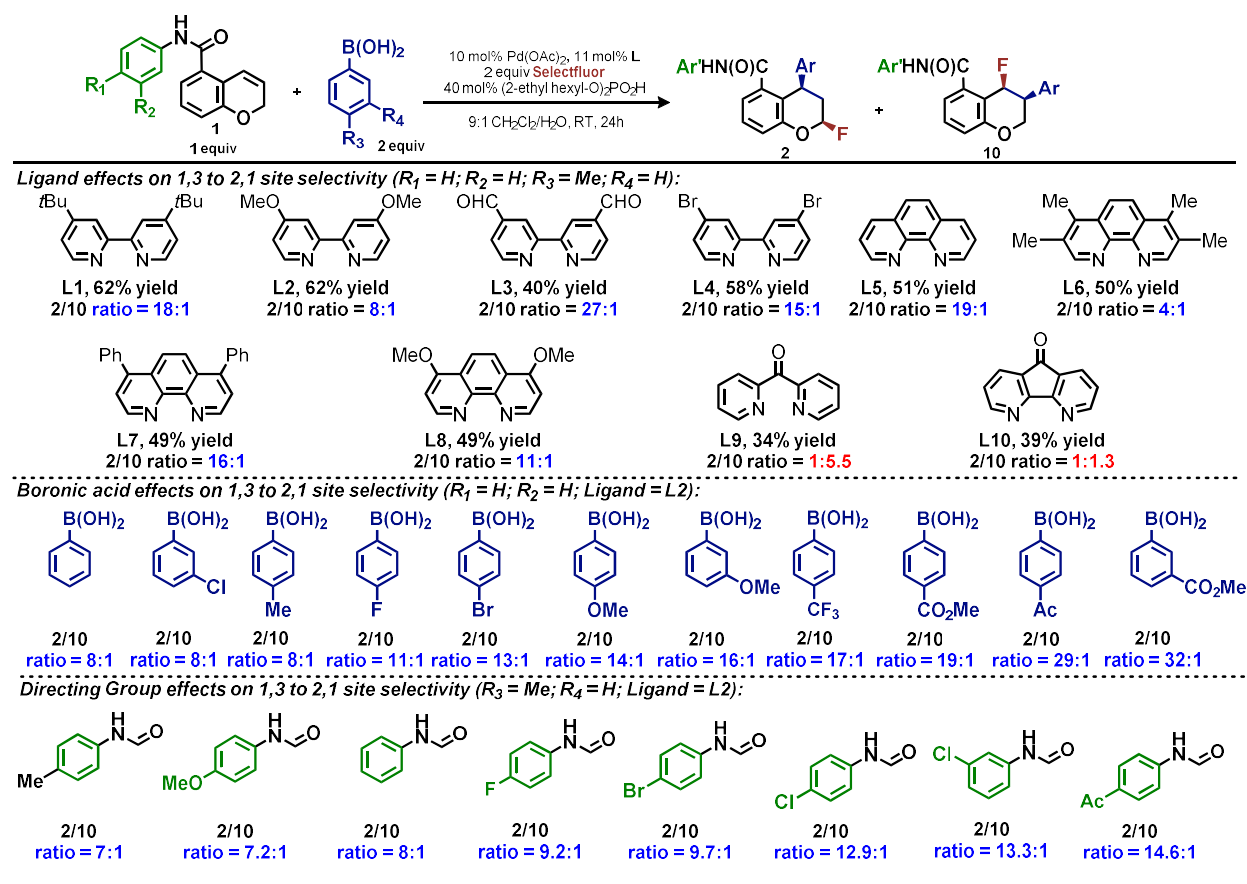
The synthetic utility of these pyranyl fluorides was further demonstrated by treating **2a** with potassium trifluoroborate salt **7** in the presence of BF₃•etherate that formed alkyne **8** in good yield and high diastereoselectivity, without erosion of the enantiomeric purity (Scheme 1.4A).⁴⁹ It

should also be noted that the arylation of pyranil fluorides with aryl stannanes has been reported.⁵⁰ In addition, the amide directing group on 2a could also be removed, affording carboxylic acid 9 in modest yield and without significant erosion of the enantiomeric excess (Scheme 1.4B). Analysis of the crude reaction mixture by ¹H-NMR after hydrolysis with LiOH/H₂O₂ revealed that 2a was formed as a significant byproduct of this reaction. We believe this is likely the result of non-selective hydrolysis of the carbamate intermediate. Therefore, the derivatization could conceivably be improved by recycling of amide 2a.



Scheme 1.4. Derivatization of 1,3-arylfuorination products. A) Derivatization of pyranil fluoride. B) Removal of amide directing group

During the development of the enantioselective variant of this reaction, we observed the formation of the 2,1-arylfuorination product **10** (Table 1.3.) in significant quantities. Given the unique nature of the 1,3-fluoroarylation reaction and the apparent ligand effect on regioselectivity, we sought to better understand the origin of this divergence. We set out to determine what experimental parameters affect the site selectivity of migratory insertion, the results of which are summarized in Table 1.3. We have identified three variables that significantly influence the observed ratio of products **2** and **10**: choice of ligand, aryl boronic acid coupling partner, and directing group. The data was utilized in the following computational and statistical analysis to develop our mechanistic hypothesis and better our understanding the factors governing reaction performance and site selectivity.



Reactions performed on 0.10 mmol scale and 2.0 mL total volume of solvent. a) Yields and product ratios determined by ¹⁹F-NMR by comparison to an internal standard (4-fluorobenzoic acid). b) Yields and product ratios are the average of two runs. c) All samples are racemic.

Table 1.3 Ratio of 1,3- and 2,1-arylation products (2/10) as a function of ligand, boronic acid and directing group^{a,b,c}

1.2.2. Ligand Effects on Regioselectivity

To elucidate the ligand features that influence the site selectivity in the arylation reaction of chromenes, various ligands were evaluated in the palladium-catalyzed arylation reaction of [2*H*]-chromene **1a** and *para*-tolyl boronic acid (Table 1.3). The results illustrate a wide variation of reaction outputs from an indiscriminating (1:1.3; Table 3, **L10**) to a highly selective (27:1; Table 1.3, **L3**) 1,3-arylation process.

Following these experiments the ground state structure of various ligated palladium dichloride complexes, PdLCl₂, were calculated using DFT. Numerous parameters were gathered from the geometry optimized structures of the palladium complexes including Natural Bond Orbital (NBO) charges, N-Pd-N bite angle, Sterimol values, and IR frequencies and intensities.⁵¹ Through linear regression analysis, Pd NBO charge was found to correlate well with the difference in transition state energies of the two regioisomers ($\Delta\Delta G^\ddagger$), which can be related to the log of the product ratios (Figure 1.1.B).⁵²⁻⁵⁵ As the Pd NBO charge becomes more positive, the $\Delta\Delta G^\ddagger$ increases, which is directly correlated to

greater selectivity for the 1,3-product. We conclude from this correlation that enhanced electrophilicity of the palladium center results in greater selectivity for the 1,3-arylfuorination product.

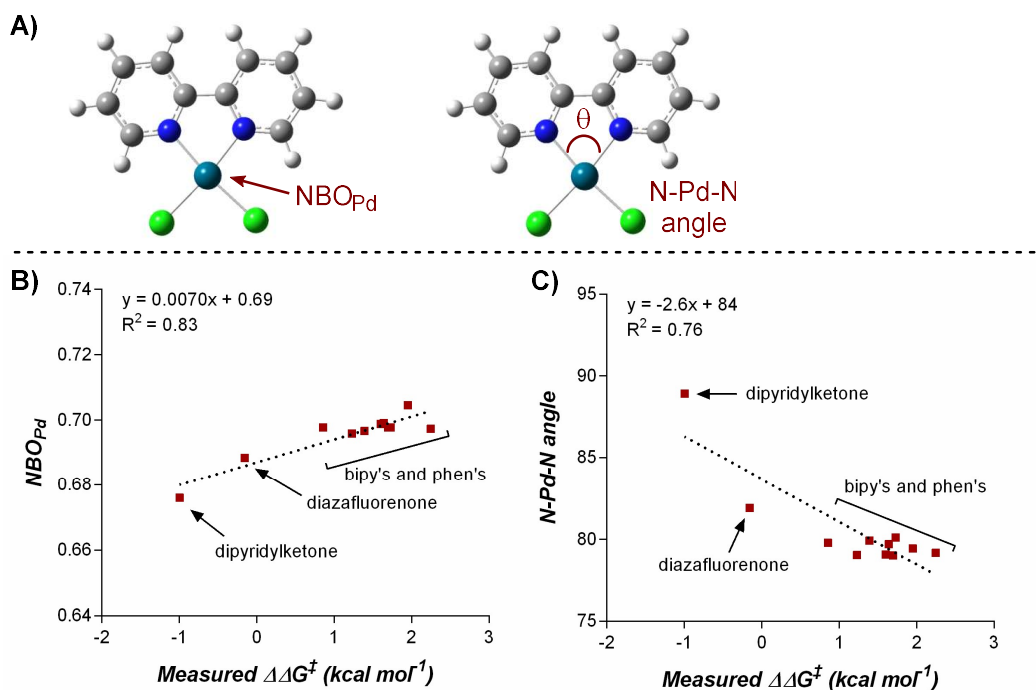


Figure 1.1. Correlation of Pd-NBO charge and ligand bite angle with measured $\Delta\Delta G^\ddagger$. A) Computed structures of palladium dichloride complexes. B) Correlation between palladium NBO charge and $\Delta\Delta G^\ddagger$. C) Correlation between ligand bite angle and $\Delta\Delta G^\ddagger$.

Additionally, the dipyriddyketone and diazafluorenone were computed to have wider bite angles as compared to the other ligands tested, which correlates to the formation of more of the 2,1-product (Figure 1.1.C). This structural distortion has previously been shown to result in complex co-ordination chemistry for diazafluorenone with palladium(II) acetate.⁵⁶ As a result, these ligands have hemi-labile behavior, suggesting they can act as both monodentate and bidentate ligands.⁵⁷ We hypothesized that this ability to act in some cases as a monodentate ligand was critical for the preferred formation of the 2,1-product. This hypothesis was further supported by the fact that when monodentate ligands, such as oxazoles and pyridines, were employed with **1a** and a variety of boronic acids exclusive formation of the 1,2-product was observed (see supporting information).

1.2.3. Aryl Coupling Partner Effects on Regioselectivity

The impact of the aryl boronic acid on site selectivity was explored in order to further understand the features contributing to the site of migratory insertion in these reactions. For this study, the standard reaction conditions were applied with substrate **1a** in conjunction with a range of arylboronic acids; 4-4'-dimethoxy-2-2'-bipyridine **L2** was chosen as the ligand since its use demonstrated moderate selectivity in the initial ligand screen (8:1; Table 1.3). Under the standard reaction conditions, the site selectivity observed

in the arylfluorination was significantly impacted as a result of changes to the boronic acid coupling partner (Table 1.3). To understand what factors drive these changes, a similar correlation analysis was applied for this collection of arylboronic acids. Through the use of univariate linear regression analysis, it was found that the IR COH bending frequency of the corresponding benzoic acid correlated to the site selectivity in migratory insertion for this diverse set of boronic acids (Figure 1.2).⁵⁸⁻⁵⁹ A more electron-withdrawing group (EWG) enhanced the formation of the 1,3-product. This correlation is consistent with our previous hypothesis that an increase in the cationic character of palladium complex favors formation of the 1,3-product.

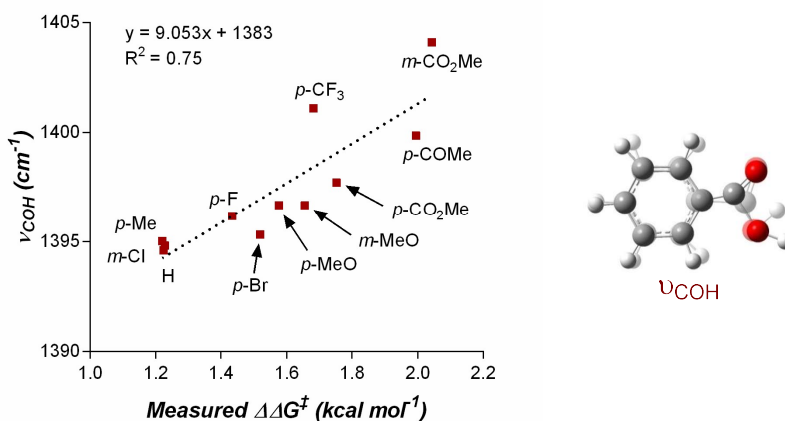


Figure 1.2. Correlation of IR stretch with measured $\Delta\Delta G^\ddagger$

1.2.4. Directing Group Effects on Regioselectivity

The final point for manipulation and analysis concerned the effect that the “directing group” has on the reaction outcome. In the report on the arylfluorination of styrenes, the directing group was incorporated in the substrate as a design element to 1) direct the regioselectivity of the migratory insertion, and 2) to prevent β -hydride elimination which was believed would lead to significant formation of a Heck-coupling side product.²² However, the results in this report and other reports on the 1,1-arylfluorination of alkenes^{25, 27} lead us to question whether the carboxamides have any directing influence on the reaction. To investigate this effect, the standard reaction conditions were once again employed with 4-4'-dimethoxy-2-2'-bipyridine **L2** as the ligand. The arylfluorination reaction site selectivity was impacted through alteration of the aryl-amide substituent, suggesting that the initial olefin insertion process is also controlled by the electronics on the arylamide of the chromene substrate (Table 1.3). In fact, a linear correlation was identified between the Hammett σ -values of various aryl substituents on the amide versus differential transition state energies for the formation of two constitutional isomers yielded in the reaction (Figure 1.3).⁶⁰

A positive slope in the Hammett plot suggests that the electronics on the arylamide is impacting the orientation of [Pd]-Ar species *via* coordination to the metal center, thus influencing the migratory insertion pathway. In general, electron donating groups (EDG)

on the arylamide decreases the selectivity for 1,3-products. We rationalized that with the use of EDG on the arylamide, coordination to the [Pd]-Ar species is more favorable, and thus the increased 2,1-product formation is a result of enhanced efficiency of coordination of the directing group.

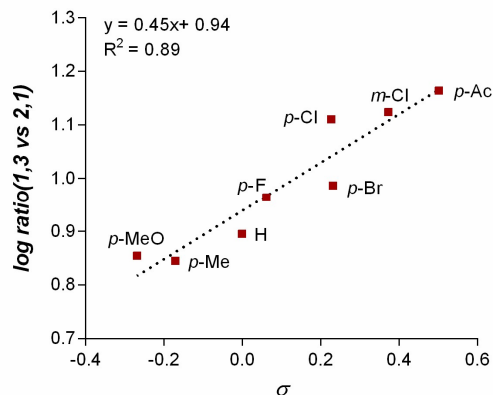


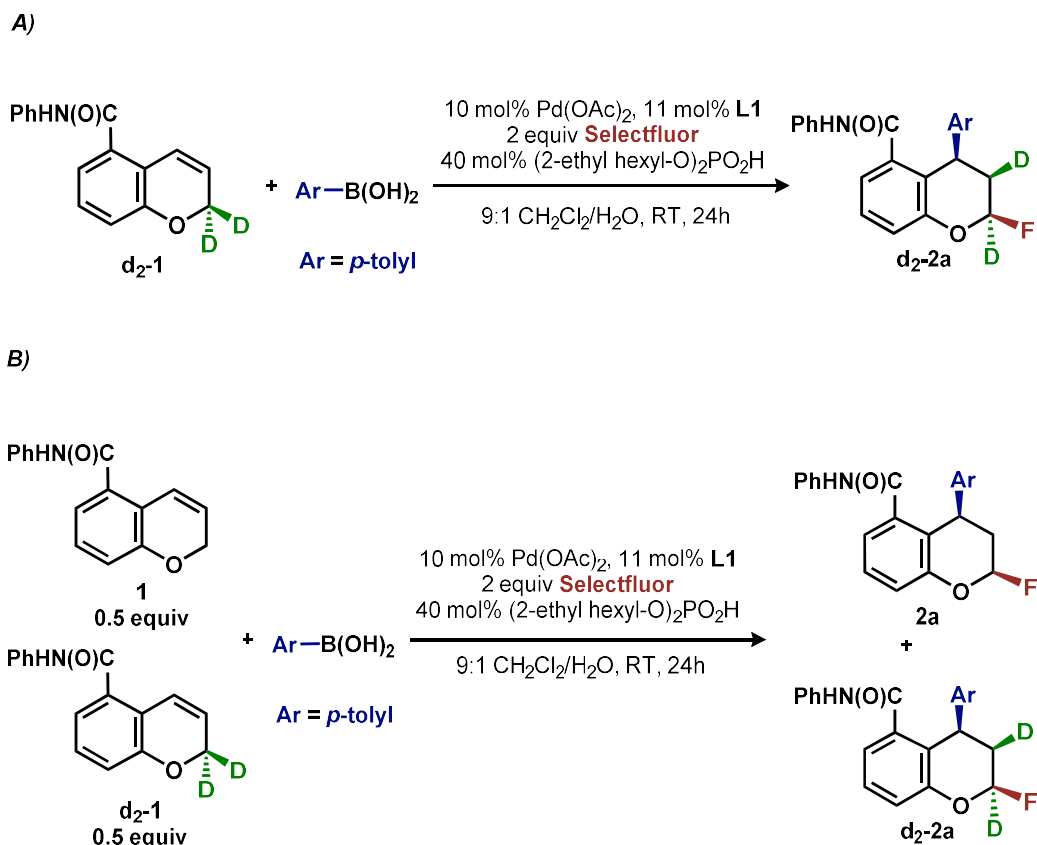
Figure 1.3. Plot of Hammett σ -values versus measured product ratio

1.2.5. Deuterium Labeling Experiments

To further probe the mechanistic divergence, we sought validation of our developing hypothesis that bifurcation occurs from the initial migratory insertion event. We assumed that the 2,1-arylfuorination product was formed in an analogous fashion to our previously reported reaction with styrenes, namely by a migratory insertion that places the palladium in the benzylic position, and the aryl-group in the homo-benzylic position, followed by C–F bond formation. For the 1,3-arylfuorination reaction, we anticipated an oxidative Heck-type mechanism would also be operative, although the possibility of alternative mechanisms, including allylic C–H palladation, were considered.⁶¹⁻⁶² We hypothesized that the 1,3-product was formed by a migratory insertion with the opposite sense of selectivity, followed by palladium migration, and C–F bond formation.

To gather further support for this latter hypothesis, we performed a deuterium labeling experiment with chromene **d2-1**, (Scheme 1.5A). The resulting product **d2-2a**, in which one deuterium migrated to the adjacent carbon, was the exclusive arylfluorination product. This is possible if a [Pd]-alkyl intermediate undergoes β -hydride elimination and reinsertion events on the carbon α to oxygen, which is suggestive of an oxidative Heck-type mechanism. In a second experiment designed to understand the palladium chain walking and probe the stereochemistry of the C–F bond-forming step, a cross-over experiment with chromene **1** and deuterated substrate **d2-1** was performed (Scheme 1.5B). The observation of a 1:1 mixture of product **2a** with no deuterium and product **d2-2a** with two deuterium atoms indicated that dissociation of an intermediate olefin from a palladium hydride species and subsequent isotopic scrambling likely did not occur,⁶³⁻⁶⁴ thereby supporting an inner-sphere C–F bond forming reductive elimination.³³ An alternative explanation for the observed 1,3-*syn*-stereodiad is reductive elimination of the α -oxy-palladium species to form the corresponding oxonium ion, which is then trapped by fluoride under thermodynamic conditions. DFT calculations revealed that the *syn*-isomer is the

thermodynamically more stable isomer by <0.5 kcal/mol. The fact that we do not observe the *trans*-product together with the small calculated thermodynamic preference for the *cis*-isomer suggest that the product is formed via an inner sphere C-F reductive elimination. In either case, the C-F bond-forming step is independent of the regio-determining step.



Scheme 1.5. Deuterium labeling experiment with chromene **d₂-1**

1.2.6. Mechanistic Proposal

Having established that both products likely arise from oxidative Heck-like mechanisms, we propose the following two pathways to rationalize the divergence in site selectivity outlined in Figures 1.4 and 1.5. In the presence of a strong bidentate ligand such as 4,4'-di-*tert*-butyl-2,2'-bipyridine **L1** (Figure 1.4), transmetalation with an arylboronic acid, followed by displacement of an anionic ligand with a chromene olefin, results in the formation of cationic palladium species, **C**. The site of migratory insertion is then controlled by the polarity of the alkene. When considering the chromene as a vinylogous enol-ether, insertion of the aryl group at the position α to the aromatic ring and the palladium at the β -position gives rise to the expected regiochemical outcome for an electron rich olefin and a cationic palladium species.⁶⁵⁻⁶⁸ Subsequent migration and oxidation results in the formation of the observed 1,3-product. In this case, the polarity bias of the olefin out competes the influence of the directing group. The correlations we found between the increased cationic character on palladium to greater selectivity for the 1,3-product

corroborates this hypothesis. Additionally, when considering the pre-migratory insertion intermediate **C**, the lack of readily available coordination site in the square planar complex, the directing group would be expected to have little influence on the regioselectivity of the migratory insertion.

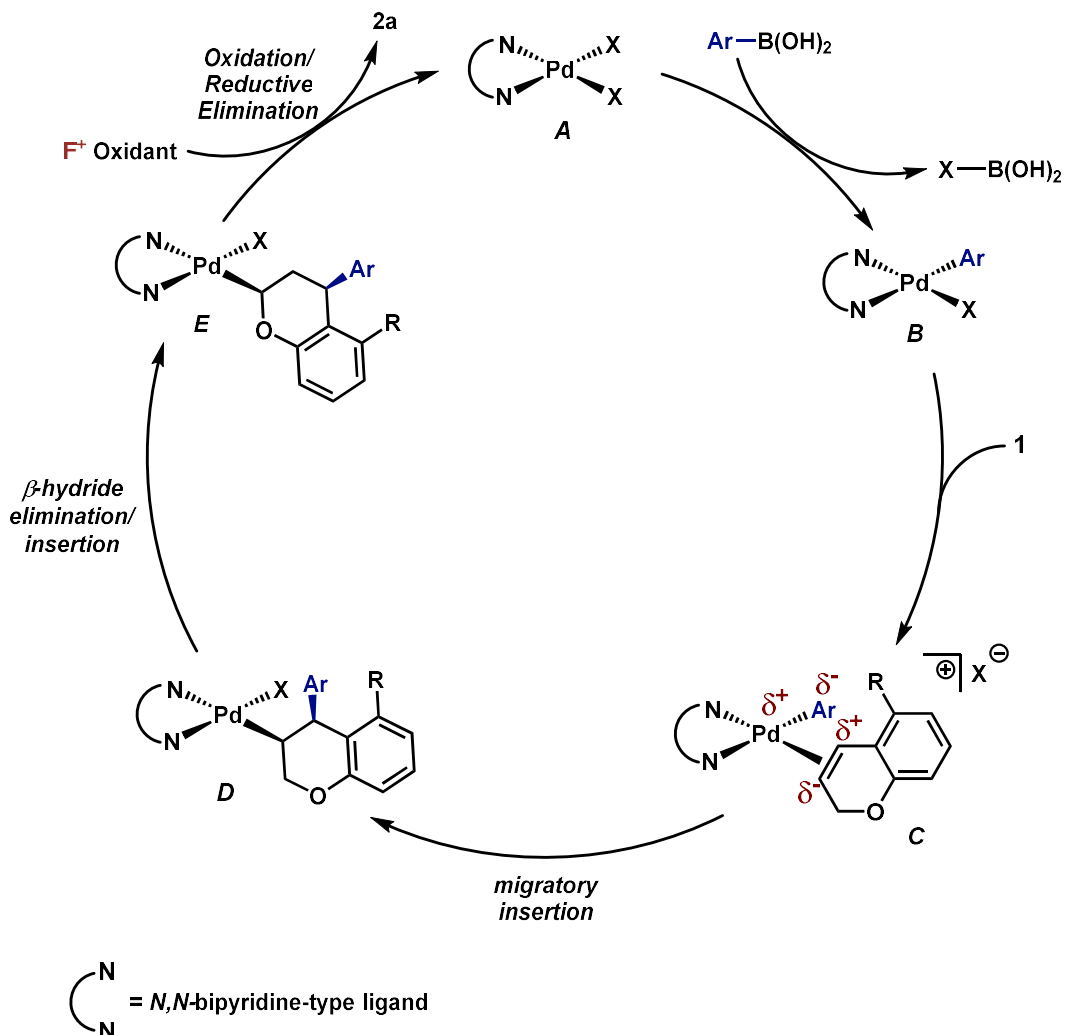
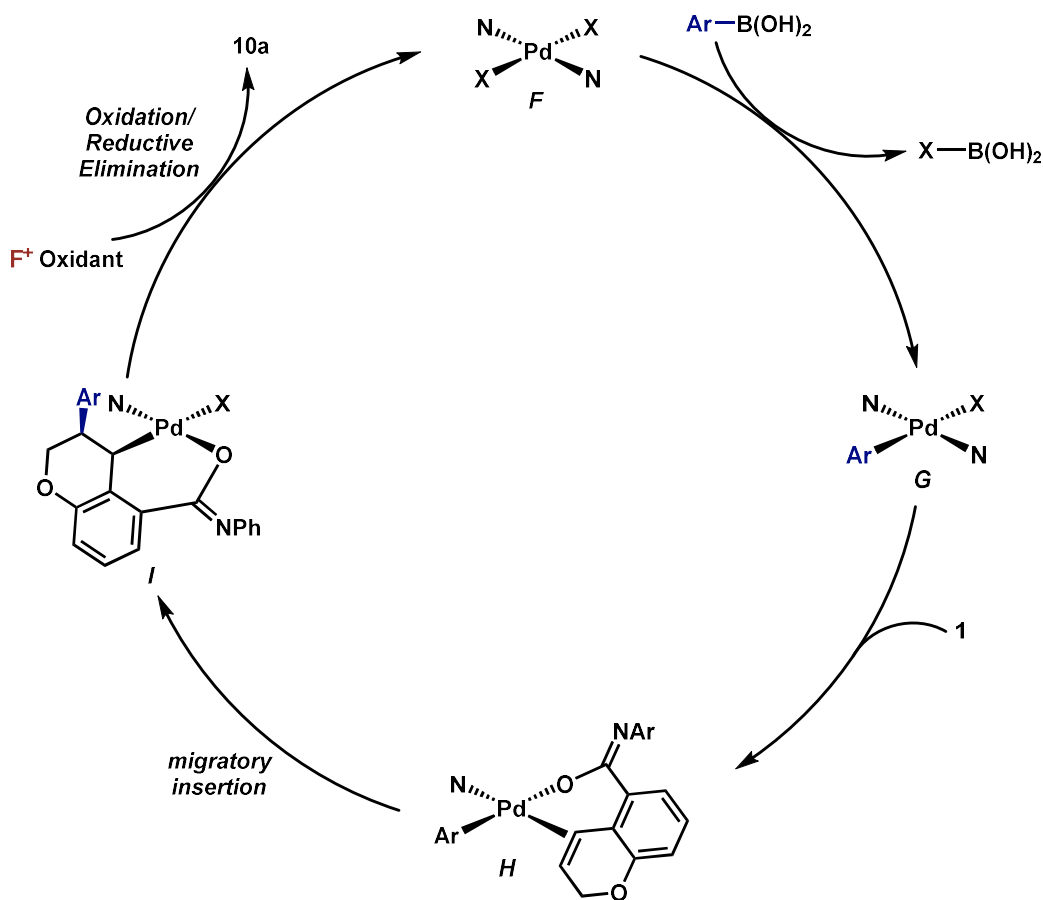


Figure 1.4. Proposed mechanisms for the formation of the 1,3-arylfluorination product

In the presence of either hemi-labile bidentate or monodentate ligands,²² we alternatively propose the mechanism outlined in Figure 1.5. After transmetalation of an arylboronic acid to form intermediate **G**, a labile ligand may allow for the formation of an intermediate such as **H**, in which the substrate is ligated by both the olefin and the *ortho*-carboxamide directing group. We propose that subsequently a directed migratory insertion occurs, placing the palladium α to the aromatic ring, and proximal to the *ortho*-amide directing group. Subsequent oxidation and reductive elimination would afford the 2,1-arylfluorination product. In this case, the open coordination site for the directing group to occupy would be more accessible, thus enhancing the influence of the directing group. In addition, our studies also indicate that the electrophilicity of the [Pd]-Ar also has an influence on the location of the migratory insertion. The proposed intermediate **H**, is a

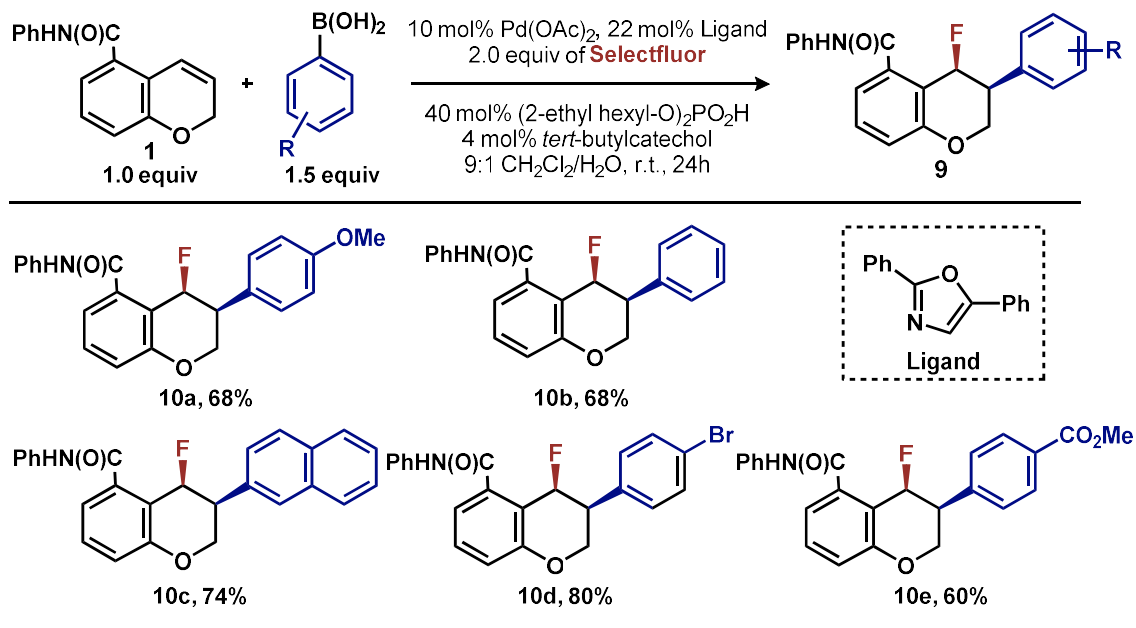
neutral palladium species and as a result is less-electrophilic than the corresponding intermediate in the mechanism in Figure 1.4; thus, the polarity of the olefin has significantly less influence in the selectivity determining step. It should be noted that similar results where significant shifts in the site of migratory insertion as a function of ligand structure in Heck reactions is preceded.⁶⁹⁻⁷⁰



N = pyridine-type ligand

Figure 5. Proposed mechanisms for the formation of the 2,1-arylfuorination product

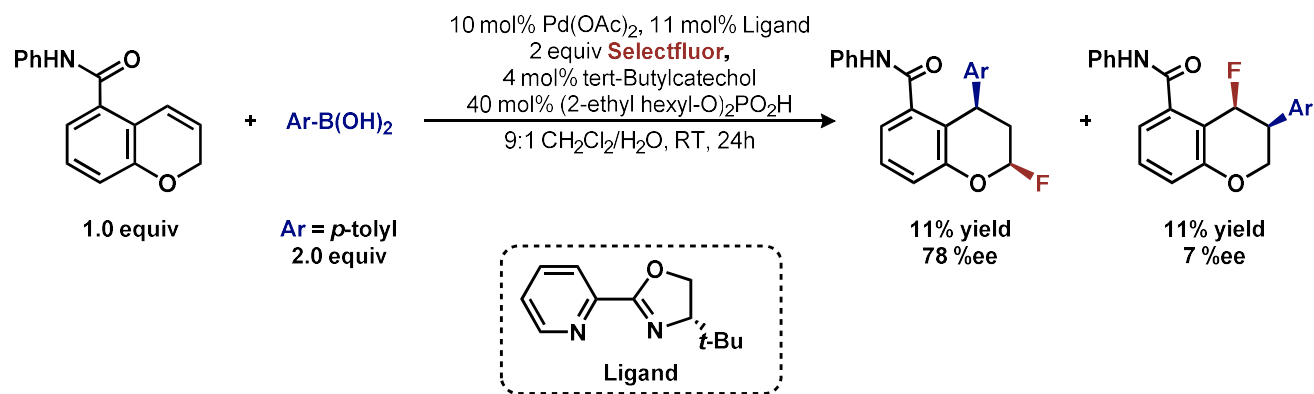
In accordance with this hypothesis, we also identified a monodentate oxazole ligand that, when employed under our reaction conditions, provides high selectivity for the 2,1-arylfuorination product (Table 1.4). Additional details on screening of monodentate ligands are provided in the supporting information.



Reaction performed on a 0.1 mmol scale and 2.0 mL total volume of solvent. a.) Yields refer to isolated yields. b.) All samples are racemic.

Table 1.4. 2,1-arylfuorination catalyzed by palladium with monodentate ligand.^{a,b}

Finally, the low enantioselectivity observed (7% ee; Scheme 1.6) for 2,1-arylfuorination products when bidentate chiral ligands are employed may also be attributed to the partial dissociation of ligand allowing directing group ligation. In contrast, high enantioselectivity was observed with the chiral bidentate PyrOx ligand for the formation of 1,3-arylfuorination product (Table 1.2). This observation is consistent with a mechanistic hypotheses discussed above in which the 1,3-arylfuorination occurs through a palladium species wherein the chiral ligands maintain their bidentate coordination.⁷¹⁻⁷³



Reactions performed on 0.1 mmol scale and 2.0 mL total volume of solvent. a.) Yields refer to isolated yields. b.) Enantiomeric excess determined by chiral HPLC

Scheme 1.6. Comparison of enantioselective 1,3-arylfuorination and 2,1-arylfuorination^{a,b}

1.3. Conclusion

We have developed a 1,3-arylfuorination of [2*H*]-chromenes; the first of the palladium-catalyzed arylhalogenation reactions that results in 1,3-relationship of the introduced substituents. In addition, we have developed an enantioselective variant of the 1,3-fluoroarylation of [2*H*]-chromenes and demonstrated the utility of the enantioenriched pyranyl fluorides by further diastereoselective C–C bond formation. We have established that both the 1,3- and 2,1-products likely arise from oxidative Heck-type mechanisms that diverge at the initial migratory insertion event. Our integrated experimental, computational, and statistical analysis revealed that the identity of the ligand, the arylboronic acid coupling partner, and the directing group all affect the site of migratory insertion. The vinylogous enol ether selectivity leading to formation of the 1,3-product is enhanced by increased electrophilic character at palladium, either by the bipyridine/phenanthroline ligand or the electronics of the aryl coupling partner. Selectivity for the 2,1-product is enhanced by increased electron donating character of the amide directing group and decreased denticity of the supporting ligand. These results should help inform the design of future arylfluorination reactions, and more broadly shed light on the subtle factors, which influence the site of functionalization in interrupted Mizoroki-Heck reactions and the role of directing groups in high-valent palladium catalyzed reactions.

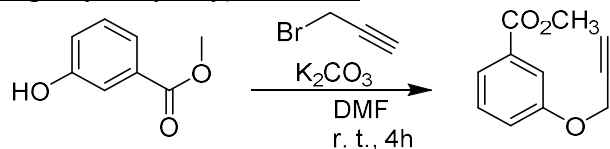
1.4. Supporting Information

1.4.1. General Information

Unless otherwise noted, reagents were obtained from commercial sources and used without further purification. All reactions were carried out without rigorous exclusion of water and air and at room temperature (23 °C) except where otherwise indicated. All reactions were magnetically stirred and monitored by analytical thin layer chromatography (TLC) using Merck 60 pre-coated silica gel plates with F254 indicator. Visualization was accomplished by UV light (254 nm). Flash column chromatography was performed using ICN SiliTech 32-63 D 60Å silica gel. Commercial grade solvents were used without further purification except as indicated below. Tetrahydrofuran (THF), diethyl ether (Et₂O), dichloromethane (CH₂Cl₂), and, *N,N'*-dimethylformamide (DMF) were dried by passing commercially available pre-dried, oxygen-free formulations through activated alumina columns. ¹H NMR, ¹³C NMR, and ¹⁹F spectra were recorded on Bruker AMX-300, AVQ-400, AVB-400, DRX-500 and AV-600 spectrometers and referenced to CDCl₃. Tetramethylsilane was used as an internal standard for ¹H NMR (δ: 0.0 ppm), and CDCl₃ for ¹³C NMR (δ: 77.23 ppm). Multiplicities are indicated by s (singlet), d (doublet), t (triplet), q (quartet), and m (multiplet). Enantiomeric excess was determined on a Shimadzu VP Series Chiral HPLC with a variable wavelength detector using chiral stationary columns. Mass spectral data were obtained from the QB3/Chemistry Mass Spectrometry Facility at the University of California, Berkeley.

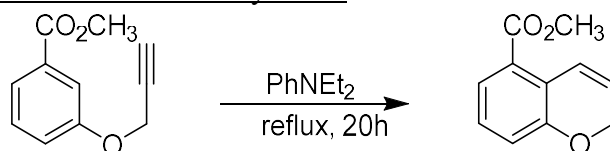
1.4.2. Preparation and Characterization of Chromene Substrates

Synthesis of methyl 3-(prop-2-yn-1-yloxy)benzoate:



To a round bottom flask equipped with a stir bar and under positive pressure of N_2 , methyl 3-hydroxybenzoate (3.04 g, 20.0 mmol 1.00 eq) and potassium carbonate (4.18 g, 30.0 mmol 1.50 eq) were added as solids and suspended in 20 ml of DMF. To the reaction mixture was added propargyl bromide (80% weight solution in toluene, 3.12 ml 28.0 mmol, 1.40 eq) was added via syringe. A slight yellow solution resulted. After stirring for 2.5 hours the reaction mixture was diluted with ethyl acetate and H_2O . The organic layer was separated and washed with 1M NaOH. The organics were again separated, dried over Na_2SO_4 , filtered, and concentrated. Residual DMF was removed in vacuo over 12 hours. The resulting yellow liquid was used crude. $^1\text{H NMR}$ (300 MHz, CDCl_3) δ 7.73-7.59 (m, 2H), 7.37 (t, $J = 8.0$ Hz, 1H), 7.18 (ddd, $J = 8.2, 2.7, 1.0$ Hz, 1H), 4.74 (d, $J = 2.4$ Hz, 2H), 3.91 (s, 3H), 2.54 (t, $J = 2.4$ Hz, 1H). Spectrum is in agreement with literature report.⁷⁴

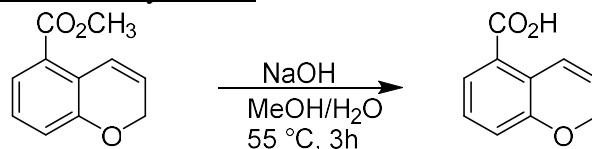
Synthesis of methyl 2H-chromene-5-carboxylate 3:



A round bottomed flask containing a stir bar and the crude methyl 3-(prop-2-yn-1-yloxy)benzoate was placed under N_2 and equipped with a reflux condenser. To the flask, 20 mL of diethyl aniline was added and the reaction mixture heated to 215°C . While heating, the solution began to turn dark brown in color beyond 150°C . The reaction mixture was heated for 24 hours, after which it was cooled to room temperature and diluted with ethyl acetate. The combined organics were washed with two times with 1 M HCl, separated, dried over Na_2SO_4 , and concentrated to afford a brown residue. The residue was purified by silica chromatography S4 (1.5%-2.5% ethyl acetate in hexanes) affording the product (1.31 g, 34% over 2 steps) as a yellow oil.

$^1\text{H NMR}$ (300 MHz, CDCl_3) δ 7.48 (dd, $J = 7.8, 1.3$ Hz, 1H), 7.31 (dtd, $J = 10.2, 1.9, 0.8$ Hz, 2H), 7.14 (t, $J = 8.0$ Hz, 1H), 7.02 – 6.92 (m, 1H), 5.94 (dt, $J = 10.2, 3.8$ Hz, 1H), 4.78 (dd, $J = 3.8, 1.9$ Hz, 2H) 3.89 (s, 3H). Spectrum is in agreement with literature report.⁷⁴

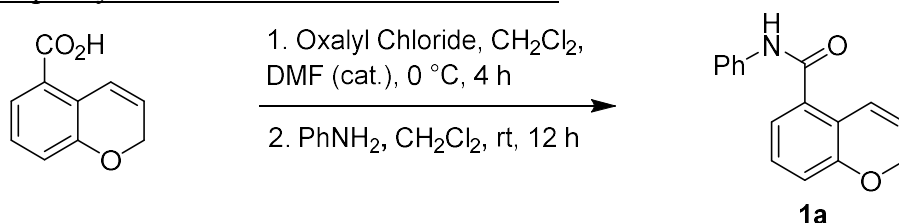
Synthesis of 2H-chromene-5-carboxylic acid



To a round bottomed flask equipped with a stir bar was added sodium hydroxide (412 mg, 10.3 mmol, 1.50 eq) was added and dissolved in 37 mL of H₂O. To the stirred solution methyl 2Hchromene-5-carboxylate (1.31 g, 1.0 eq, 6.87 mmol) was added in 17 mL of MeOH resulting in a cloudy mixture. The reaction mixture was heated to 55 °C at which point a clear yellow solution formed. After heating for the 3 hours, the contents of the flask were cooled to room temperature and the MeOH was removed by a rotary evaporator. To the remaining aqueous solution, 15 mL of 1 M HCl was added forming a colorless precipitate. The precipitate was filtered and rinsed with water on a Büchner funnel and dried in vacuo for 12 hours affording the product (846 mg, 70% yield) as a colorless powder.

¹H NMR (300 MHz, CDCl₃) δ 7.63 (dd, J = 7.8, 1.3 Hz, 1H), 7.42 (d, J = 10.2 Hz, 1H), 7.18 (t, J = 8.0 Hz, 1H), 7.03 (d, J = 8.0 Hz, 1H), 5.97 (dt, J = 10.3, 3.8 Hz, 1H), 4.80 (dd, J = 3.8, 1.9 Hz, 2H). Spectrum is in agreement with literature report.⁷⁵

Synthesis of N-phenyl-2H-chromene-5-carboxamide **1a**:



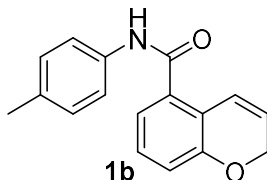
To a solution of the 2-H-chromene-5-carboxylic acid (264 mg, 1.5 mmol, 1.00 equiv) in dcm (10 mL) at 0 °C was added dropwise oxalyl chloride (381 mg, 3.0 mmol, 2.0 equiv) followed by a catalytic amount of dry dmf (2 drops). The reaction was allowed to stir at rt until completion (typically 4 h). The solvent was then removed under reduced pressure to afford the corresponding crude acid chloride. Aniline (168 mg, 1.8 mmol, 1.2 equiv) was added to solution of acid chloride in dcm (20 mL). Reaction was stirred for 12 h at rt followed by quenching with sat. NaHCO₃ (20 mL) solution. Organic layers were dried over MgSO₄, filtered, evaporated and purified by silica chromatography (10-40% EtOAc:hexanes) to give the compound **1a** as a white powder (300 mg, 80%) .

¹H NMR (400 MHz, CDCl₃) δ 7.61 (m, 3H), 7.37 (t, J = 7.9 Hz, 2H), 7.21 – 7.06 (m, 3H), 6.94 – 6.83 (m, 2H), 5.88 (dt, J = 10.1, 3.7 Hz, 1H), 4.81 (dd, J = 3.8, 1.9 Hz, 2H).

¹³C NMR (101 MHz, CDCl₃) δ 166.6, 155.0, 138.1, 133.8, 129.3, 129.1, 124.9, 123.5, 122.2, 120.9, 120.1, 119.9, 118.7, 65.3.

HRMS (ESI) m/z (M+H)⁺ calculated for C₁₆H₁₄NO₂: 252.1019 observed 252.1019.

Synthesis of N-(*p*-tolyl)-2H-chromene-5-carboxamide **1b**:



The same general procedure as that for the synthesis of **1a** was followed using 2-H-chromene-5-carboxylic acid (264 mg, 1.5 mmol, 1.00 equiv), oxalyl chloride (381 mg, 3.0 mmol, 2.0 equiv), *p*-toluidine (193 mg, 1.8 mmol, 1.2 equiv), and dmf (2 drops). The compound was purified by

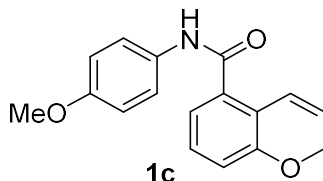
silica chromatography (10-40% EtOAc:hexanes) to give the compound **1b** as a white powder (334 mg, 84%) .

¹H NMR (400 MHz, CDCl₃) δ 7.50 (d, *J* = 8.3 Hz, 3H), 7.21 – 7.05 (m, 4H), 6.90 (t, *J* = 8.2 Hz, 2H), 5.89 (dt, *J* = 10.1, 3.7 Hz, 1H), 4.82 (dd, *J* = 3.7, 1.8 Hz, 2H), 2.34 (s, 3H).

¹³C NMR (101 MHz, CDCl₃) δ 166.5, 155.1, 135.5, 134.6, 133.9, 129.8, 129.1, 123.5, 122.3, 120.9, 120.1, 119.9, 118.6, 65.3, 21.1.

HRMS (ESI) *m/z* (M+H)⁺ calculated for C₁₇H₁₅NO₂: 266.1176 observed: 266.1190.

Synthesis of N-(4-methoxyphenyl)-2H-chromene-5-carboxamide **1c**:



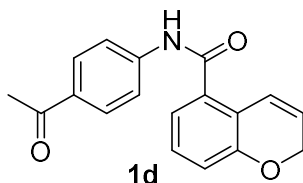
The same general procedure as that for the synthesis of **1a** was followed using 2-H-chromene-5-carboxylic acid (264 mg, 1.5 mmol, 1.00 equiv), oxalyl chloride (381 mg, 3.0 mmol, 2.0 equiv), *p*-anisidine (222 mg, 1.8 mmol, 1.2 equiv), and dmf (2 drops). The compound was purified by silica chromatography (10-40% EtOAc:hexanes) to give the compound **1c** as a white powder (312 mg, 74%) .

¹H NMR (400 MHz, CDCl₃) δ 7.52 (d, *J* = 8.9 Hz, 2H), 7.41 (s, 1H), 7.13 (dd, *J* = 18.5, 7.1 Hz, 2H), 6.91 (d, *J* = 8.8 Hz, 4H), 5.89 (d, *J* = 10.1 Hz, 1H), 4.82 (dd, *J* = 3.7, 1.8 Hz, 2H), 3.82 (s, 3H).

¹³C NMR (101 MHz, CDCl₃) δ 166.5, 156.9, 155.1, 133.9, 131.1, 129.1, 123.5, 122.3, 121.9, 121.0, 119.9, 118.6, 114.5, 65.3, 55.7.

HRMS (ESI) *m/z* (M+H)⁺ calculated for C₁₇H₁₆NO₃: 282.1125 observed: 282.1125.

Synthesis of N-(4-acetylphenyl)-2H-chromene-5-carboxamide **1d**:



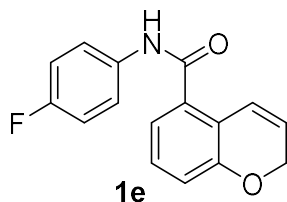
The same general procedure as that for the synthesis of **1a** was followed using 2-H-chromene-5-carboxylic acid (264 mg, 1.5 mmol, 1.00 equiv), oxalyl chloride (381 mg, 3.0 mmol, 2.0 equiv), *p*-acetylaniline (243 mg, 1.8 mmol, 1.2 equiv), and dmf (2 drops). The compound was purified by silica chromatography (10-40% EtOAc:hexanes) to give the compound **1d** as a white powder (264 mg, 60%) .

¹H NMR (400 MHz, CDCl₃) δ 8.01 (d, *J* = 8.7 Hz, 2H), 7.74 (s, 2H), 7.72 (bs, 1H), 7.21 (t, *J* = 7.8 Hz, 1H), 7.17 – 7.11 (m, 1H), 6.97 (d, *J* = 8.0 Hz, 1H), 6.90 (d, *J* = 10.1 Hz, 1H), 5.94 (dt, *J* = 10.1, 3.7 Hz, 1H), 4.86 (dd, *J* = 3.7, 1.9 Hz, 2H), 2.62 (s, 3H).

¹³C NMR (101 MHz, CDCl₃) δ 197.1, 166.7, 155.2, 142.3, 133.4, 133.1, 130.1, 129.2, 123.9, 122.0, 121.1, 119.9, 119.2, 119.1, 65.3, 26.7.

HRMS (ESI) *m/z* (M+H)⁺ calculated for C₁₈H₁₆NO₃: 294.1125 observed: 294.1130.

Synthesis of N-(4-fluorophenyl)-2H-chromene-5-carboxamide **1e**:



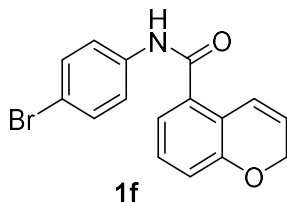
The same general procedure as that for the synthesis of **1a** was followed using 2-H-chromene-5-carboxylic acid (264 mg, 1.5 mmol, 1.00 equiv), oxalyl chloride (381 mg, 3.0 mmol, 2.0 equiv), *p*-fluoroaniline (200 mg, 1.8 mmol, 1.2 equiv), and dmf (2 drops). The compound was purified by silica chromatography (10-40% EtOAc:hexanes) to give the compound **1e** as a white powder (238 mg, 59%).

¹H NMR (400 MHz, CDCl₃) δ 7.62 – 7.55 (m, 2H), 7.15 (t, *J* = 7.8 Hz, 1H), 7.11 – 7.03 (m, 3H), 6.97 – 6.83 (m, 3H), 5.89 (dt, *J* = 10.1, 3.7 Hz, 1H), 4.81 (dd, *J* = 3.7, 1.8 Hz, 2H).

¹³C NMR (101 MHz, CDCl₃) δ 166.6, 159.7 (d, *J* = 244.0 Hz), 155.1, 134.0 (d, *J* = 2.8 Hz), 133.5, 129.1, 123.6, 122.1, 121.9 (d, *J* = 7.9 Hz), 119.9, 118.8, 116.0 (d, *J* = 22.5 Hz), 115.9, 65.2.

HRMS (ESI) *m/z* (M+H)⁺ calculated for C₁₆H₁₃FNO₂: 270.0925 observed: 270.0926.

Synthesis of N-(4-bromophenyl)-2H-chromene-5-carboxamide **1f**:



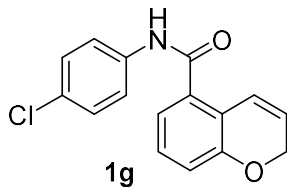
The same general procedure as that for the synthesis of **1a** was followed using 2-H-chromene-5-carboxylic acid (264 mg, 1.5 mmol, 1.00 equiv), oxalyl chloride (381 mg, 3.0 mmol, 2.0 equiv), *p*-bromoaniline (310 mg, 1.8 mmol, 1.2 equiv), and dmf (2 drops). The compound was purified by silica chromatography (10-40% EtOAc:hexanes) to give the compound **1f** as a white powder (205 mg, 62%).

¹H NMR (400 MHz, CDCl₃) δ 7.50 (q, *J* = 8.9, 8.5 Hz, 5H), 7.18 (t, *J* = 7.8 Hz, 1H), 7.10 (d, *J* = 6.8 Hz, 1H), 6.93 (d, *J* = 8.0 Hz, 1H), 6.87 (d, *J* = 10.1 Hz, 1H), 5.91 (dt, *J* = 10.1, 3.7 Hz, 1H), 4.83 (dd, *J* = 3.7, 1.9 Hz, 2H).

¹³C NMR (101 MHz, CDCl₃) δ 166.5, 155.1, 137.1, 132.3, 129.1, 123.8, 122.1, 121.6, 121.0, 120.3, 119.8, 118.9, 117.5, 65.3.

HRMS (ESI) *m/z* (M+H)⁺ calculated for C₁₆H₁₃NO₂Br: 330.0124 observed: 330.0133.

Synthesis of N-(4-chlorophenyl)-2H-chromene-5-carboxamide **1g**:



The same general procedure as that for the synthesis of **1a** was followed using 2-H-chromene-5-carboxylic acid (264 mg, 1.5 mmol, 1.00 equiv), oxalyl chloride (381 mg, 3.0 mmol, 2.0 equiv),

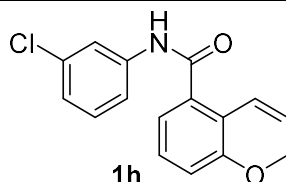
p-chloroaniline (230 mg, 1.8 mmol, 1.2 equiv), and dmf (2 drops). The compound was purified by silica chromatography (10-40% EtOAc:hexanes) to give the compound **1g** as a white powder (236 mg, 55%).

¹H NMR (400 MHz, CDCl₃) δ 7.57 (d, *J* = 8.7 Hz, 3H), 7.33 (d, *J* = 8.8 Hz, 2H), 7.16 (t, *J* = 7.8 Hz, 1H), 7.09 (d, *J* = 7.0 Hz, 1H), 6.92 (d, *J* = 8.0 Hz, 1H), 6.85 (d, *J* = 10.1 Hz, 1H), 5.89 (dt, *J* = 10.1, 3.7 Hz, 1H), 4.82 (dd, *J* = 3.7, 1.8 Hz, 2H).

¹³C NMR (101 MHz, CDCl₃) δ 166.6, 155.1, 136.6, 133.4, 129.8, 129.3, 129.1, 123.7, 122.1, 121.3, 121.0, 119.9, 118.9, 65.2.

HRMS (ESI) *m/z* (M+H)⁺ calculated for C₁₆H₁₃NO₂Cl: 286.0629 observed: 286.0633.

Synthesis of N-(3-chlorophenyl)-2H-chromene-5-carboxamide **1h**:



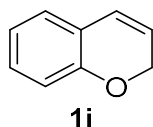
The same general procedure as that for the synthesis of **1a** was followed using 2-H-chromene-5-carboxylic acid (264 mg, 1.5 mmol, 1.00 equiv), oxalyl chloride (381 mg, 3.0 mmol, 2.0 equiv), *m*-chloroaniline (230 mg, 1.8 mmol, 1.2 equiv), and dmf (2 drops). The compound was purified by silica chromatography (10-40% EtOAc:hexanes) to give the compound **1h** as a white powder (194 mg, 50%).

¹H NMR (400 MHz, CDCl₃) δ 7.76 (s, 1H), 7.58 (s, 1H), 7.44 (d, *J* = 7.9 Hz, 1H), 7.28 (d, *J* = 8.1 Hz, 1H), 7.20 – 7.11 (m, 2H), 7.08 (dd, *J* = 7.6, 1.1 Hz, 1H), 6.97 – 6.89 (m, 1H), 6.86 (d, *J* = 10.1 Hz, 1H), 5.90 (dt, *J* = 10.1, 3.7 Hz, 1H), 4.82 (dd, *J* = 3.7, 1.9 Hz, 2H).

¹³C NMR (101 MHz, CDCl₃) δ 166.6, 155.1, 139.1, 135.0, 133.3, 130.3, 129.1, 124.9, 123.8, 122.0, 121.0, 120.1, 119.9, 119.0, 118.0, 65.3.

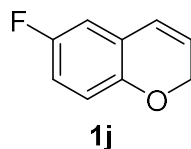
HRMS (ESI) *m/z* (M+H)⁺ calculated for C₁₆H₁₃NO₂Cl: 286.0629 observed: 286.0635.

Synthesis of 2H-chromene **1i**:



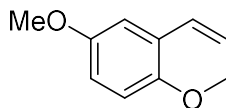
Compound was prepared according to literature procedure.⁷⁶ Analytical data matches the literature.⁷⁷

Synthesis of 6-fluoro-2H-chromene **1j**:



Compound was prepared according to literature procedure. Analytical data matches the literature.⁷⁶

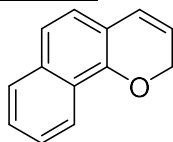
Synthesis of 6-methoxy-2H-chromene **1k**:



1k

Compound was prepared according to literature procedure. Analytical data matches the literature.⁷⁶

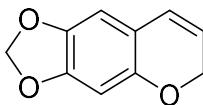
Synthesis of 6H-[1,3]dioxolo[4,5-g]chromene **1l**:



3

Compound **1l** was prepared according to literature procedure. Analytical data matches the literature.⁷⁶

Synthesis of 2H-benzo[h]chromene **1m**:



4

Compound **1m** was prepared according to literature procedure. Analytical data matches the literature.⁷⁶

1.4.3. Optimization, Preparation, and Characterization of Arylfluorination Products

Procedure A: Synthesis of racemic 1,3-arylfluorination products

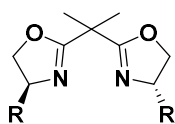
Preparation of the catalyst (10 mol %):

Pd(OAc)₂ (2.2 mg, 0.010 mmol, 0.10 eq) was added to a solution of 4,4'-di-*tert*-butyl-2,2'-bipyridine (2.9 mg, 0.011 mmol, 0.11 eq) in CH₂Cl₂ (1 ml) and the reaction mixture was stirred for 30 min.

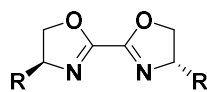
The catalyst solution was then added to a solution of chromene **1** (25.0 mg, 0.100 mmol, 1.00 eq), aryl boronic acid (0.200 mmol, 2.00 eq), bis(2-ethylhexyl) hydrogen phosphate (12.8 mg, 0.040 mmol, 0.40 eq), Selectfluor (71.0 mg, 0.200 mmol, 2.00 eq) and *tert*-butyl catechol (0.6 mg, 0.004 mmol, 0.04 eq) in CH₂Cl₂ (0.8 ml)/water (0.2 ml). The reaction mixture was vigorously stirred for 24 h. The reaction mixture was diluted with CH₂Cl₂, dried with Na₂SO₄, filtered through celite, and concentrated under reduce pressure. The residue was purified by column chromatography to give the fluorinated products **2-5**.

Optimization of 1,3- asymmetric reaction conditions and 2,1- reaction conditions

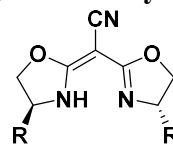
Chiral ligand classes surveyed for enantioselective 1,3-fluoroarylation



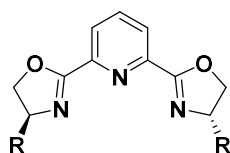
Trace Conversion



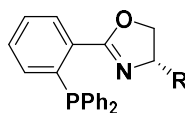
Trace Conversion



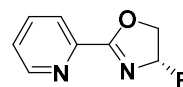
Decomposition
and 1,2 product



Trace Conversion

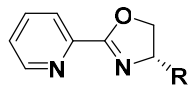


No Conversion

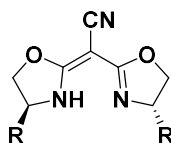


1:1 mixture
85% ee

Ligands surveyed that afforded 1,2-fluoroarylation product



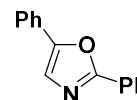
Formed as side
product



Decomposition
and 1,2 product

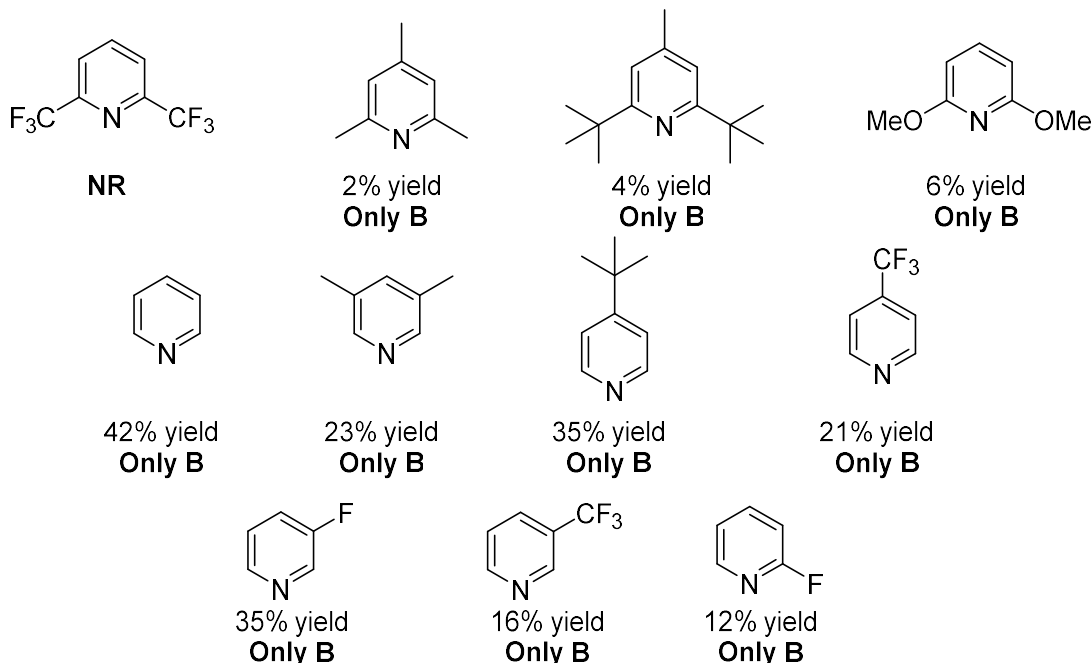
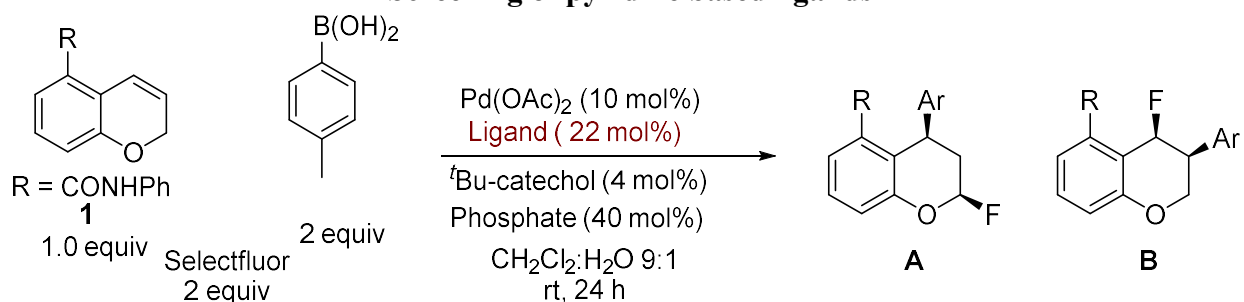


1,2 product formed
exclusively



1,2 product formed
exclusively

Screening of pyridine based ligands



Procedure B: Synthesis of racemic 2,1-arylfurorination products

Preparation of the catalyst (10 mol %):

Pd(OAc)_2 (2.2 mg, 0.010 mmol, 0.10 eq) was added to a solution of 2,5-diphenyloxazole (4.9 mg, 0.022 mmol) in CH_2Cl_2 (1 ml) and the reaction mixture was stirred for 30 min.

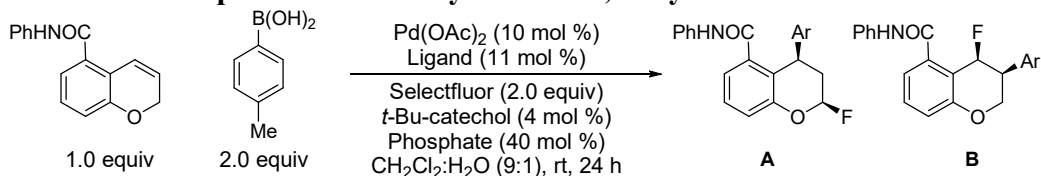
The catalyst solution was then added to a solution of chromene **1** (25.0 mg, 0.100 mmol, 1.00 eq), aryl boronic acid (0.200 mmol, 2.00 eq), bis(2-ethylhexyl) hydrogen phosphate (12.8 mg, 0.040 mmol, 0.40 eq), Selectfluor (71.0 mg, 0.200 mmol, 2.00 eq) and *tert*-butyl catechol (0.6 mg, 0.004 mmol, 0.04 eq) in CH_2Cl_2 (0.8 ml)/water (0.2 ml). The reaction mixture was vigorously stirred for 24 h. The reaction mixture was diluted with CH_2Cl_2 , dried with Na_2SO_4 , filtered through celite, and concentrated under reduced pressure. The residue was purified by column chromatography to give the fluorinated products **9**.

Procedure C: synthesis of enantioenriched 1,3-arylfurorination products

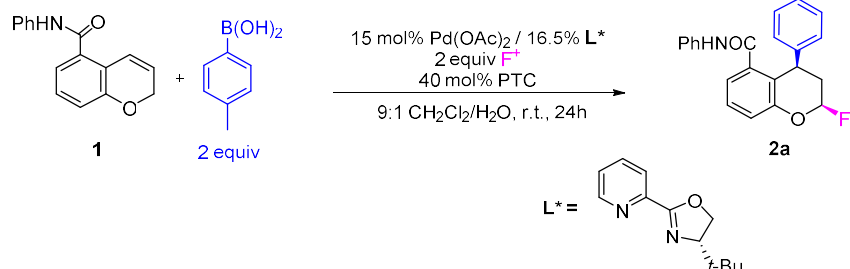
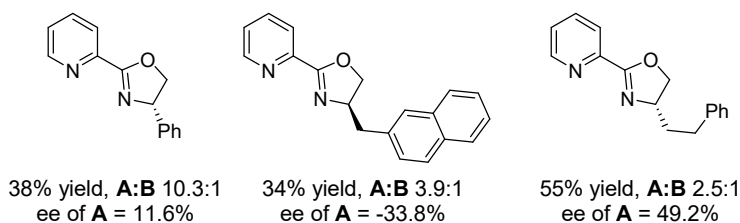
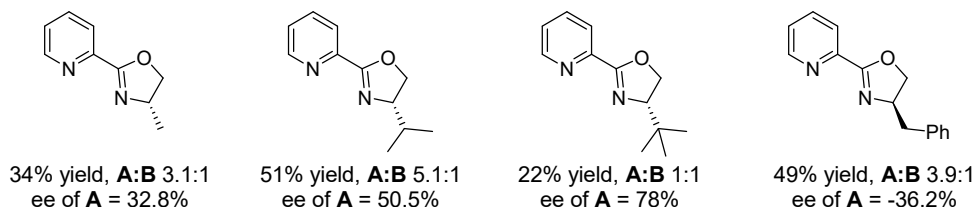
The palladium complex **6** was prepared as previously reported in the literature.⁴⁸

To a round bottom flask, chromene **1** (25.0 mg, 0.100 mmol, 1.00 eq), aryl boronic acid (0.150 mmol, 1.50 eq), bis(2-ethylhexyl) hydrogen phosphate (12.8 mg, 0.040 mmol, 0.40 eq), Selectfluor (71.0 mg, 0.200 mmol, 2.00 eq), *tert*-butyl catechol (0.6 mg, 0.004 mmol, 0.04 eq), and palladium complex **5** (6.8 mg, 0.0150 mmol, 0.15 eq) were added and placed under N₂. To the flask, 1,2-dichloroethane (1.5 ml)/water (0.5 ml) was added. The reaction mixture was vigorously stirred for 24 h. The reaction mixture was diluted with CH₂Cl₂, dried with Na₂SO₄, filtered through celite, and concentrated under reduce pressure. The residue was purified by column chromatography to give the fluorinated product. The enantiomeric excess was determined by chiral HPLC analysis.

Optimization of Asymmetric 1,3-arylfluorination



PyrOx Ligand Screen

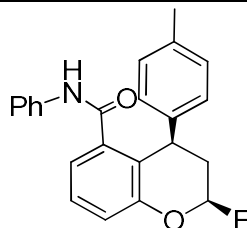


Entry	Solvent	Additive	1,3:1,2 ratio ^{ab}	% ee ^c
1	DCM/H ₂ O 9:1	-	1:1	85%
2	DCM/H ₂ O 9:1	2 eq KF	5:1	80%
3	DCM/H ₂ O 9:1	1 eq KF	5:1	86%

4	DCM/H ₂ O 9:1	0.5 eq KF	2:1	-
5	DCM/H ₂ O 9:1	1 eq CsF	3:1 ^d	-
6	DCM/H ₂ O 9:1	1 eq NaF	4:1	86%
7	DCM/H ₂ O 9:1	1 eq NaF	>10:1 ^e	-
8	DCE/H ₂ O 9:1	1 eq NaF	4:1	89%
9	CHCl ₃ /H ₂ O 9:1	1 eq NaF	1:1	-
10	DCE/H ₂ O 3:1	1 eq NaF	5:1	89%
11	DCE/H ₂ O 3:1	1.5 eq NaF	5:1 ^f	90%

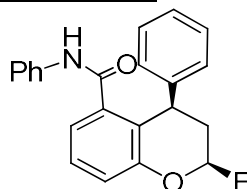
Standard conditions: 1 equiv Chromene, 2 equiv boronic acid, 15 mol% Pd(OAc)₂, 16.5 mol% PyOx, 2 equiv Selectfluor, 40 mol% bis(2-ethylhexyl)hydrogenphosphate, 4 mol% *t*-butyl catechol, CH₂Cl₂/H₂O 9:1, N₂ atmosphere, 23⁰ C, 24h.; (a) Reactions reach full conversion of the starting material unless otherwise noted. (b) Determined by ¹H and ¹⁹F NMR; (c) Determined by Chiral HPLC; (d) Large amount of side product formation; (e) Reaction run at 0⁰ C, trace conversion. (f) 1.5 equiv boronic acid, less side product formation.

2-fluoro-N-phenyl-4-(p-tolyl)chroman-5-carboxamide 2a:



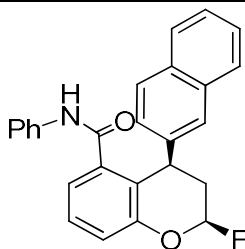
- ¹H NMR (400 MHz, CDCl₃) δ 7.36 (t, *J* = 7.8 Hz, 1H), 7.25 - 7.14 (m, 4H), 7.08 – 6.91 (m, 7H), 6.06 (d, *J* = 55.8 Hz, 1H), 4.75 – 4.67 (m, 1H), 2.58 – 2.33 (m, 2H), 2.26 (s, 3H).
- ¹⁹F NMR (377 MHz, CDCl₃): -118.4
- ¹³C NMR (101 MHz, CDCl₃) δ 166.9, 151.4, 141.4, 138.3, 137.1, 136.3, 129.3, 128.7, 128.7, 128.1, 128.1, 124.5, 121.7, 120.9, 120.0, 119.7, 104.9 (d, *J* = 221.5), 34.0, 33.8, 21.0.
- HRMS (ESI): M+H⁺ found 362.1550; C₂₃H₂₁FNO₂ requires 362.1551

2-fluoro-N,4-diphenylchroman-5-carboxamide 2b:



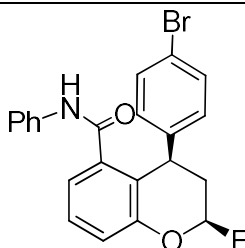
- **¹H NMR** (400 MHz, CDCl₃) δ 7.37 (t, *J* = 7.8 Hz, 1H), 7.26 – 7.00 (m, 10H), 6.99 – 6.91 (m, 2H), 6.06 (d, *J* = 55.7 Hz, 1H), 4.78 (d, *J* = 5.6 Hz, 1H), 2.60 – 2.37 (m, 2H).
- **¹⁹F NMR** (377 MHz, CDCl₃): -118.2
- **¹³C NMR** (101 MHz, CDCl₃) δ 167.0, 151.6, 144.6, 138.3, 137.1, 128.9, 128.8, 128.8, 128.3, 126.8, 124.7, 121.8, 120.8, 120.3, 119.9, 104.9 (d, *J* = 221.7), 34.2, 34.0, 33.8.
- **HRMS** (ESI): M+H⁺ found 348.1392; C₂₂H₁₉FNO₂ requires 348.1394

2-fluoro-4-(naphthalen-2-yl)-N-phenylchroman-5-carboxamide **2c**:



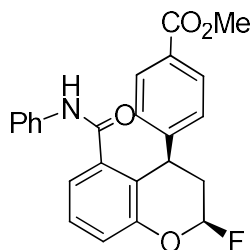
- **¹H NMR** (600 MHz, CDCl₃) δ 7.75 (d, *J* = 7.7 Hz, 1H), 7.72 (d, *J* = 8.5 Hz, 1H), 7.63 (d, *J* = 7.7 Hz, 1H), 7.51 (s, 1H), 7.44 – 7.37 (m, 3H), 7.29 – 7.27 (m, 1H), 7.25 – 7.21 (m, 2H), 6.98 (t, *J* = 7.6 Hz, 2H), 6.94 – 6.88 (m, 2H), 6.66 (d, *J* = 7.8 Hz, 2H), 6.09 (d, *J* = 55.6 Hz, 1H), 4.94 (d, *J* = 6.8 Hz, 1H), 2.67 – 2.48 (m, 2H).
- **¹⁹F NMR** (377 MHz, CDCl₃): -118.3
- **¹³C NMR** (151 MHz, CDCl₃) δ 167.1, 151.6, 141.9, 138.4, 136.8, 133.5, 132.4, 129.0, 128.6, 128.4, 127.8, 127.6, 127.1, 126.6, 126.3, 125.9, 124.6, 121.7, 121.1, 120.2, 119.9, 104.9 (d, *J* = 221.6), 34.4, 33.9, 33.7.
- **HRMS** (ESI): M+H⁺ found 398.1549; C₂₆H₂₁FNO₂ requires 398.1551

4-(4-bromophenyl)-2-fluoro-N-phenylchroman-5-carboxamide **2d**:



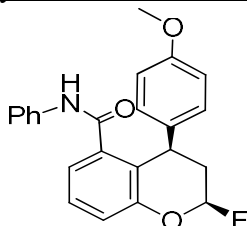
- **¹H NMR** (400 MHz, CD₂Cl₂) δ 7.38 (t, *J* = 7.9 Hz, 1H), 7.33 – 7.15 (m, 6H), 7.14 – 7.02 (m, 3H), 6.96 (d, *J* = 8.2 Hz, 2H), 6.06 (d, *J* = 55.3 Hz, 1H), 4.85 (d, *J* = 6.1 Hz, 1H), 2.58 – 2.42 (m, 2H).
- **¹⁹F NMR** (377 MHz, CDCl₃): -118.2
- **¹³C NMR** (101 MHz, CD₂Cl₂) δ 166.7, 151.8, 144.1, 138.1, 137.6, 131.5, 130.5, 129.2, 129.1, 125.1, 121.4, 121.3, 120.7, 120.4, 120.2, 105.3 (d, *J* = 221.2 Hz), 33.7 (d, *J* = 21.2 Hz), 33.3.
- **HRMS** (ESI): M+H⁺ found 426.0500; C₂₂H₁₈BrFNO₂ requires 426.0499

methyl 4-(2-fluoro-5-(phenylcarbamoyl)chroman-4-yl)benzoate **2e**:



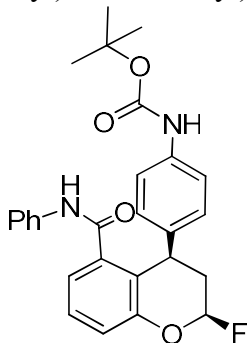
- **¹H NMR** (400 MHz, CD₂Cl₂) δ 7.87 (d, *J* = 8.4 Hz, 2H), 7.39 (t, *J* = 7.8 Hz, 1H), 7.26 – 7.13 (m, 6H), 7.08 – 7.01 (m, 4H), 6.96 (s, 1H), 6.06 (dt, *J* = 55.2, 2.3 Hz, 1H), 4.98 (dd, *J* = 7.1, 2.8 Hz, 1H), 3.82 (s, 3H), 2.60 – 2.47 (m, 2H).
- **¹⁹F NMR** (377 MHz, CDCl₃): -118.2
- **¹³C NMR** (101 MHz, CDCl₃) 167.0, 166.9, 151.7, 149.9, 138.0, 137.0, 129.9, 129.2, 129.0, 128.6, 128.5, 125.0, 121.4, 120.8, 120.4, 120.2, 104.8 (d, *J* = 223.2 Hz), 52.2, 33.8, 33.6 (d, *J* = 21.2 Hz).
- **HRMS** (ESI): M+H⁺ found 406.1446 ; C₂₄H₂₁FNO₄ requires 406.1449.

2-fluoro-4-(4-methoxyphenyl)-N-phenylchromane-5-carboxamide 2f:



- **¹H NMR** (500 MHz, CDCl₃) δ 7.34 (t, *J* = 7.8 Hz, 1H), 7.24 – 7.18 (m, 3H), 7.17 – 7.13 (m, 1H), 7.09 – 6.97 (m, 5H), 6.92 (s, 1H), 6.73 (d, *J* = 8.7 Hz, 2H), 6.06 (dt, *J* = 55.8, 2.4 Hz, 1H), 4.70 (t, *J* = 4.7 Hz, 1H), 3.69 (s, 3H), 2.53 – 2.36 (m, 2H).
- **¹⁹F NMR** (377 MHz, CDCl₃): -118.0
- **¹³C NMR** (101 MHz, CD₂Cl₂) δ 167.0, 158.6, 151.8, 138.5, 137.8, 136.9, 129.6, 129.0, 128.9, 124.8, 121.8, 121.7, 120.4, 119.9, 114.0, 105.5 (d, *J* = 221.2 Hz), 55.5, 34.2 (d, *J* = 20.2 Hz), 33.4.
- **HRMS**(ESI): M+H⁺ found 378.1497; C₂₃H₂₁FNO₃ requires 378.1500.

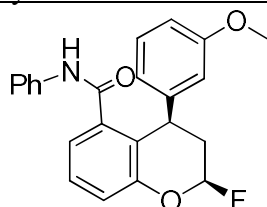
tert-butyl (4-(2-fluoro-5-(phenylcarbamoyl)chroman-4-yl)phenyl)carbamate 2g:



- **¹H NMR** (500 MHz, CDCl₃) δ 7.34 (t, *J* = 7.9 Hz, 1H), 7.23 – 7.12 (m, 6H), 7.08 – 7.03 (m, 3H), 7.00 (d, *J* = 8.2 Hz, 2H), 6.93 (s, 1H), 6.35 (s, 1H), 6.04 (d, *J* = 55.5 Hz, 1H), 4.72 (t, *J* = 4.8 Hz, 1H), 2.54 – 2.34 (m, 2H), 1.50 (s, 9H).

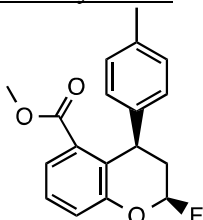
- **¹⁹F NMR** (377 MHz, CDCl₃): -118.1
- **¹³C NMR** (126 MHz, CDCl₃) δ 167.1, 152.8, 151.6, 139.2, 138.3, 137.2, 137.1, 129.1, 129.1, 128.9, 124.8, 121.7, 121.3, 120.4, 119.9, 118.8, 105.0 (d, *J* = 221.8 Hz), 34.0 (d, *J* = 20.2 Hz), 33.6, 28.5.
- **HRMS** (ESI): M+H⁺ found 463.2033; C₂₇H₂₈FN₂O₄ requires 463.2028.

2-fluoro-4-(3-methoxyphenyl)-N-phenylchromane-5-carboxamide **2h**:



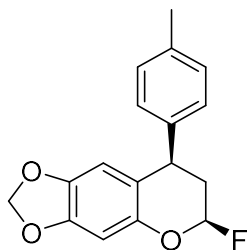
- **¹H NMR** (600 MHz, CDCl₃) δ 7.35 (t, *J* = 7.9 Hz, 1H), 7.24 – 7.18 (m, 3H), 7.15 (ddd, *J* = 7.9, 4.4, 3.2 Hz, 2H), 7.07 – 7.03 (m, 1H), 7.01 (d, *J* = 7.6 Hz, 1H), 6.98 (s, 1H), 6.05 (dt, *J* = 55.9, 2.3 Hz, 1H), 4.71 (d, *J* = 6.7 Hz, 1H), 3.66 (s, 3H), 2.61 – 2.34 (m, 2H).
- **¹⁹F NMR** (377 MHz, CDCl₃): -117.3
- **¹³C NMR** (151 MHz, CDCl₃): δ 167.1, 160.0, 151.6, 146.3, 138.5, 137.3, 129.8, 129.0, 128.9, 124.8, 121.9, 120.8, 120.2, 119.9, 114.8, 111.9, 104.9 (d, *J* = 222.0 Hz), 55.4, 34.3, 33.9 (d, *J* = 19.6 Hz).
- **HRMS** (ESI): M+H⁺ found 378.1492; C₂₃H₂₁FNO₃ requires 378.1500.

methyl 2-fluoro-4-(p-tolyl)chromane-5-carboxylate **3**:



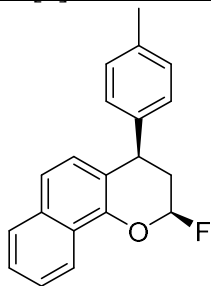
- **¹H NMR** (600 MHz, CDCl₃) δ 7.54 (d, *J* = 7.6 Hz, 1H), 7.32 (t, *J* = 7.9 Hz, 1H), 7.20 (d, *J* = 8.3 Hz, 1H), 7.01 (d, *J* = 7.7 Hz, 2H), 6.88 (d, *J* = 7.7 Hz, 2H), 6.03 (dt, *J* = 55.6, 2.1 Hz, 1H), 5.08 (d, *J* = 7.5 Hz, 1H), 3.54 (s, 3H), 2.59 – 2.38 (m, 3H), 2.27 (s, 3H).
- **¹⁹F NMR** (377 MHz, CDCl₃): -119.2
- **¹³C NMR** (151 MHz, CDCl₃) δ 167.6, 151.8, 142.1, 135.6, 131.7, 129.0, 128.2, 127.8, 125.0, 124.2, 121.7, 104.9 (d, *J* = 222.0 Hz), 52.11, 34.3 (d, *J* = 19.6 Hz), 33.9, 21.25.
- **HRMS** (ESI): M+Na⁺ found 323.1051 ; C₁₈H₁₇FO₃Na requires 323.1054.

6-fluoro-8-(p-tolyl)-7,8-dihydro-6H-[1,3]dioxolo[4,5-g]chromene **4**:



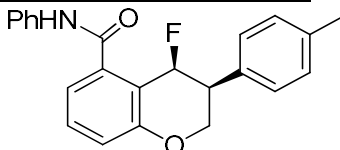
- **¹H NMR** (500 MHz, CD₂Cl₂) δ 7.10 (d, *J* = 7.8 Hz, 2H), 7.02 (d, *J* = 7.9 Hz, 2H), 6.51 (s, 1H), 6.31 (d, *J* = 0.8 Hz, 1H), 5.99 (ddd, *J* = 56.1, 4.1, 2.7 Hz, 1H), 5.89 (d, *J* = 1.4 Hz, 2H), 4.07 (t, *J* = 6.2 Hz, 1H), 2.53 – 2.32 (m, 2H), 2.31 (s, 3H).
- **¹⁹F NMR** (377 MHz, CD₂Cl₂): -120.5
- **¹³C NMR** (126 MHz, CD₂Cl₂) δ 147.7, 146.1, 143.2, 141.7, 136.6, 129.4, 128.51 (d, *J* = 2.5 Hz), 116.5, 108.8, 106.1 (d, *J* = 220.5 Hz), 101.8, 99.0, 37.2, 35.2 (d, *J* = 21.4 Hz), 21.1.
- **HRMS** (EI): M⁺ found 286.1007 ; C₁₇H₁₅FO₃ requires 286.1005.

2-fluoro-4-(p-tolyl)-3,4-dihydro-2H-benzo[h]chromene 5:



- **¹H NMR** (500 MHz, CD₂Cl₂) δ 8.31 – 8.21 (m, 1H), 7.81 (dd, *J* = 7.2, 2.1 Hz, 1H), 7.53 (ddt, *J* = 10.7, 7.0, 3.5 Hz, 2H), 7.44 (d, *J* = 8.5 Hz, 1H), 7.10 (d, *J* = 7.8 Hz, 2H), 7.02 (m, 3H), 6.36 – 6.17 (m, 1H), 4.34 (dd, *J* = 7.4, 4.3 Hz, 1H), 2.73 – 2.50 (m, 2H), 2.31 (s, 3H).
- **¹⁹F NMR** (377 MHz, CD₂Cl₂): -121.4
- **¹³C NMR** (126 MHz, CD₂Cl₂) δ 146.4, 141.8, 136.5, 134.0, 129.3, 128.7, 128.0, 127.9, 126.7, 126.3, 125.2, 121.9, 121.7, 118.2, 106.1 (d, *J* = 219.2 Hz), 37.3, 35.1 (d, *J* = 20.2 Hz), 21.1.
- **HRMS** (EI): M⁺ found 292.1264 ; C₂₀H₁₇FO requires 292.1263.

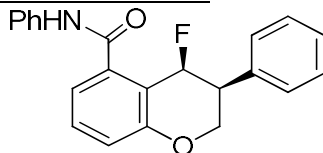
4-fluoro-N-phenyl-3-(p-tolyl)chroman-5-carboxamide 10a:



- **¹H NMR** (500 MHz, CDCl₃) δ 8.01 (br d, *J* = 5.6 Hz, 1H), 7.60 (d, *J* = 7.6 Hz, 2H), 7.44 (td, *J* = 8.2, 2.1 Hz, 1H), 7.36 – 7.31 (m, 3H), 7.22 – 7.16 (m, 4H), 7.14 (dd, *J* = 10.6, 4.2 Hz, 1H), 7.09 (d, *J* = 8.3 Hz, 1H), 5.96 (d, *J* = 50.6 Hz, 1H), 4.63 (ddd, *J* = 12.8, 10.7, 1.9 Hz, 1H), 4.40 (dd, *J* = 10.6, 4.1 Hz, 1H), 3.34 (dddd, *J* = 33.2, 12.9, 3.9, 2.1 Hz, 1H), 2.36 (s, 3H).
- **¹⁹F NMR** (377 MHz, CDCl₃): -158.1
- **¹³C NMR** (126 MHz, CDCl₃) δ 166.1, 139.1, 137.7, 137.6, 133.0, 131.8, 129.5, 129.4, 129.2, 129.1, 128.4, 128.4, 125.1, 124.7, 121.0, 120.9, 120.0, 120.0, 119.9, 84.7 (d, *J* = 172.0), 64.1 (d, *J* = 3.5), 42.6 (d, *J* = 19.6), 21.1.

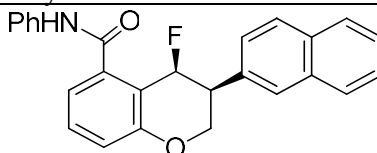
- **HRMS** (EI): M⁺ found 361.1480, C₂₃H₂₀FNO₂ requires 361.1481

4-fluoro-N,3-diphenylchroman-5-carboxamide **10b**:



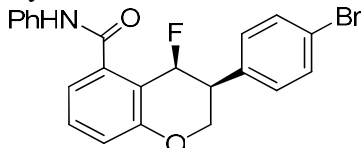
- **¹H NMR** (600 MHz, CDCl₃) δ 8.03 (br s, 1H), 7.61 (d, *J* = 7.8 Hz, 2H), 7.45 (td, *J* = 8.2, 1.7 Hz, 1H), 7.40 – 7.30 (m, 8H), 7.14 (t, *J* = 7.4 Hz, 1H), 7.10 (d, *J* = 8.3 Hz, 1H), 6.00 (d, *J* = 50.6 Hz, 1H), 4.70 – 4.62 (m, 1H), 4.43 (dd, *J* = 10.6, 4.0 Hz, 1H), 3.37 (dd, *J* = 33.1, 11.5 Hz, 1H).
- **¹⁹F NMR** (377 MHz, CDCl₃): -158.3
- **¹³C NMR** (151 MHz, CDCl₃) δ 166.2, 155.1, 155.1, 139.2, 137.8, 136.2, 131.9, 131.8, 129.2, 128.9, 128.6, 128.6, 128.0, 124.8, 121.0, 121.0, 120.1, 84.6 (d, *J* = 171.8), 64.1 (d, *J* = 2.7), 43.1 (d, *J* = 19.3).
- **HRMS** (EI): M⁺ found 347.1319, C₂₂H₁₈FNO₂ requires 347.1322

4-fluoro-3-(naphthalen-2-yl)-N-phenylchroman-5-carboxamide **10c**:



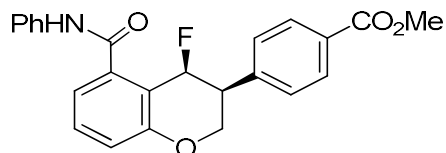
- **¹H NMR** (400 MHz, CDCl₃) δ 8.06 (br s, 1H), 7.89 – 7.81 (m, 3H), 7.77 (s, 1H), 7.60 (d, *J* = 7.9 Hz, 2H), 7.53 – 7.40 (m, 4H), 7.32 (dd, *J* = 15.2, 7.5 Hz, 3H), 7.17 – 7.08 (m, 2H), 6.09 (d, *J* = 50.6 Hz, 1H), 4.77 (t, *J* = 11.7 Hz, 1H), 4.53 (dd, *J* = 10.6, 3.7 Hz, 1H), 3.53 (dd, *J* = 33.0, 11.8 Hz, 1H).
- **¹⁹F NMR** (377 MHz, CDCl₃): -157.8
- **¹³C NMR** (151 MHz, CDCl₃) δ 166.2, 155.1, 155.1, 139.2, 137.8, 133.6, 133.5, 132.9, 131.9, 131.9, 129.2, 128.6, 128.0, 127.8, 127.5, 127.5, 126.5, 126.3, 124.8, 121.1, 120.1, 116.5, 116.4, 84.6 (d, *J* = 171.9), 64.2, 43.2 (d, *J* = 19.4).
- **HRMS** (ESI): M+H⁺ found 398.1549; C₂₆H₂₁FNO₂ requires 398.1551

3-(4-bromophenyl)-4-fluoro-N-phenylchroman-5-carboxamide **10d**:



- **¹H NMR** (400 MHz, CD₂Cl₂) δ 7.93 (s, 1H), 7.58 (d, *J* = 7.5 Hz, 2H), 7.53 – 7.42 (m, 3H), 7.40 – 7.27 (m, 3H), 7.22 (d, *J* = 8.2 Hz, 2H), 7.17 – 7.09 (m, 2H), 6.00 (d, *J* = 50.7 Hz, 1H), 4.58 (t, *J* = 11.5 Hz, 1H), 4.39 (d, *J* = 9.7 Hz, 1H), 3.40 (dd, *J* = 32.4, 11.8 Hz, 1H).
- **¹⁹F NMR** (377 MHz, CDCl₃): -158.7
- **¹³C NMR** (101 MHz, CD₂Cl₂) δ 166.2, 155.3, 139.3, 138.2, 135.8, 132.1, 132.0, 131.7, 130.7, 129.4, 125.0, 122.0, 120.9, 120.2, 116.7 (d, *J* = 19.2 Hz), 84.3 (d, *J* = 172.7 Hz), 64.1, 42.8 (d, *J* = 20.2 Hz).
- **HRMS** (ESI): M+H⁺ found 426.0500; C₂₂H₁₈BrFNO₂ requires 426.0499

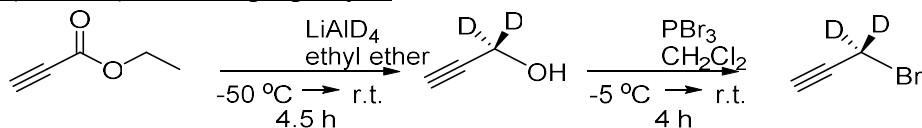
methyl 4-(4-fluoro-5-(phenylcarbamoyl)chroman-3-yl)benzoate 10e:



- **¹H NMR** (400 MHz, CD₂Cl₂) δ 8.01 (d, *J* = 8.4 Hz, 2H), 7.93 (bs, 1H), 7.58 (d, *J* = 7.8 Hz, 2H), 7.50 – 7.39 (m, 3H), 7.35 – 7.26 (m, 3H), 7.12 (dd, *J* = 18.8, 7.9 Hz, 2H), 6.07 (d, *J* = 50.7 Hz, 1H), 4.64 (t, *J* = 11.8 Hz, 1H), 4.44 (dd, *J* = 10.6, 3.4 Hz, 1H), 3.88 (s, 3H), 3.47 (dd, *J* = 32.3, 12.3 Hz, 1H).
- **¹⁹F NMR** (377 MHz, CDCl₃): -158.8
- **¹³C NMR** (101 MHz, CD₂Cl₂) δ 166.9, 166.2, 155.4, 141.8, 139.3, 138.2, 132.1, 130.1, 129.4, 129.0, 125.0, 120.9, 120.2, 120.1, 116.7 (d, *J* = 19.2 Hz), 84.2 (d, *J* = 172.7 Hz), 64.1, 52.4, 43.3 (d, *J* = 19.2 Hz).
- **HRMS** (ESI): M+H⁺ found 406.1445 ; C₂₄H₂₁FNO₄ requires 406.1449.

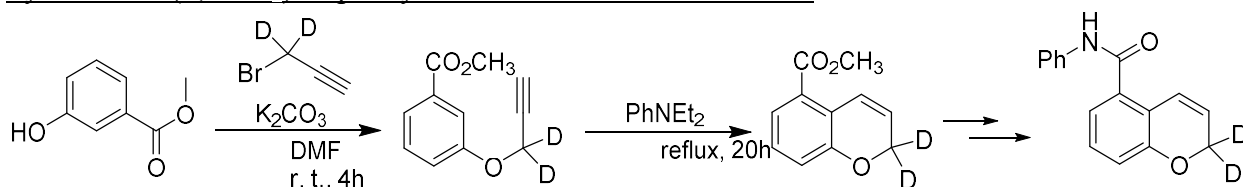
1.4.4. Preparation and Characterization of Deuterated Substrate

Synthesis of (1,1-2H₂)-1-bromoprop-2-yne



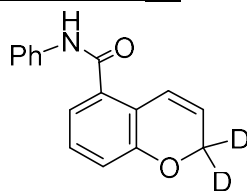
The deuterio alkyne was synthesized according to a literature report.⁷⁸

Synthesis of (2,2-2H₂)-N-phenyl-2H-chromene-5-carboxamide



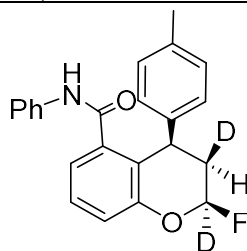
The deuterated chromene was synthesized via an analogous procedure as the non-deuterated substrate using the d₂-propargyl bromide.

N-phenyl-2H-chromene-2,2-d₂-5-carboxamide **d₂-1**:



- **¹H NMR** (400 MHz, CHCl₃) δ 7.61 (d, *J* = 8.1 Hz, 3H), 7.37 (t, *J* = 7.8 Hz, 2H), 7.21 – 7.06 (m, 3H), 6.89 (dd, *J* = 12.1, 9.0 Hz, 2H), 5.87 (d, *J* = 10.1 Hz, 1H).
- **¹³C NMR** (101 MHz, CDCl₃) δ 166.6, 155.0, 138.1, 133.8, 129.3, 129.0, 124.9, 123.3, 122.3, 120.9, 120.1, 119.9, 118.7.
- **HRMS** (ESI): M+H⁺ found 254.1146; C₁₆H₁₂²H₂NO₂ requires 254.1145.

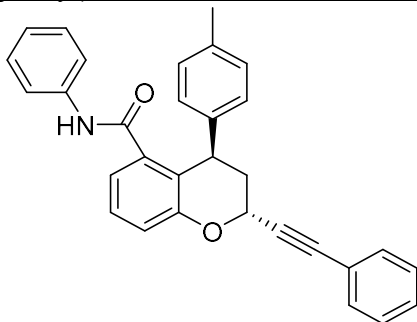
2-fluoro-N-phenyl-4-(p-tolyl)chromane-2,3-d₂-5-carboxamide **d₂-2a**:



- **¹H NMR** (500 MHz, CDCl₃) δ 7.35 (t, *J* = 7.9 Hz, 1H), 7.19 (m, 4H), 7.04 (m, 3H), 7.00 – 6.94 (m, 4H), 6.92 (s, 1H), 4.69 (d, *J* = 7.5 Hz, 1H), 2.42 (dd, *J* = 38.4, 7.6 Hz, 1H), 2.25 (s, 3H).
- **¹⁹F NMR** (377 MHz, CDCl₃): -118.5
- **¹³C NMR** (126 MHz, CDCl₃) δ 167.1, 151.6, 141.6, 138.4, 137.3, 136.5, 129.5, 128.9, 128.8, 128.3, 124.7, 121.9, 121.1, 120.2, 119.8, 33.9, 21.2.
- **HRMS** (ESI): M+H⁺ found 364.1675; C₂₃H₁₉²H₂FNO₂ requires 364.1676.

1.4.5. Preparation and Characterization Derivatization Products

N-phenyl-2-(phenylethynyl)-4-(p-tolyl)chromane-5-carboxamide 8:



Procedure:

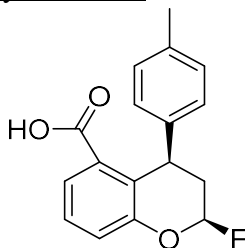
An adapted procedure from the literature was used.⁴⁹ 2-pyranyl fluoride **2a** (17.8 mg, 0.050 mmol, 1.0 eq) and trifluoroborate salt **7** (12.5 mg, 0.060 mmol, 1.2 eq) were added to a 1 dram vial with a septum cap and placed under an atmosphere of N₂. The solids were dissolved in 0.3 mL of dry acetonitrile and stirred. To the vial, boron trifluoride etherate (8 μL, 0.065 mmol, 1.3 eq) was added via syringe. A yellow solution resulted. The solution was stirred for 20 minutes. The contents of the vial were diluted with CH₂Cl₂ and washed 2 times with a saturated solution of NaHCO₃. The organic layer was separated, dried over Na₂SO₄, and concentrated. The crude solid was purified by silica chromatography (15:1 pentane/ ethyl acetate) to afford **8** as a colorless powder (13 mg, 59%).

• **¹H NMR** (600 MHz, CDCl₃) δ 7.44 (dd, *J* = 7.9, 1.7 Hz, 2H), 7.35 – 7.27 (m, 4H), 7.20 (dd, *J* = 8.4, 7.3 Hz, 2H), 7.14 (d, *J* = 8.0 Hz, 2H), 7.10 (d, *J* = 7.8 Hz, 2H), 7.08 – 7.03 (m, 1H), 7.03 – 6.96 (m, 4H), 6.92 (s, 1H), 5.04 (dd, *J* = 11.0, 2.5 Hz, 1H), 4.74 (dd, *J* = 5.3, 3.3 Hz, 1H), 2.52 (ddd, *J* = 13.8, 11.0, 5.3 Hz, 1H), 2.32 (t, *J* = 2.9 Hz, 1H), 2.30 (s, 3H).

• **¹³C NMR** (151 MHz, CDCl₃) δ 167.3, 154.8, 142.3, 138.3, 137.5, 136.9, 132.1, 129.8, 128.9, 128.9, 128.7, 128.6, 128.5, 124.6, 122.3, 120.6, 120.6, 120.0, 119.7, 86.8, 86.1, 63.0, 37.6, 37.0, 21.2.

• **HRMS** (ESI): M+Na⁺ found 466.1778; C₃₁H₂₅NO₂Na requires 466.1785.

2-fluoro-4-(p-tolyl)chromane-5-carboxylic acid 9:



Procedure:

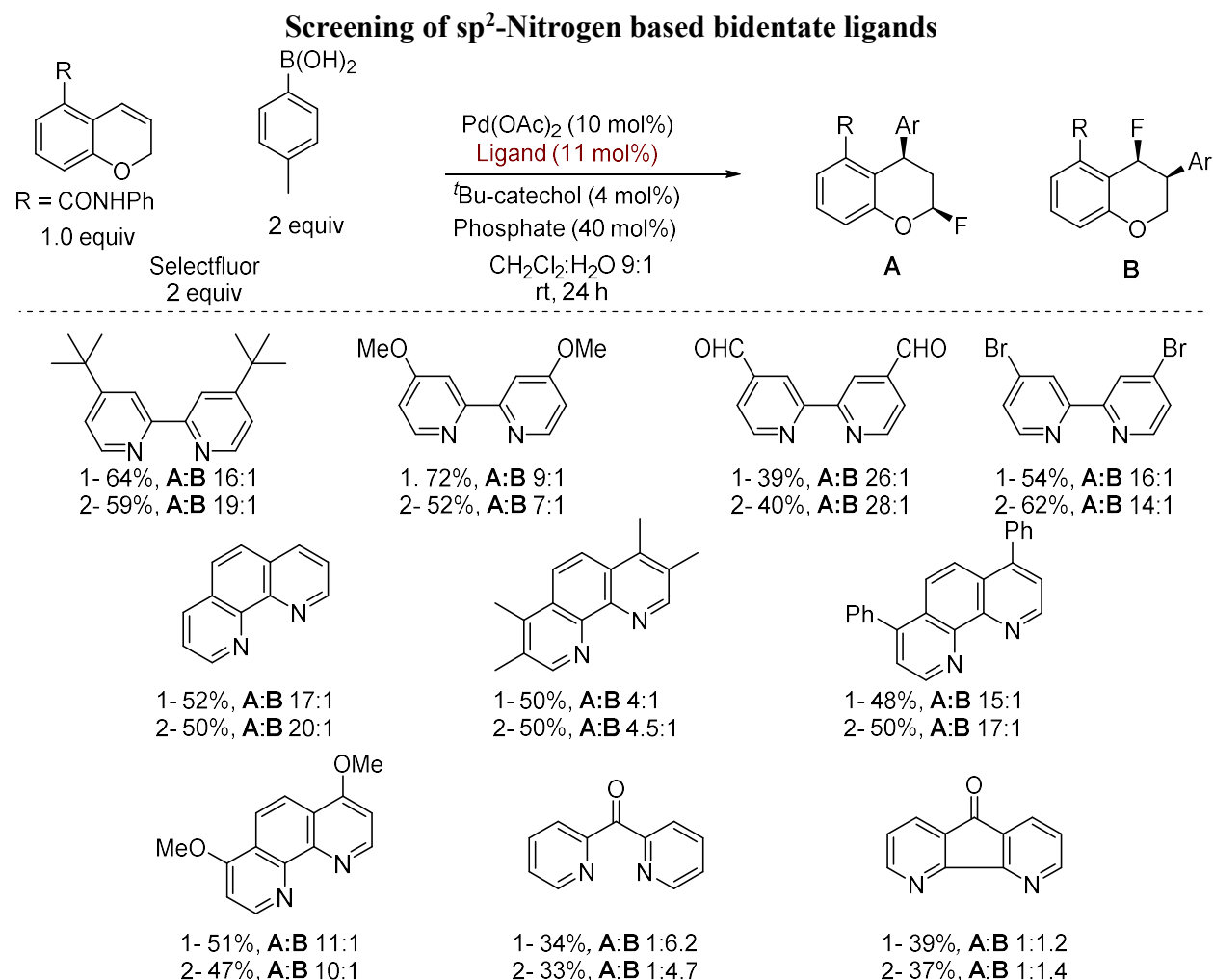
2-pyranyl fluoride **2a** (35.0 mg, 0.097 mmol, 1.0 eq) and 4-dimethylaminopyridine (85.0 mg, 0.146 mmol, 1.5 eq) were added to a 1 dram vial with a septum cap. The solids were dissolved in 0.8 mL of 1,2-dichloroethane and stirred. To the vial, di-*tert*-butyl dicarbonate (40.0 mg, 0.388 mmol, 4.0 eq) was added as a solution in 0.2 ml of 1,2-dichloroethane. The reaction mixture was then heated to 60 °C and stirred for 36 hours. A yellow solution resulted. The reaction mixture was

cooled to room temperature, and the contents of the vial were diluted with CH₂Cl₂ and washed with a saturated aqueous solution of NH₄Cl. The organic layer was separated, dried over Na₂SO₄, and concentrated. Full consumption of **2a** was confirmed by ¹H-NMR analysis of the crude reaction mixture. The crude mixture was utilized without purification. In a round bottomed flask, the resulting residue was dissolved in 1.6 mL of tetrahydrofuran and 0.4 mL of H₂O and stirred. To the flask, as a 30% by weight aqueous solution, H₂O₂ (195 μL, 1.940 mmol, 20.0 eq) was added via syringe. As a solid, LiOH (23 mg, 0.970 mmol, 10.0 eq) was added. The reaction mixture was stirred at room temperature for 18 hours. The contents of the flask were diluted with CH₂Cl₂ and washed with a saturated aqueous solution of NH₄Cl. The organic layer was separated, dried over Na₂SO₄, and concentrated. Analysis of the crude reaction mixture revealed that both **9** and **2a** were present in the reaction mixture in a 1.0:0.4 ratio, respectively. The crude solid was purified by silica chromatography (25:25:1 pentane/CHCl₃/Et₂O to 25:1 CHCl₃/Et₂O) to afford **9** as a colorless powder (12.3 mg, 44%).

- **¹H NMR** (600 MHz, CD₂Cl₂) δ 7.70 (d, *J* = 7.7 Hz, 1H), 7.37 (t, *J* = 8.0 Hz, 1H), 7.26 (d, *J* = 8.2 Hz, 1H), 7.00 (d, *J* = 7.7 Hz, 2H), 6.84 (d, *J* = 7.7 Hz, 2H), 6.03 (d, *J* = 56.1 Hz, 1H), 5.17 (d, *J* = 7.2 Hz, 1H), 2.60 – 2.35 (m, 2H), 2.26 (s, 3H).
- **¹⁹F NMR** (377 MHz, CDCl₃): -118.8
- **¹³C NMR** (151 MHz, CDCl₃) δ ¹³C NMR (151 MHz, CD₂Cl₂) δ 169.5, 152.1, 142.4, 135.9, 129.0, 128.5, 127.9 (d, *J* = 30.2 Hz), 126.2, 125.5, 122.8, 105.3 (d, *J* = 222.0 Hz), 34.1 (d, *J* = 21.1 Hz), 33.55, 21.08.
- **HRMS** (ESI): M⁺ found 285.0929; C₁₇H₁₄O₃F requires 285.0932.

For analysis by chiral HPLC, further derivatization to the corresponding methyl ester, **3**, was necessary. A general procedure for derivatization was used as follows: A sample of **9** (12.3 mg, 0.043 mmol, 1.0 eq) in a 1 dram septum capped vial was dissolved in 0.3 mL of C₆H₆ and 0.3 mL of MeOH. To the vial, as a 2.0M solution in Et₂O, trimethylsilyldiazomethane (22 μL, 0.043 mmol, 1.0 eq) was added via syringe. The solution became yellow. The solution was stirred for 45 minutes, after which the reaction mixture was diluted with CH₂Cl₂ and H₂O. The organic layer was separated, dried over MgSO₄, and concentrated to afford a colorless oil, **3**, quantitatively. No further purification was necessary.

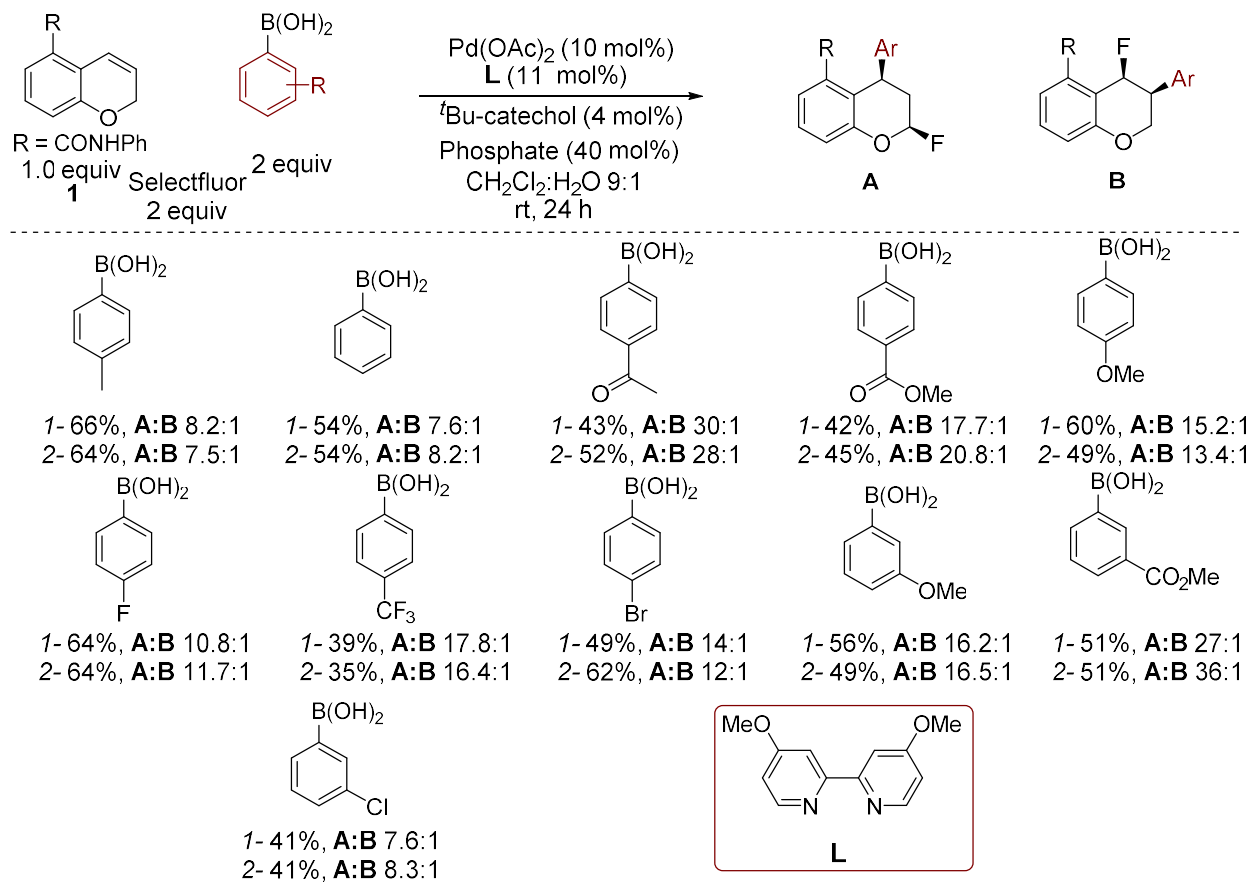
1.4.6. Experimental Data Set for Statistical Analysis



Procedure D

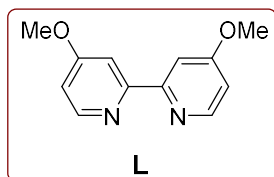
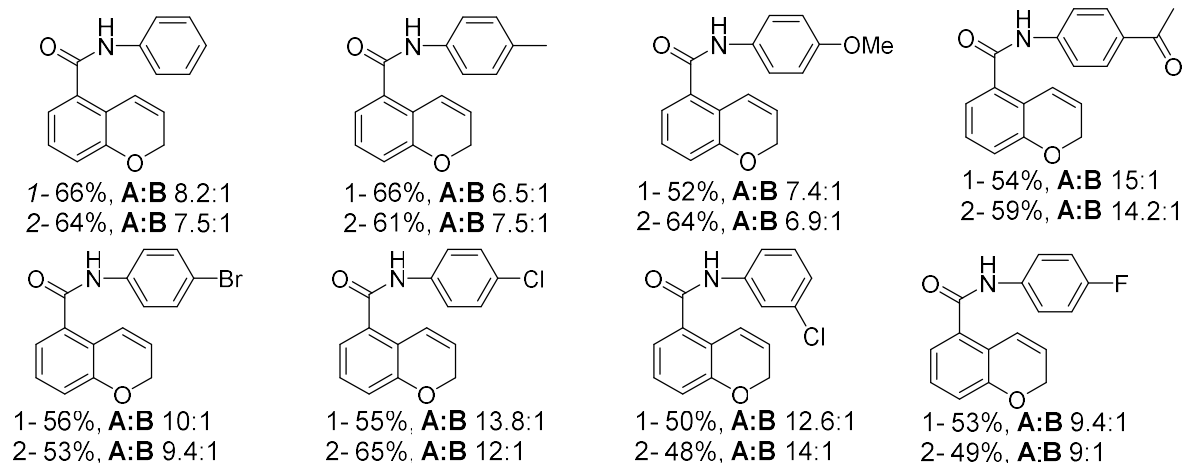
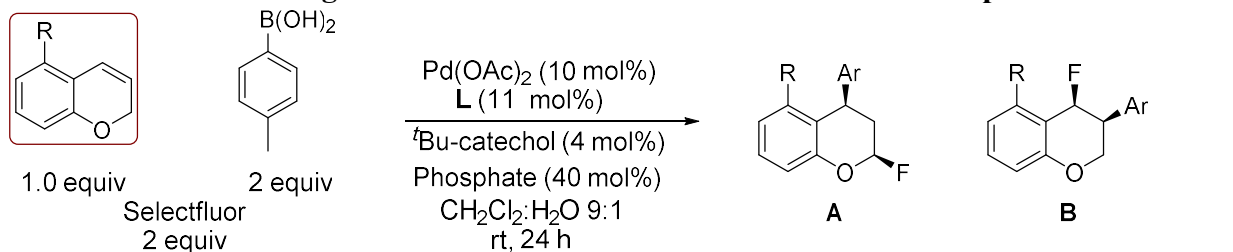
Pd(OAc)₂ (2.2 mg, 0.010 mmol, 0.10 equiv) was added to a solution of **Ligand** (0.011 mmol, 0.11 equiv) in CH₂Cl₂ (1 ml) and the reaction mixture was stirred for 30 min. The catalyst solution was then added to a solution of chromene **1** (25.0 mg, 0.100 mmol, 1.00 equiv), *p*-tolyl phenylboronic acid (27 mg, 0.200 mmol, 2.00 equiv), bis(2-ethylhexyl) hydrogen phosphate (12.8 mg, 0.040 mmol, 0.40 equiv), Selectfluor (71.0 mg, 0.200 mmol, 2.00 equiv) and *tert*-butyl catechol (0.6 mg, 0.004 mmol, 0.04 equiv) in CH₂Cl₂ (0.8 ml)/water (0.2 ml). The reaction mixture was vigorously stirred for 24 h. The reaction mixture was diluted with CH₂Cl₂, dried with Na₂SO₄, filtered through celite, and concentrated under reduce pressure. Then, a known amount of 4-fluorobenzoic acid as an internal standard was added to the crude extract. Yield and regioselectivity was determined using ¹⁹F NMR (CD₂Cl₂, 400 MHz, d1=10). The reaction was repeated twice and results obtained are described above. *Note*: 1- and 2- represents first and second run, respectively. The percentage figure represents total yield (A+B) of the reaction.

Screening of various boronic acids



Procedure: The general procedure **D** was followed with the following modification. Ligand **L** (0.011 mmol, 0.11 equiv) and different boronic acids (0.022 mmol, 0.22 equiv) as described in the Table 4 were used. The yields and selectivities were obtained by ¹⁹F NMR using 4-fluorobenzoic acid as an internal standard and are described below.

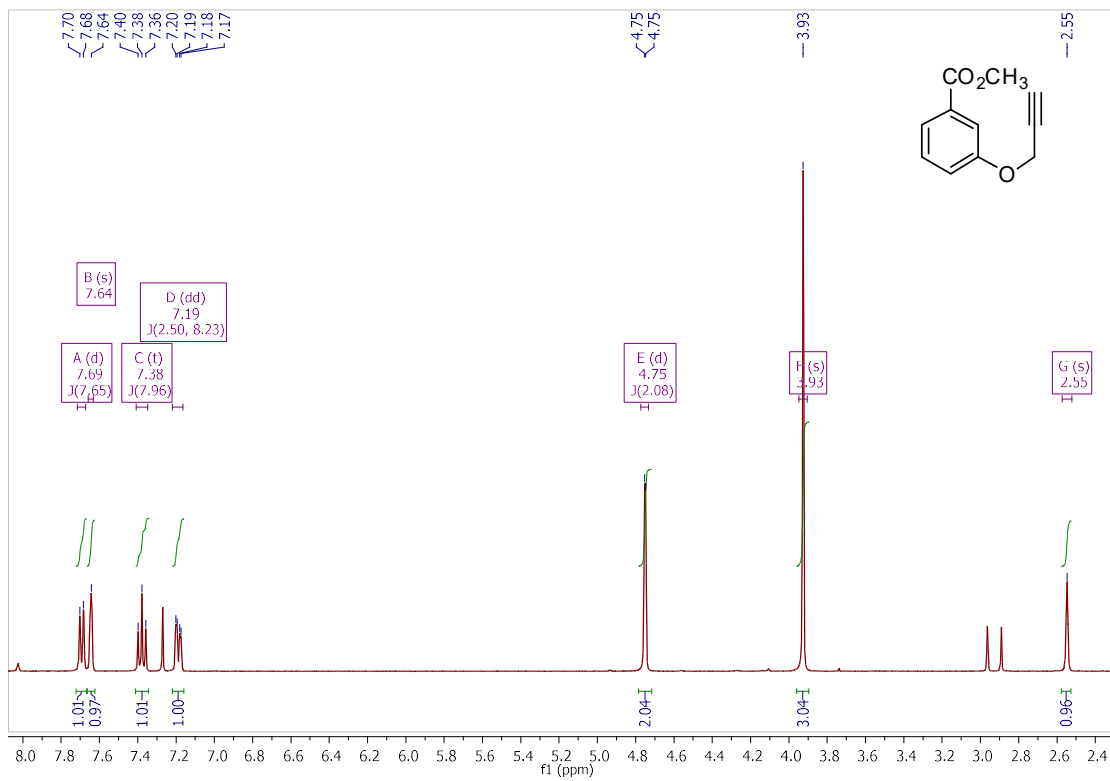
Screening of different chromene substrates for Hammett plot



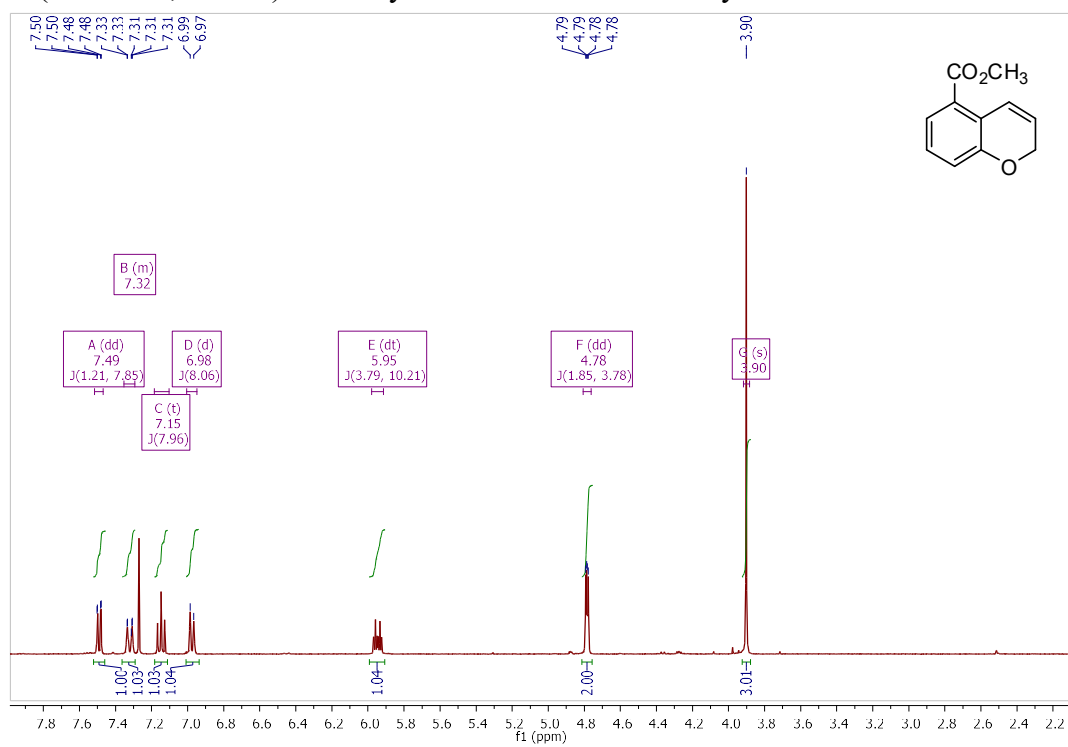
Procedure: The general procedure **D** was followed with the following modification. Ligand **L** and the chromene substrates as shown above were used and the corresponding yield and selectivity obtained is described below each substrate. The yields and selectivities were obtained by ¹⁹F NMR using 4-fluorobenzoic acid as an internal standard. The product formation was later confirmed by LCMS.

1.4.7. Spectral Data

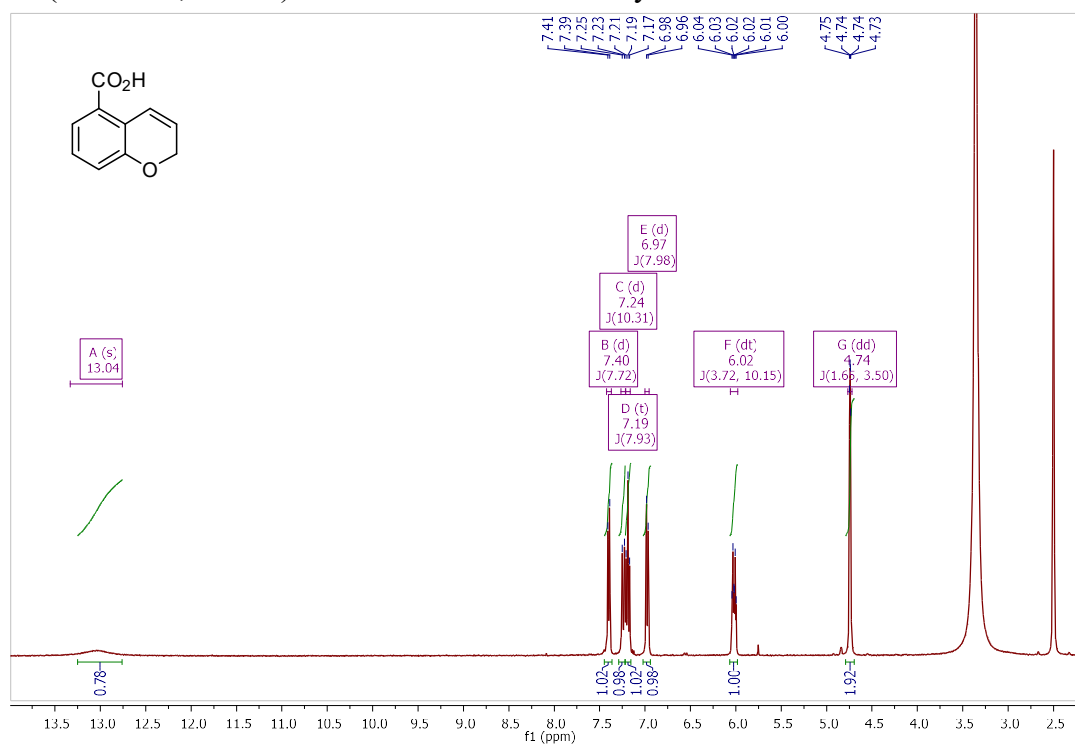
^1H NMR (400 MHz, CDCl_3) of methyl 3-(prop-2-yn-1-yloxy)benzoate



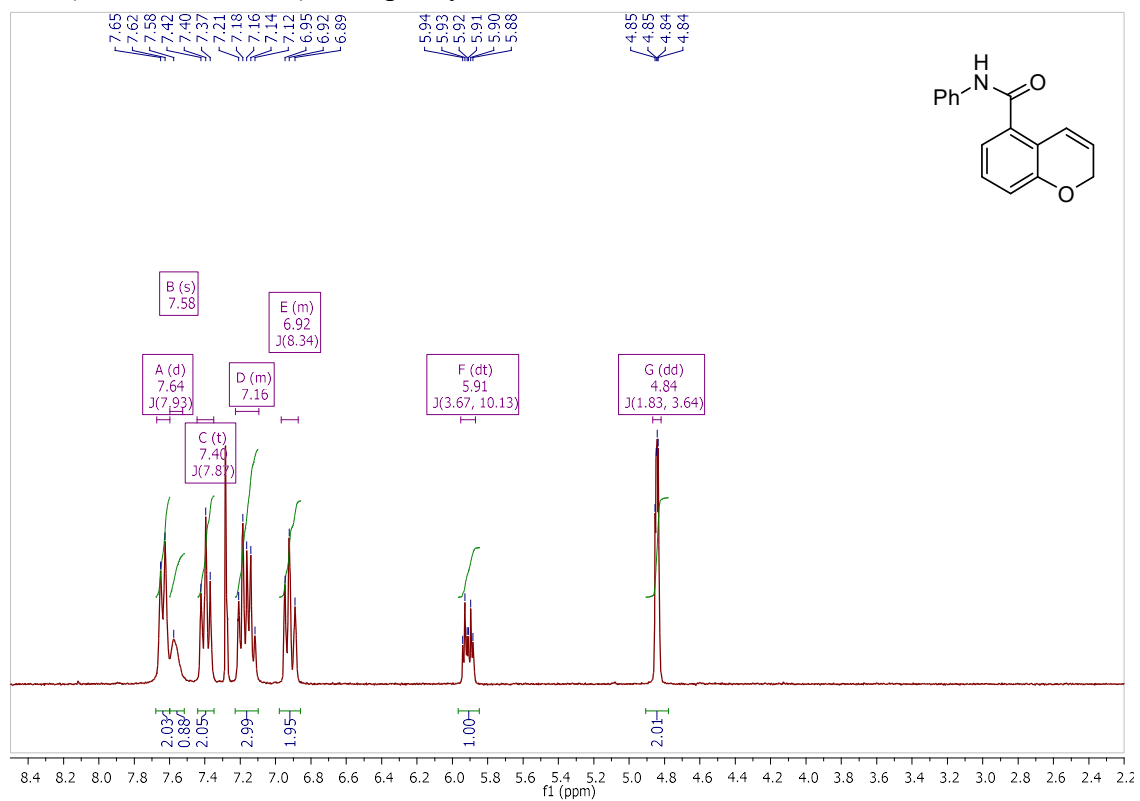
^1H NMR (400 MHz, CDCl_3) of methyl 2H-chromene-5-carboxylate **3**



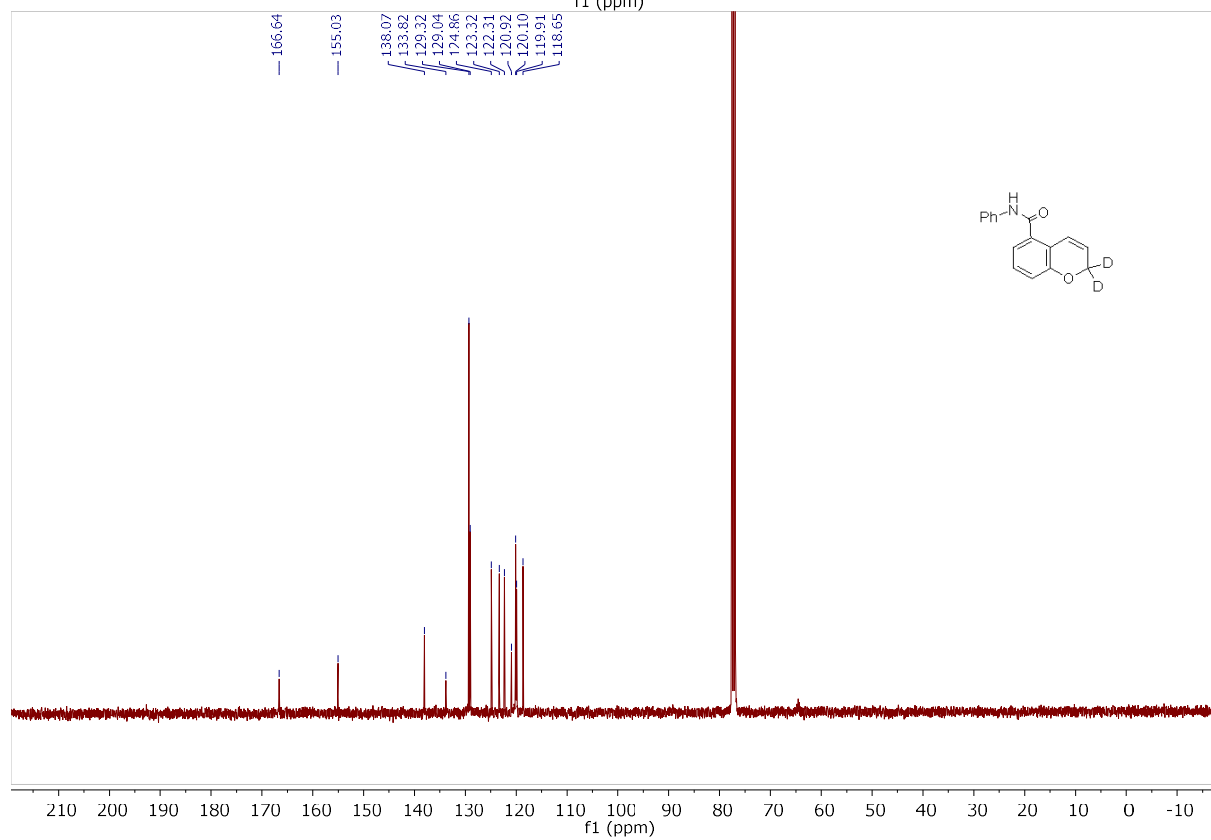
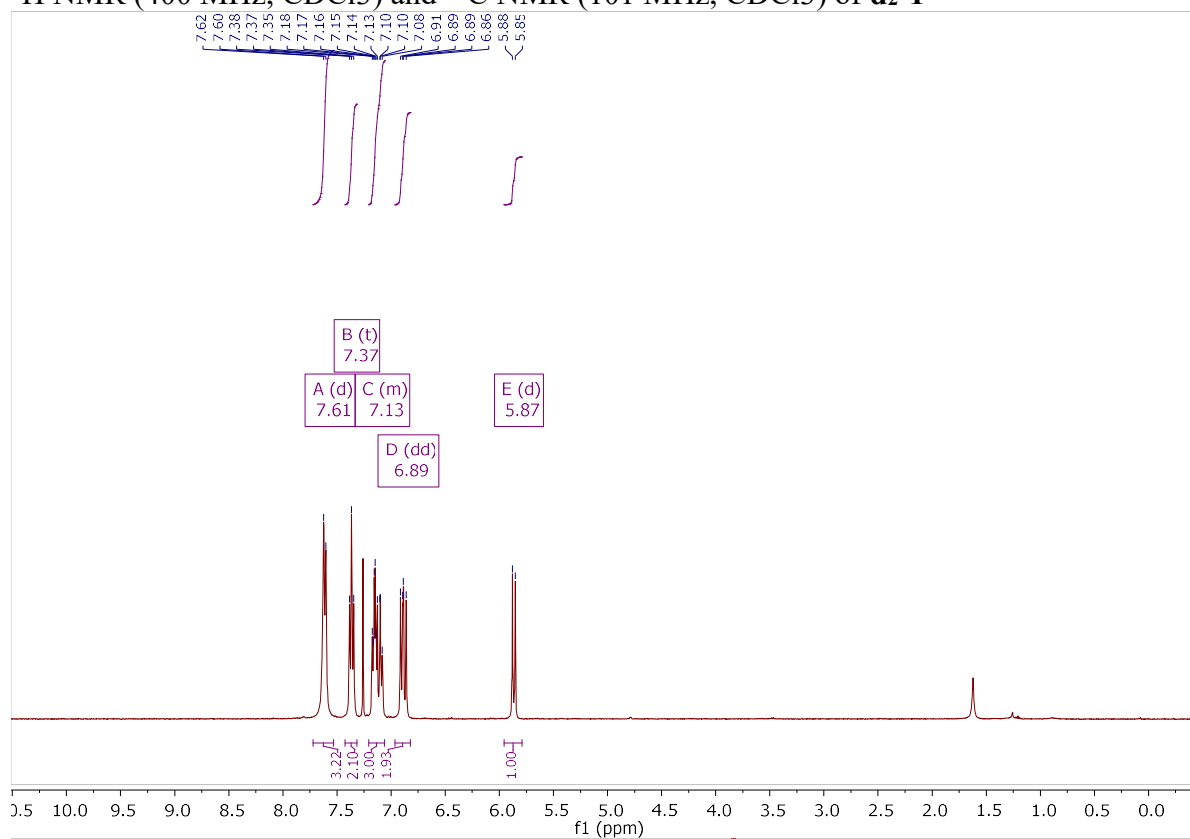
¹H NMR (400 MHz, CDCl₃) of 2H-chromene-5-carboxylic acid **9**



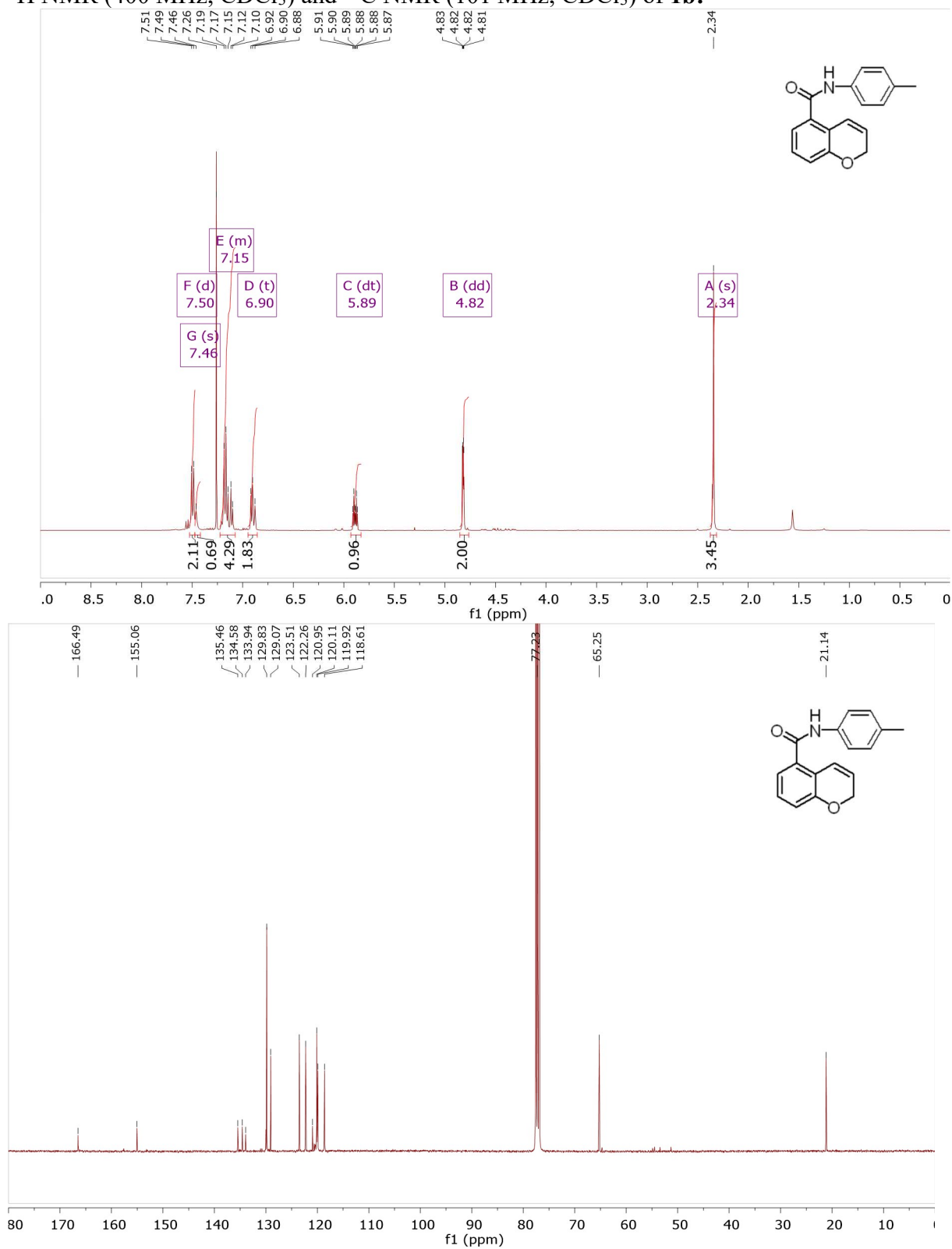
^1H NMR (300 MHz, CDCl_3) of N-phenyl-2H-chromene-5-carboxamide **1a**



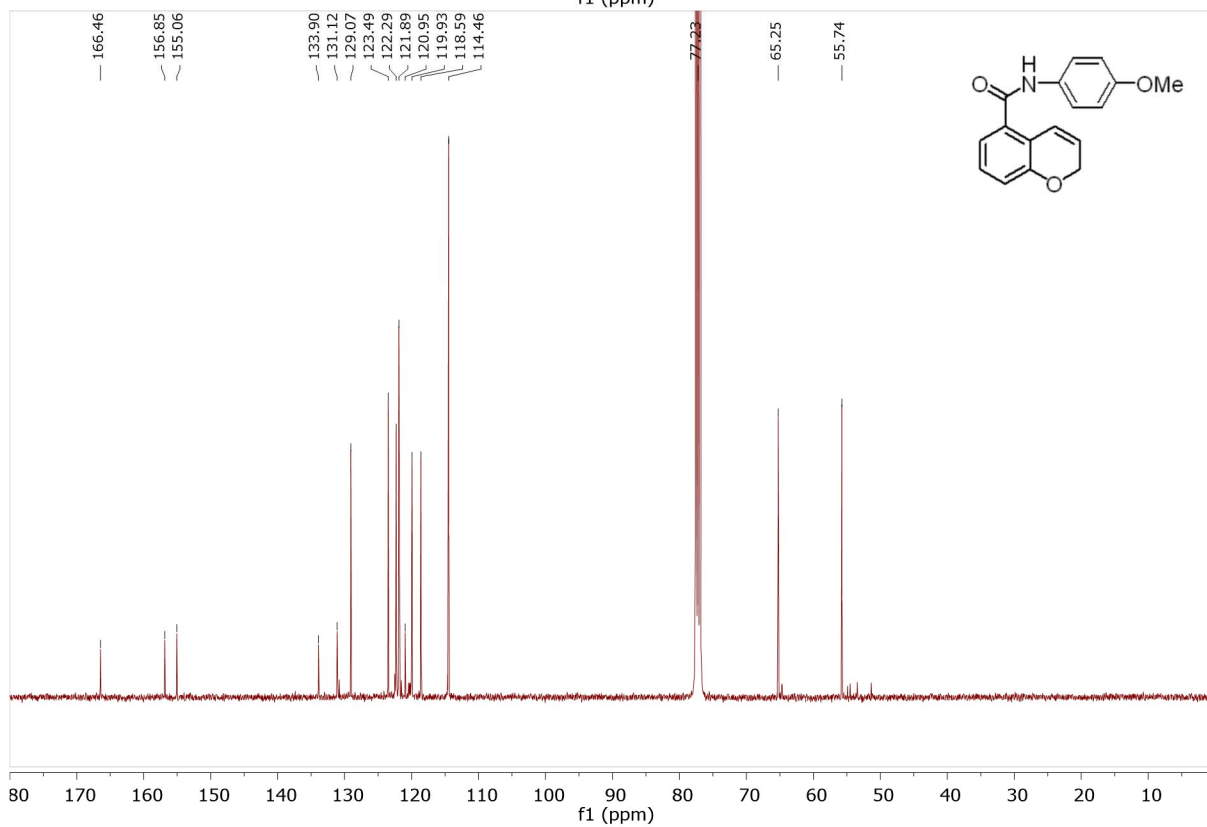
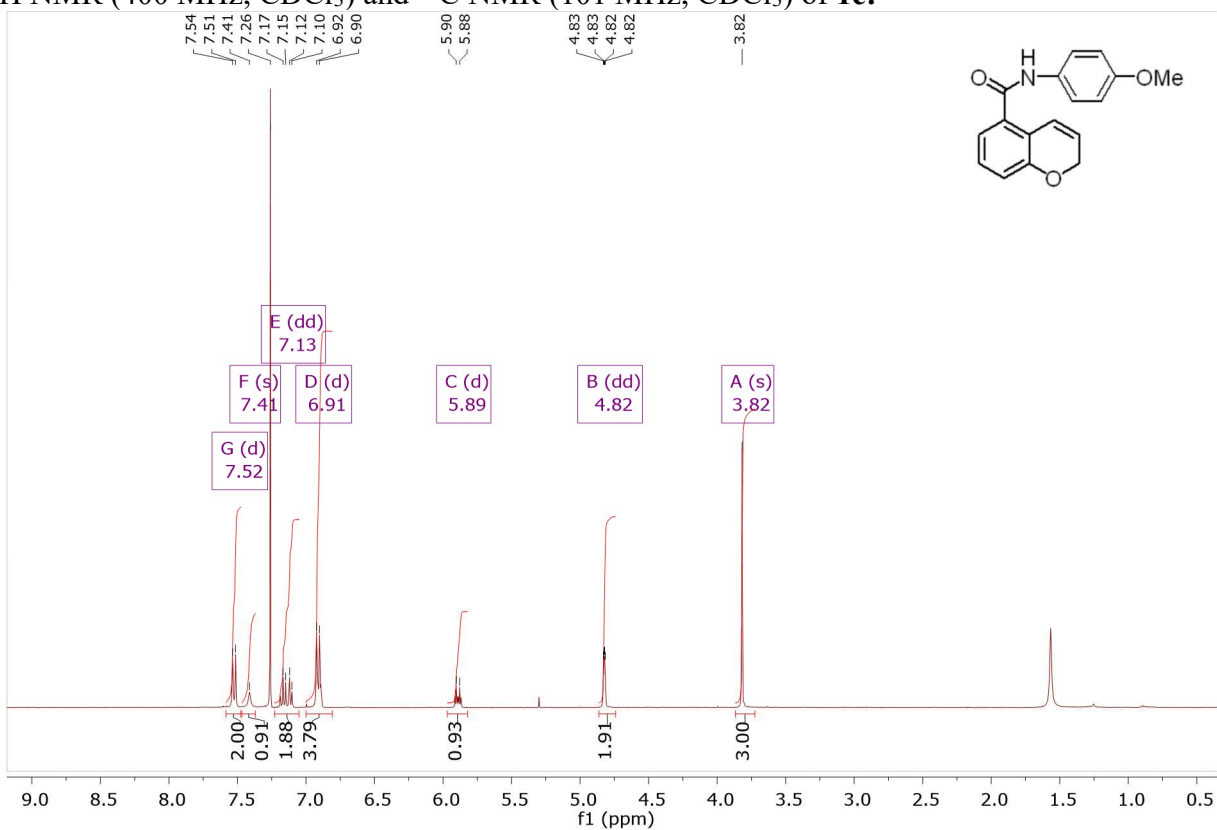
¹H NMR (400 MHz, CDCl₃) and ¹³C NMR (101 MHz, CDCl₃) of d₂-1



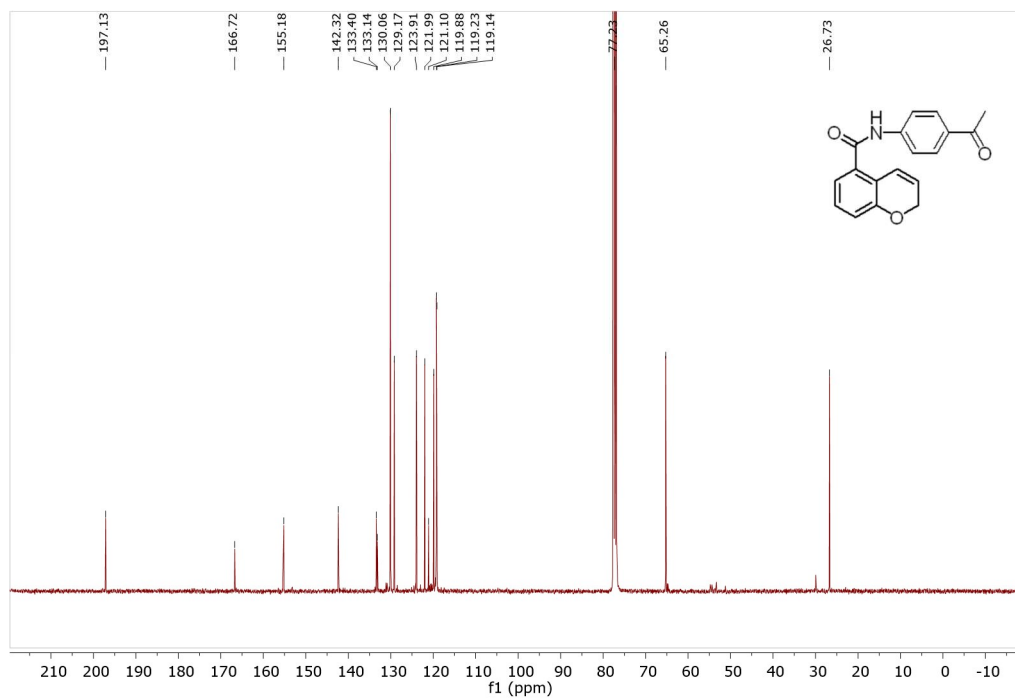
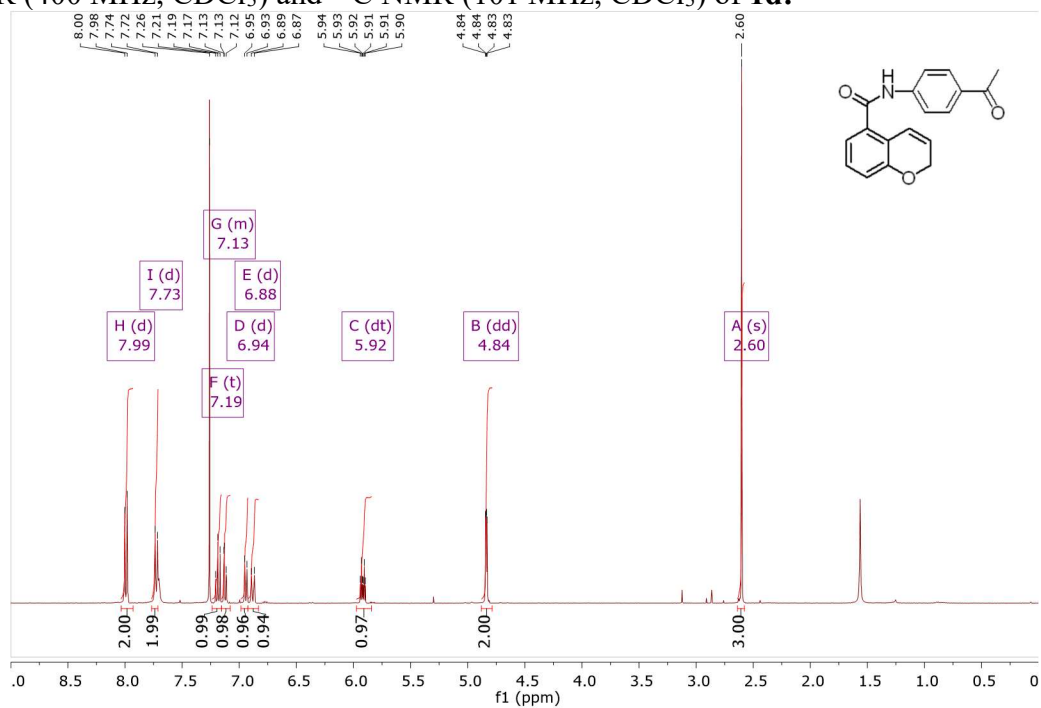
^1H NMR (400 MHz, CDCl_3) and ^{13}C NMR (101 MHz, CDCl_3) of **1b**:



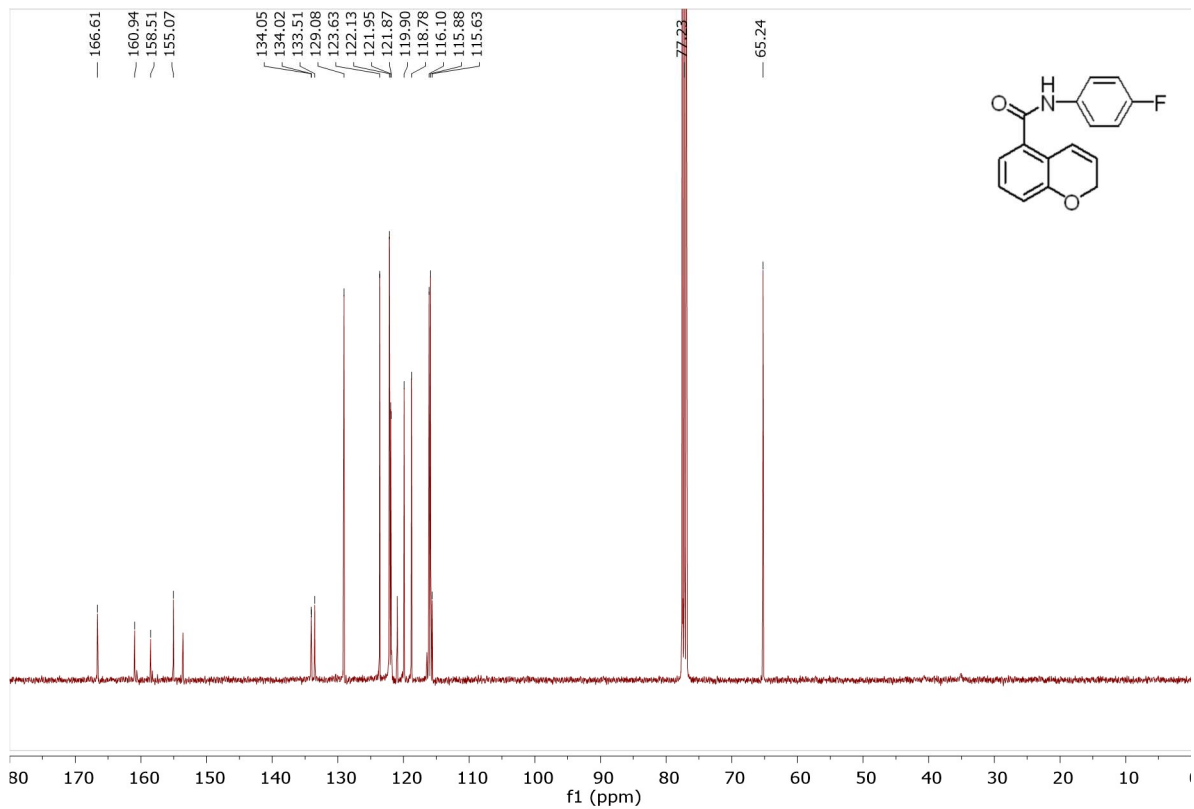
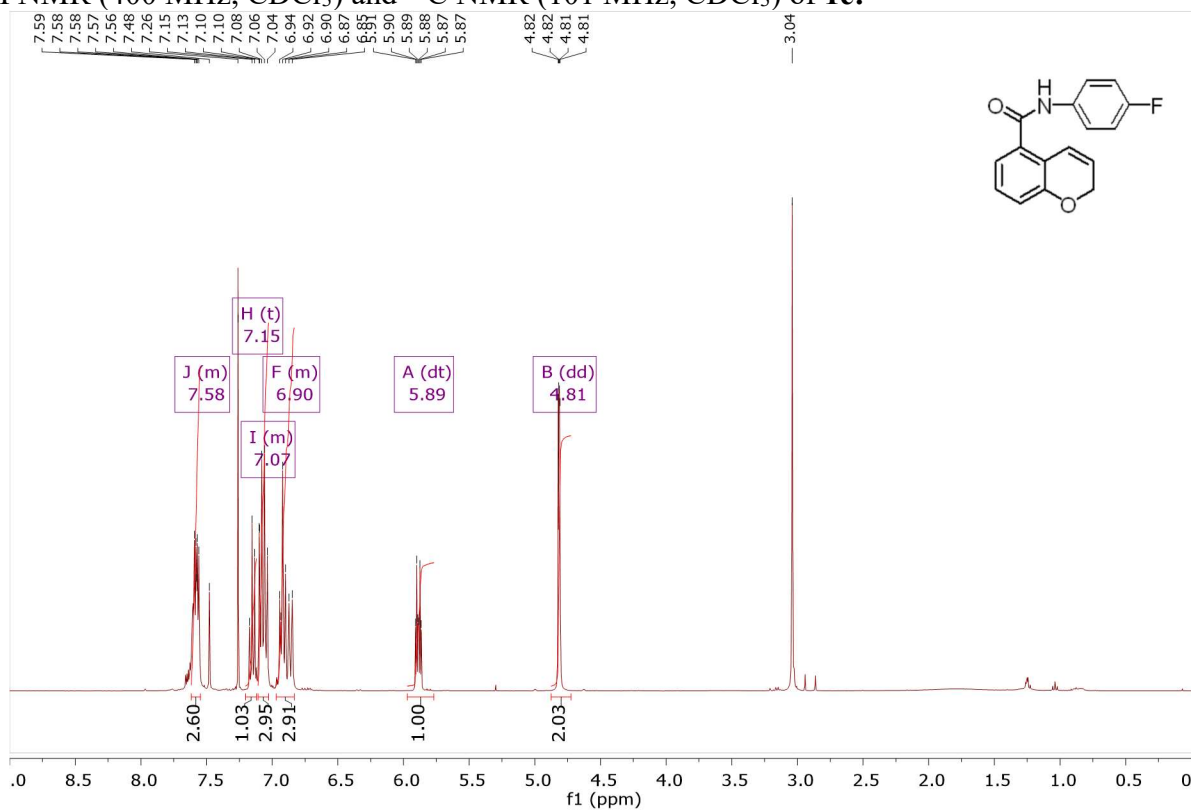
^1H NMR (400 MHz, CDCl_3) and ^{13}C NMR (101 MHz, CDCl_3) of **1c**:



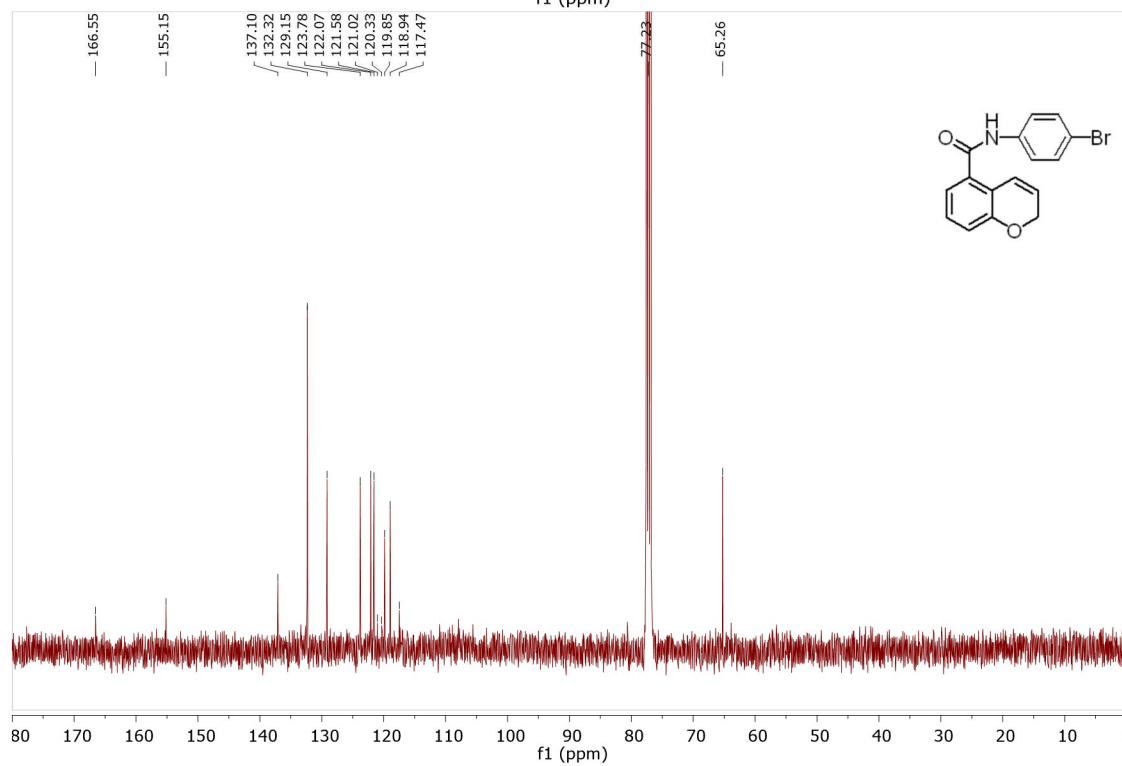
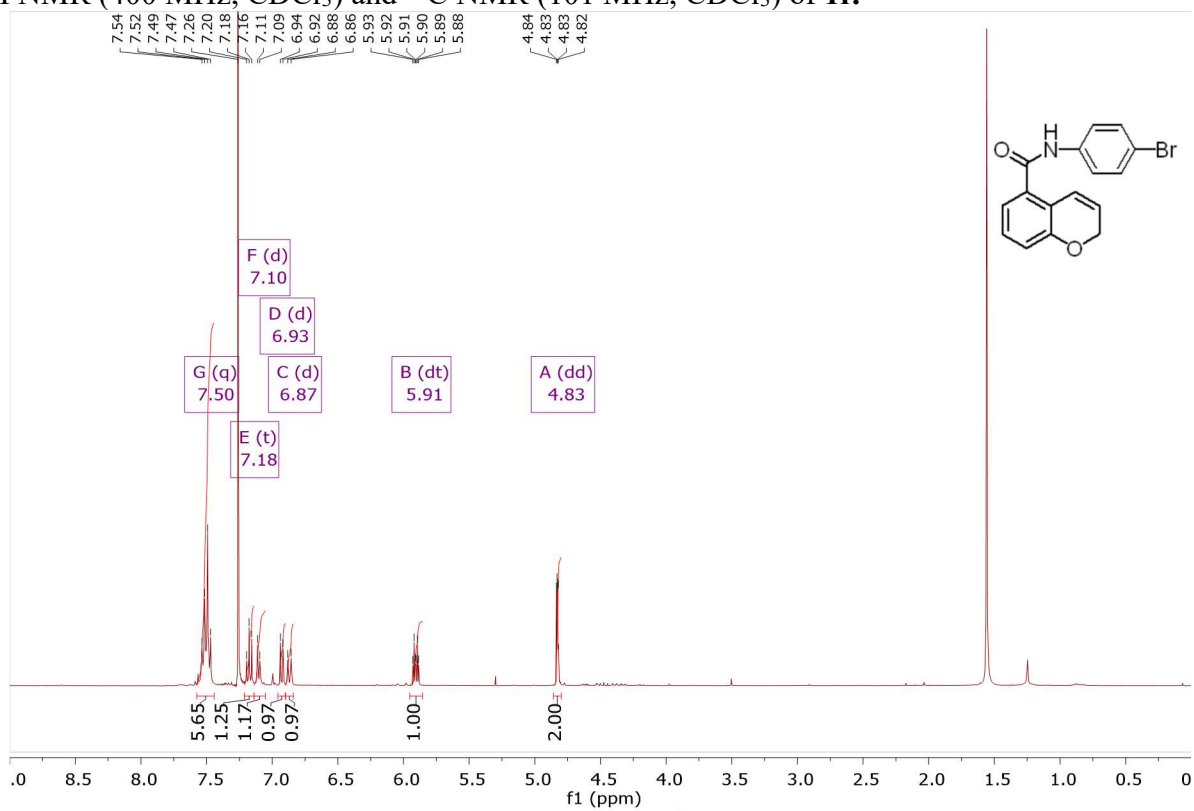
^1H NMR (400 MHz, CDCl_3) and ^{13}C NMR (101 MHz, CDCl_3) of **1d**:



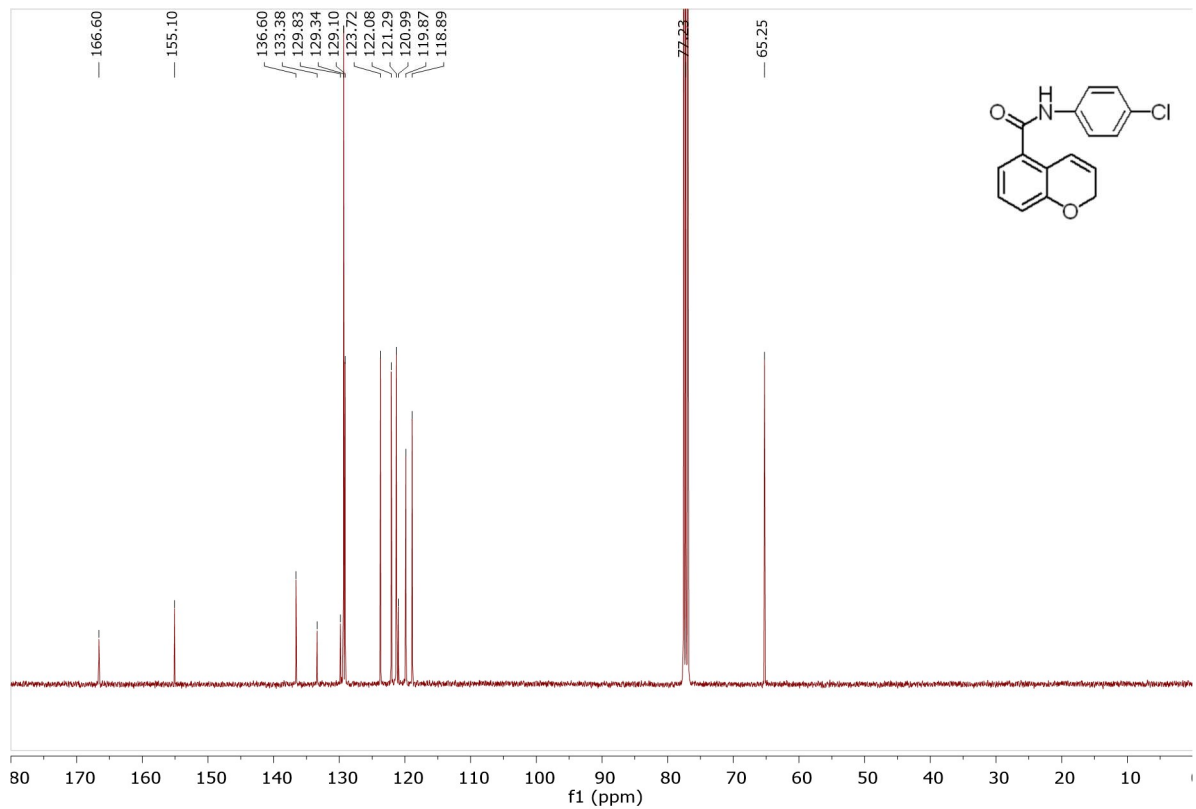
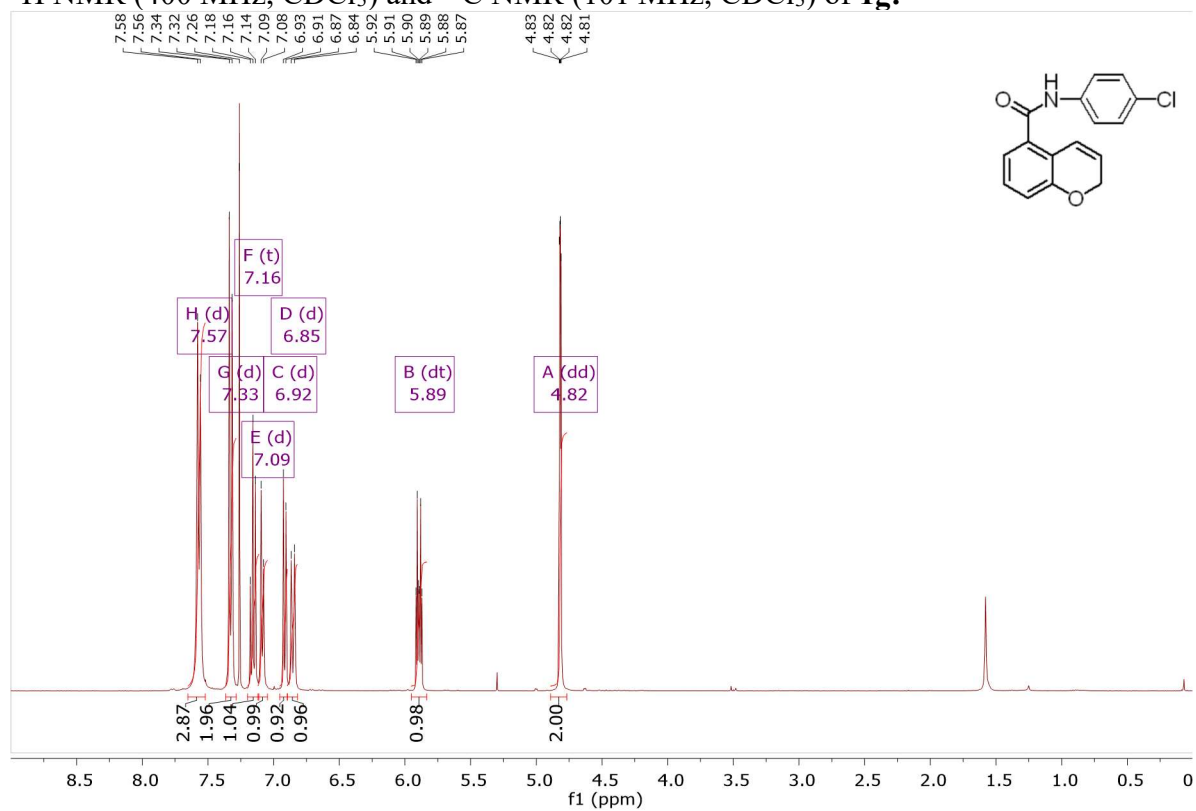
^1H NMR (400 MHz, CDCl_3) and ^{13}C NMR (101 MHz, CDCl_3) of **1e**:



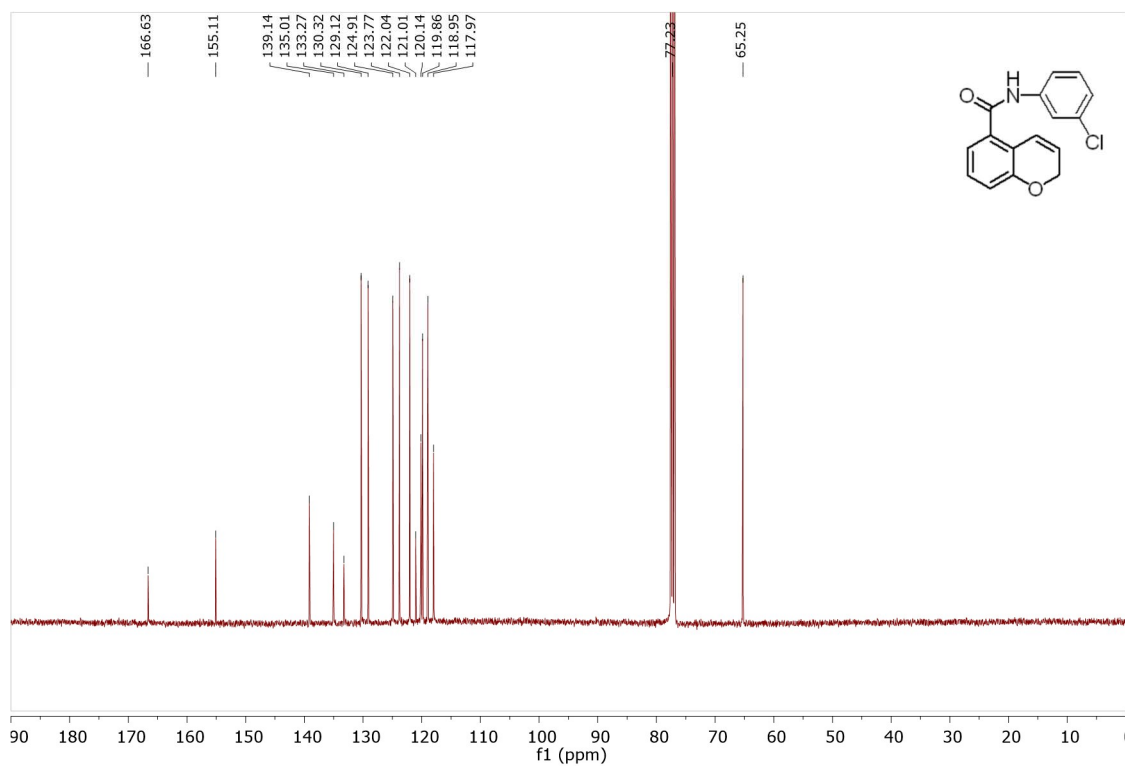
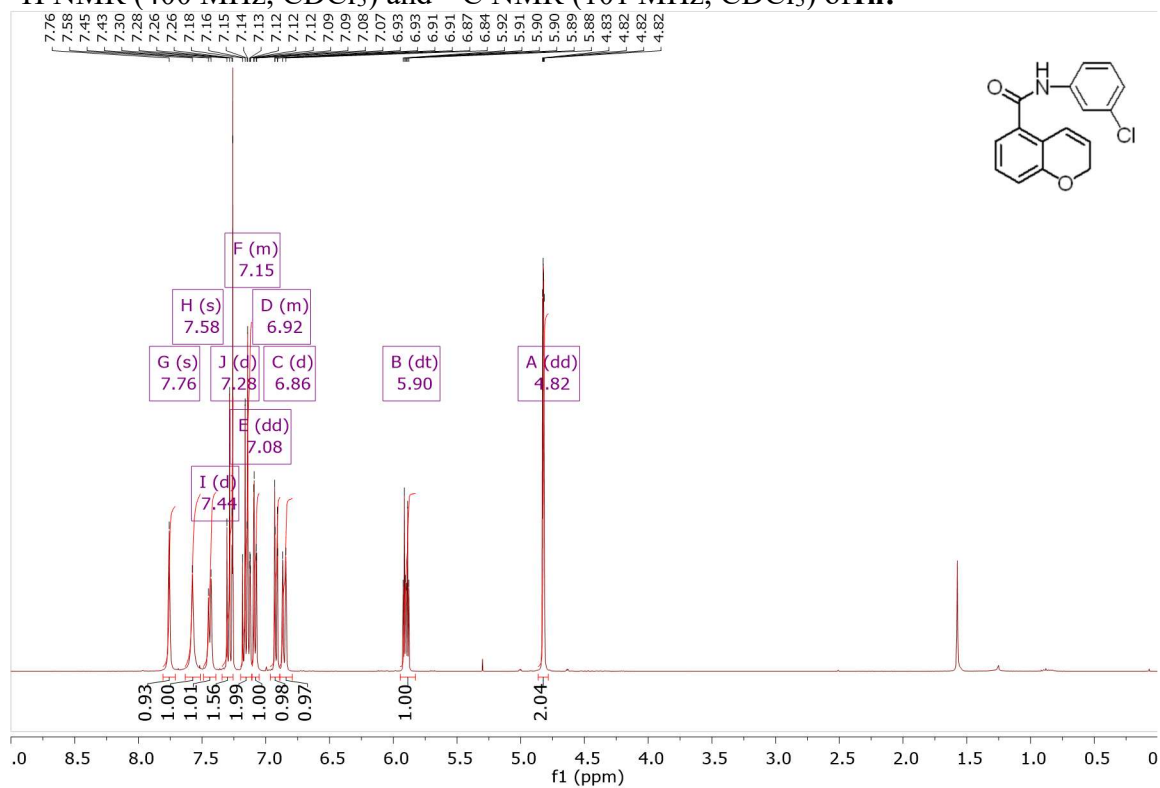
^1H NMR (400 MHz, CDCl_3) and ^{13}C NMR (101 MHz, CDCl_3) of **1f**:



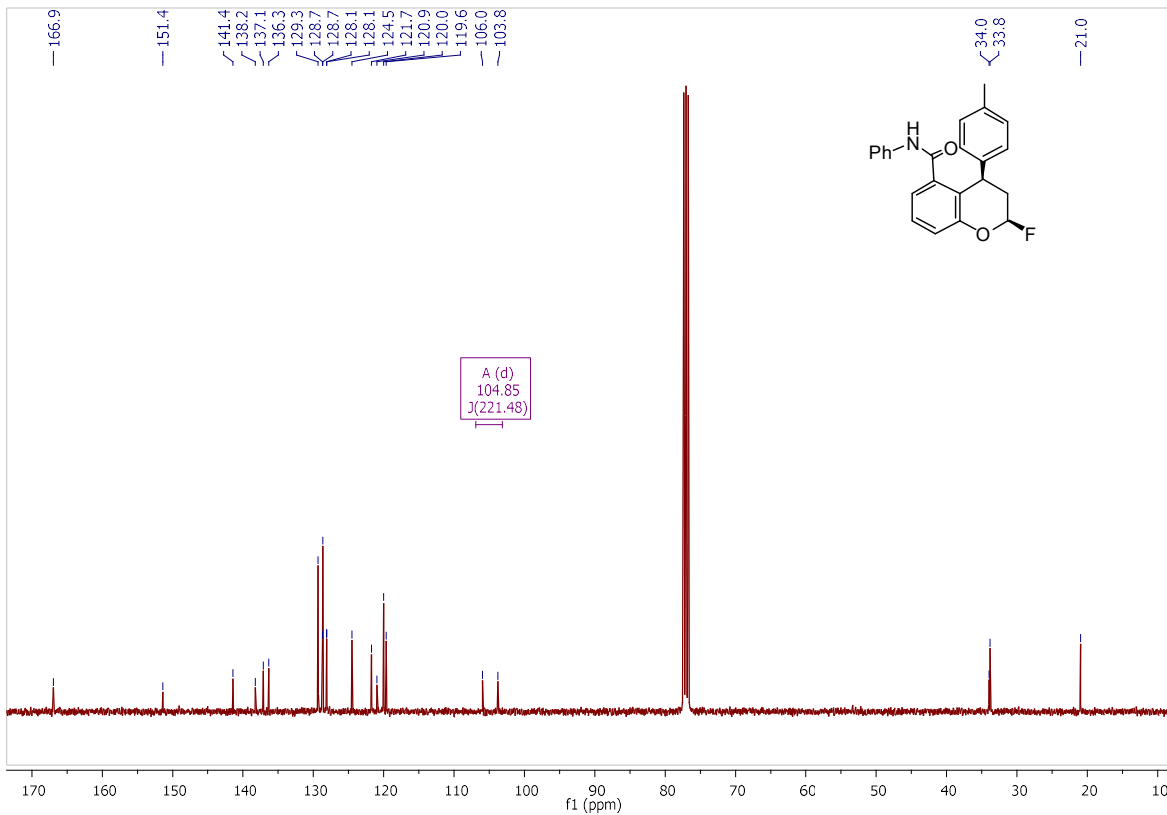
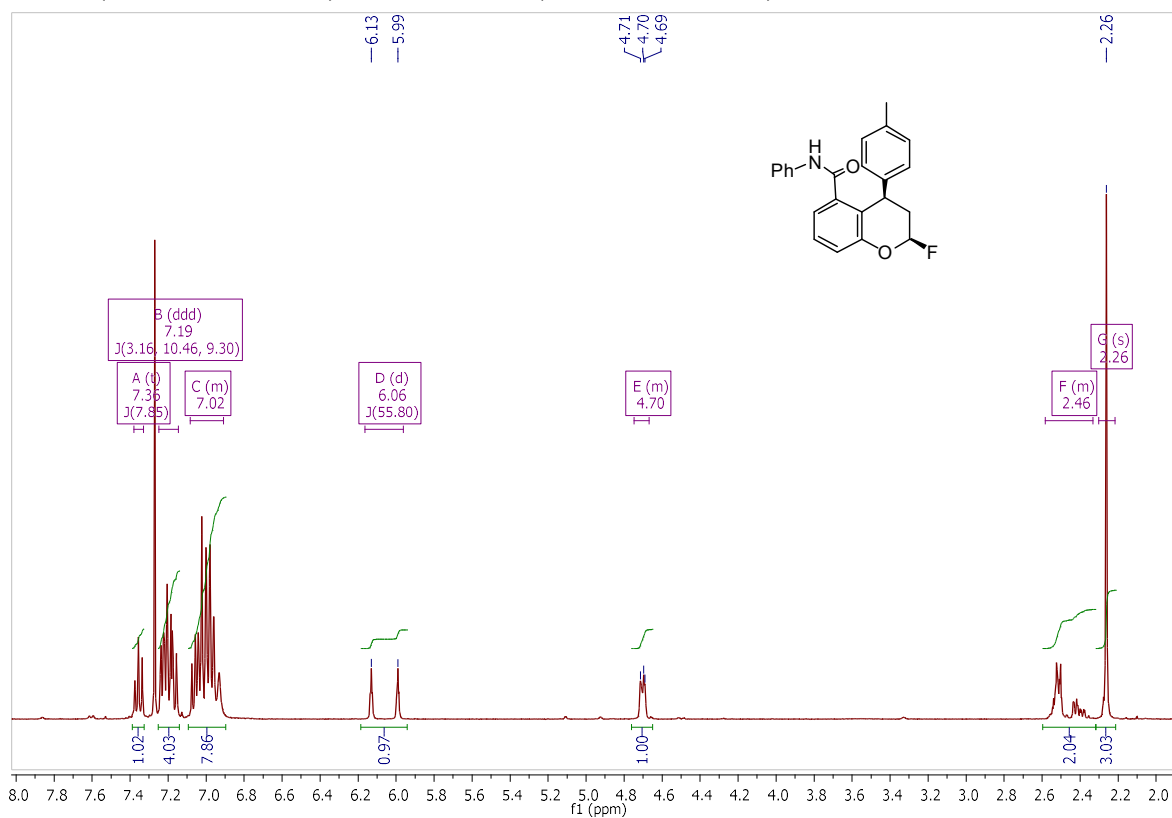
^1H NMR (400 MHz, CDCl_3) and ^{13}C NMR (101 MHz, CDCl_3) of **1g**:



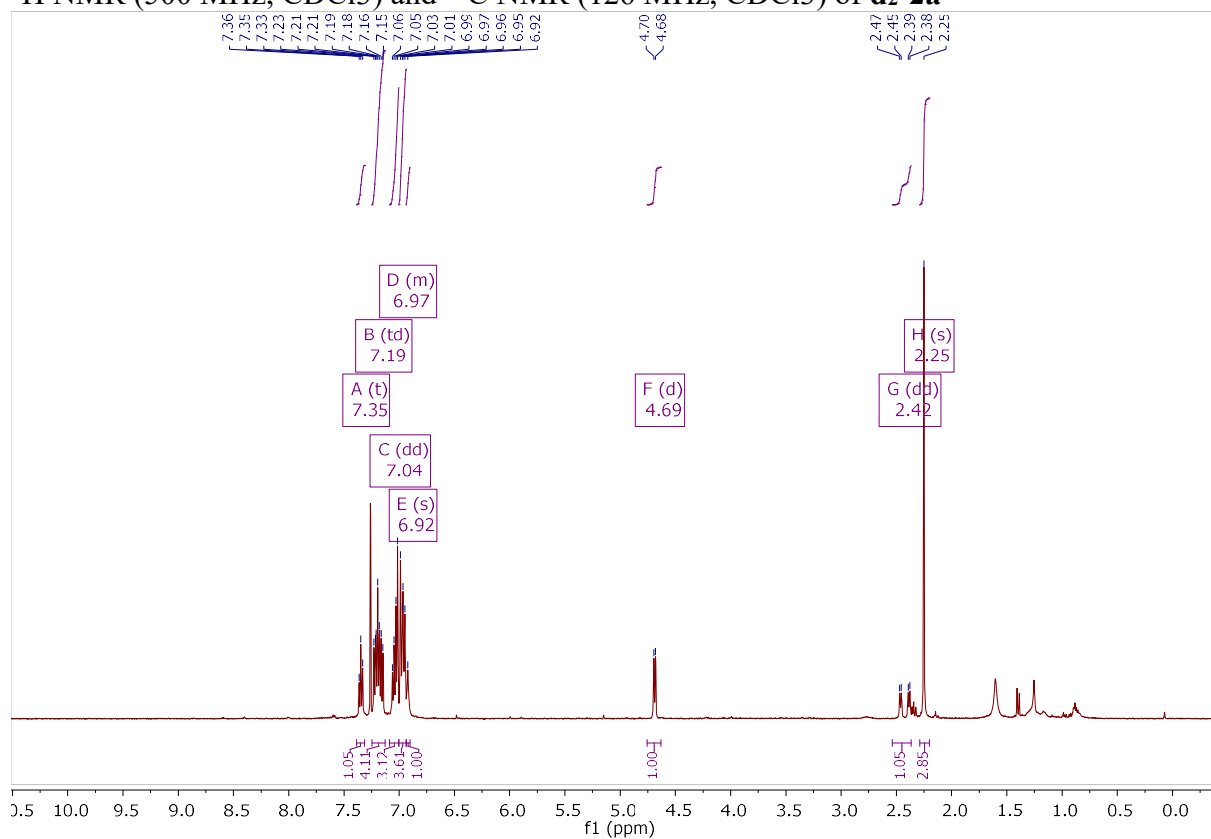
^1H NMR (400 MHz, CDCl_3) and ^{13}C NMR (101 MHz, CDCl_3) of **1h**:

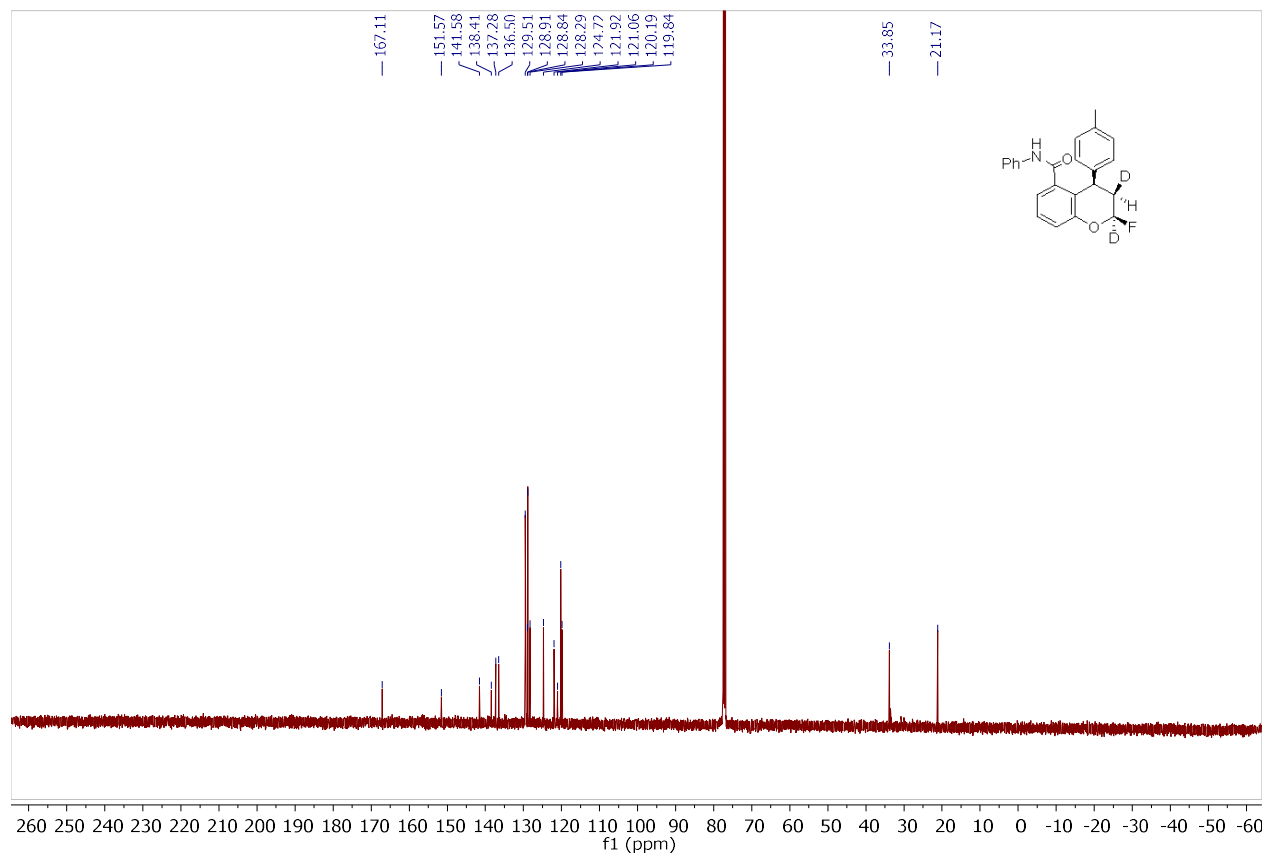


^1H NMR (400 MHz, CDCl_3) and ^{13}C NMR (101 MHz, CDCl_3) of **2a**:

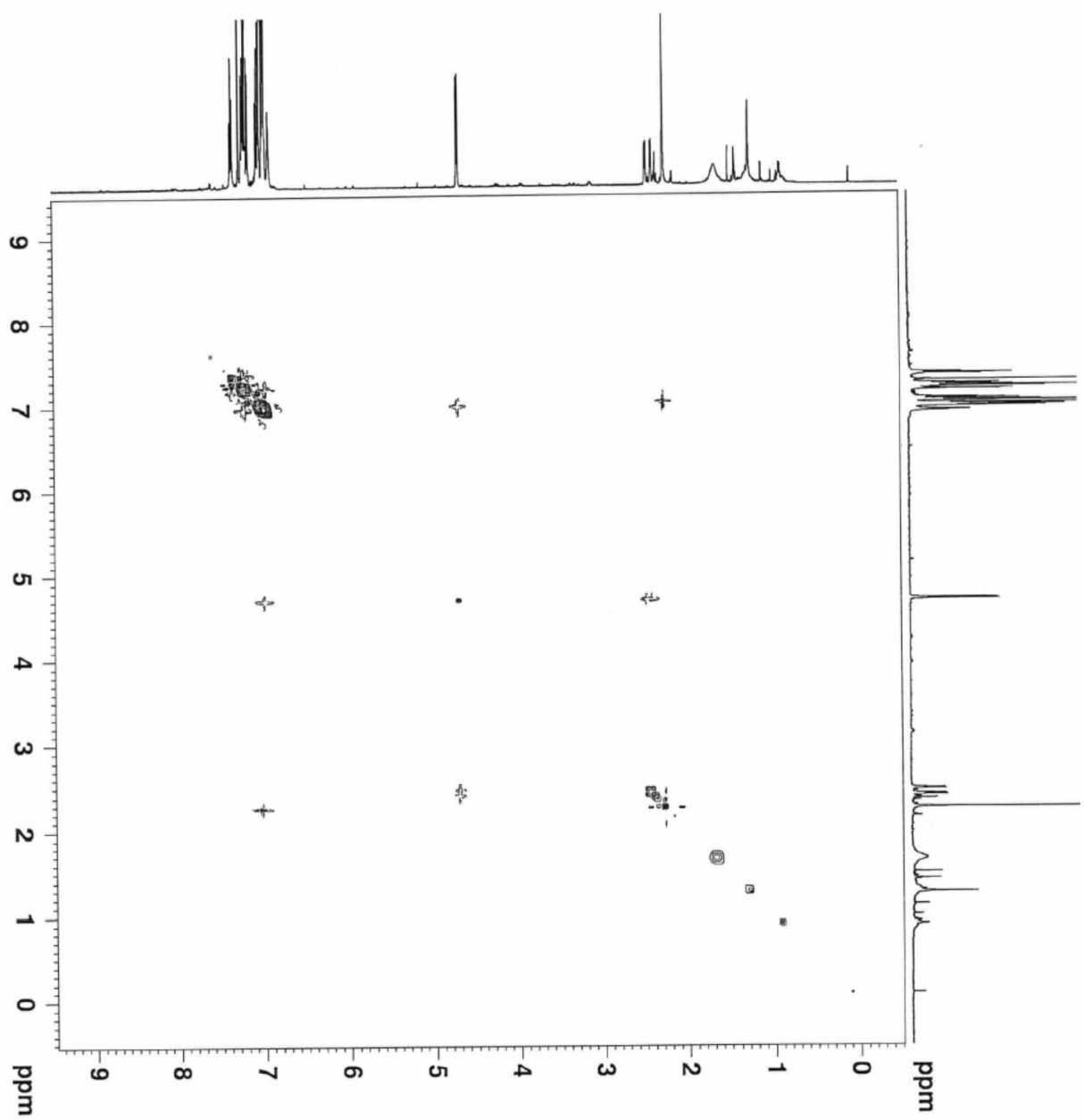


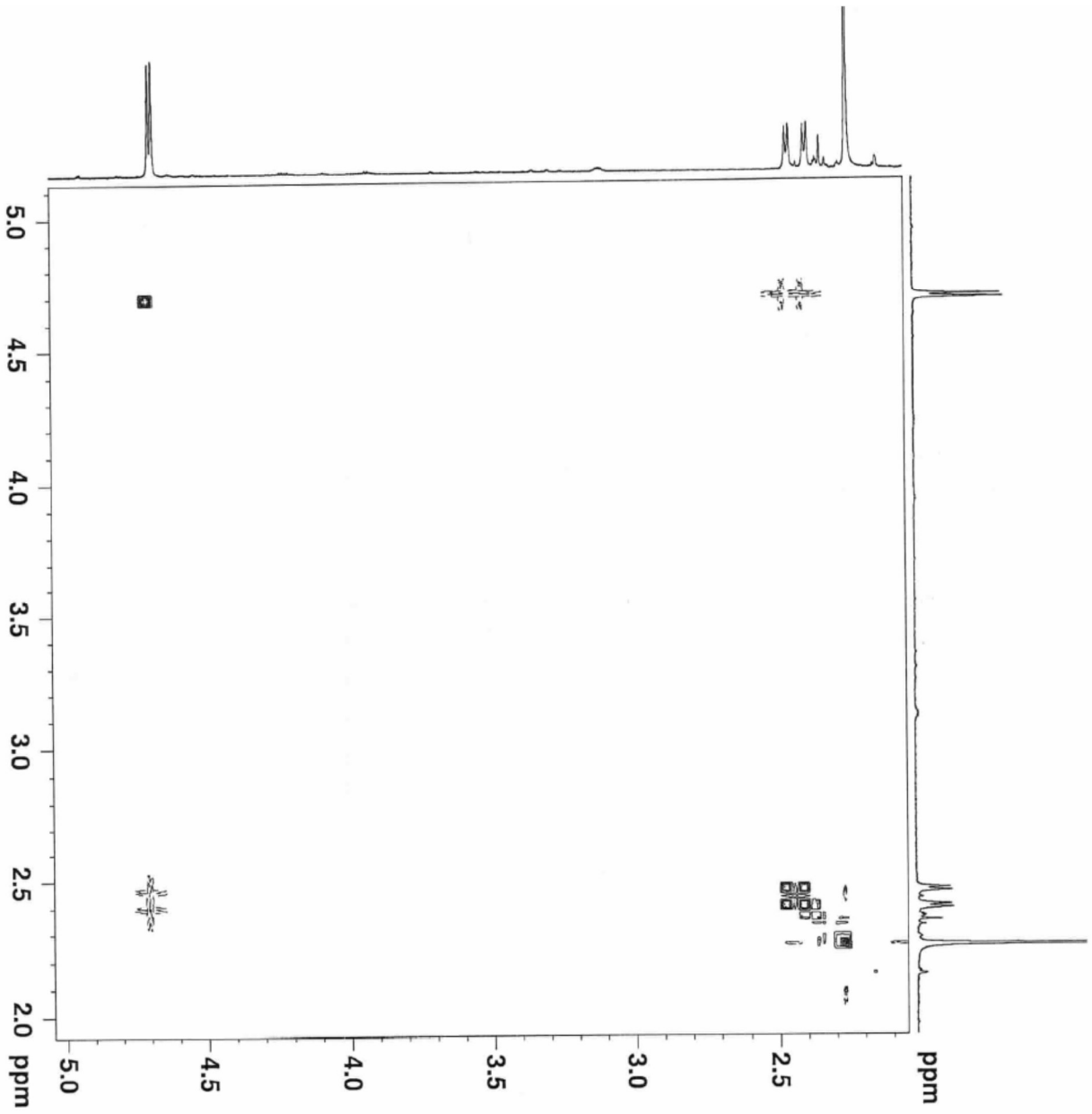
^1H NMR (500 MHz, CDCl_3) and ^{13}C NMR (126 MHz, CDCl_3) of **d2-2a**



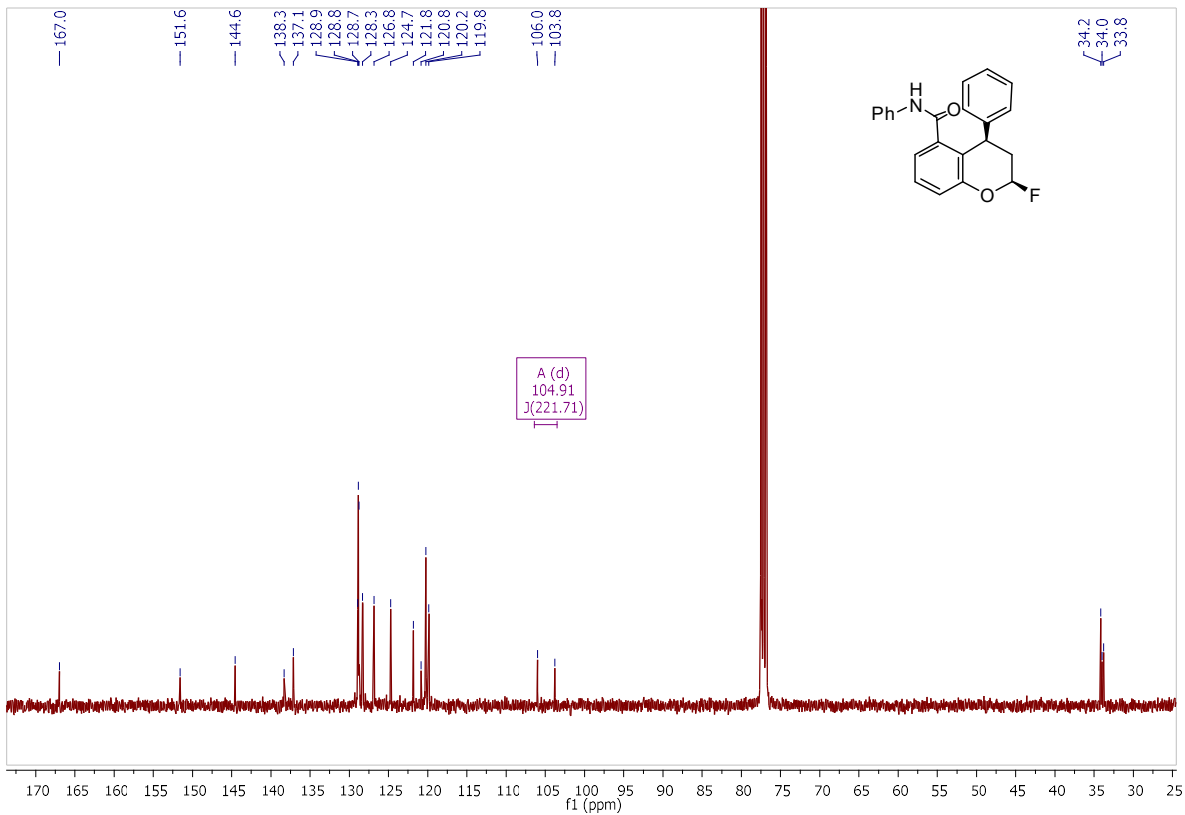
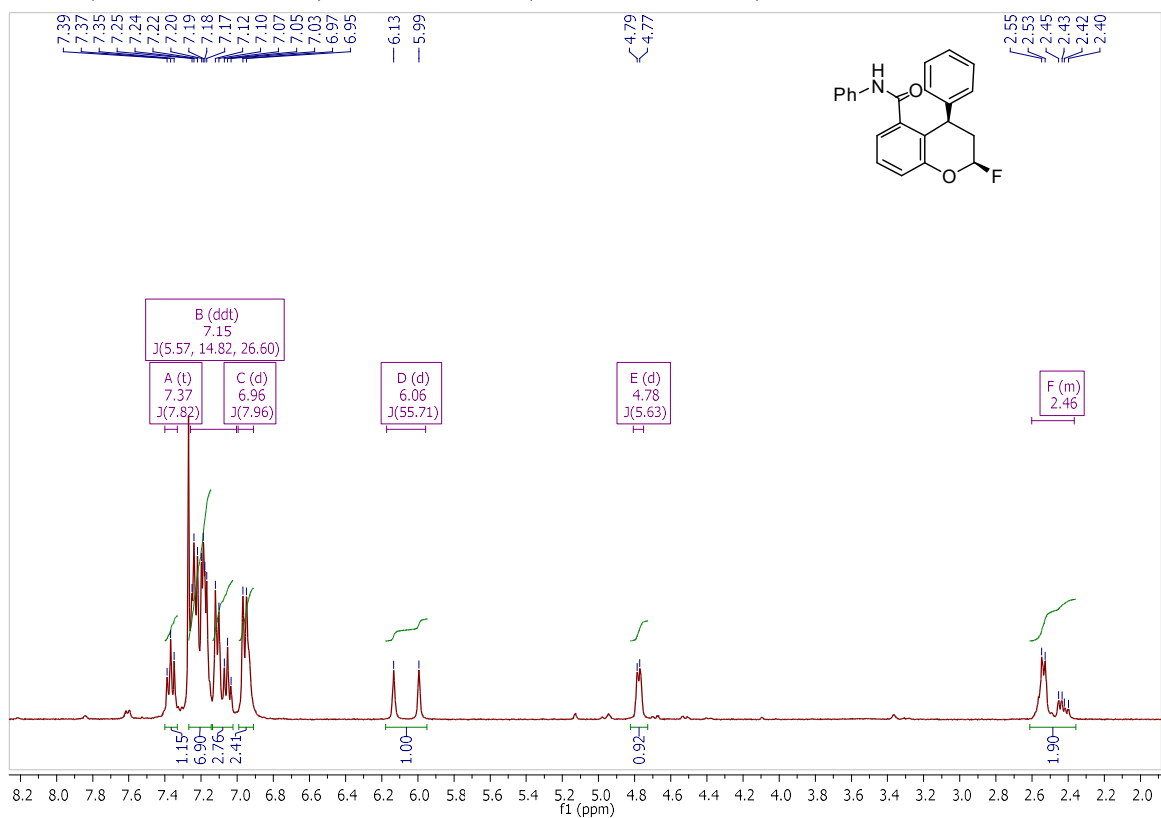


^1H 2D NOESY spectrum of **d₂-2a** :

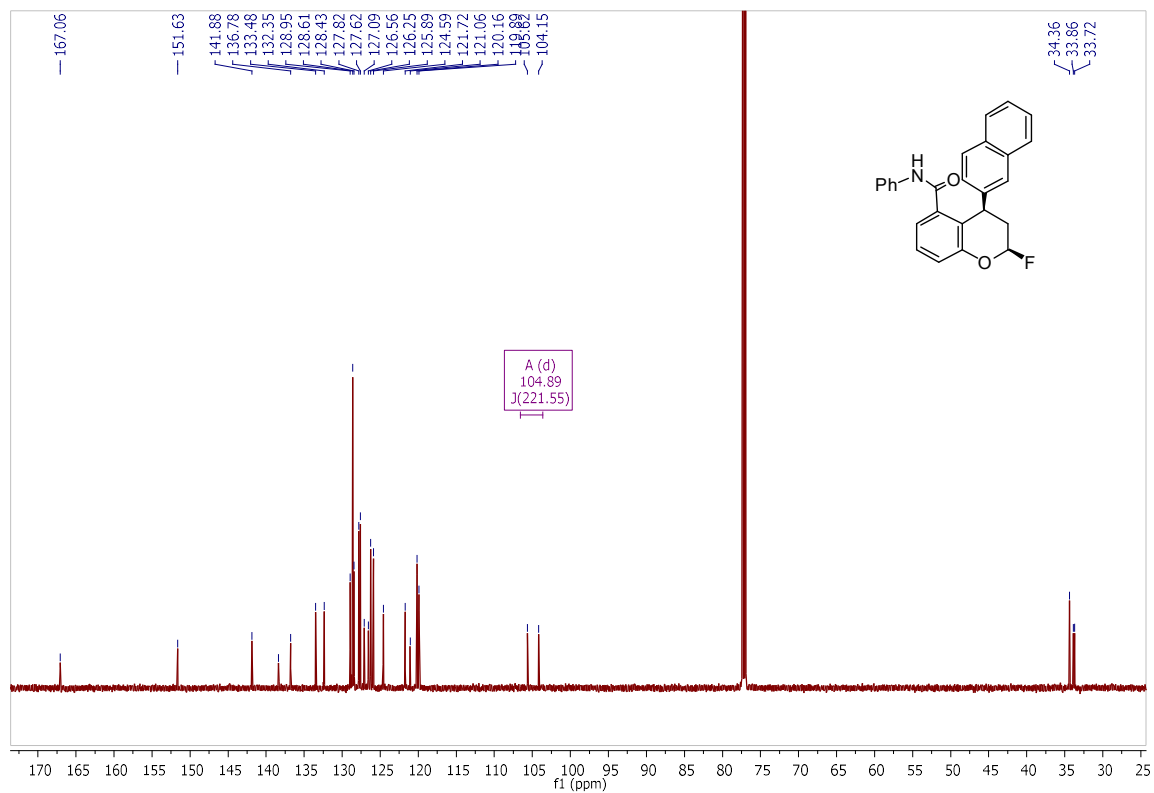
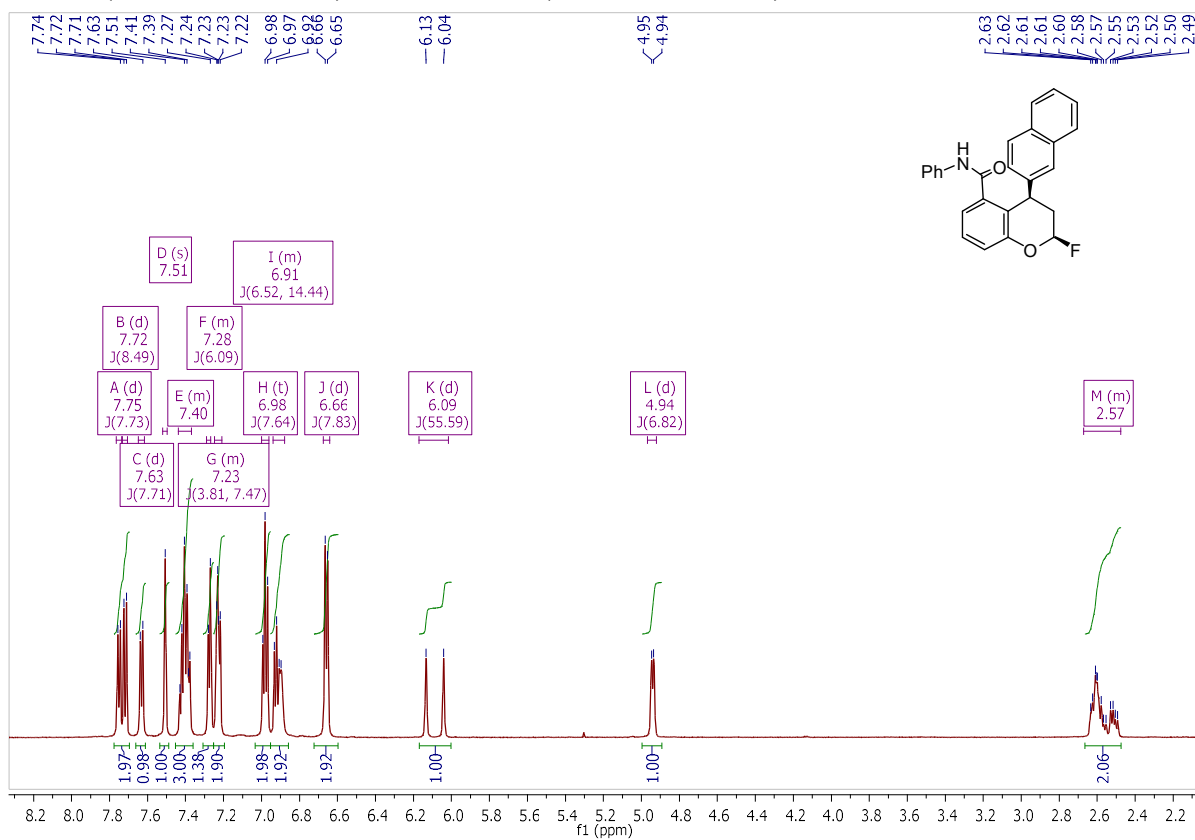




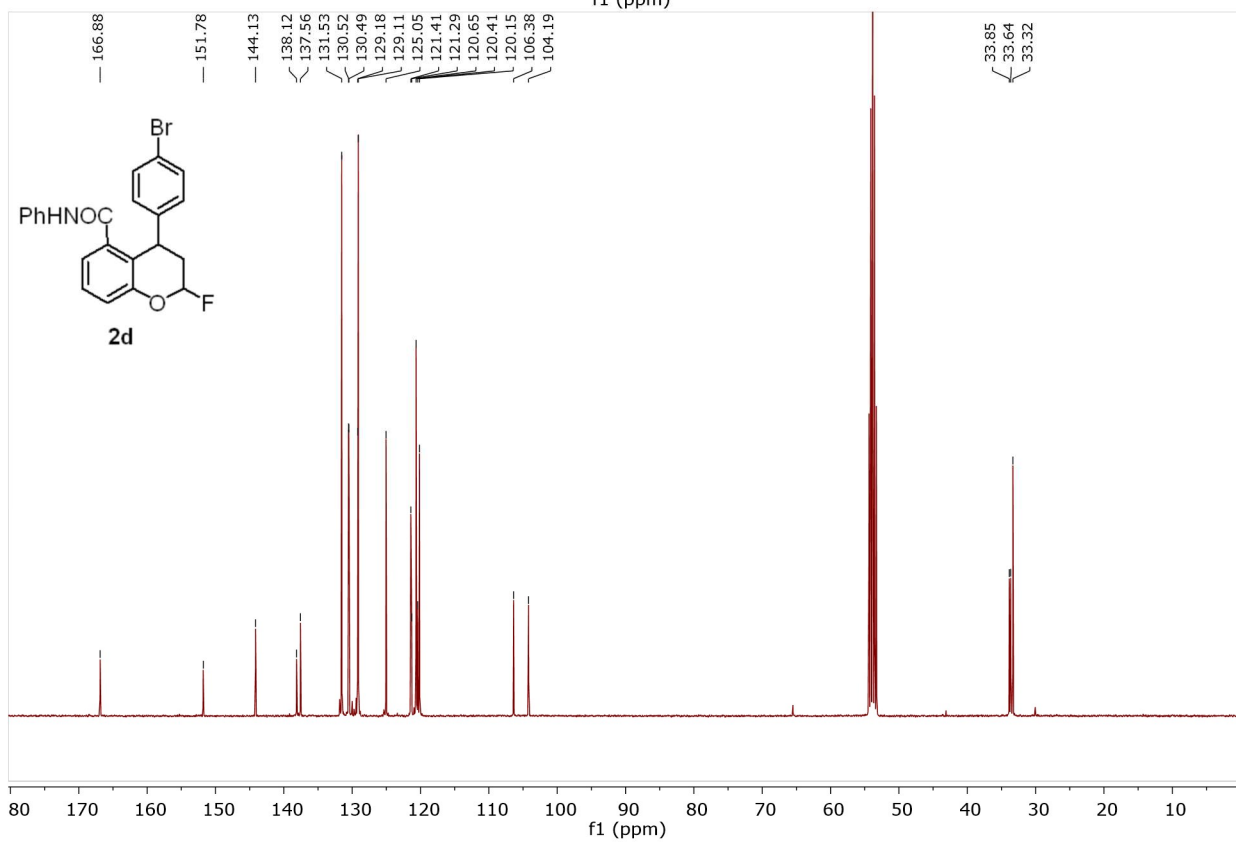
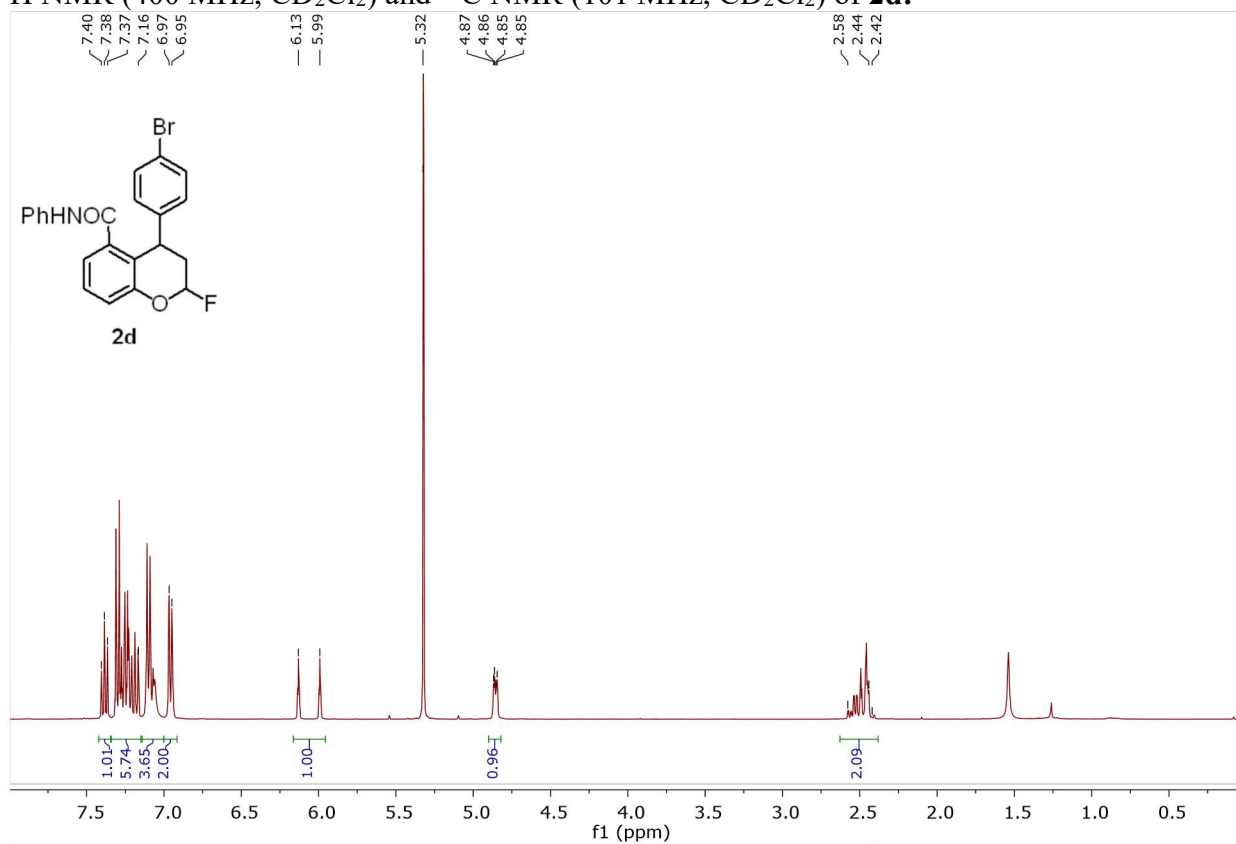
^1H NMR (400 MHz, CDCl_3) and ^{13}C NMR (101 MHz, CDCl_3) of **2b**:



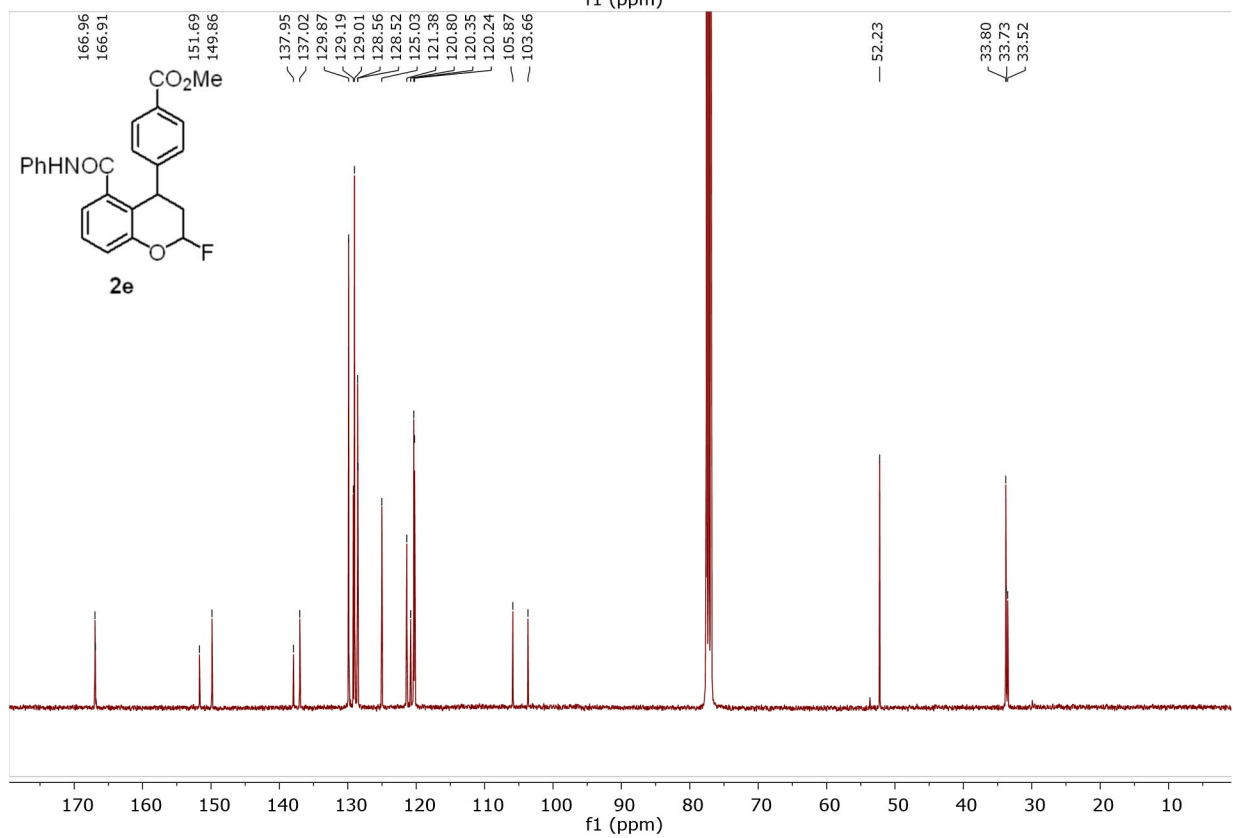
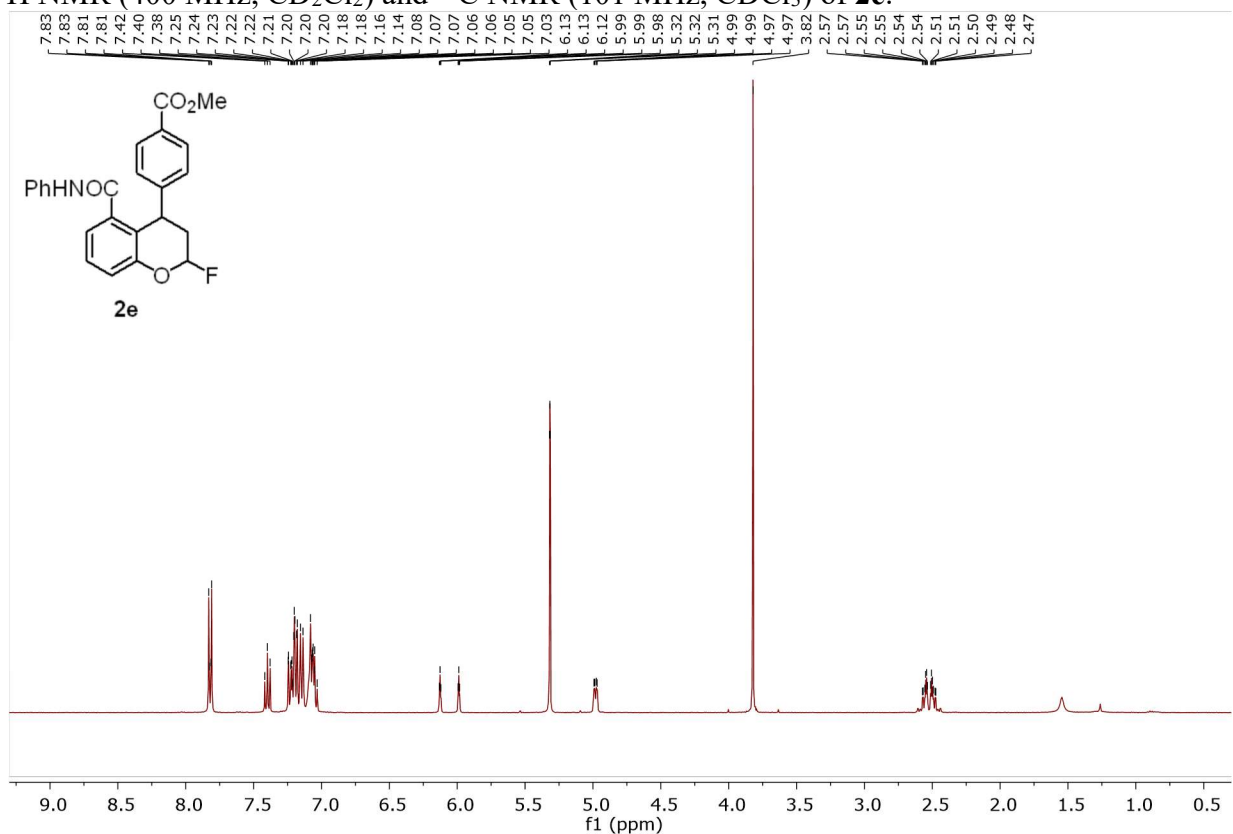
^1H NMR (600 MHz, CDCl_3) and ^{13}C NMR (151 MHz, CDCl_3) of **2c**:



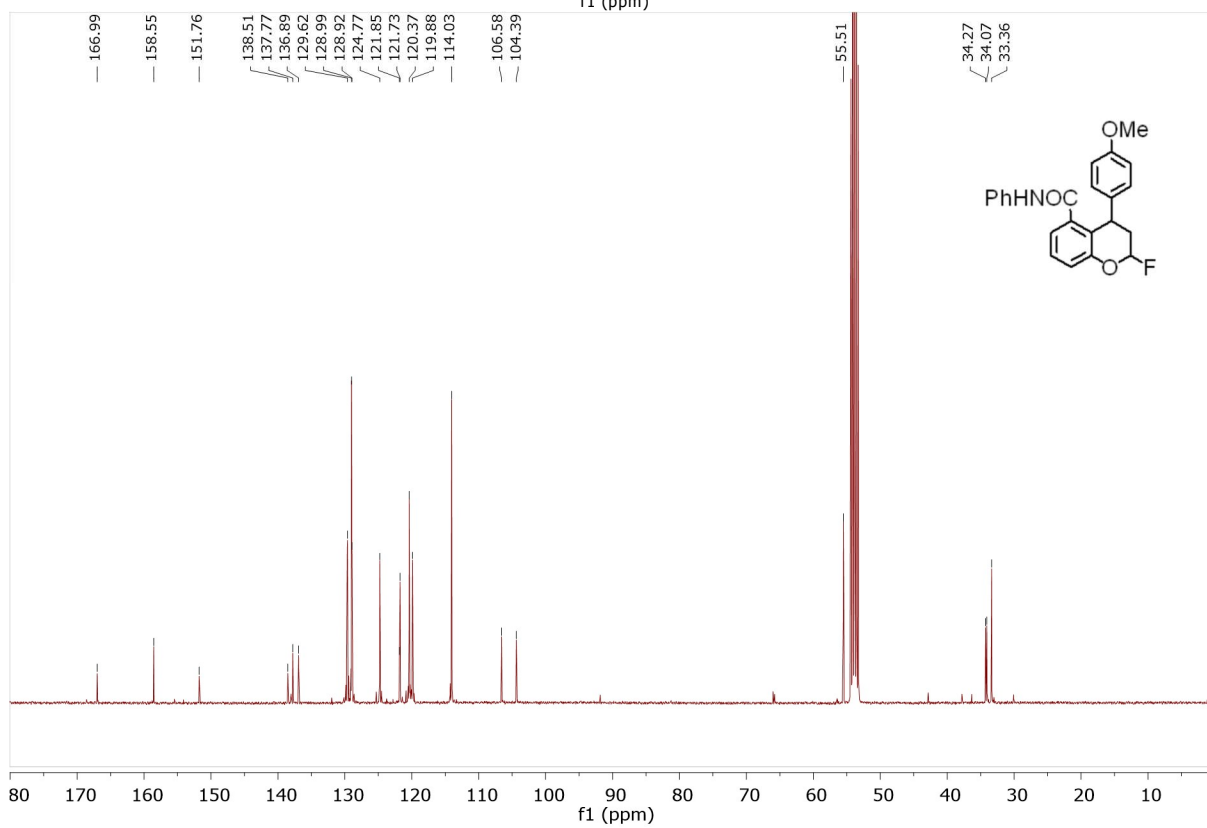
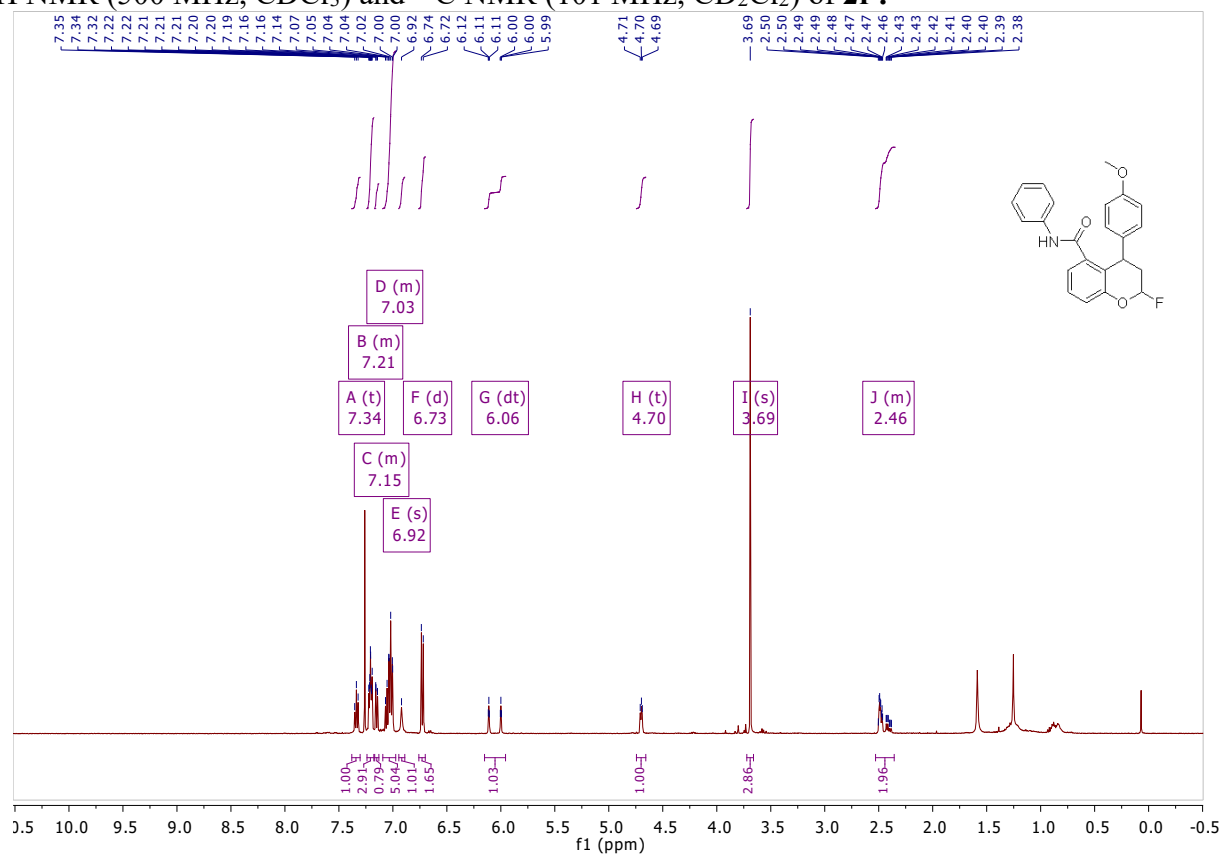
^1H NMR (400 MHz, CD_2Cl_2) and ^{13}C NMR (101 MHz, CD_2Cl_2) of **2d**:



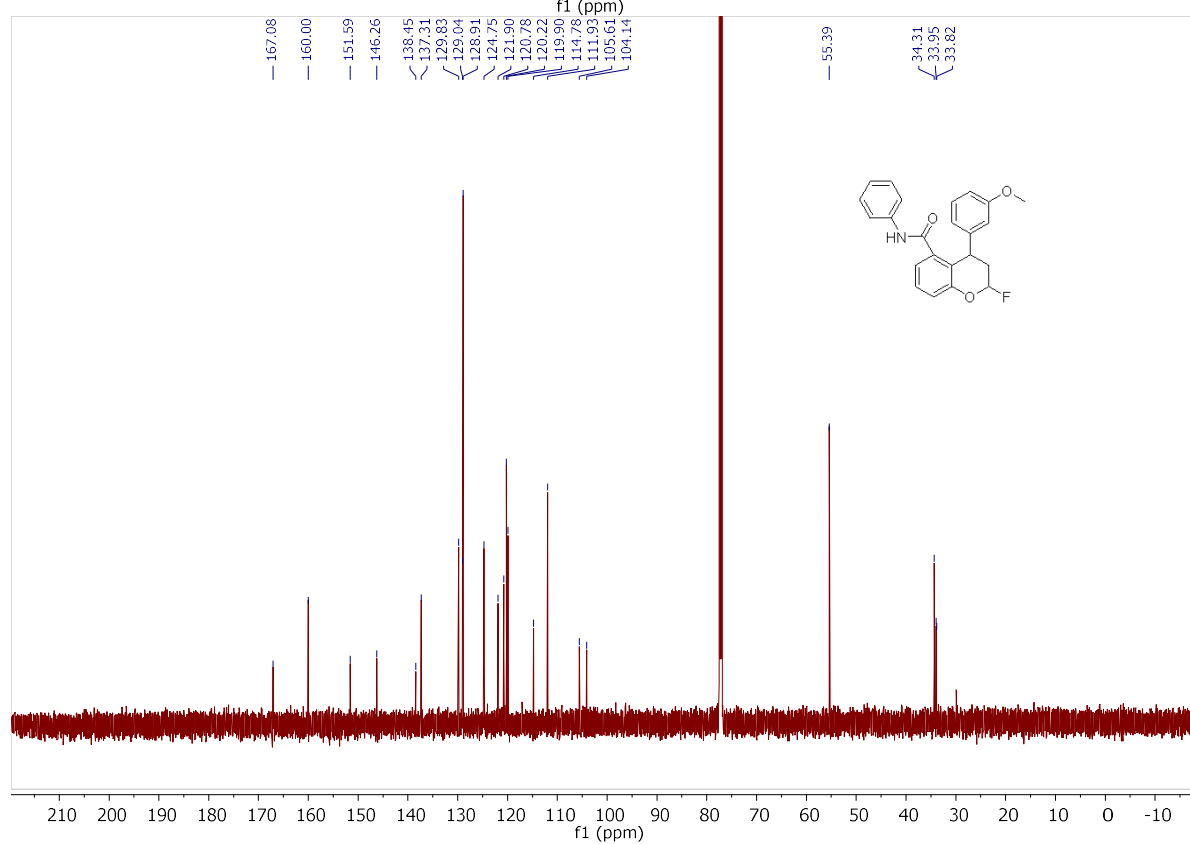
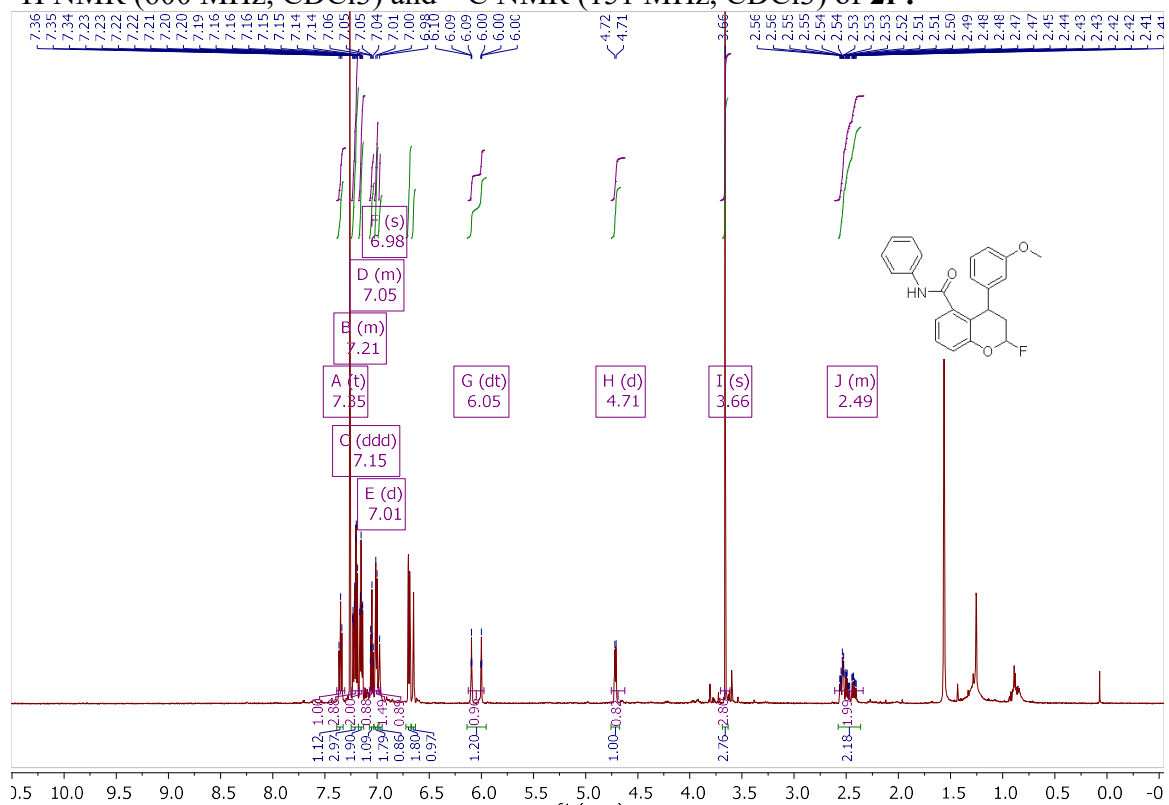
^1H NMR (400 MHz, CD_2Cl_2) and ^{13}C NMR (101 MHz, CDCl_3) of **2e**:



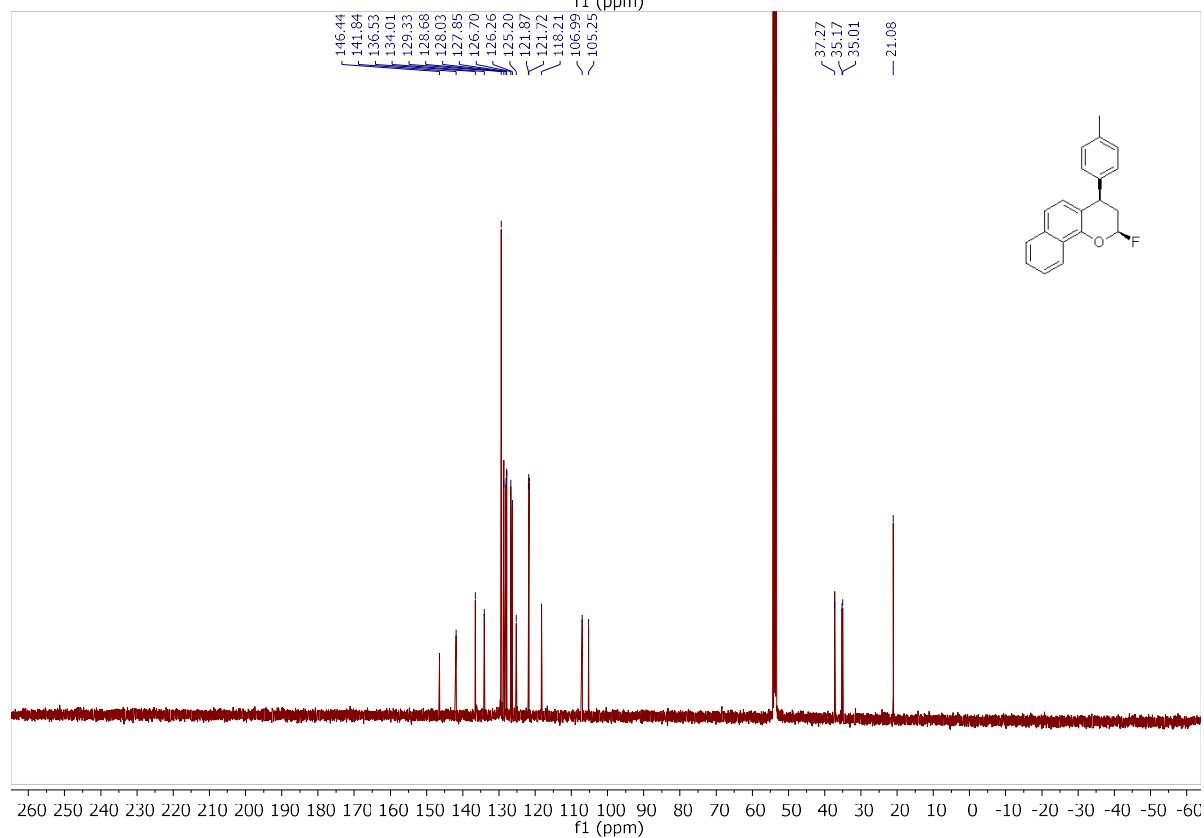
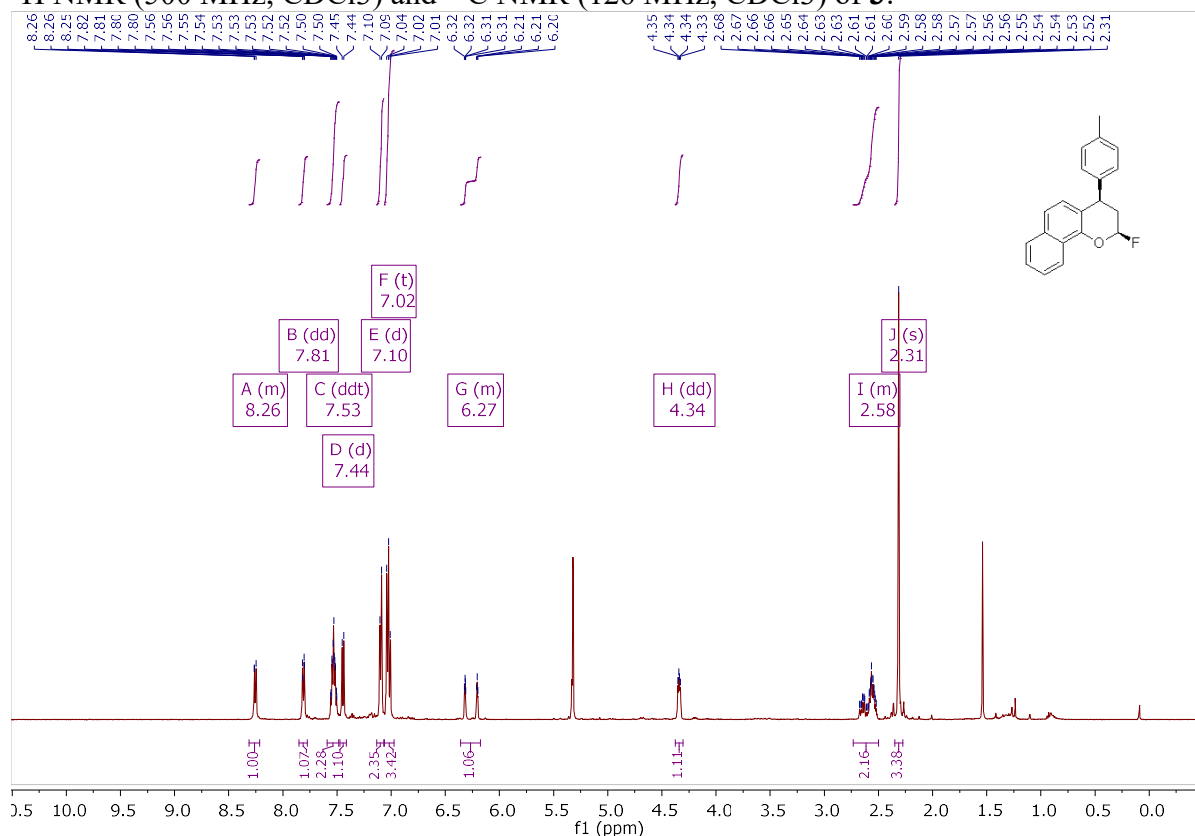
^1H NMR (500 MHz, CDCl_3) and ^{13}C NMR (101 MHz, CD_2Cl_2) of **2f**:



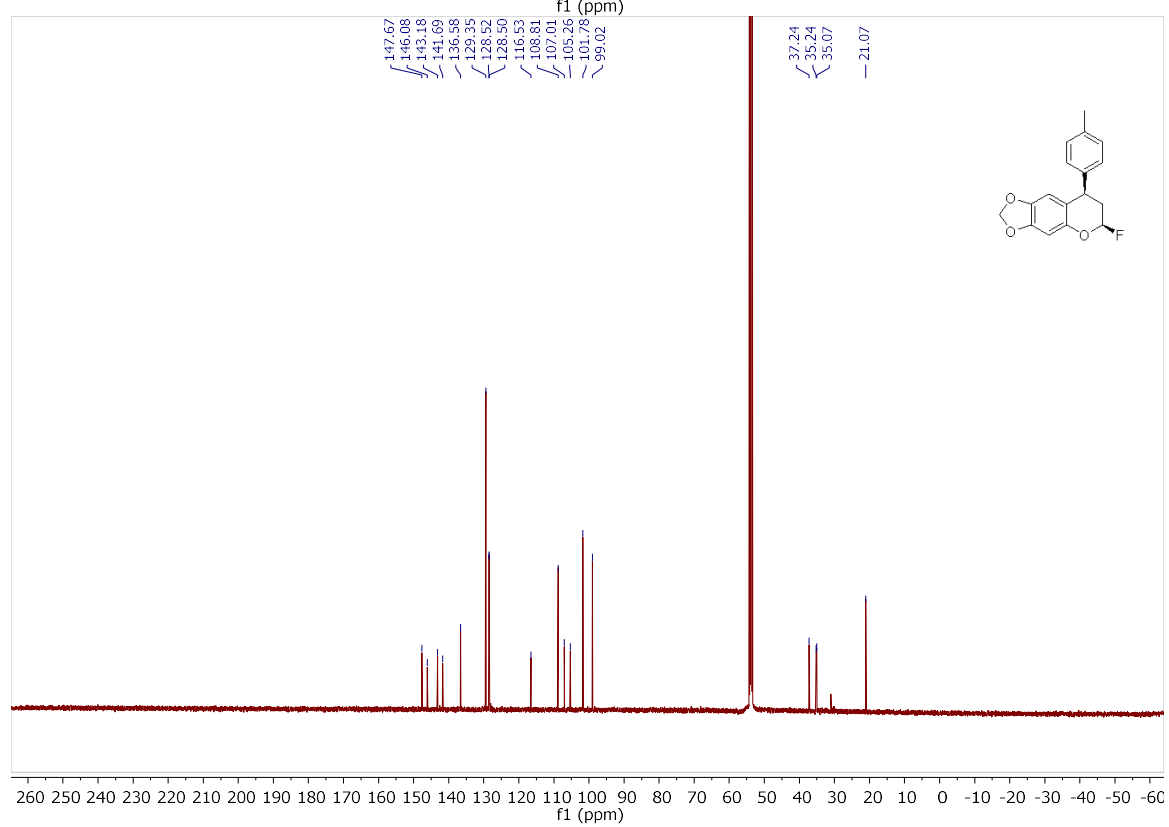
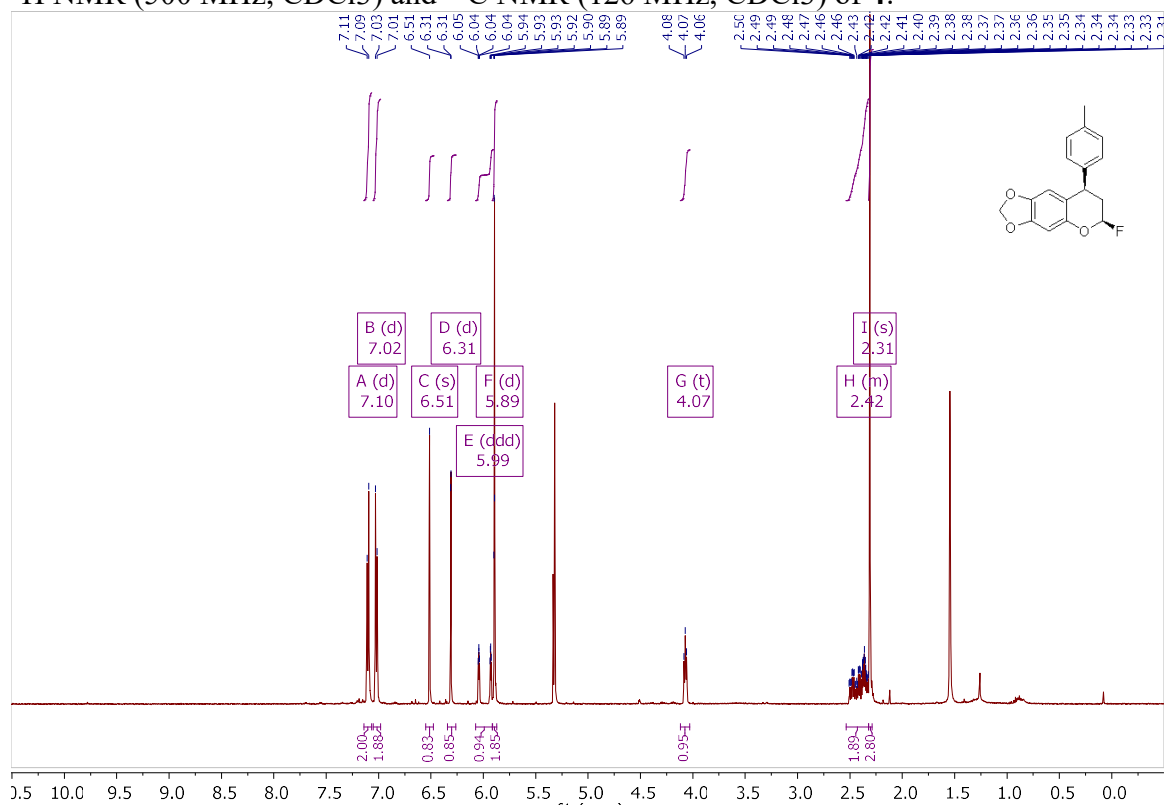
^1H NMR (600 MHz, CDCl_3) and ^{13}C NMR (151 MHz, CDCl_3) of **2f**:



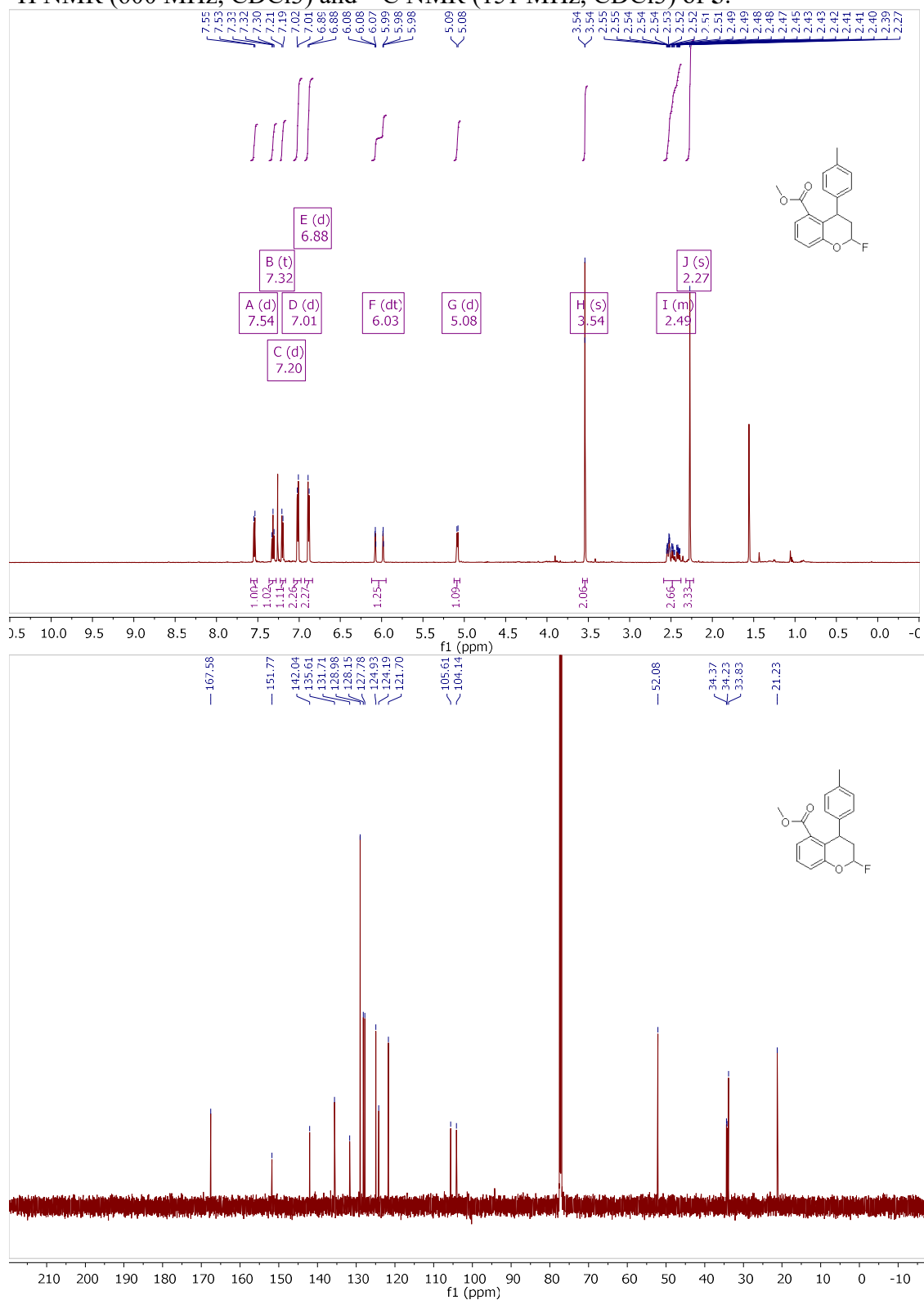
¹H NMR (500 MHz, CDCl₃) and ¹³C NMR (126 MHz, CDCl₃) of **3**:



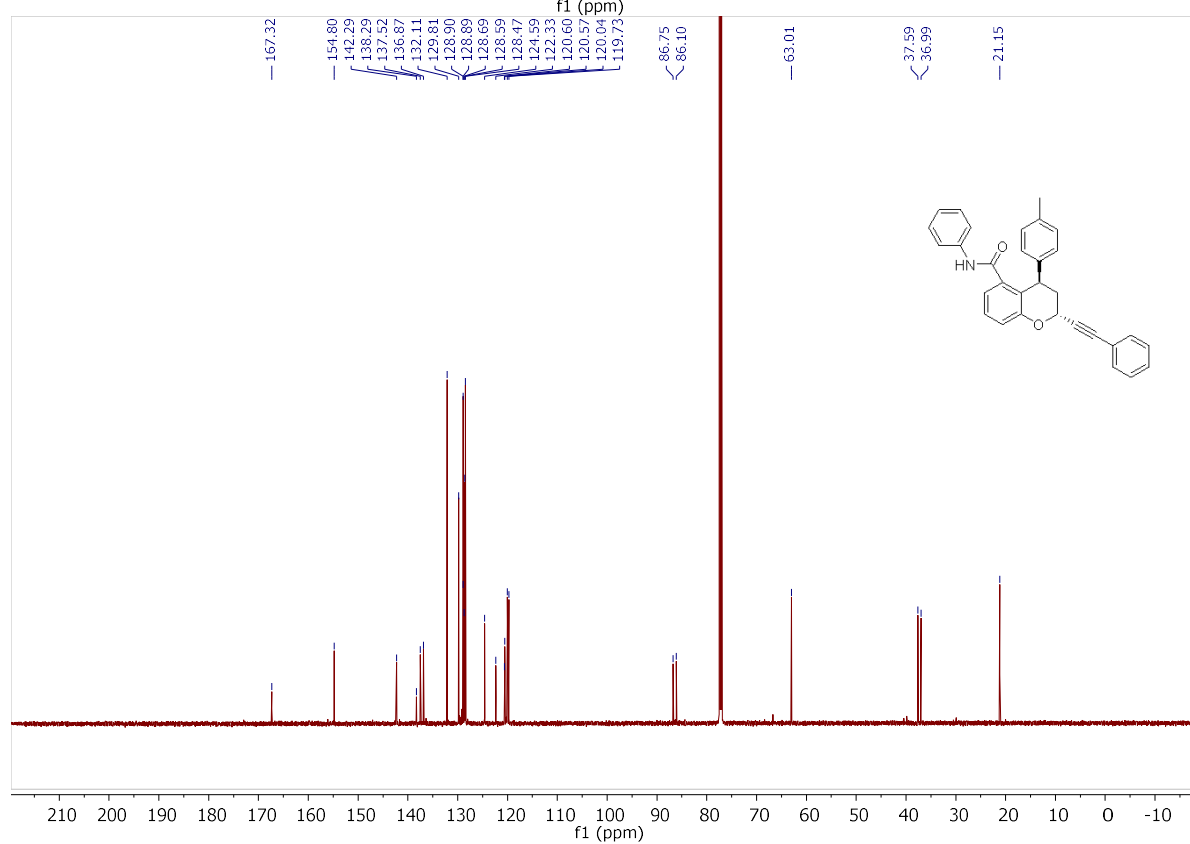
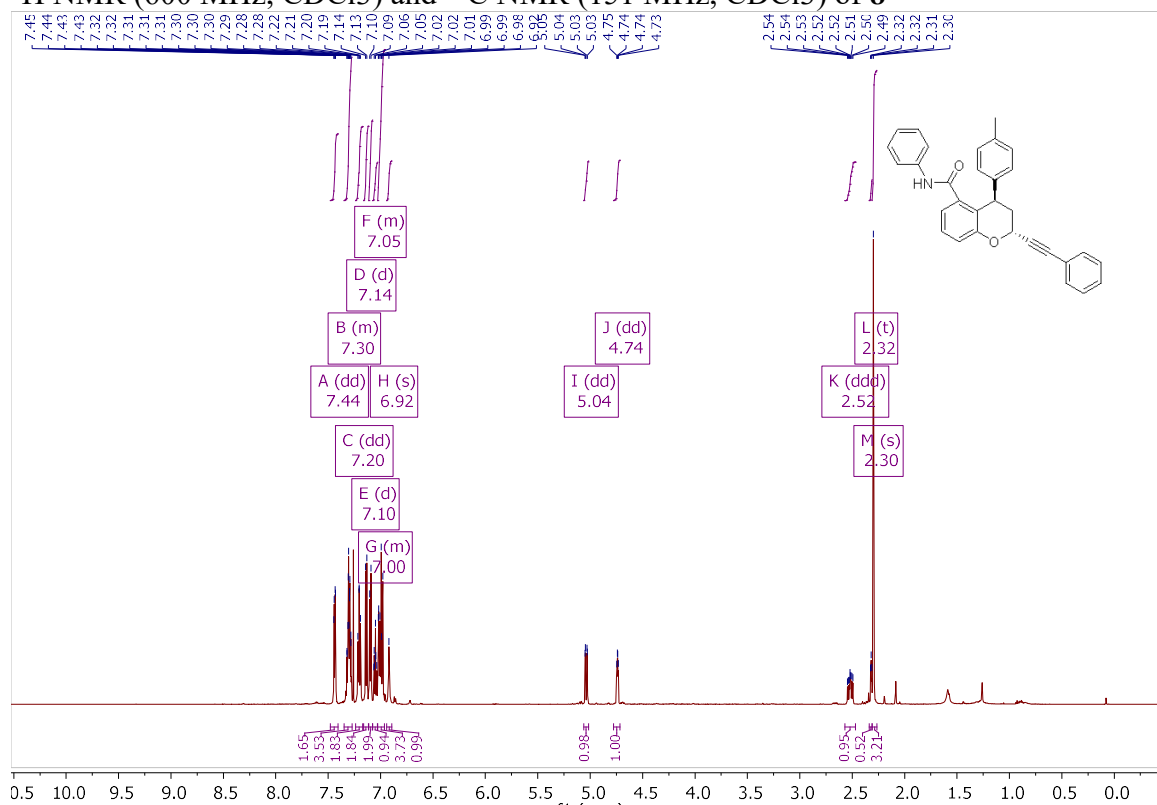
^1H NMR (500 MHz, CDCl_3) and ^{13}C NMR (126 MHz, CDCl_3) of 4:



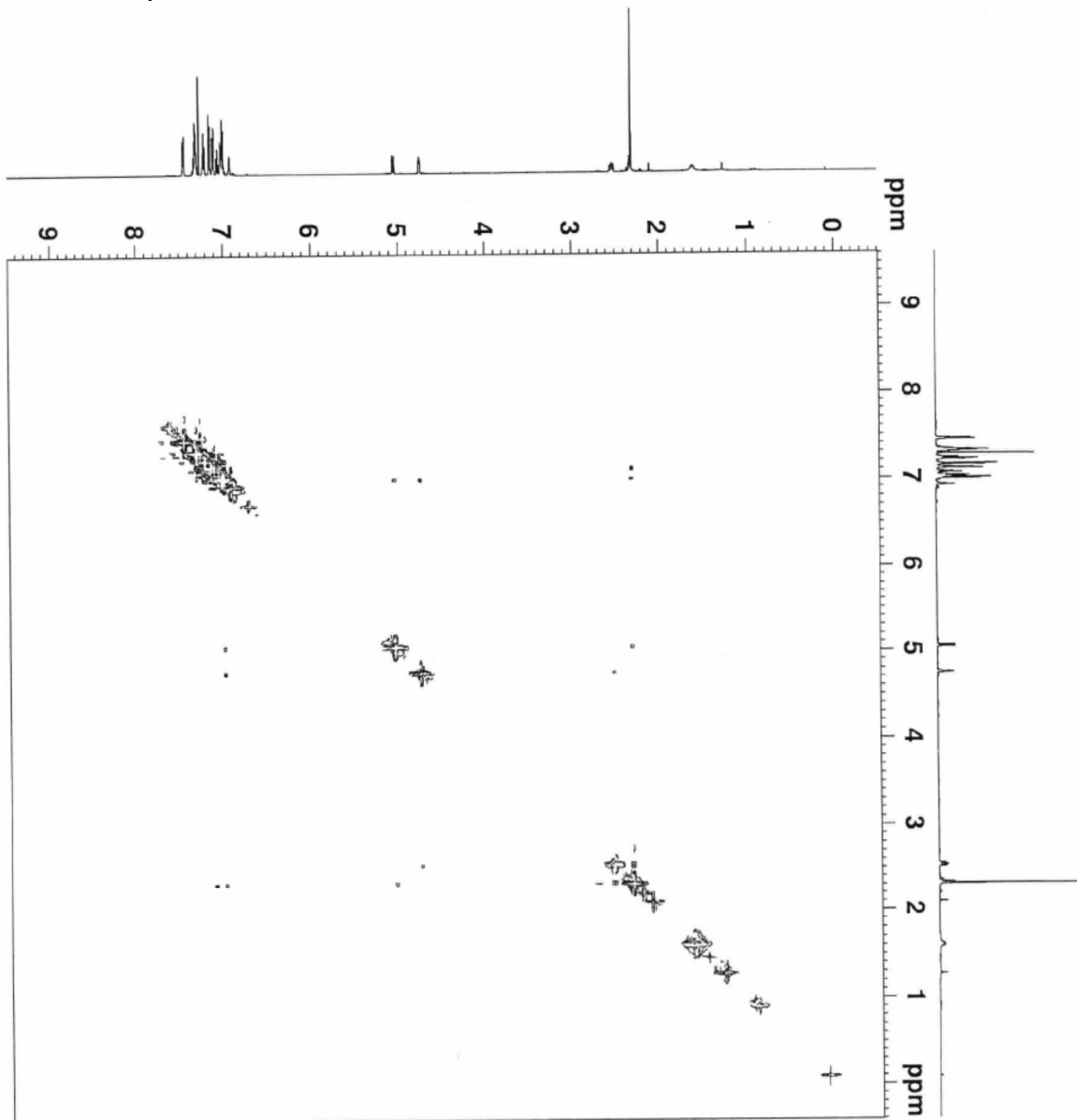
^1H NMR (600 MHz, CDCl_3) and ^{13}C NMR (151 MHz, CDCl_3) of **5**:

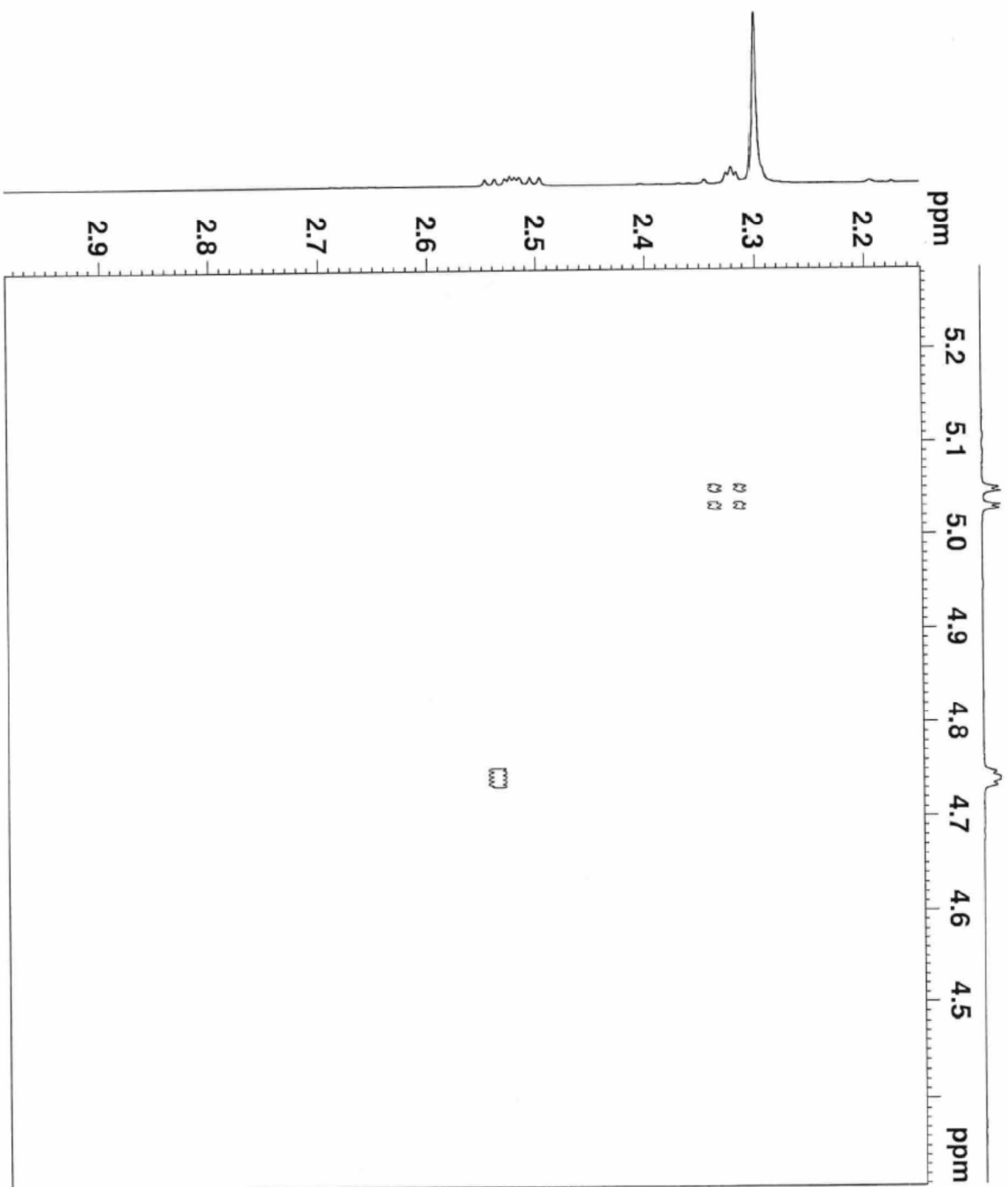


^1H NMR (600 MHz, CDCl_3) and ^{13}C NMR (151 MHz, CDCl_3) of **8**

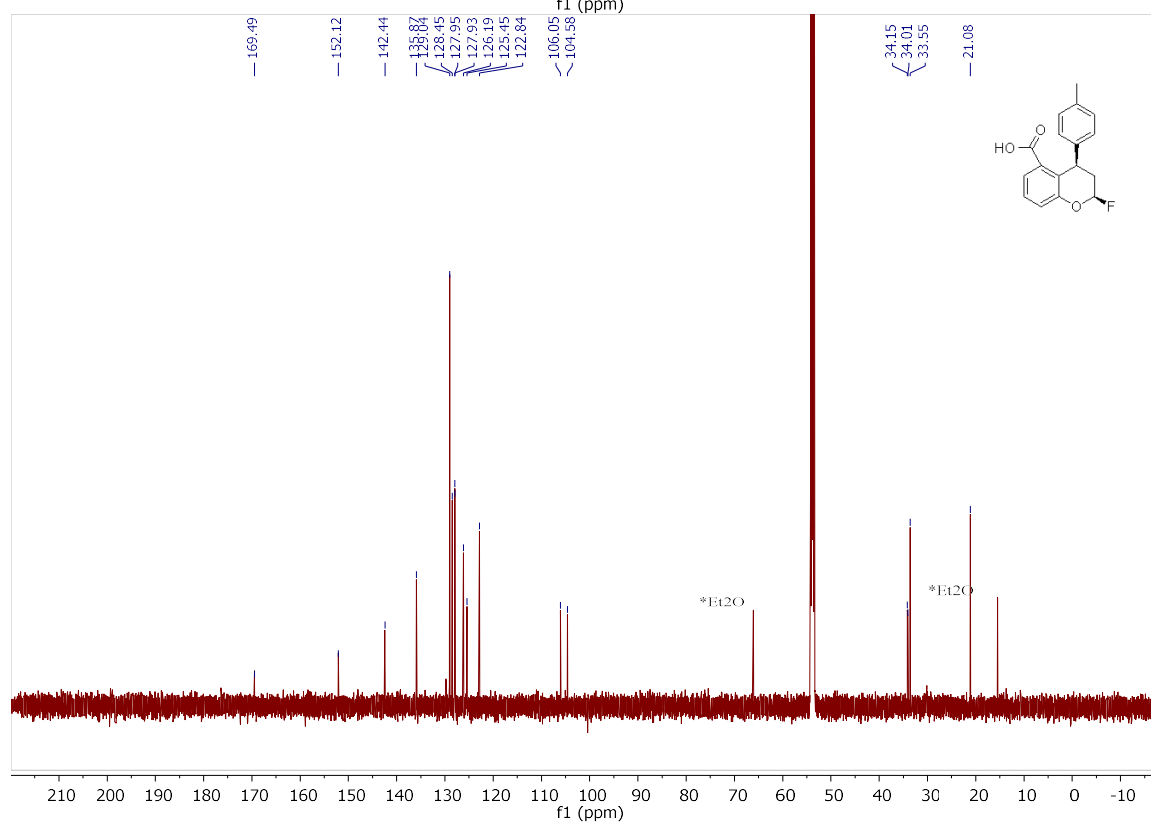
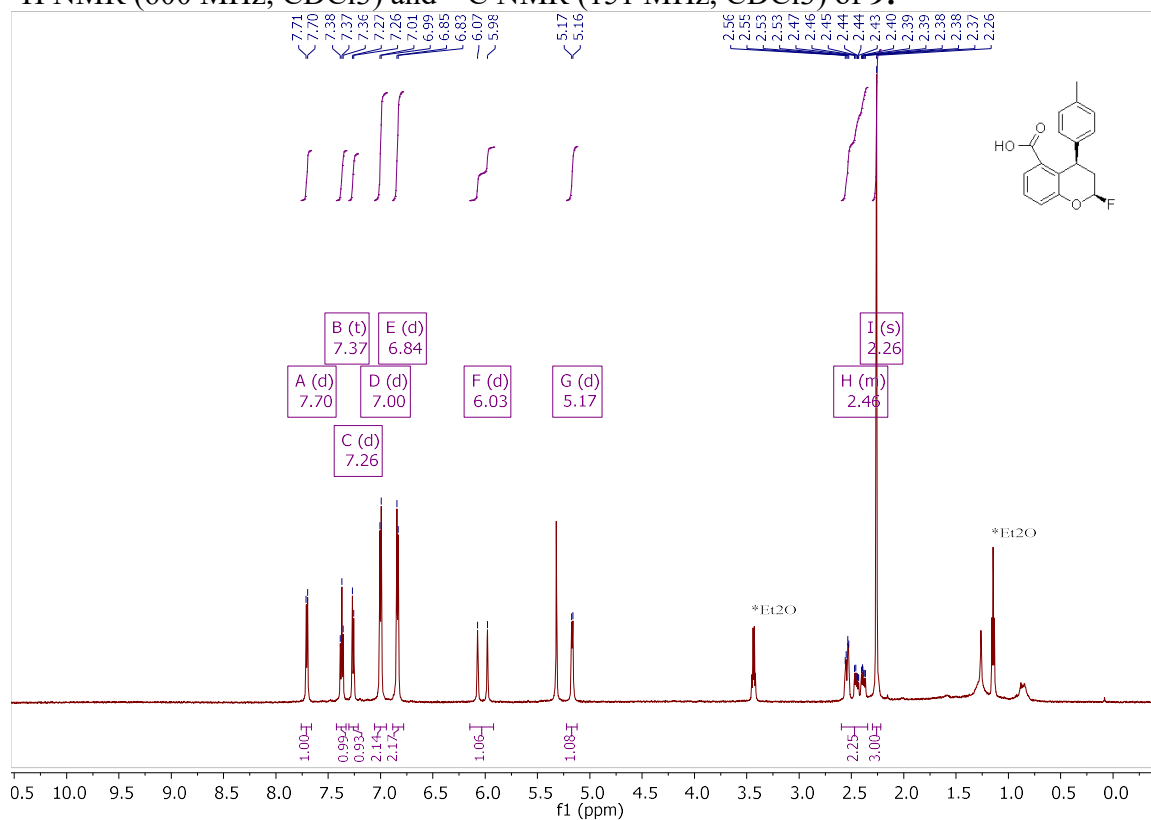


^1H 2D NOESY spectrum of **8**:

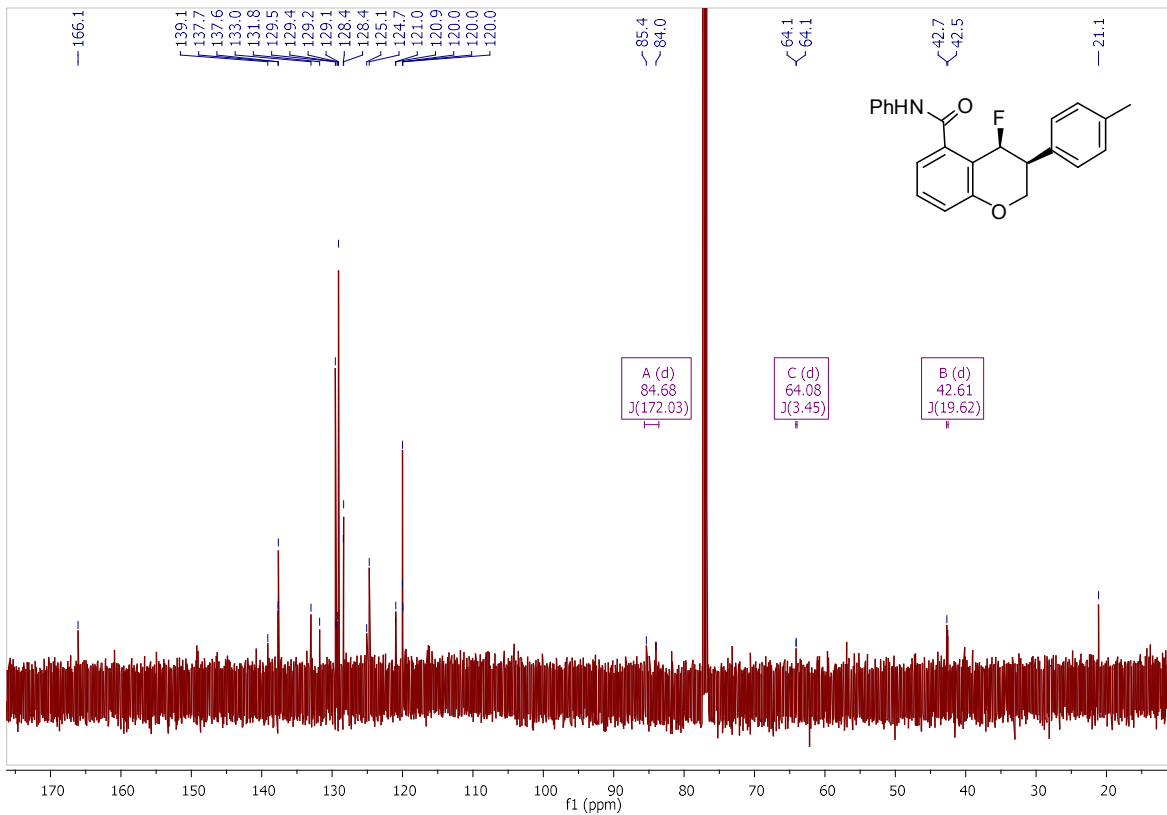
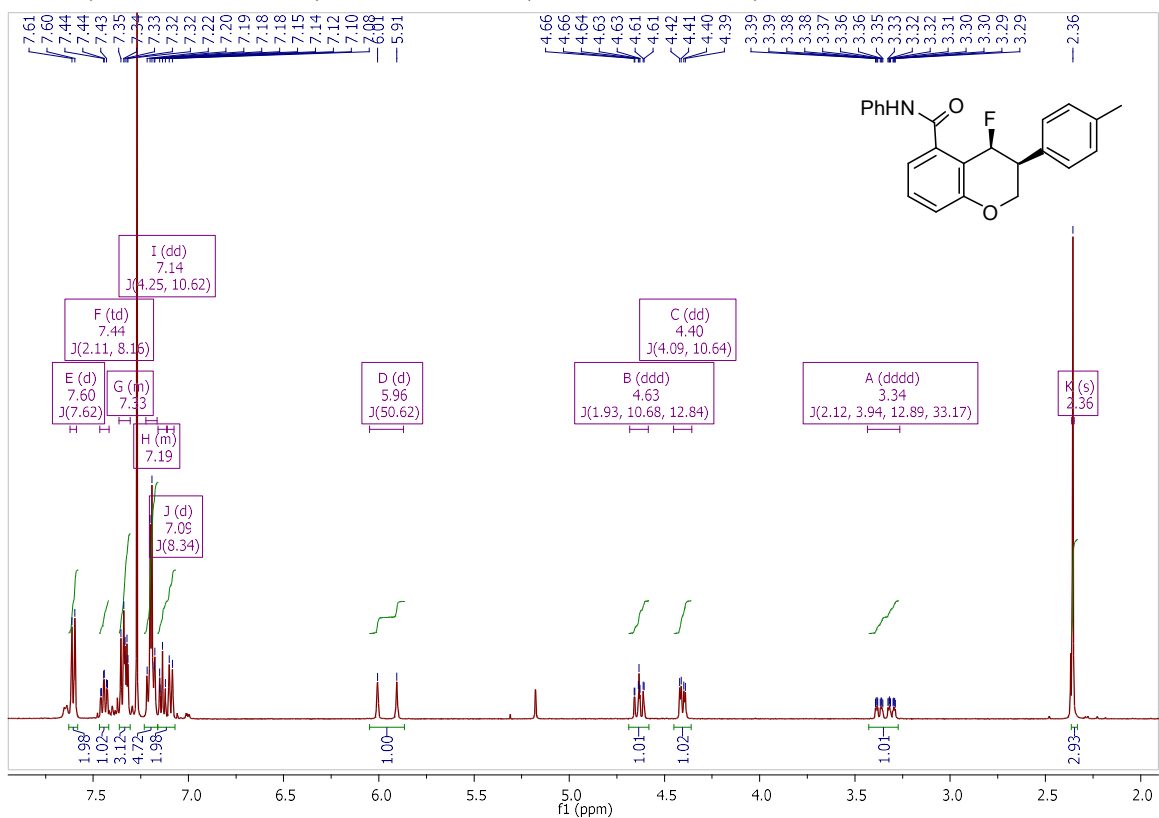




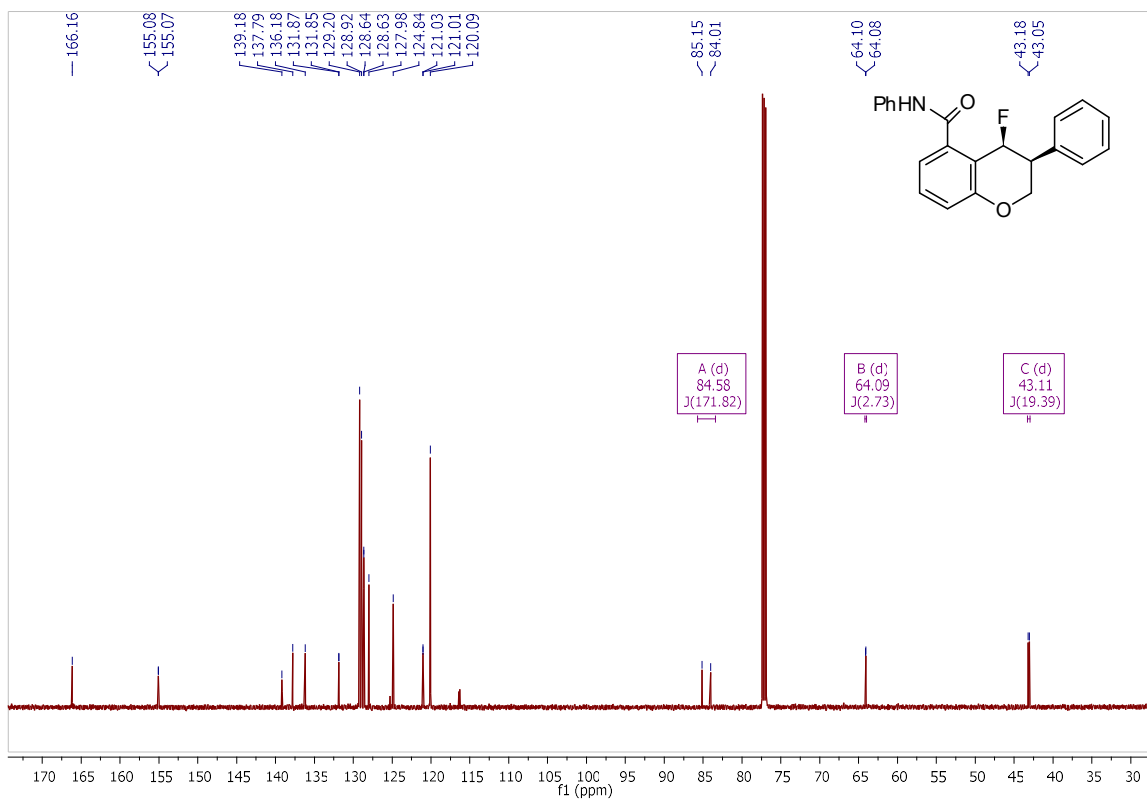
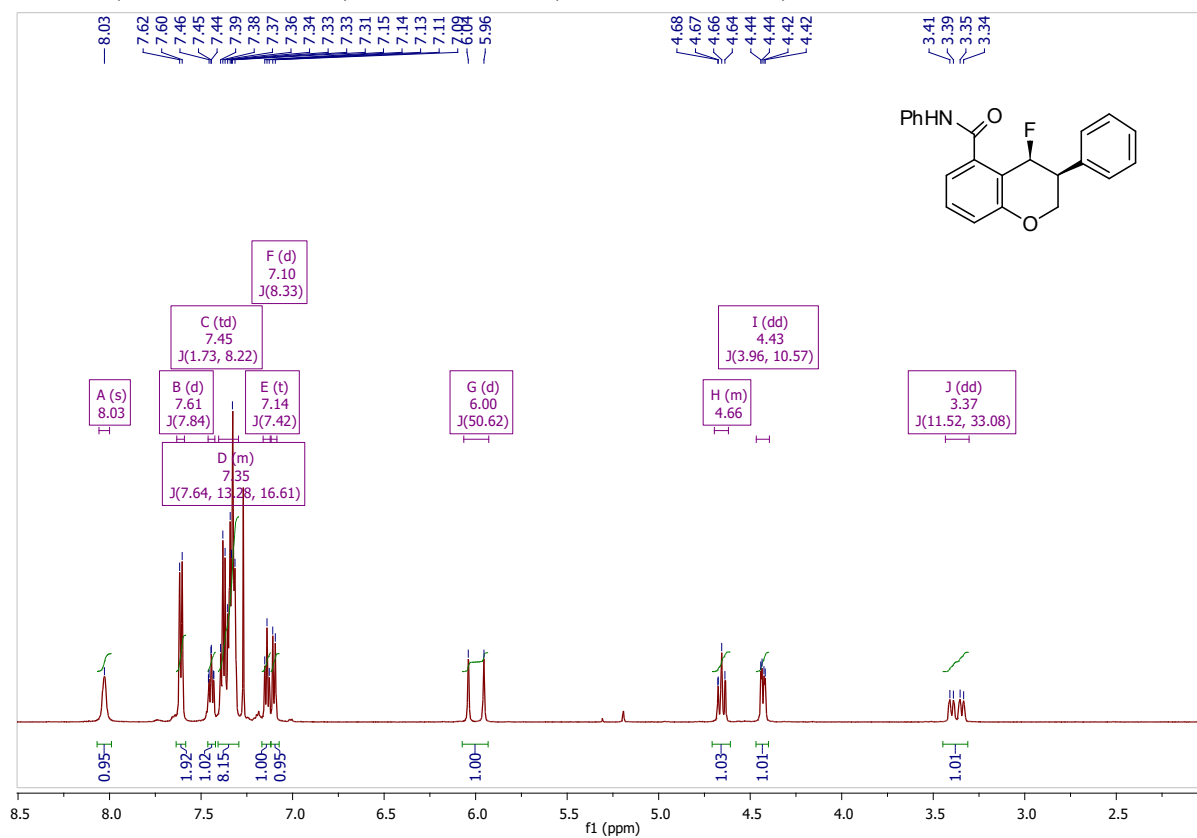
^1H NMR (600 MHz, CDCl_3) and ^{13}C NMR (151 MHz, CDCl_3) of **9**:



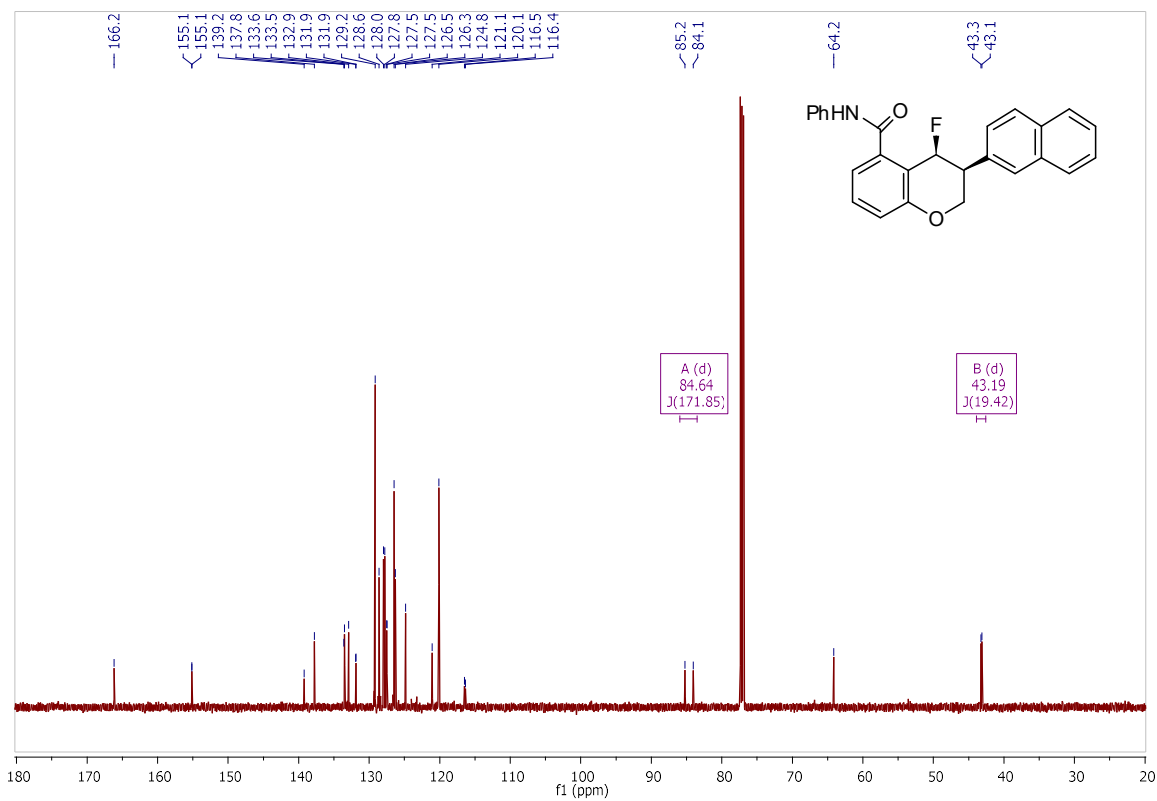
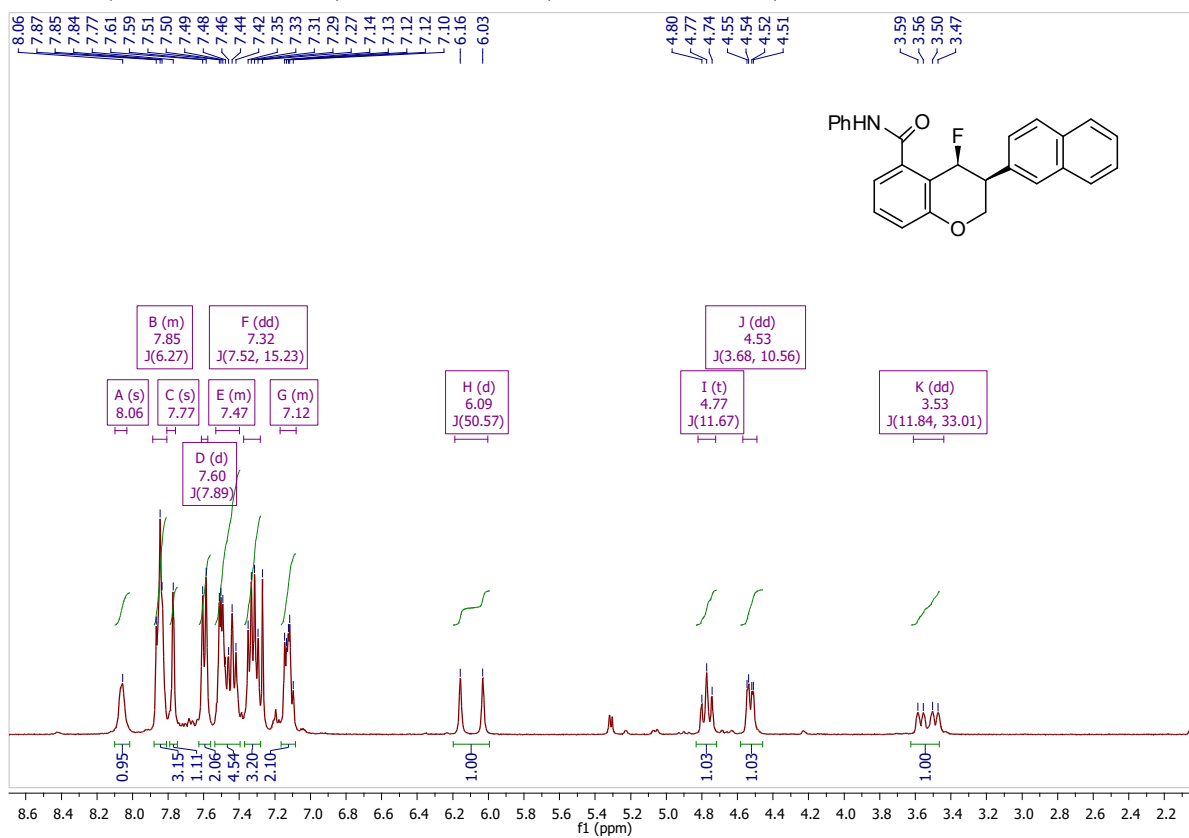
^1H NMR (500 MHz, CDCl_3) and ^{13}C NMR (126 MHz, CDCl_3) of **10a**:



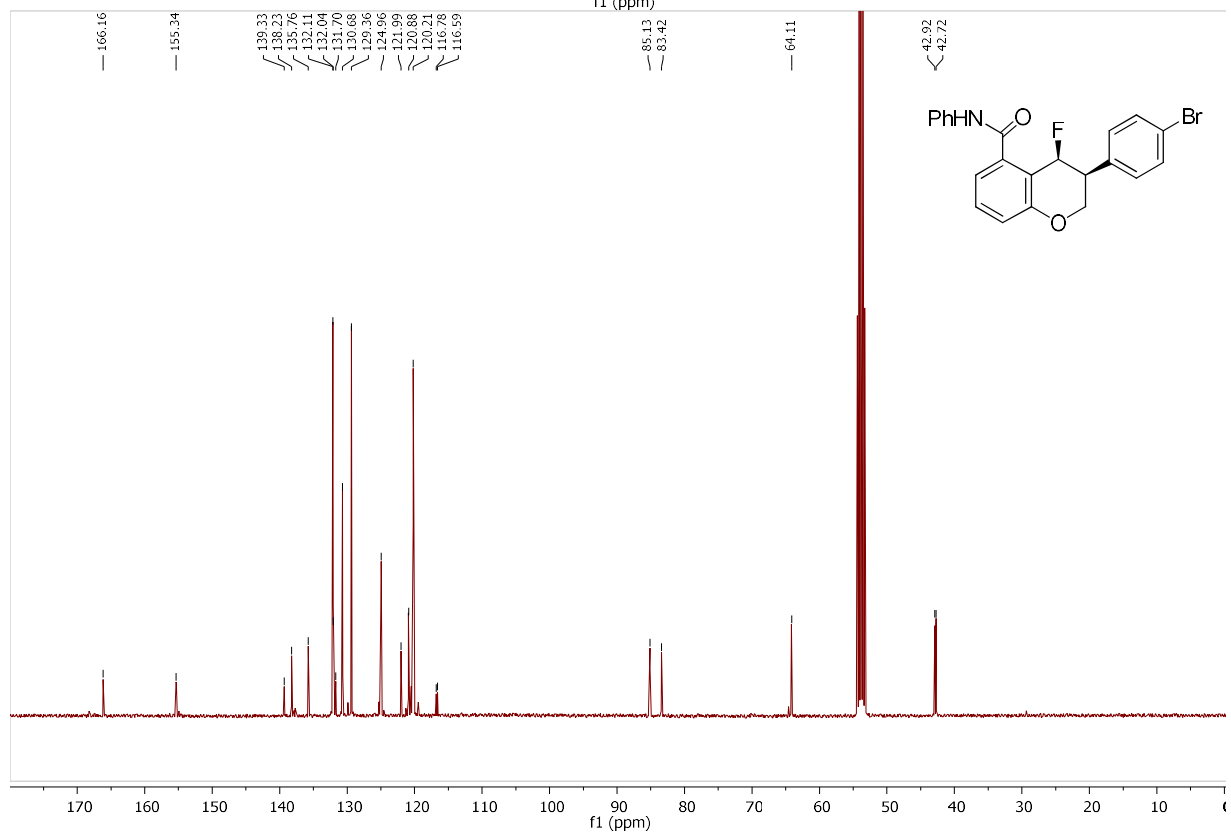
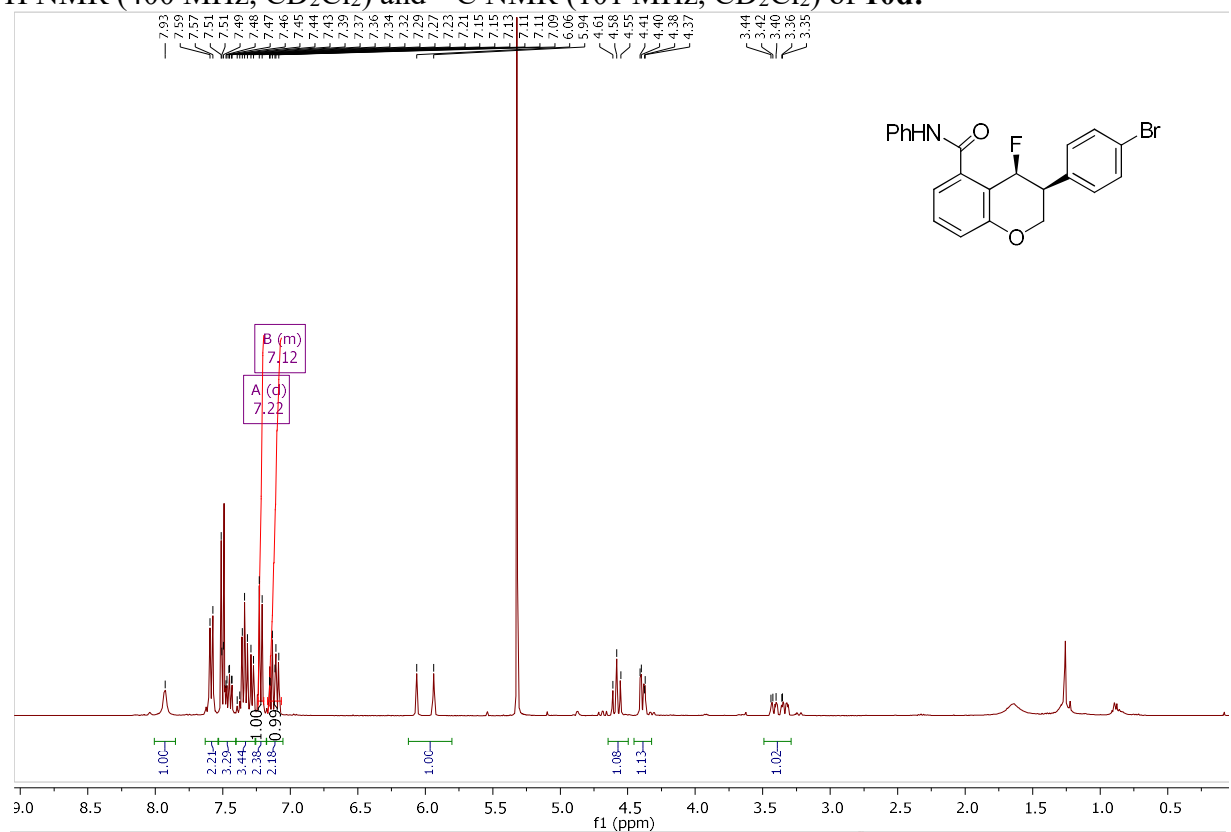
^1H NMR (600 MHz, CDCl_3) and ^{13}C NMR (151 MHz, CDCl_3) of **10b**:



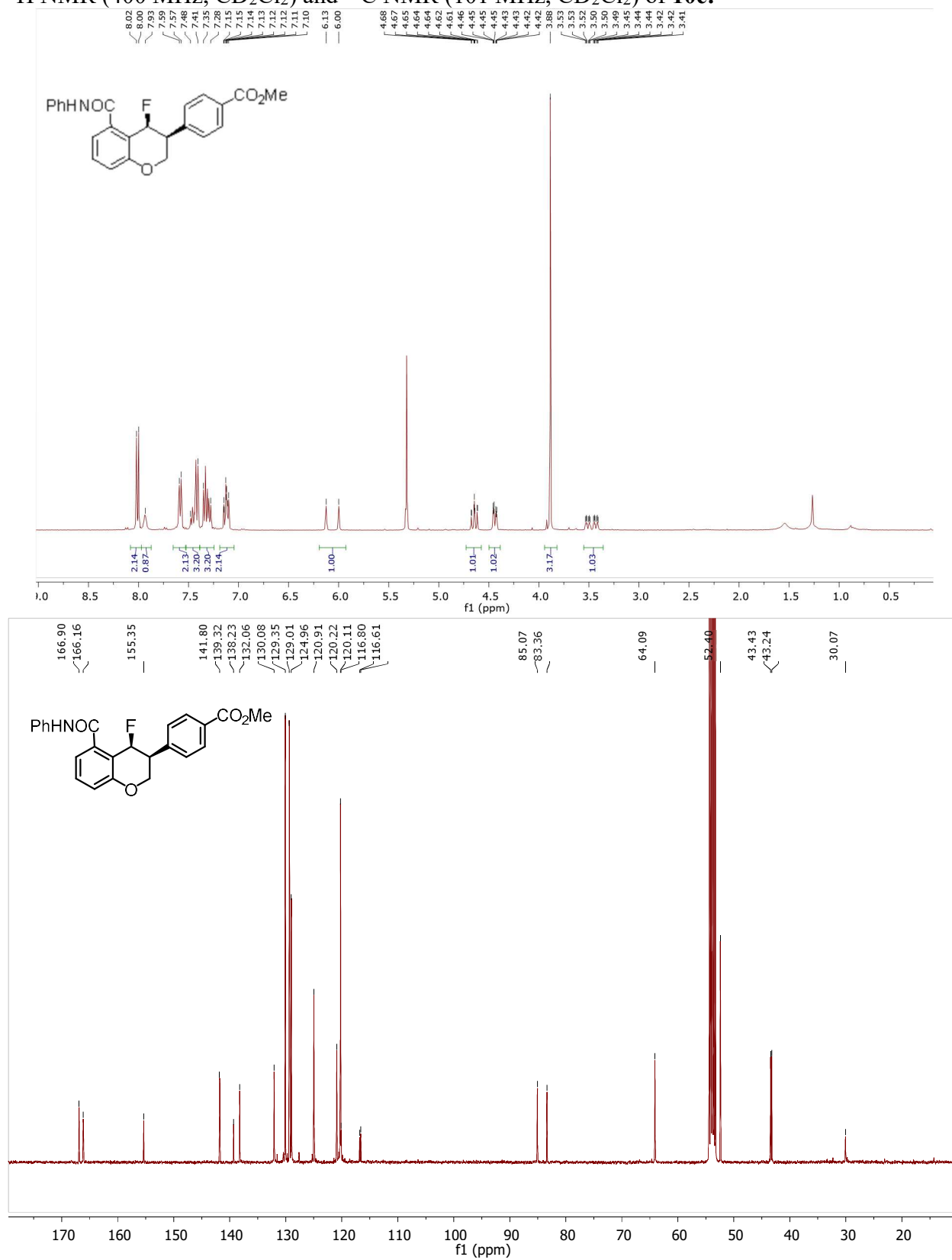
^1H NMR (400 MHz, CDCl_3) and ^{13}C NMR (151 MHz, CDCl_3) of **10c**:



^1H NMR (400 MHz, CD_2Cl_2) and ^{13}C NMR (101 MHz, CD_2Cl_2) of **10d**:

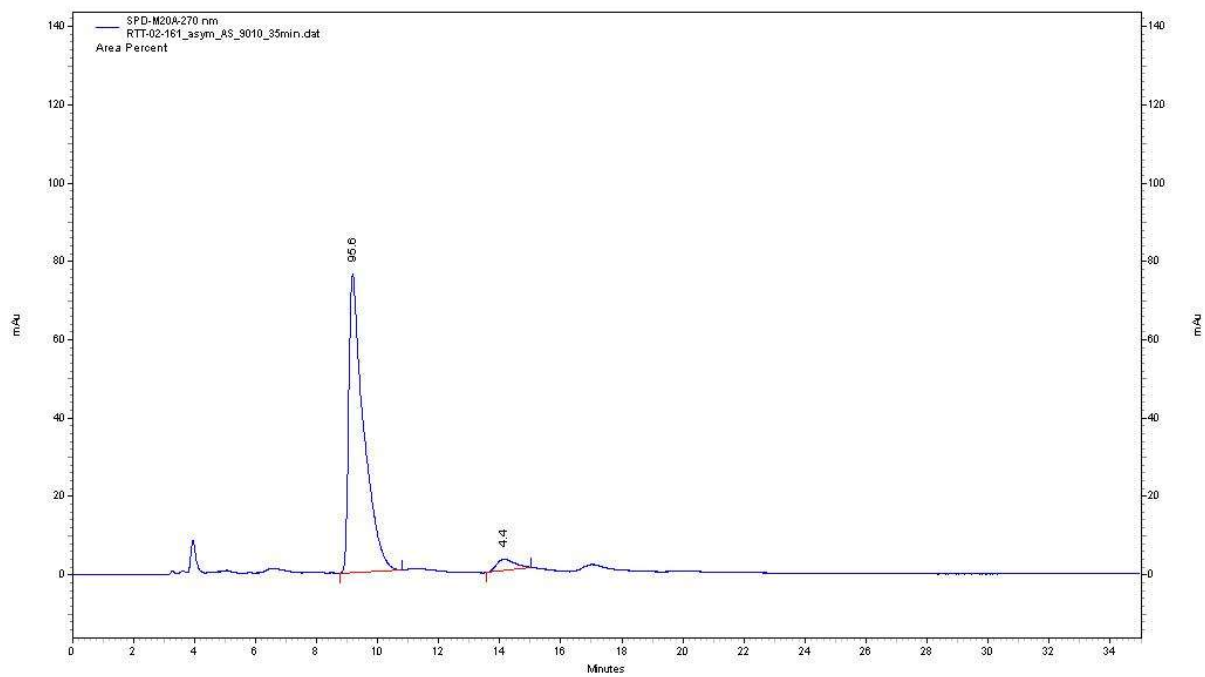
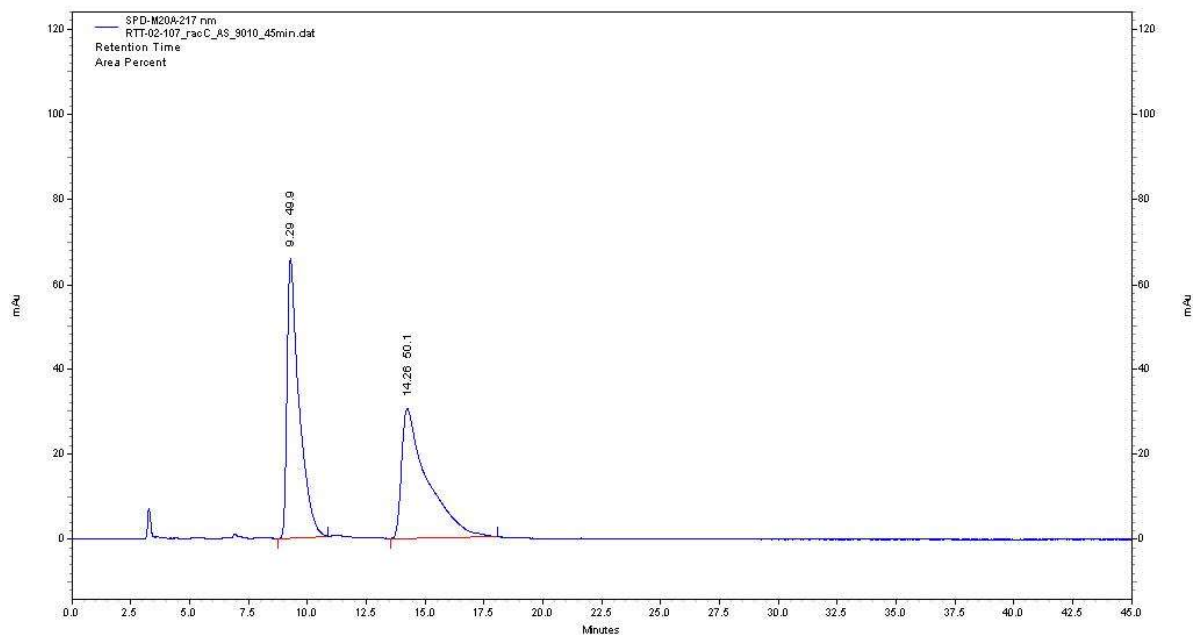
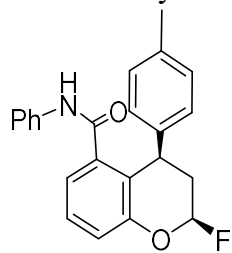


^1H NMR (400 MHz, CD_2Cl_2) and ^{13}C NMR (101 MHz, CD_2Cl_2) of **10e**:

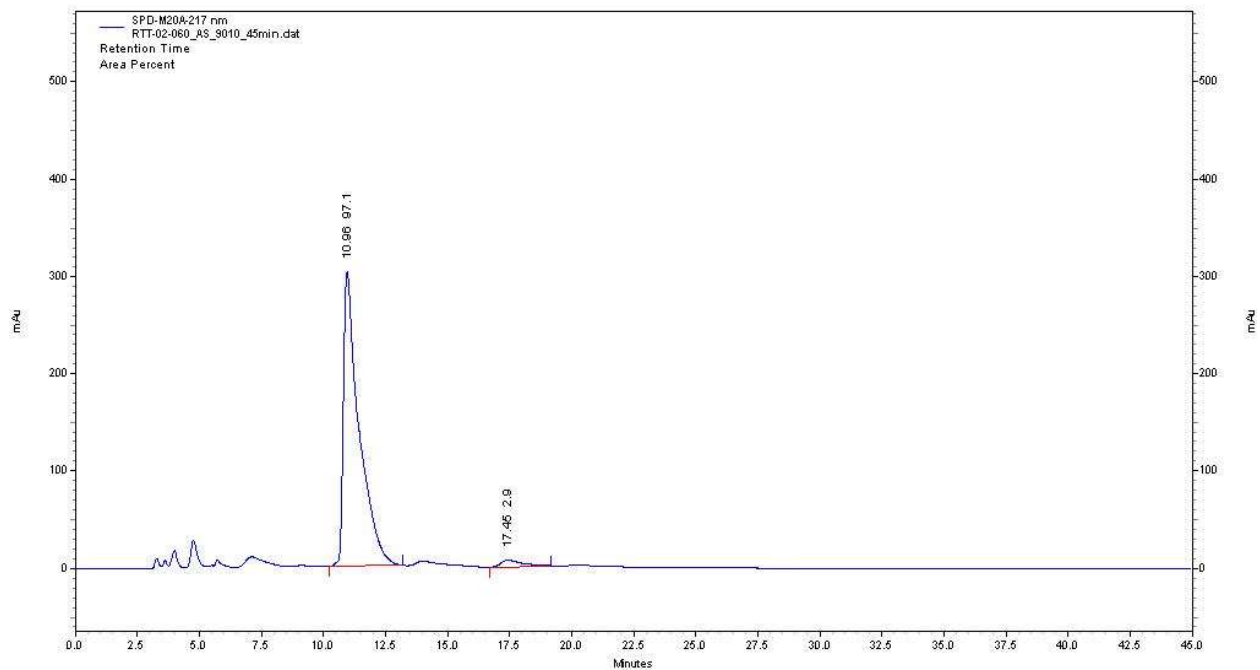
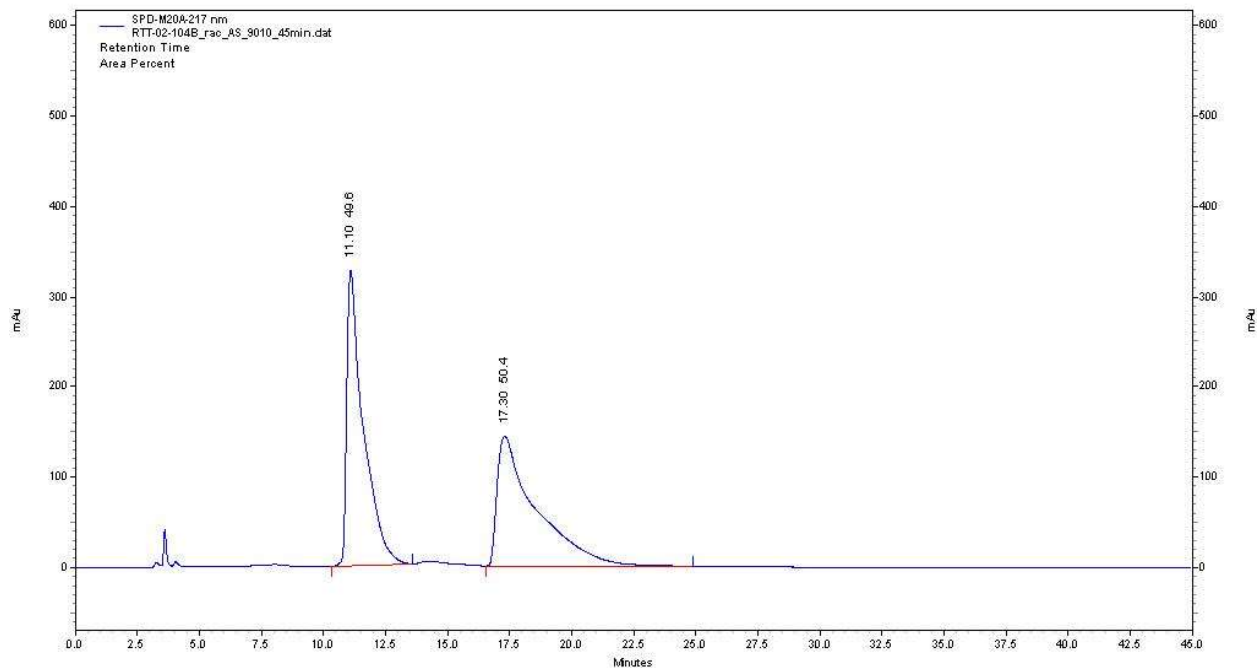
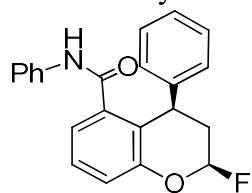


1.4.8. Chiral HPLC/SFC Analysis

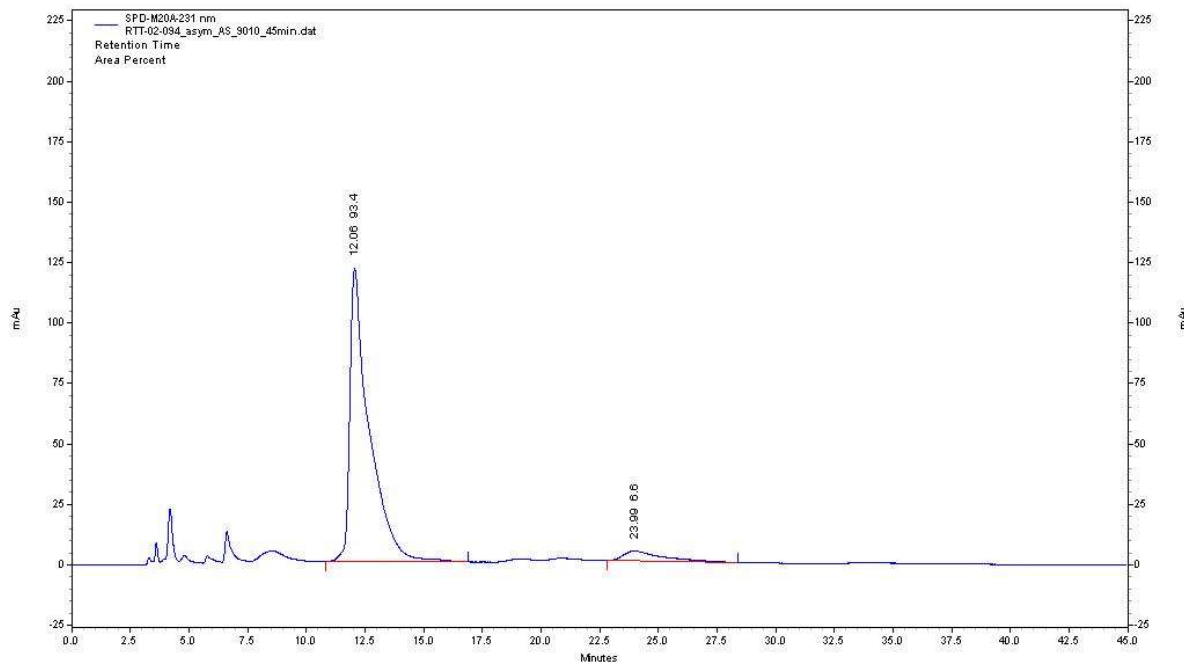
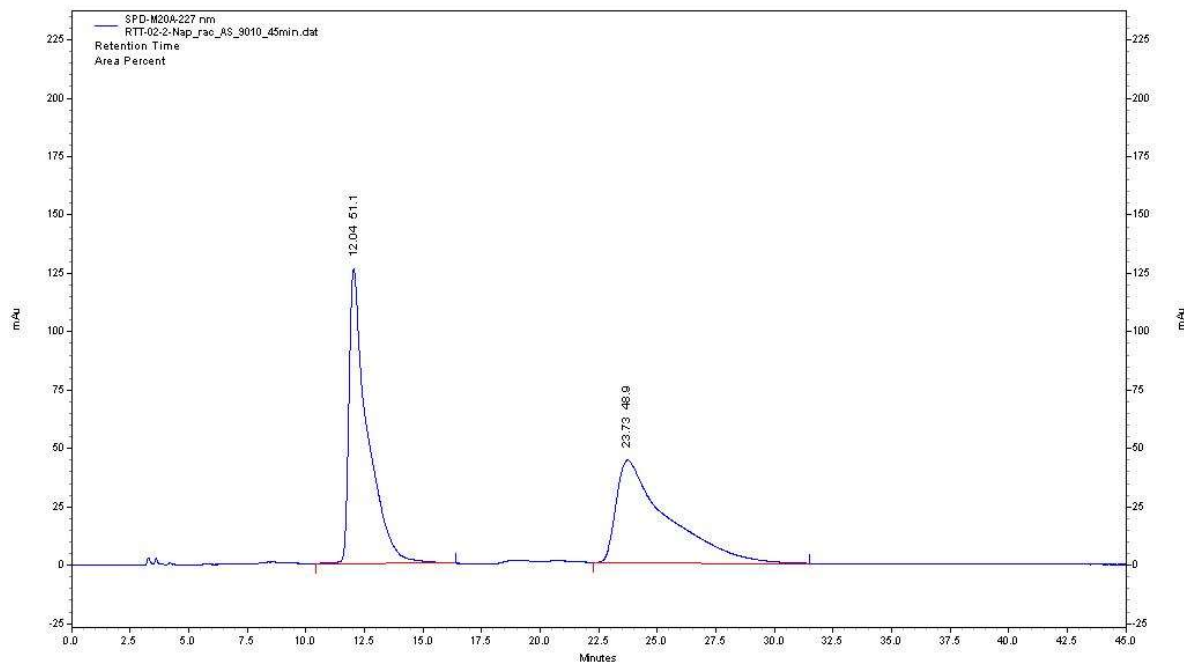
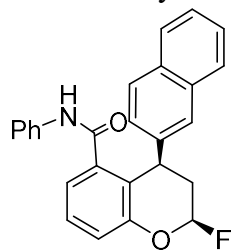
HPLC Analysis of 2a



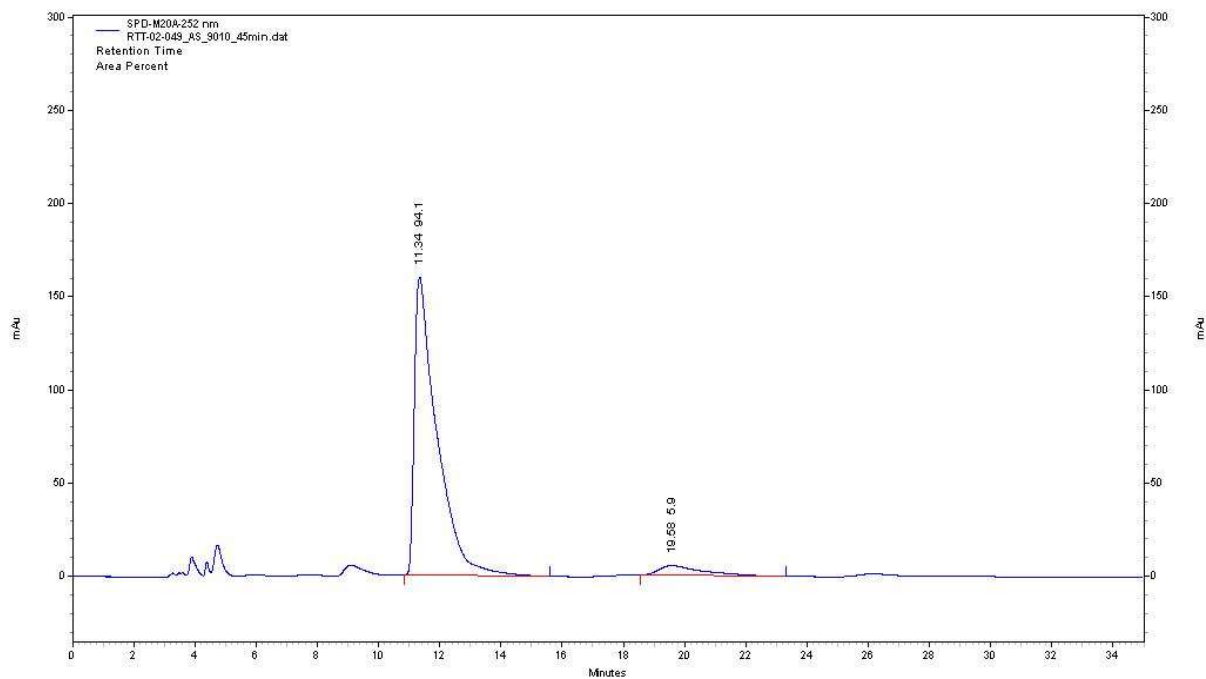
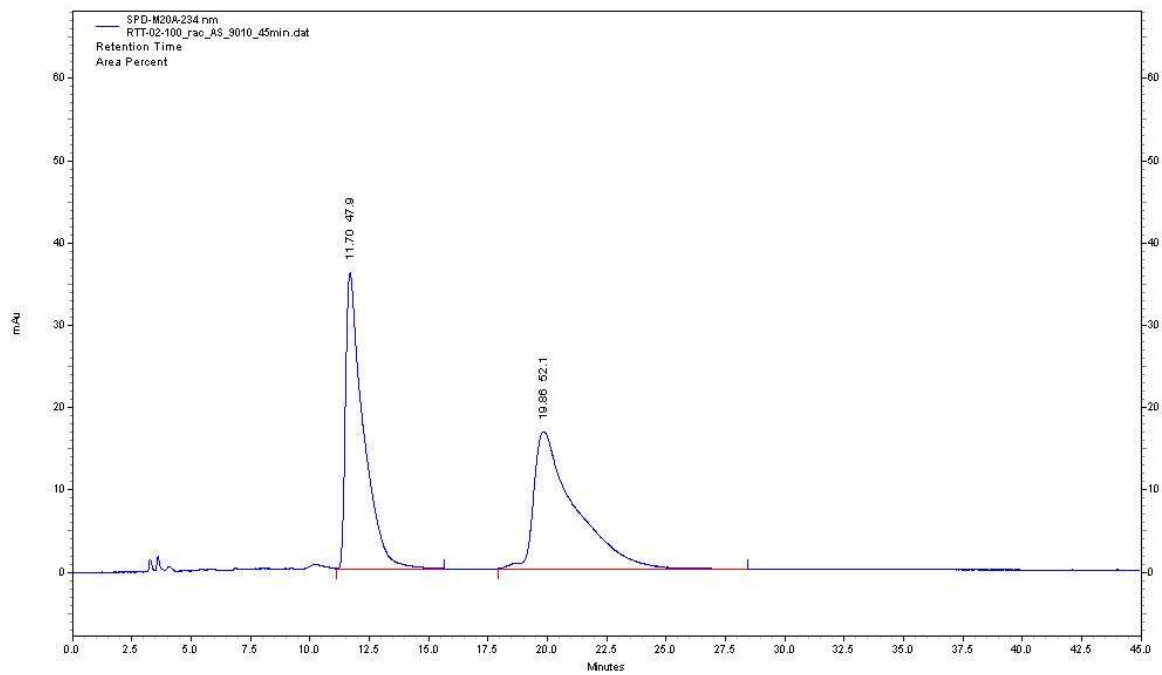
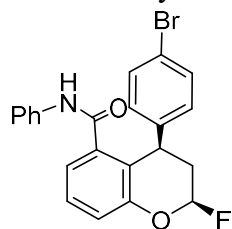
HPLC Analysis of **2b**



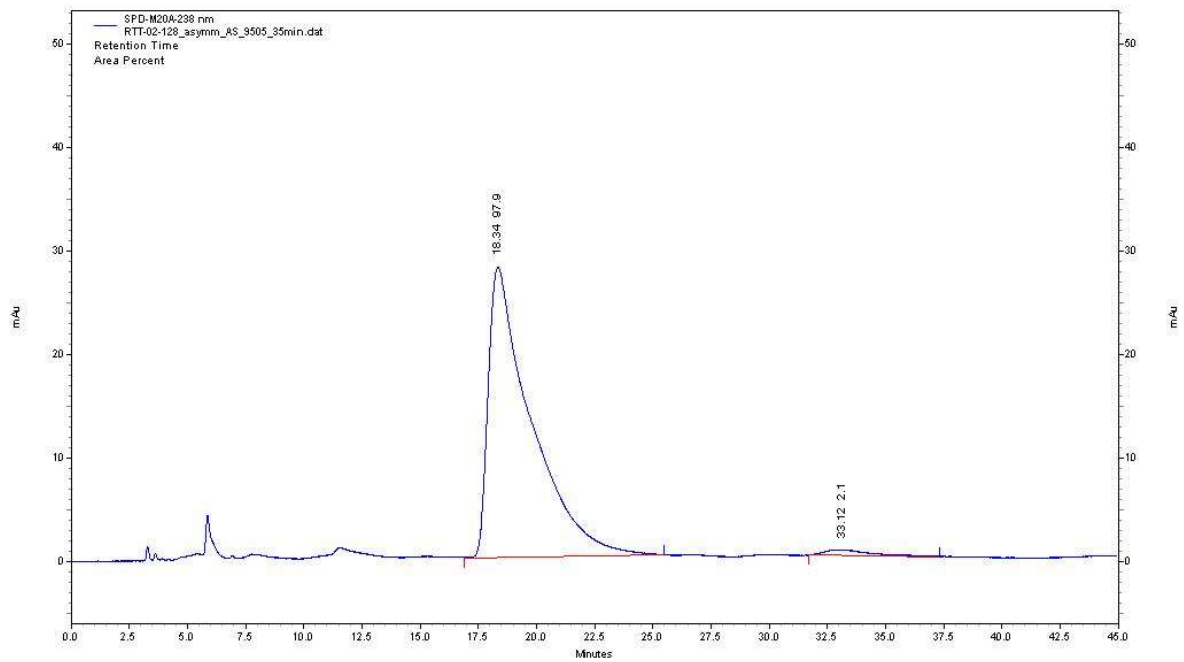
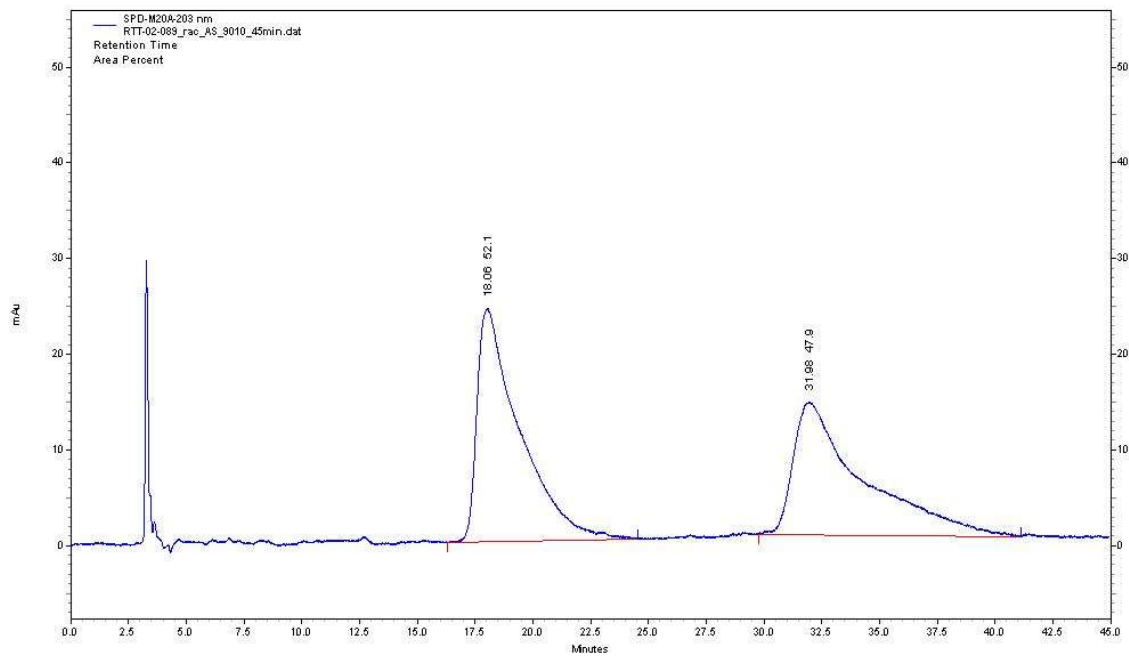
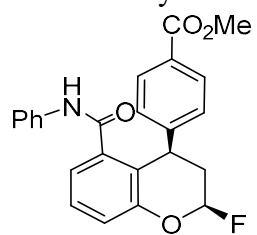
HPLC Analysis of 2c



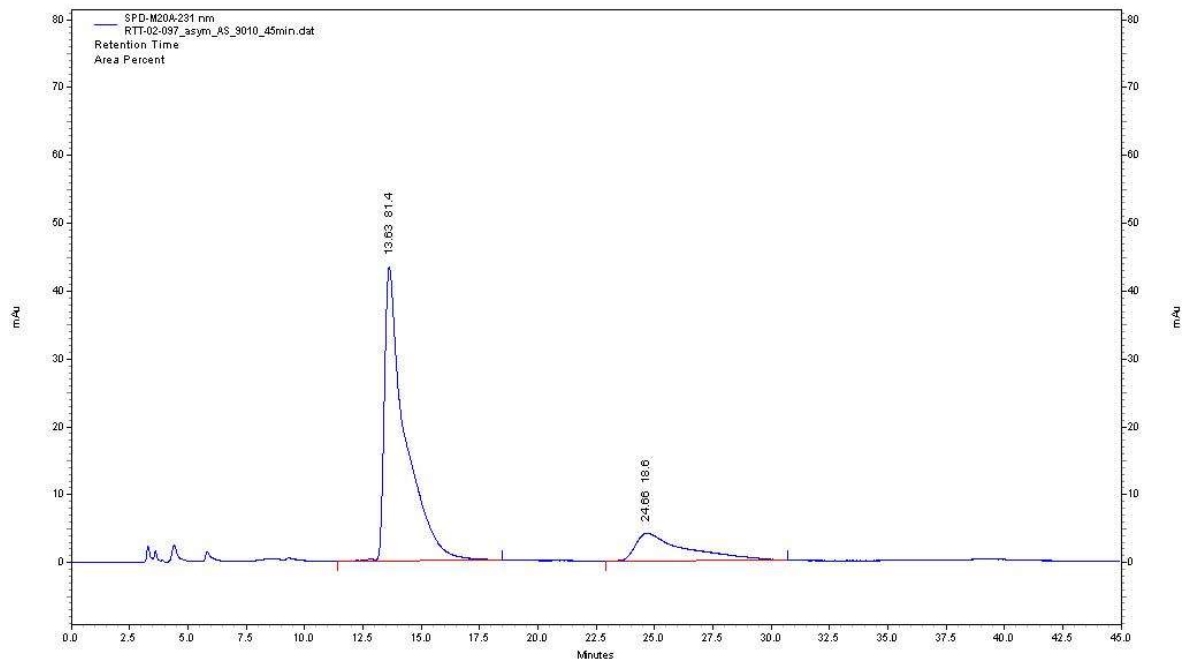
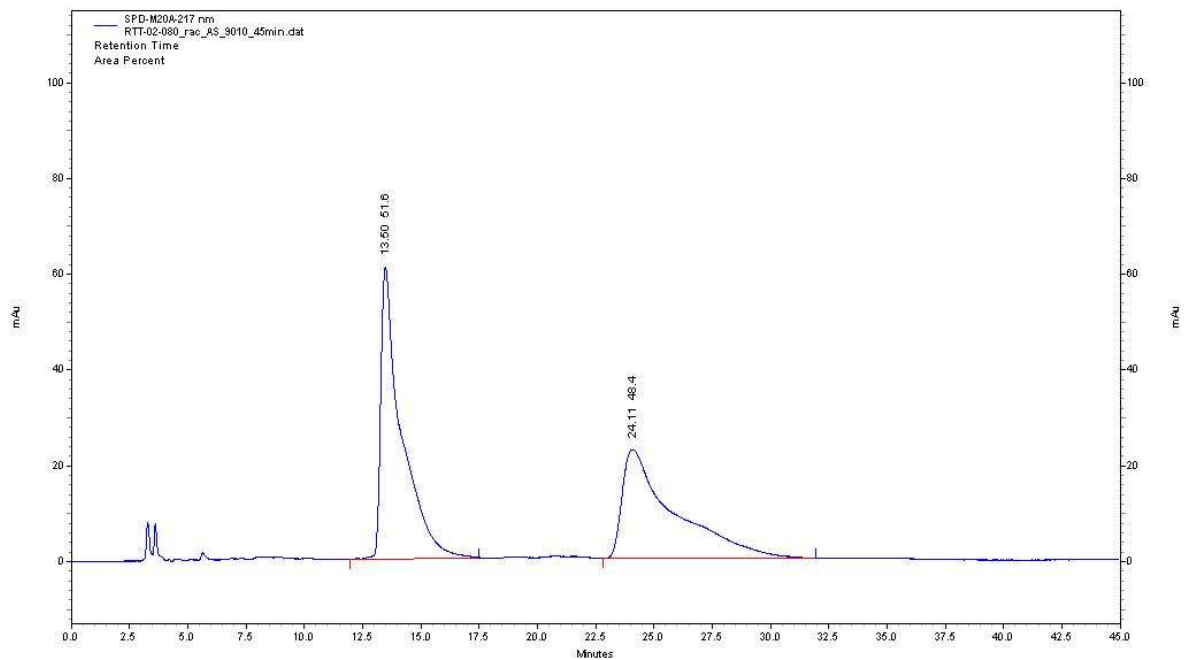
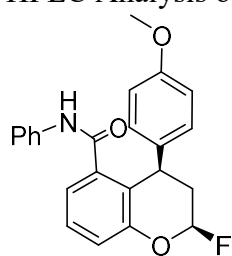
HPLC Analysis of 2d



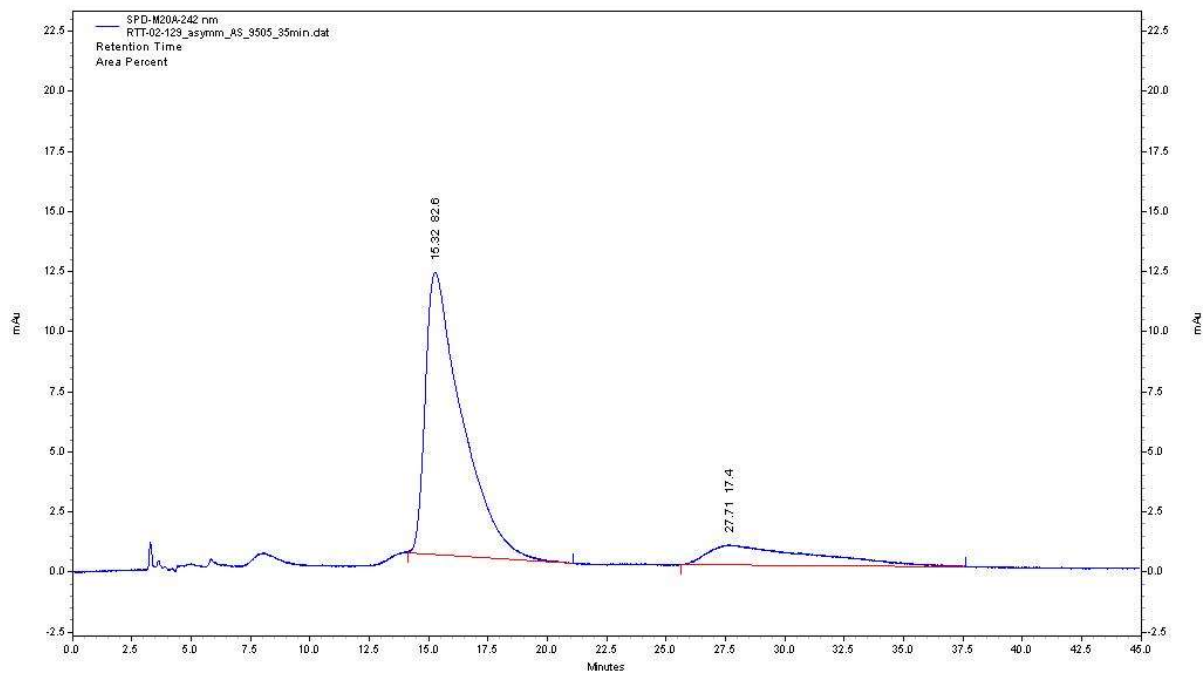
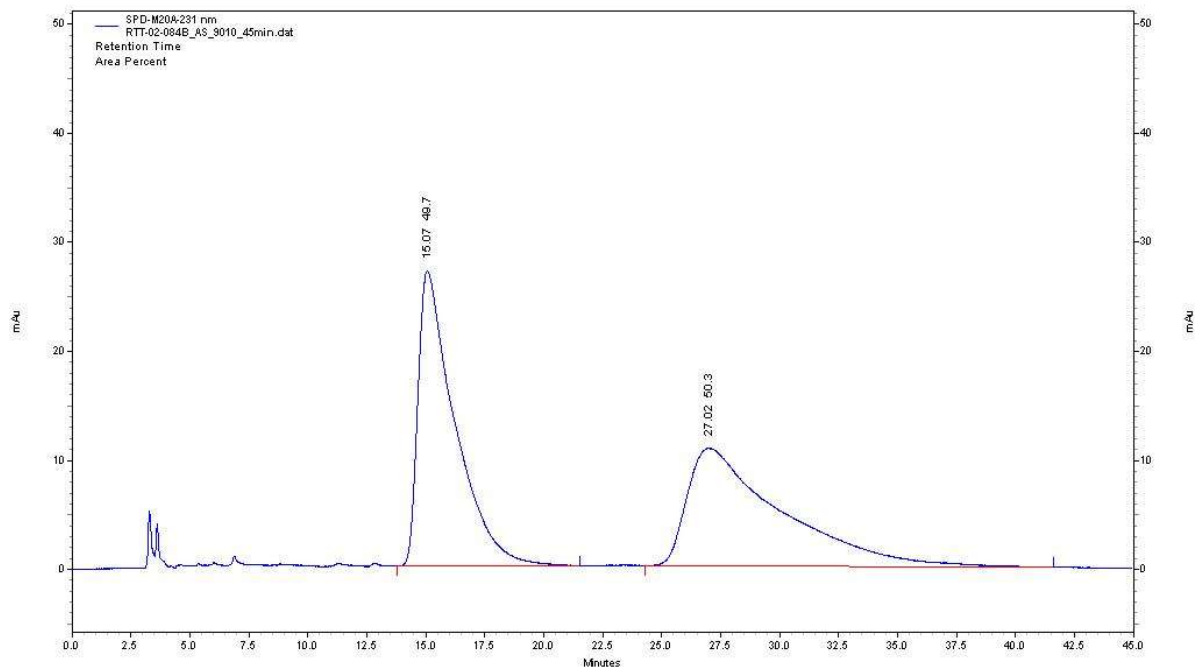
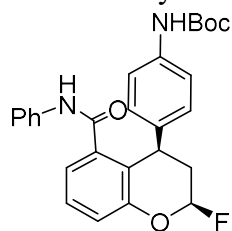
HPLC Analysis of **2e**



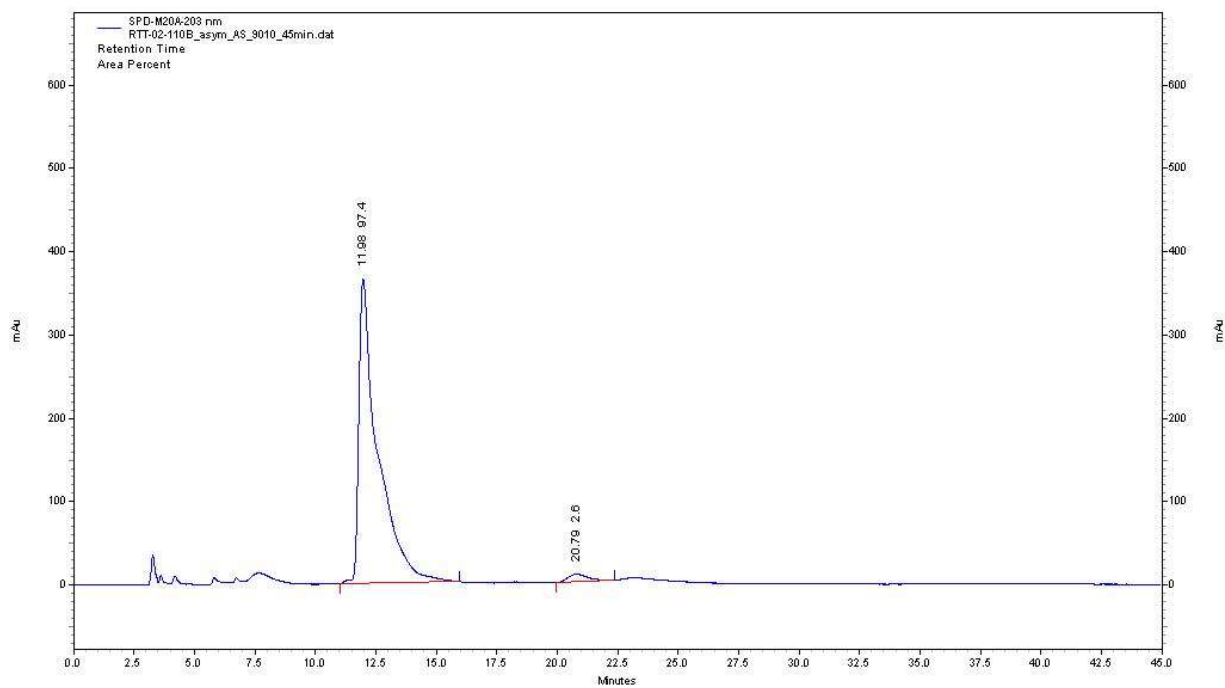
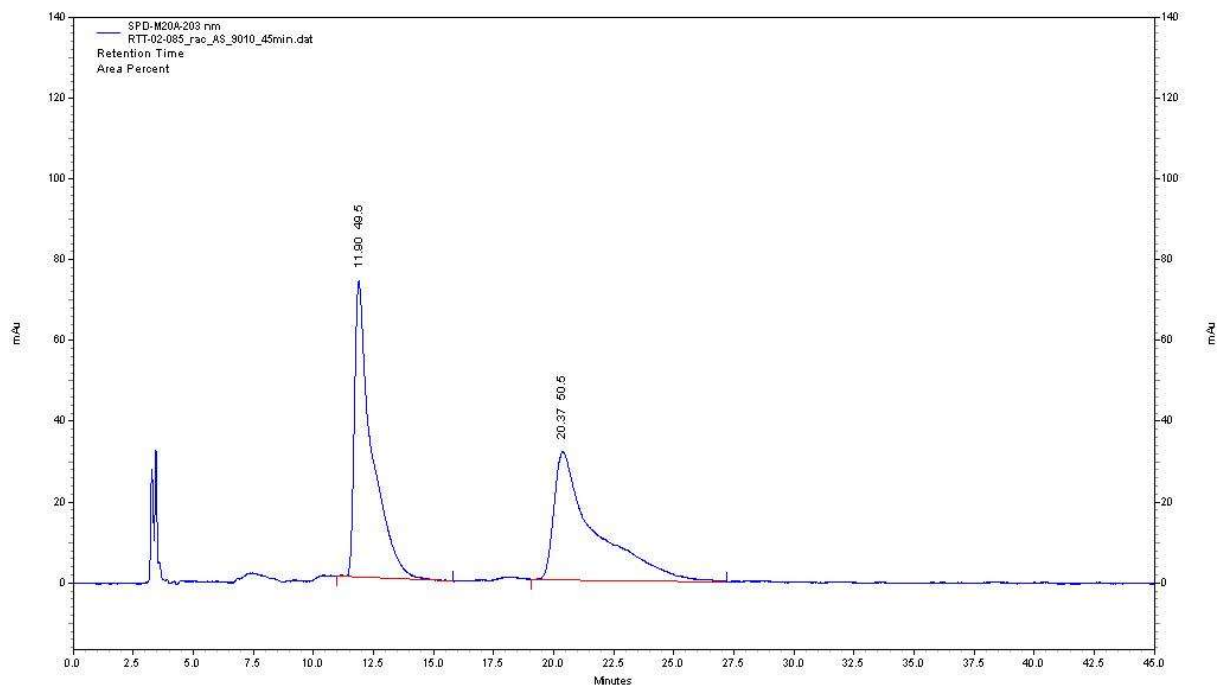
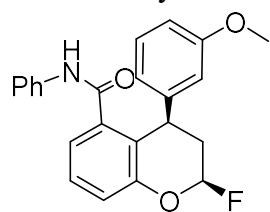
HPLC Analysis of 2f



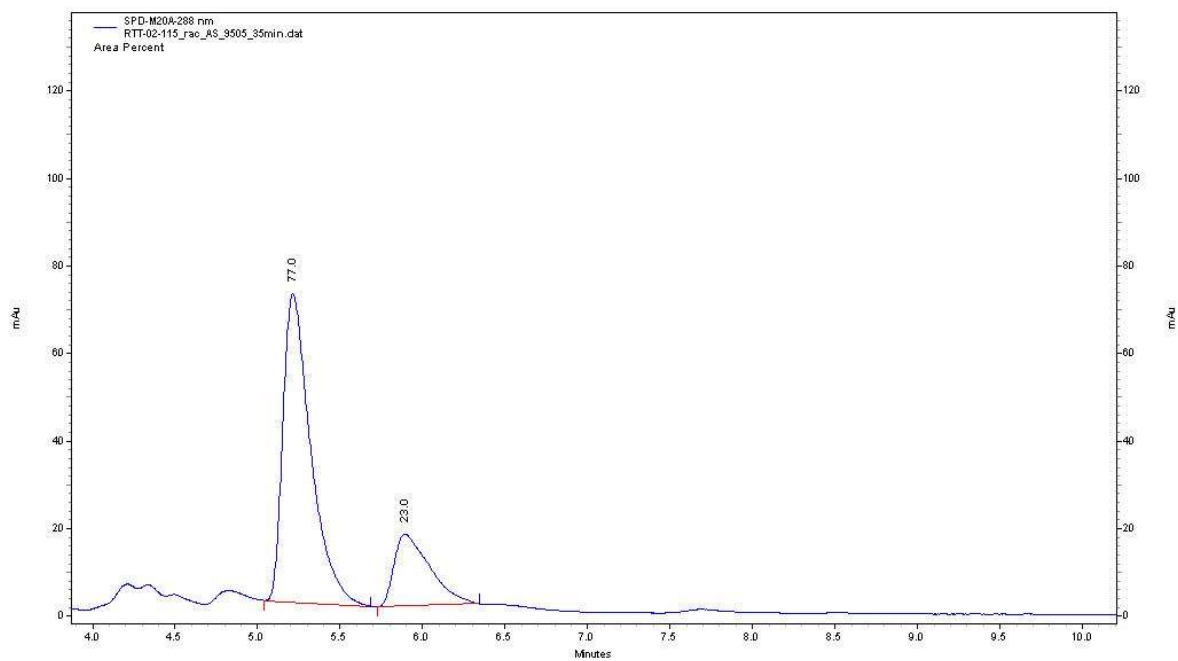
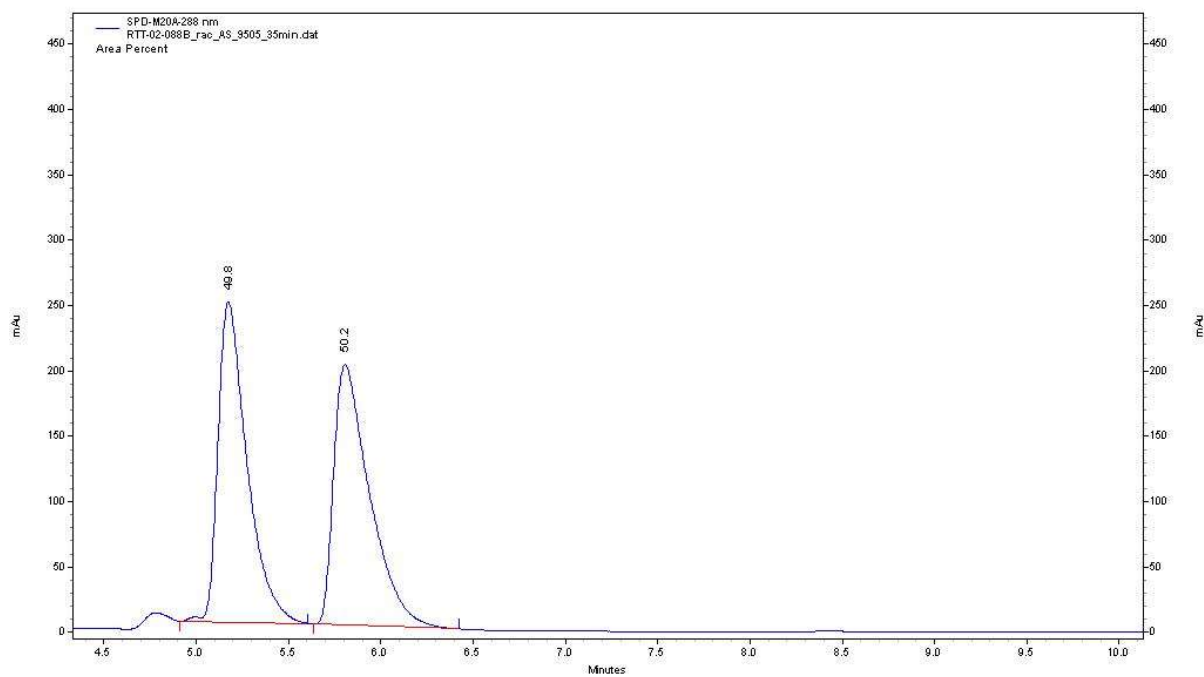
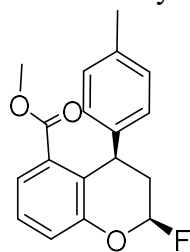
HPLC Analysis of 2g



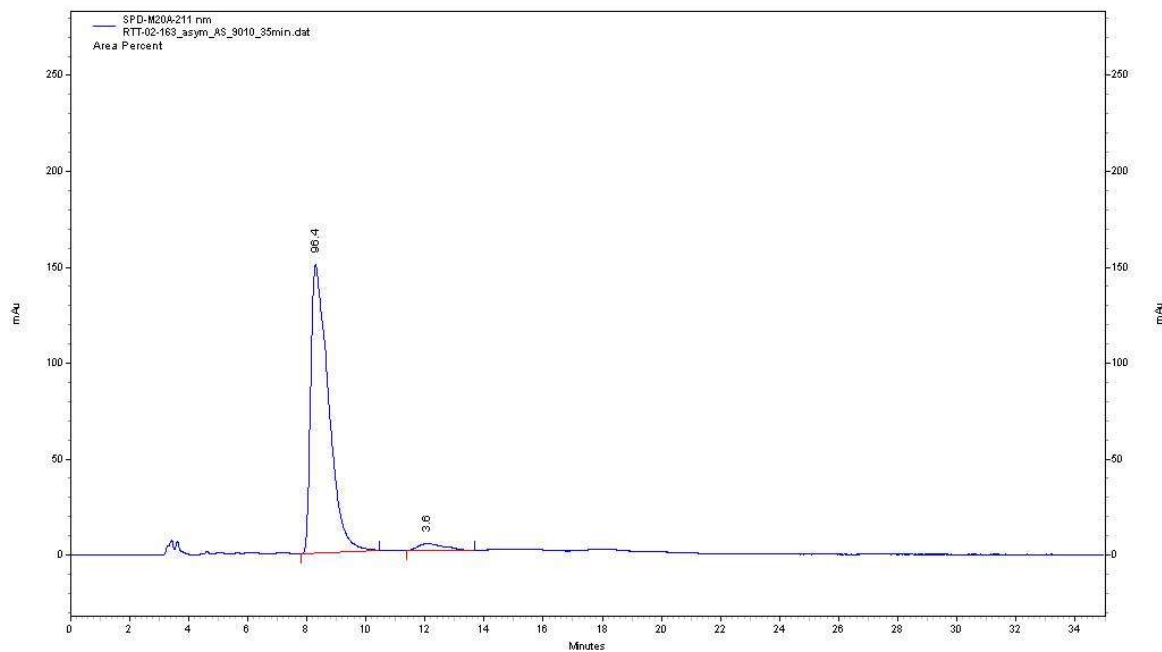
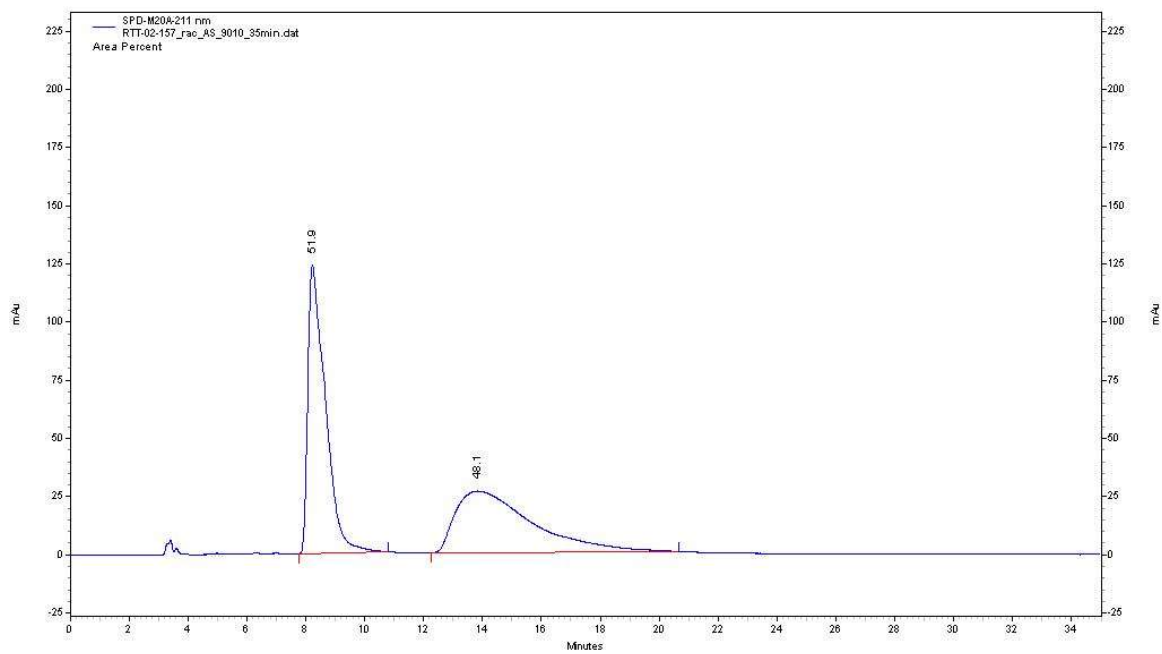
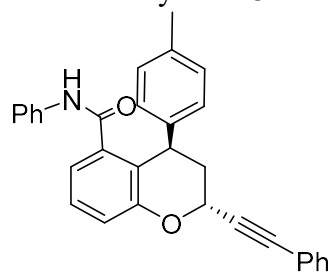
HPLC Analysis of 2h



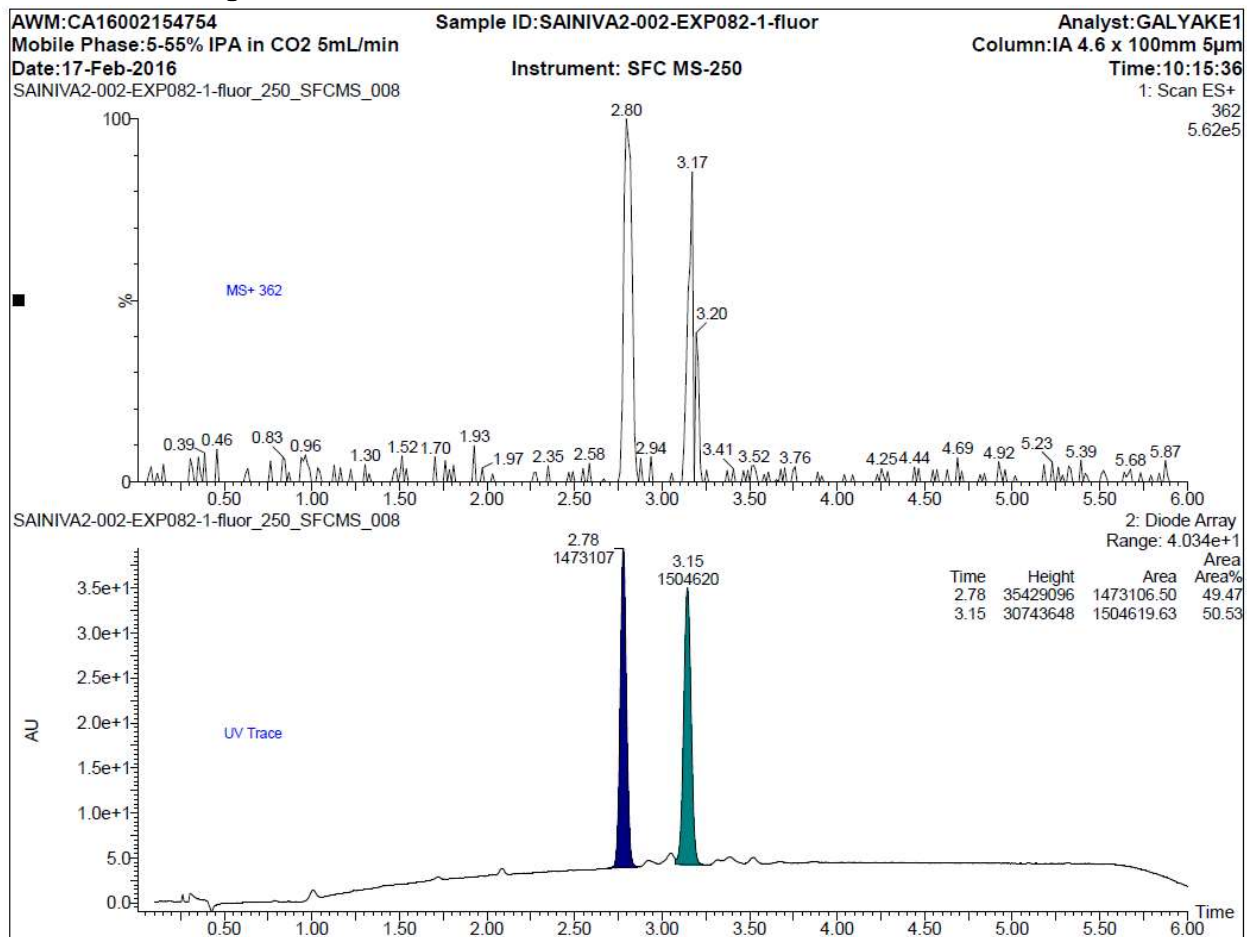
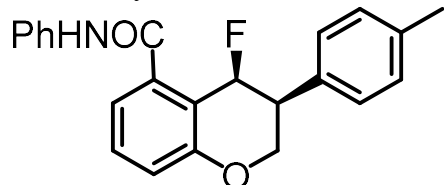
HPLC Analysis of 3

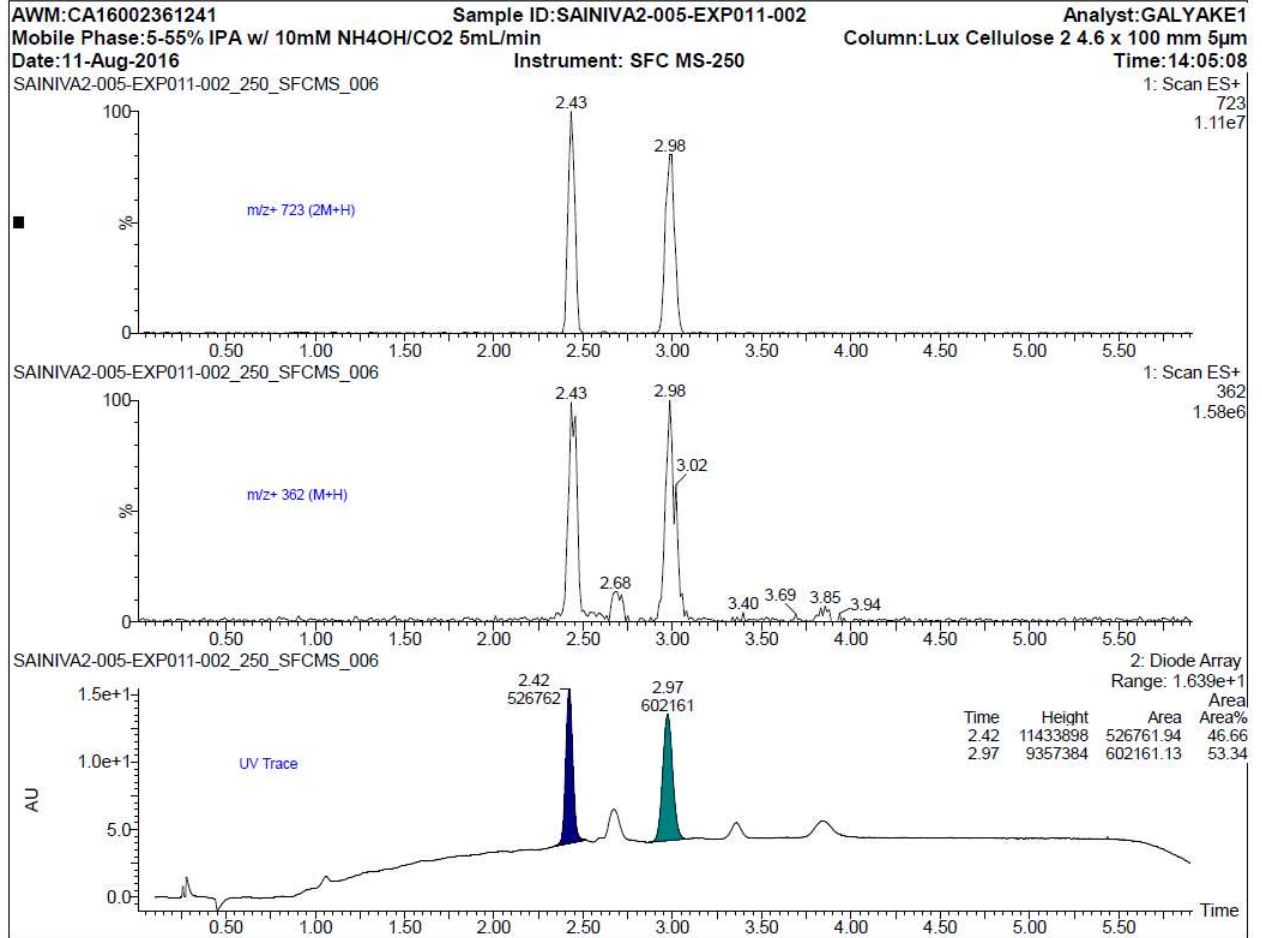


HPLC Analysis of 8



SFC Analysis of **10a**:





1.4.9. X-ray Crystallographic Data for *rac-2d*:

X-ray crystallography quality crystals of **rac-2d** were grown by solvent layering from CHCl₃ and *n*-pentane. A colorless needle 0.01 x 0.02 x 0.06 mm in size was mounted on a Cryoloop with Paratone oil. Data were collected in a nitrogen gas stream at 100(2) K using phi and omega scans. Crystal-to-detector distance was 60 mm and exposure time was 5 seconds per frame using a scan width of 1.0°. Data collection was 99.7% complete to 67.00° in ω . A total of 24648 reflections were collected covering the indices, $-18 \leq h \leq 18$, $-14 \leq k \leq 14$, $-11 \leq l \leq 12$. 3399 reflections were found to be symmetry independent, with an Rint of 0.0469. Indexing and unit cell refinement indicated a primitive, monoclinic lattice. The space group was found to be P2(1)/c (No. 14). The data were integrated using the Bruker SAINT software program and scaled using the SADABS software program. Solution by direct methods (SIR-2011) produced a complete heavy-atom phasing model consistent with the proposed structure. All non-hydrogen atoms were refined anisotropically by full-matrix least-squares (SHELXL-2014). All hydrogen atoms were placed using a riding model. Their positions were constrained relative to their parent atom using the appropriate HFIX command in SHELXL-2014.

Crystal data and structure refinement for *rac-2d*.

Identification code	shelx	
Empirical formula	C ₂₂ H ₁₇ Br F N O ₂	
Formula weight	426.27	
Temperature	100(2) K	
Wavelength	1.54178 Å	
Crystal system	Monoclinic	
Space group	P 21/c	
Unit cell dimensions	a = 15.3026(6) Å	∠ = 90°.
	b = 12.0184(4) Å	∠ = 90.552(3)°.
	c = 10.1214(4) Å	∠ = 90°.
Volume	1861.37(12) Å ³	
Z	4	
Density (calculated)	1.521 Mg/m ³	
Absorption coefficient	3.238 mm ⁻¹	
F(000)	864	
Crystal size	0.060 x 0.020 x 0.010 mm ³	
Theta range for data collection	2.888 to 68.325°.	
Index ranges	-18 ≤ h ≤ 18, -14 ≤ k ≤ 14, -11 ≤ l ≤ 12	
Reflections collected	24648	
Independent reflections	3399 [R(int) = 0.0469]	
Completeness to theta = 67.000°	99.7 %	
Absorption correction	Semi-empirical from equivalents	
Max. and min. transmission	0.7531 and 0.6139	
Refinement method	Full-matrix least-squares on F ²	
Data / restraints / parameters	3399 / 0 / 244	
Goodness-of-fit on F ²	1.038	
Final R indices [I > 2σ(I)]	R1 = 0.0372, wR2 = 0.0915	
R indices (all data)	R1 = 0.0447, wR2 = 0.0963	
Extinction coefficient	n/a	
Largest diff. peak and hole	0.870 and -0.325 e.Å ⁻³	

Atomic coordinates ($\times 10^4$) and equivalent isotropic displacement parameters ($\text{\AA}^2 \times 10^3$) for *rac-2d*. U(eq) is defined as one third of the trace of the orthogonalized U^{ij} tensor.

	x	y	z	U(eq)
$\bar{C}(1)$	1366(2)	-2975(2)	9430(3)	21(1)
C(2)	2218(2)	-3351(2)	9158(3)	23(1)
C(3)	2366(2)	-4394(2)	8630(3)	25(1)
C(4)	1664(2)	-5106(2)	8371(3)	26(1)
C(5)	823(2)	-4749(2)	8586(3)	25(1)
C(6)	680(2)	-3686(2)	9094(3)	23(1)
C(7)	-386(2)	-2307(2)	9520(3)	27(1)
C(8)	233(2)	-1759(2)	10480(3)	26(1)
C(9)	1195(2)	-1850(2)	10055(3)	22(1)
C(10)	2993(2)	-2631(2)	9515(3)	23(1)
C(11)	4292(2)	-1739(2)	8571(3)	28(1)
C(12)	4440(2)	-950(3)	7600(3)	34(1)
C(13)	5193(2)	-298(3)	7664(4)	42(1)
C(14)	5783(2)	-435(3)	8692(4)	42(1)
C(15)	5629(2)	-1215(3)	9650(4)	40(1)
C(16)	4888(2)	-1887(3)	9598(3)	33(1)
C(17)	1513(2)	-890(2)	9198(3)	21(1)
C(18)	1516(2)	-926(2)	7825(3)	26(1)
C(19)	1861(2)	-63(2)	7087(3)	28(1)
C(20)	2215(2)	845(2)	7741(3)	24(1)
C(21)	2200(2)	921(2)	9092(3)	24(1)
C(22)	1849(2)	54(2)	9813(3)	24(1)
N(1)	3519(2)	-2401(2)	8484(2)	26(1)
O(1)	-190(1)	-3413(2)	9261(2)	27(1)
O(2)	3128(1)	-2322(2)	10653(2)	27(1)
F(1)	-365(1)	-1730(1)	8314(2)	31(1)
Br(1)	2791(1)	1982(1)	6774(1)	33(1)

Bond lengths [Å] and angles [°] for *rac-2d*.

C(1)-C(6)	1.393(4)
C(1)-C(2)	1.410(4)
C(1)-C(9)	1.516(4)
C(2)-C(3)	1.383(4)
C(2)-C(10)	1.509(4)
C(3)-C(4)	1.396(4)
C(3)-H(3)	0.9500
C(4)-C(5)	1.376(4)
C(4)-H(4)	0.9500
C(5)-C(6)	1.394(4)
C(5)-H(5)	0.9500
C(6)-O(1)	1.383(3)
C(7)-O(1)	1.389(3)
C(7)-F(1)	1.405(3)
C(7)-C(8)	1.502(4)
C(7)-H(7)	1.0000
C(8)-C(9)	1.542(4)
C(8)-H(8A)	0.9900
C(8)-H(8B)	0.9900
C(9)-C(17)	1.526(4)
C(9)-H(9)	1.0000
C(10)-O(2)	1.226(3)
C(10)-N(1)	1.353(4)
C(11)-C(12)	1.385(4)
C(11)-C(16)	1.389(4)
C(11)-N(1)	1.428(4)
C(12)-C(13)	1.395(4)
C(12)-H(12)	0.9500
C(13)-C(14)	1.381(5)
C(13)-H(13)	0.9500
C(14)-C(15)	1.371(5)
C(14)-H(14)	0.9500
C(15)-C(16)	1.392(4)
C(15)-H(15)	0.9500
C(16)-H(16)	0.9500
C(17)-C(18)	1.390(4)
C(17)-C(22)	1.391(4)
C(18)-C(19)	1.386(4)
C(18)-H(18)	0.9500
C(19)-C(20)	1.384(4)
C(19)-H(19)	0.9500
C(20)-C(21)	1.371(4)
C(20)-Br(1)	1.902(3)
C(21)-C(22)	1.383(4)

C(21)-H(21)	0.9500
C(22)-H(22)	0.9500
N(1)-H(1)	0.8800

C(6)-C(1)-C(2)	116.8(2)
C(6)-C(1)-C(9)	121.2(2)
C(2)-C(1)-C(9)	122.1(2)
C(3)-C(2)-C(1)	121.5(2)
C(3)-C(2)-C(10)	118.7(2)
C(1)-C(2)-C(10)	119.7(2)
C(2)-C(3)-C(4)	119.9(3)
C(2)-C(3)-H(3)	120.0
C(4)-C(3)-H(3)	120.0
C(5)-C(4)-C(3)	119.9(3)
C(5)-C(4)-H(4)	120.0
C(3)-C(4)-H(4)	120.0
C(4)-C(5)-C(6)	119.6(3)
C(4)-C(5)-H(5)	120.2
C(6)-C(5)-H(5)	120.2
O(1)-C(6)-C(1)	123.2(2)
O(1)-C(6)-C(5)	114.7(2)
C(1)-C(6)-C(5)	122.1(2)
O(1)-C(7)-F(1)	107.5(2)
O(1)-C(7)-C(8)	113.9(2)
F(1)-C(7)-C(8)	109.1(2)
O(1)-C(7)-H(7)	108.8
F(1)-C(7)-H(7)	108.8
C(8)-C(7)-H(7)	108.8
C(7)-C(8)-C(9)	112.8(2)
C(7)-C(8)-H(8A)	109.0
C(9)-C(8)-H(8A)	109.0
C(7)-C(8)-H(8B)	109.0
C(9)-C(8)-H(8B)	109.0
H(8A)-C(8)-H(8B)	107.8
C(1)-C(9)-C(17)	112.3(2)
C(1)-C(9)-C(8)	110.4(2)
C(17)-C(9)-C(8)	114.6(2)
C(1)-C(9)-H(9)	106.3
C(17)-C(9)-H(9)	106.3
C(8)-C(9)-H(9)	106.3
O(2)-C(10)-N(1)	124.5(3)
O(2)-C(10)-C(2)	121.6(2)
N(1)-C(10)-C(2)	113.9(2)
C(12)-C(11)-C(16)	120.5(3)
C(12)-C(11)-N(1)	118.6(3)
C(16)-C(11)-N(1)	120.9(3)

C(11)-C(12)-C(13)	119.5(3)
C(11)-C(12)-H(12)	120.2
C(13)-C(12)-H(12)	120.2
C(14)-C(13)-C(12)	120.1(3)
C(14)-C(13)-H(13)	119.9
C(12)-C(13)-H(13)	119.9
C(15)-C(14)-C(13)	119.9(3)
C(15)-C(14)-H(14)	120.1
C(13)-C(14)-H(14)	120.1
C(14)-C(15)-C(16)	121.1(3)
C(14)-C(15)-H(15)	119.5
C(16)-C(15)-H(15)	119.5
C(11)-C(16)-C(15)	118.9(3)
C(11)-C(16)-H(16)	120.6
C(15)-C(16)-H(16)	120.6
C(18)-C(17)-C(22)	117.9(2)
C(18)-C(17)-C(9)	123.3(2)
C(22)-C(17)-C(9)	118.8(2)
C(19)-C(18)-C(17)	121.4(3)
C(19)-C(18)-H(18)	119.3
C(17)-C(18)-H(18)	119.3
C(20)-C(19)-C(18)	118.8(3)
C(20)-C(19)-H(19)	120.6
C(18)-C(19)-H(19)	120.6
C(21)-C(20)-C(19)	121.3(3)
C(21)-C(20)-Br(1)	118.5(2)
C(19)-C(20)-Br(1)	120.1(2)
C(20)-C(21)-C(22)	119.1(2)
C(20)-C(21)-H(21)	120.5
C(22)-C(21)-H(21)	120.5
C(21)-C(22)-C(17)	121.5(3)
C(21)-C(22)-H(22)	119.3
C(17)-C(22)-H(22)	119.3
C(10)-N(1)-C(11)	124.4(2)
C(10)-N(1)-H(1)	117.8
C(11)-N(1)-H(1)	117.8
C(6)-O(1)-C(7)	117.4(2)

Symmetry transformations used to generate equivalent atoms:

Anisotropic displacement parameters ($\text{\AA}^2 \times 10^3$) for *rac-2d*. The anisotropic displacement factor exponent takes the form: $-2 \sin^2[\theta] (h^2 a^{*2} U^{11} + \dots + 2 h k a^* b^* U^{12})$

	U11	U22	U33	U23	U13	U12
C(1)	29(1)	20(1)	14(1)	4(1)	1(1)	1(1)
C(2)	28(1)	24(1)	16(1)	4(1)	2(1)	0(1)
C(3)	29(1)	25(1)	20(1)	2(1)	3(1)	4(1)
C(4)	39(2)	20(1)	20(1)	0(1)	2(1)	2(1)
C(5)	34(1)	22(1)	19(1)	3(1)	0(1)	-4(1)
C(6)	28(1)	23(1)	17(1)	5(1)	0(1)	0(1)
C(7)	27(1)	27(1)	28(2)	5(1)	4(1)	3(1)
C(8)	29(1)	24(1)	24(1)	2(1)	5(1)	2(1)
C(9)	27(1)	21(1)	19(1)	2(1)	1(1)	0(1)
C(10)	25(1)	22(1)	21(2)	1(1)	1(1)	3(1)
C(11)	26(1)	31(1)	28(2)	-8(1)	6(1)	-3(1)
C(12)	37(2)	38(2)	28(2)	-2(1)	5(1)	-6(1)
C(13)	44(2)	40(2)	42(2)	-6(2)	16(2)	-13(1)
C(14)	31(2)	48(2)	48(2)	-17(2)	10(1)	-11(1)
C(15)	24(1)	53(2)	43(2)	-16(2)	3(1)	-1(1)
C(16)	30(1)	38(2)	30(2)	-4(1)	3(1)	1(1)
C(17)	22(1)	19(1)	21(1)	0(1)	0(1)	2(1)
C(18)	36(2)	19(1)	22(1)	-1(1)	-1(1)	-2(1)
C(19)	42(2)	24(1)	18(1)	1(1)	1(1)	-2(1)
C(20)	26(1)	21(1)	25(1)	3(1)	2(1)	2(1)
C(21)	26(1)	22(1)	23(1)	-5(1)	1(1)	-1(1)
C(22)	29(1)	25(1)	19(1)	-4(1)	2(1)	-1(1)
N(1)	27(1)	30(1)	19(1)	-2(1)	2(1)	-4(1)
O(1)	26(1)	23(1)	31(1)	2(1)	1(1)	-2(1)
O(2)	28(1)	33(1)	20(1)	-2(1)	0(1)	-1(1)
F(1)	35(1)	31(1)	26(1)	7(1)	-2(1)	4(1)
Br(1)	42(1)	26(1)	32(1)	8(1)	4(1)	-6(1)

Hydrogen coordinates ($\times 10^4$) and isotropic displacement parameters ($\text{\AA}^2 \times 10^3$) for *rac-2d*.

	x	y	z	U(eq)
H(3)	2946	-4627	8443	30
H(4)	1767	-5836	8048	31
H(5)	343	-5223	8389	30
H(7)	-991	-2264	9881	33
H(8A)	167	-2109	11359	31
H(8B)	76	-964	10564	31
H(9)	1554	-1827	10886	27
H(12)	4032	-854	6896	41
H(13)	5301	241	6998	51
H(14)	6295	12	8737	51
H(15)	6034	-1300	10360	48
H(16)	4793	-2437	10255	39
H(18)	1276	-1555	7384	31
H(19)	1856	-95	6149	34
H(21)	2428	1560	9528	29
H(22)	1838	105	10749	29
H(1)	3375	-2677	7707	31

Hydrogen bonds for *rac-2d* [\AA and $^\circ$].

D-H...A	d(D-H)	d(H...A)	d(D...A)	\angle (DHA)
---------	--------	----------	----------	----------------

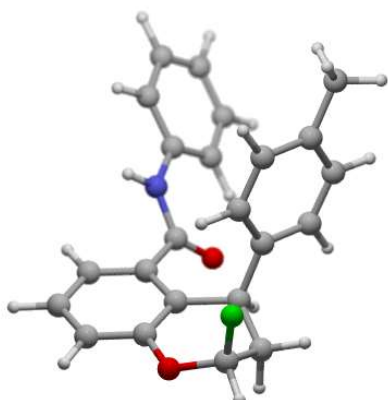
1.4.10. DFT Calculations

DFT for *cis*- and *trans*- 1,3-Arylfluorination Products

Density functional theory (DFT) calculations were performed with Gaussian 09 revision D01. Geometry optimizations were carried out at the B3LYP level of theory with the 6-31G(d) basis set. Optimized geometries were verified as a minima by frequency computations (zero imaginary frequencies). Single-point energy calculations on the optimized geometries were then evaluated using different density functionals and the triple-zeta valence quality def2-TZVPP basis set, within the SMD/IEF-PCM model (dichloromethane). The thermal corrections evaluated from the unscaled vibrational frequencies at the B3LYP/6-31G(d) level on the optimized geometries were then added to these electronic energies to obtain the free energies.

Level of theory	ΔG_{trans} (H)	ΔG_{cis} (H)	$\Delta\Delta G$ (kcal/mol)
B3LYP-D3/Def2TZVPP//B3LYP/6-31G(d)	-1193,784844	-1193,785210	0.2
M062X/Def2TZVPP//B3LYP/6-31G(d)	-1193,255521	-1193,256118	0.4
wB97XD/Def2TZVPP//B3LYP/6-31G(d)	-1193,338696	-1193,338928	0.1

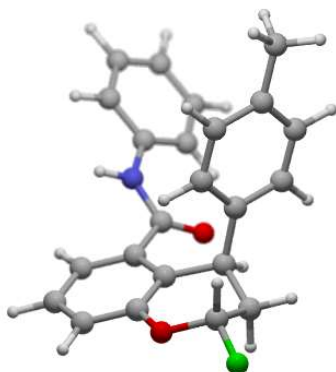
Cartesian coordinates



cis

C	2.063478000	-3.498878000	9.462858000
C	3.383647000	-3.921528000	9.188372000
C	3.627527000	-5.138860000	8.543560000
C	2.564865000	-5.962666000	8.165411000
C	1.260913000	-5.566418000	8.424425000
C	1.020531000	-4.344933000	9.063853000
C	-0.671707000	-2.772870000	9.674276000
C	0.303289000	-2.160004000	10.658846000
C	1.767114000	-2.174542000	10.154978000
C	4.563655000	-3.107398000	9.665544000
C	6.766021000	-2.250800000	8.793077000
C	7.517474000	-2.128112000	7.613282000
C	8.755738000	-1.493016000	7.628204000
C	9.264367000	-0.971008000	8.819092000
C	8.515427000	-1.094025000	9.989920000
C	7.272332000	-1.727235000	9.992764000
C	2.143215000	-0.950619000	9.314909000
C	1.925407000	-0.872766000	7.933760000
C	2.271420000	0.273260000	7.219439000
C	2.849776000	1.380849000	7.852350000
C	3.068179000	1.300325000	9.232746000
C	2.727642000	0.153360000	9.948594000
N	5.525946000	-2.918544000	8.699594000
O	-0.312647000	-4.070431000	9.295043000
O	4.654899000	-2.692870000	10.816394000
F	-0.759618000	-1.980774000	8.535201000
C	3.253307000	2.607289000	7.067239000
H	4.650571000	-5.461139000	8.371595000
H	2.757251000	-6.912937000	7.675755000
H	0.409424000	-6.178700000	8.145350000
H	-1.683984000	-2.861643000	10.077877000

H	0.232785000	-2.747454000	11.582811000
H	-0.013904000	-1.139076000	10.890364000
H	2.402673000	-2.136823000	11.043061000
H	7.126441000	-2.532621000	6.681470000
H	9.322568000	-1.407454000	6.704986000
H	10.230746000	-0.475227000	8.832793000
H	8.899407000	-0.691437000	10.923660000
H	6.690896000	-1.816573000	10.899136000
H	1.466154000	-1.705656000	7.411855000
H	2.084078000	0.308508000	6.148065000
H	3.521534000	2.140733000	9.754256000
H	2.928013000	0.111205000	11.016757000
H	5.272655000	-3.229550000	7.771171000
H	2.630678000	2.734583000	6.175120000
H	4.296347000	2.539965000	6.729311000
H	3.168156000	3.516858000	7.671781000



trans

C	2.147467000	-3.435812000	9.428133000
C	3.457745000	-3.906447000	9.189522000
C	3.670352000	-5.127200000	8.538224000
C	2.585702000	-5.898397000	8.113882000
C	1.291133000	-5.446375000	8.322280000
C	1.078532000	-4.221077000	8.968294000
C	-0.566919000	-2.605673000	9.666016000
F	-1.809000000	-2.772686000	10.228436000
C	0.427256000	-2.173687000	10.718509000
C	1.861852000	-2.126423000	10.147427000
C	4.654675000	-3.129700000	9.686473000
C	6.926267000	-2.405997000	8.870318000
C	7.725975000	-2.363540000	7.716784000
C	8.989005000	-1.780358000	7.754507000
C	9.474927000	-1.231138000	8.942631000
C	8.678377000	-1.274653000	10.087362000
C	7.409911000	-1.855090000	10.067172000

C	2.107456000	-0.886067000	9.286114000
C	1.850417000	-0.850608000	7.910182000
C	2.043601000	0.319333000	7.173028000
C	2.507979000	1.491414000	7.779422000
C	2.771414000	1.452366000	9.155719000
C	2.578684000	0.286731000	9.893088000
N	5.662294000	-3.023675000	8.753482000
O	-0.238542000	-3.862091000	9.103771000
O	4.722068000	-2.663113000	10.819190000
C	2.748537000	2.748899000	6.977097000
H	4.682699000	-5.495746000	8.399882000
H	2.754046000	-6.853043000	7.623738000
H	0.426028000	-6.016228000	7.998912000
H	-0.671856000	-1.874292000	8.855539000
H	0.374879000	-2.899829000	11.538591000
H	0.131023000	-1.196381000	11.111159000
H	2.545154000	-2.065779000	10.996527000
H	7.353053000	-2.789743000	6.787161000
H	9.592923000	-1.756816000	6.851379000
H	10.460554000	-0.775762000	8.974308000
H	9.044471000	-0.850434000	11.018682000
H	6.792511000	-1.882743000	10.953477000
H	1.505598000	-1.746364000	7.399753000
H	1.831873000	0.317197000	6.105819000
H	3.140704000	2.345479000	9.655530000
H	2.803103000	0.282440000	10.957369000
H	5.436375000	-3.370249000	7.830746000
H	2.209053000	2.725849000	6.024590000
H	3.814664000	2.877228000	6.747112000
H	2.428114000	3.642281000	7.524958000

DFT for Statistical Analysis

DFT Calculations

Compounds were geometrically optimized, with an ultrafine integration grid and ideal gas phase approximation using Gaussian 09 software.⁷⁹ DFT calculations of benzoic acid (as surrogates for arylboronic acid) ground state structures were performed using M06-2x functional and a triple zeta potential basis set (JUN-CC-PVTZ).⁸⁰ DFT calculations of PdCl₂ complexes were performed using B3LYP functional and LANL2DZ basis set for the palladium atom and 6-31G(d,p) basis set for other atoms. NBO charges⁵⁵ and torsion angles were obtained from the geometry optimized structures. Hammett values were acquired from the compilation made by Hansch, Leo, and Taft.⁶⁰

According to Curtin-Hammett principle,⁸¹ the relative rate of formation of competing products (X and Y) is logarithmically related to the difference in transition state energies, represented by the measured $\Delta\Delta G^\ddagger$ (equation 1), where R is the gas constant and T is temperature. To derive measured $\Delta\Delta G^\ddagger$ values, product ratios resulting from differences in selectivity were obtained experimentally.

$$\text{measured } \Delta\Delta G^\ddagger = -RT \ln \left(\frac{X}{Y} \right) \quad (1)$$

Regioselectivity ratios (rr) of 1,3- vs 2,1-arylfluorinated product and corresponding measured $\Delta\Delta G^\ddagger$ from reactions run with various arylboronic acids.

<i>R</i>	<i>Trial 1</i> <i>rr</i>	<i>Trial 2</i> <i>rr</i>	<i>Average</i> <i>rr</i>	<i>Measure</i> <i>d</i> $\Delta\Delta G^\ddagger$
p-Me	8.2	7.5	7.9	1.22
H	7.6	8.2	7.9	1.22
p-COMe	30.0	28.0	29.0	1.99
p-CO ₂ Me	17.7	20.8	19.3	1.75
p-OMe	15.2	13.4	14.3	1.58
p-F	10.8	11.7	11.3	1.43
p-CF ₃	17.8	16.4	17.1	1.68
p-Br	14.0	12.0	13.0	1.52
m-OMe	16.2	16.5	16.4	1.66
m-				
CO ₂ Me	27.0	36.0	31.5	2.04
m-Cl	7.6	8.3	8.0	1.23

$\Delta\Delta G^\ddagger$ is reported in kcal/mol.

Calculated parameters for benzoic acids as surrogates for arylboronic acids.

<i>R</i>	ν_{COH}	$\nu_{C=O}$	<i>NBO_C</i>	<i>NBO_{=O}</i>	<i>NBO_O</i>	<i>NBO_H</i>
p-Me	1395.02	1844.66	0.78588	-0.60618	-0.70599	0.50033
H	1394.60	1847.85	0.80516	-0.60208	-0.70358	0.50087
p-COMe	1399.86	1851.01	0.80289	-0.59612	-0.69999	0.50263
p-CO ₂ Me	1397.72	1851.64	0.80291	-0.59567	-0.70074	0.50254
p-OMe	1396.68	1839.37	0.80480	-0.61182	-0.70667	0.49976
p-F	1396.19	1847.75	0.80562	-0.60242	-0.70414	0.50193
p-CF ₃	1401.11	1854.66	0.78303	-0.59324	-0.70152	0.50390
p-Br	1395.33	1849.58	0.80491	-0.59850	-0.70255	0.50251
m-OMe	1396.67	1847.51	0.80599	-0.60040	-0.70218	0.50019
m-CO ₂ Me	1404.11	1850.19	0.80428	-0.59917	-0.70153	0.50178
m-Cl	1394.82	1852.53	0.80547	-0.59554	-0.70118	0.50252

Regioselectivity ratios (rr) of 1,3- vs 2,1-arylfluorinated product and corresponding measured $\Delta\Delta G^\ddagger$ from reactions run with various ligands.

<i>R</i>	<i>Trial 1 rr</i>	<i>Trial 2 rr</i>	<i>Average rr</i>	<i>Measured $\Delta\Delta G^\ddagger$</i>	<i>NBO_{Pd}</i>	<i>N-Pd-N angle</i>
bpyH	47	42	44.5	2.25	0.69727	79.18
bpytBu	16	19	17.5	1.70	0.69774	79.02
bpyMeO	9	7	8.0	1.23	0.69592	79.05
bpyCHO	26	28	27.0	1.95	0.70455	79.44
bpyBr	16	14	15.0	1.60	0.69882	79.09
phenH	17	20	18.5	1.73	0.69779	80.13
phenMe	4	4.5	4.25	0.86	0.69779	79.80
phenPh	15	17	16.0	1.64	0.69909	79.71
phenOMe	11	10	10.5	1.39	0.69662	79.93
dipyridylketone	0.16	0.21	0.19	-0.99	0.67595	88.93
diazafluorenone	0.83	0.71	0.77	-0.15	0.68843	81.95

$\Delta\Delta G^\ddagger$ is reported in kcal/mol.

Calculated parameters of PdLCl₂ complexes.

<i>R</i>	<i>NBO_{Pd}</i>	<i>N-Pd-N angle</i>
bpyH	0.69727	79.18
bpytBu	0.69774	79.02
bpyMeO	0.69592	79.05
bpyCHO	0.70455	79.44
bpyBr	0.69882	79.09
phenH	0.69779	80.13
phenMe	0.69779	79.80
phenPh	0.69909	79.71
phenOMe	0.69662	79.93
dipyridylketone	0.67595	88.93
diazafluorenone	0.68843	81.95

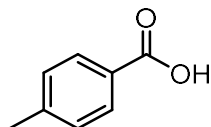
Table 15. Regioselectivity ratios (rr) of 1,3- vs 2,1-arylfluorinated product and corresponding measured $\Delta\Delta G^\ddagger$ from reactions run with various chromene derivatives.

<i>R</i>	<i>Trial 1</i> <i>rr</i>	<i>Trial 2</i> <i>rr</i>	<i>Average</i> <i>rr</i>	<i>log(1,3 vs</i> <i>2,1)</i>	σ
p-MeO	7.4	6.9	7.15	0.85	-0.268
p-Me	6.5	7.5	7	0.85	-0.170
H	8.2	7.5	7.85	0.89	0.000
p-F	9.4	9	9.2	0.96	0.062
p-Cl	13.8	12	12.9	1.11	0.227
p-Br	10	9.4	9.7	0.99	0.232
m-Cl	12.6	14	13.3	1.12	0.373
p-Ac	15	14.2	14.6	1.16	0.502

Cartesian Coordinates of Geometry Optimized Structures

benzoic acids

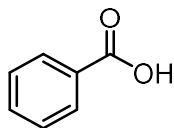
p-Me



C	0.01585300	-1.18043900	-0.00046100
C	0.69479800	0.03528100	-0.00007300
C	-0.02119700	1.22592400	-0.00038400
C	-1.40566400	1.20074200	-0.00086500
C	-2.09820700	-0.00711500	-0.00092100
C	-1.36715300	-1.19470100	-0.00098400
C	2.17540700	0.10956600	0.00027900
O	2.81336200	1.12865700	0.00040300

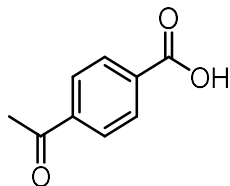
H	0.52268400	2.16035600	-0.00047100
O	2.76678400	-1.10215000	0.00051500
H	3.72007700	-0.94452100	0.00078200
H	0.57432800	-2.10515500	-0.00062500
C	-3.60005100	-0.04406700	0.00137000
H	-3.97456200	-0.59589800	-0.86127400
H	-3.97199100	-0.54629100	0.89513400
H	-4.02137700	0.95861300	-0.02558100
H	-1.89366300	-2.14100400	-0.00165800
H	-1.95937100	2.13069400	-0.00141400

H



C	-0.44402200	-1.19534300	0.00000300
C	0.21414500	0.03015800	0.00000100
C	-0.51131500	1.21709800	-0.00000900
C	-1.89521100	1.17807200	-0.00001800
C	-2.55361800	-0.04512600	-0.00001800
C	-1.83002100	-1.22936000	-0.00000600
C	1.69655400	0.12263600	0.00001000
O	2.31942600	1.15033800	0.00001000
H	0.02644800	2.15487200	-0.00000900
O	2.30214000	-1.08088000	0.00002000
H	3.25377400	-0.91298100	0.00002600
H	0.12950800	-2.11060000	0.00001300
H	-2.34520100	-2.17929700	-0.00000400
H	-2.46171800	2.09828100	-0.00002400
H	-3.63440400	-0.07475400	-0.00002000

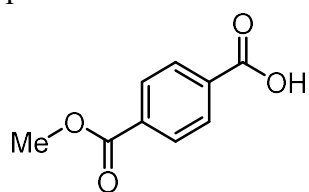
p-COMe



C	0.75387100	-1.19713600	-0.00010900
C	1.39803500	0.03767500	0.00005600
C	0.66028200	1.21495300	0.00016400
C	-0.72312400	1.15915000	0.00010600
C	-1.37448200	-0.07194600	-0.00005800
C	-0.62781100	-1.24769700	-0.00016200
C	2.88194100	0.14936200	0.00012300
O	3.48709000	1.18679100	0.00026300

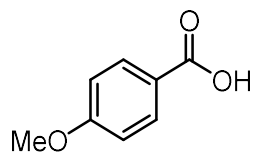
H	1.18540900	2.15963000	0.00029300
O	3.49953700	-1.04561000	0.00001000
H	4.45023800	-0.87123500	0.00006400
H	1.33804100	-2.10549500	-0.00019100
H	-1.15363100	-2.19196200	-0.00028500
H	-1.29081500	2.07893000	0.00019200
C	-2.87314700	-0.18115500	-0.00012000
O	-3.40427000	-1.26515900	-0.00020300
C	-3.68588100	1.08881600	-0.00007700
H	-3.45333100	1.68978600	0.87979700
H	-3.45308200	1.69002800	-0.87971900
H	-4.73979800	0.83000300	-0.00025300

p-CO₂Me



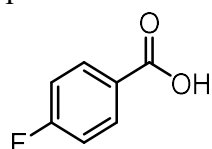
C	1.22816500	1.20896200	0.00018000
C	1.81363100	-0.05345800	-0.00001800
C	1.02324200	-1.19778400	-0.00019500
C	-0.35543300	-1.08354400	-0.00017500
C	-0.94165300	0.17882000	0.00002400
C	-0.15098200	1.32253100	0.00020100
C	3.29119900	-0.23094400	-0.00004700
O	3.85017900	-1.29384200	-0.00019900
H	1.50643900	-2.16452500	-0.00034800
O	3.96152600	0.93566000	0.00011500
H	4.90337700	0.71864000	0.00008300
H	1.85261600	2.08993700	0.00031700
H	-0.63432700	2.28913300	0.00035700
H	-0.98025000	-1.96402600	-0.00031200
C	-2.42295600	0.36026800	0.00006800
O	-2.97034900	1.43069500	0.00024500
O	-3.08436900	-0.80237400	-0.00011300
C	-4.50750000	-0.69047900	-0.00008100
H	-4.84232700	-0.15419300	-0.88556900
H	-4.88534000	-1.70712700	-0.00064300
H	-4.84235700	-0.15518100	0.88599300

p-OMe



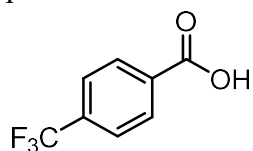
C	-0.54036400	-1.25921700	-0.00000100
C	-1.10322000	0.01844700	0.00001000
C	-0.27295300	1.13031900	0.00003700
C	1.10518200	0.98855300	0.00005900
C	1.65889000	-0.29081900	0.00006200
C	0.82810500	-1.41383700	0.00002300
C	-2.56500500	0.23625900	-0.00001300
O	-3.10388200	1.31210600	-0.00000200
H	-0.72332700	2.11335600	0.00003000
O	-3.27191500	-0.91314400	-0.00005100
H	-4.20495200	-0.66250400	-0.00006400
H	-1.18431500	-2.12656000	-0.00002100
H	1.28665600	-2.39234900	0.00002000
H	1.73158200	1.86698300	0.00006100
O	2.98595500	-0.54028400	0.00005700
C	3.86948900	0.56222200	-0.00011000
H	4.87193800	0.14617600	-0.00032700
H	3.73002700	1.17697800	-0.89167400
H	3.73038400	1.17693400	0.89154100

p-F



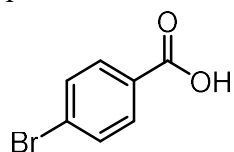
C	-0.02419300	-1.18621600	0.00000600
C	0.64653300	0.03313600	0.00000300
C	-0.07009400	1.22634300	-0.00000600
C	-1.45265600	1.20957700	-0.00001400
C	-2.09278900	-0.01675200	-0.00001100
C	-1.40848900	-1.21753200	-0.00000100
C	2.12719200	0.11305200	0.00001100
O	2.75798600	1.13593600	0.00000900
H	0.47468000	2.15990100	-0.00000800
O	2.72118000	-1.09608900	0.00002000
H	3.67462700	-0.93852200	0.00002400
H	0.53959700	-2.10729900	0.00001300
H	-1.96052200	-2.14590900	0.00000100
H	-2.03835900	2.11710000	-0.00002200
F	-3.43070800	-0.04152100	-0.00001800

p-CF₃



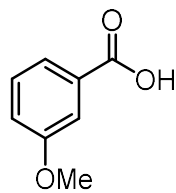
C	-1.01934400	-1.17122900	0.00003600
C	-1.70568300	0.03997600	0.00000800
C	-1.01221400	1.24296100	-0.00004600
C	0.37336700	1.24293100	-0.00008100
C	1.05146300	0.03417300	-0.00005300
C	0.36359800	-1.17285800	0.00001500
C	-3.19348700	0.09687500	0.00000800
O	-3.83476100	1.11153000	-0.00003500
H	-1.57173800	2.16757300	-0.00006800
O	-3.76480100	-1.12051700	0.00005700
H	-4.72177400	-0.98394300	0.00004900
H	-1.56941600	-2.10032100	0.00004400
H	0.91183300	-2.10523500	-0.00002900
H	0.92323900	2.17238600	-0.00013500
C	2.55436100	-0.00807700	-0.00001200
F	3.02531600	-0.65730200	-1.07343800
F	3.02540400	-0.65395300	1.07539900
F	3.09949900	1.21046800	-0.00188200

p-Br



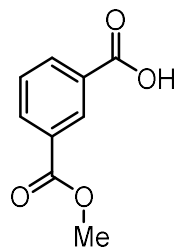
C	-1.08086200	-1.17814400	-0.00001000
C	-1.76098700	0.03467400	-0.00000600
C	-1.05313100	1.23171900	0.00000300
C	0.33033200	1.22383500	0.00000700
C	0.99439000	0.00511500	0.00000300
C	0.30449000	-1.19763200	-0.00000600
C	-3.24420100	0.10341400	-0.00001000
O	-3.88061600	1.12224900	-0.00000700
H	-1.60244700	2.16282000	0.00000600
O	-3.82770300	-1.10986500	-0.00001800
H	-4.78274700	-0.96167200	-0.00002000
H	-1.63533600	-2.10508200	-0.00001600
H	0.84429300	-2.13290900	-0.00000900
H	0.89042900	2.14708700	0.00001400
Br	2.88606200	-0.01563400	0.00000900

m-OMe



C	-0.06746300	-0.70787700	0.00020400
C	1.00403700	0.16787900	0.00006400
C	0.80094100	1.54713600	-0.00000100
C	-0.49090000	2.03256500	0.00005200
C	-1.58137300	1.16620200	0.00015500
C	-1.36808400	-0.20794700	0.00024700
C	2.40565400	-0.32859600	-0.00007100
O	3.37977700	0.37475100	-0.00023500
H	1.65728000	2.20519200	-0.00009600
O	2.49293100	-1.67245900	-0.00001500
H	3.43442600	-1.88994700	-0.00015300
H	0.08346900	-1.77713700	0.00025600
H	-0.66722400	3.09927400	0.00000600
H	-2.58171400	1.57183900	0.00018700
O	-2.35724400	-1.13503300	0.00044000
C	-3.69063600	-0.67415900	-0.00054100
H	-4.31807500	-1.55999000	-0.00025500
H	-3.90295100	-0.07866100	0.89039500
H	-3.90198100	-0.07985900	-0.89250800

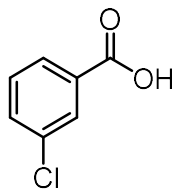
m-CO₂Me



C	-0.77288200	0.59735200	0.00000000
C	0.26156100	-0.32947700	0.00000000
C	1.57677200	0.11741400	0.00000000
C	1.85726800	1.48035400	0.00000000
C	0.82173700	2.40068600	0.00000000
C	-0.49253500	1.95989400	0.00000000
H	2.89144100	1.79582200	0.00000000
H	1.03803100	3.45949600	0.00000000
H	-1.31937800	2.65668500	0.00000000
C	-2.20389200	0.18119700	0.00000000
O	-3.12893800	0.94968500	0.00000100
O	-2.35410200	-1.14796500	0.00000000
C	-3.70597000	-1.60591100	0.00000000

H	-4.22515000	-1.24568100	0.88574300
H	-4.22515100	-1.24567600	-0.88574000
H	-3.65230100	-2.68919200	-0.00000300
H	0.04487500	-1.38661700	0.00000000
C	2.72341100	-0.82831600	0.00000000
O	2.34239100	-2.11904200	0.00000000
O	3.87874600	-0.49944300	0.00000000
H	3.15004100	-2.64987900	0.00000000

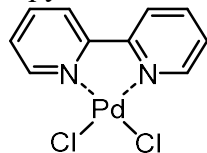
m-Cl



C	0.20187900	-0.61564900	-0.00000400
C	-0.93114000	0.19006800	-0.00000200
C	-0.81745600	1.57547200	0.00000800
C	0.43821200	2.15895900	0.00001700
C	1.57868000	1.36765200	0.00001500
C	1.44719800	-0.01240200	0.00000500
C	-2.29748900	-0.39842500	-0.00001100
O	-3.31385200	0.24088500	-0.00001000
H	-1.71822200	2.17228400	0.00001000
O	-2.29081700	-1.74370500	-0.00002000
H	-3.21387200	-2.03021200	-0.00002600
H	0.11426500	-1.69153500	-0.00001200
H	0.53684800	3.23526800	0.00002500
H	2.56435800	1.81042900	0.00002200
Cl	2.87262800	-1.00398400	0.00000300

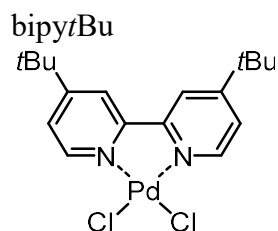
ligands

bipyH



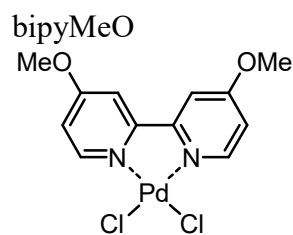
C	0.43838500	-2.66065300	0.00006800
C	1.77380600	-0.73776300	-0.00002300
C	2.93260100	-1.51628600	-0.00004300
C	2.82397000	-2.90443500	-0.00000100
C	1.55889600	-3.48659300	0.00006200
H	-0.58130000	-3.03328600	0.00010200
H	3.90828500	-1.04694600	-0.00008600

H	3.71775900	-3.51954100	-0.00001400
H	1.43015200	-4.56273900	0.00010200
C	1.77380100	0.73777400	-0.00002800
C	2.93259000	1.51630500	-0.00007300
C	2.82394900	2.90445400	-0.00003700
H	3.90827800	1.04697300	-0.00013500
C	0.43836600	2.66065500	0.00007500
C	1.55887000	3.48660200	0.00004600
H	3.71773400	3.51956700	-0.00007200
H	-0.58132200	3.03328000	0.00012300
H	1.43011900	4.56274800	0.00008300
N	0.54985300	-1.32530700	0.00002400
N	0.54984300	1.32530900	0.00003400
Pd	-1.05274600	-0.00000400	0.00000800
Cl	-2.66331900	1.67456000	-0.00001000
Cl	-2.66330900	-1.67457600	-0.00005700



C	-2.65822100	-0.82469600	-0.00055600
C	-0.73816000	0.49431600	-0.00017700
C	-1.51348200	1.65521800	0.00010000
C	-2.90884200	1.58383300	0.00003100
C	-3.47126100	0.29921600	-0.00040100
H	-3.04348200	-1.83939900	-0.00076200
H	-1.02054200	2.61642900	0.00045600
H	-4.54565600	0.15861100	-0.00055000
C	0.73814800	0.49432500	-0.00010500
C	1.51345800	1.65523600	-0.00045700
C	2.90881800	1.58386500	-0.00017100
H	1.02050600	2.61644100	-0.00100600
C	2.65822300	-0.82466700	0.00065600
C	3.47125000	0.29925300	0.00051400
H	3.04349400	-1.83936600	0.00100900
H	4.54564600	0.15866000	0.00088200
N	-1.32070500	-0.72869200	-0.00040100
N	1.32070700	-0.72867600	0.00031500
C	-3.80486800	2.82400200	0.00030400
C	3.80484300	2.82403600	-0.00027400
C	4.69249200	2.79821400	1.26386100
H	5.34570200	3.67631500	1.27864000
H	4.08195500	2.81060100	2.17191700

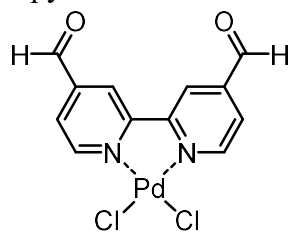
H	5.32730200	1.90879300	1.29685800
C	4.69637800	2.79566400	-1.26159900
H	4.08865300	2.80594900	-2.17156400
H	5.34940100	3.67390100	-1.27624100
H	5.33158800	1.90640500	-1.29076600
C	-4.69536400	2.79608600	1.26237700
H	-4.08688800	2.80673300	2.17183600
H	-5.34840900	3.67430400	1.27723100
H	-5.33049900	1.90679900	1.29239300
C	-4.69355900	2.79773500	-1.26308300
H	-5.34671800	3.67587600	-1.27765900
H	-4.08377800	2.80973000	-2.17165200
H	-5.32847800	1.90836300	-1.29521800
C	-2.99234300	4.12882500	0.00178400
H	-2.35847100	4.21468300	-0.88676700
H	-3.67472300	4.98325600	0.00211000
H	-2.35940900	4.21320900	0.89114600
C	2.99232500	4.12886000	-0.00292300
H	2.35995000	4.21278100	-0.89272700
H	2.35789500	4.21518500	0.88518300
H	3.67470800	4.98328900	-0.00324700
Pd	0.00001100	-2.33033100	-0.00001500
Cl	-1.68092200	-3.93873800	-0.00057300
Cl	1.68096600	-3.93871400	0.00060100



C	-2.65681900	-0.21049800	-0.00000800
C	-0.73898800	1.11688200	-0.00011800
C	-1.50570200	2.27223700	-0.00014200
C	-2.90503800	2.17399100	-0.00006900
C	-3.48960900	0.90199600	-0.00000800
H	-3.03888700	-1.22690600	0.00004500
H	-1.05730800	3.25695000	-0.00019900
H	-4.56140800	0.75726500	0.00004300
C	0.73899400	1.11688000	-0.00013200
C	1.50571200	2.27223000	-0.00004800
C	2.90504800	2.17398100	-0.00001300
H	1.05732100	3.25694500	0.00003000
C	2.65682000	-0.21050600	-0.00019600
C	3.48961600	0.90198500	-0.00011400
H	3.03888600	-1.22691500	-0.00024600

H	4.56141300	0.75724500	-0.00011000
N	-1.32237500	-0.11223800	-0.00005400
N	1.32237700	-0.11224300	-0.00018700
O	3.57872100	3.33870200	0.00013100
O	-3.57871900	3.33870700	-0.00005200
C	-5.00594600	3.29423900	0.00011200
H	-5.38446200	2.78963500	0.89576500
H	-5.33384000	4.33312300	0.00016300
H	-5.38467400	2.78965700	-0.89546300
C	5.00594500	3.29423900	0.00032100
H	5.38469600	2.78975800	-0.89530200
H	5.33382900	4.33312600	0.00049400
H	5.38444400	2.78953900	0.89592800
Pd	-0.00000200	-1.71491300	-0.00002700
Cl	-1.68470900	-3.32197600	0.00026300
Cl	1.68470000	-3.32198100	-0.00004800

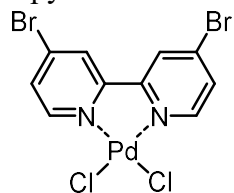
bipyCHO



C	0.26055400	-2.66200300	0.00016600
C	-1.07991400	-0.73742300	0.00013800
C	-2.23689100	-1.50911000	0.00006000
C	-2.12815200	-2.90173400	0.00000500
C	-0.86184200	-3.48590300	0.00009400
H	1.28017100	-3.03488100	0.00020400
H	-3.22577900	-1.06711900	-0.00001000
H	-0.74036200	-4.56438300	0.00008000
C	-1.07981600	0.73749500	0.00010300
C	-2.23669400	1.50932800	0.00013600
C	-2.12778000	2.90193700	-0.00000300
H	-3.22563600	1.06745900	0.00026500
C	0.26089900	2.66190700	-0.00017400
C	-0.86139500	3.48594600	-0.00020400
H	1.28056500	3.03465200	-0.00029500
H	-0.73977900	4.56441000	-0.00034900
N	0.14678600	-1.32744100	0.00013400
N	0.14695700	1.32735800	0.00000200
C	-3.36317700	-3.73669100	-0.00019800
C	-3.36270200	3.73704700	0.00006400
O	-4.48024200	-3.26540700	-0.00032500
O	-4.47982500	3.26590000	0.00029200

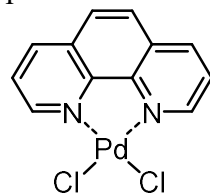
H	-3.19095600	-4.83241000	-0.00024200
H	-3.19034700	4.83274500	-0.00010000
Pd	1.74447200	-0.00010800	-0.00005100
Cl	3.35387100	-1.66958700	0.00015300
Cl	3.35390600	1.66937200	-0.00009400

bipyBr



C	2.66050200	0.85806100	0.00018900
C	0.73840400	-0.47152600	-0.00000700
C	1.50775000	-1.63456800	-0.00005700
C	2.89537000	-1.51785400	0.00003200
C	3.48952200	-0.25869400	0.00017500
H	3.03973100	1.87584100	0.00026100
H	1.04734000	-2.61287100	-0.00015600
H	4.56554900	-0.14093500	0.00026300
C	-0.73839100	-0.47154100	-0.00000300
C	-1.50771300	-1.63460000	-0.00006700
C	-2.89533500	-1.51791500	0.00003000
H	-1.04728200	-2.61289300	-0.00018600
C	-2.66051700	0.85800500	0.00022200
C	-3.48951300	-0.25876700	0.00019600
H	-3.03976700	1.87577700	0.00031000
H	-4.56554200	-0.14103200	0.00029100
N	1.32468100	0.75198400	0.00009200
N	-1.32469400	0.75195600	0.00011500
Br	3.96571300	-3.07869500	-0.00003200
Br	-3.96564500	-3.07877900	-0.00005600
Pd	-0.00002600	2.35634400	0.00001600
Cl	-1.67621900	3.96011600	-0.00008600
Cl	1.67612500	3.96016000	-0.00015900

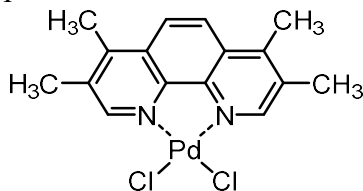
phenH



C	1.33559800	3.45201000	0.00034100
C	2.57163100	2.83587700	0.00017800
C	2.64605100	1.42484600	0.00002500

C	1.42470900	0.71548600	0.00016800
C	0.16455400	2.67145200	0.00025700
C	3.87441200	0.68213000	-0.00030800
C	1.42472000	-0.71548000	0.00011400
C	2.64606900	-1.42482900	-0.00012700
C	3.87442100	-0.68210000	-0.00039500
C	2.57165600	-2.83586000	-0.00011600
H	3.48656400	-3.42064200	-0.00022300
C	1.33562600	-3.45200000	0.00007600
C	0.16457500	-2.67145100	0.00016200
H	4.81008500	1.23241300	-0.00046700
H	1.24739100	4.53236400	0.00045400
H	3.48653800	3.42066200	0.00018700
H	-0.83473100	3.09625000	0.00016000
H	4.81010100	-1.23237200	-0.00062600
H	1.24742500	-4.53235500	0.00009900
H	-0.83468700	-3.09628500	0.00015900
N	0.21568700	1.34363700	0.00024000
N	0.21570400	-1.34363300	0.00020500
Pd	-1.38198900	-0.00000400	-0.00000100
Cl	-2.97266300	-1.69066100	0.00015500
Cl	-2.97269400	1.69063900	-0.00045300

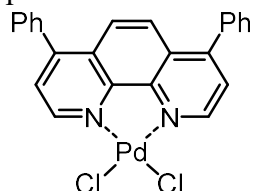
phenMe



C	3.47196900	0.92685900	-0.00001000
C	2.86123100	2.18143600	0.00000700
C	1.43792900	2.24080800	0.00001100
C	0.71567000	1.02995900	0.00000000
C	2.66109200	-0.22824000	-0.00001500
C	0.68287100	3.46215200	0.00002500
C	-0.71567600	1.02995500	-0.00000200
C	-1.43794200	2.24079900	-0.00000200
C	-0.68289100	3.46214800	0.00001800
C	-2.86124200	2.18141800	-0.00001500
C	-3.47197300	0.92683700	-0.00000800
C	-2.66109000	-0.22825700	-0.00000400
H	1.21311900	4.40713300	0.00004000
H	3.08385200	-1.22887700	-0.00002200
H	-1.21314500	4.40712500	0.00003500
H	-3.08384300	-1.22889700	-0.00000100
N	1.33642200	-0.18117700	-0.00000900

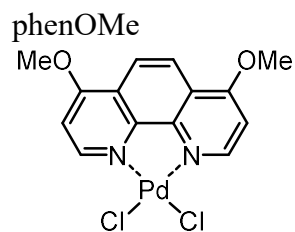
N	-1.33642000	-0.18118600	-0.00000500
C	3.66002000	3.45766100	0.00001700
H	3.42669000	4.06473300	-0.88157700
H	3.42664100	4.06475100	0.88158600
H	4.73235500	3.26865600	0.00004900
C	-3.66004700	3.45763100	-0.00002200
H	-3.42700200	4.06452100	0.88177600
H	-3.42640300	4.06491000	-0.88138700
H	-4.73238000	3.26860800	-0.00042600
C	4.96930400	0.74264600	-0.00002600
H	5.43091900	1.19655900	-0.88318200
H	5.43094900	1.19662700	0.88307900
H	5.22478400	-0.31883400	0.00001000
C	-4.96930700	0.74262600	-0.00000300
H	-5.43093900	1.19662600	0.88309900
H	-5.43093300	1.19652800	-0.88316000
H	-5.22479200	-0.31885300	0.00005300
Pd	0.00000600	-1.77962300	-0.00000100
Cl	-1.69527800	-3.37237900	0.00001500
Cl	1.69529900	-3.37236900	0.00000300

phenPh



C	-3.44492900	0.25288500	-0.05854300
C	-2.86169800	-1.00698400	0.00274200
C	-1.43545400	-1.07820300	0.00722600
C	-0.71730600	0.13928200	-0.00645500
C	-2.65954300	1.41348200	-0.07325100
C	-0.68262800	-2.29963800	0.00068600
C	0.71733200	0.13910000	0.00660500
C	1.43517200	-1.07856800	-0.00700900
C	0.68203400	-2.29981100	-0.00029500
C	2.86143500	-1.00770900	-0.00266200
C	3.44498700	0.25202000	0.05849200
C	2.65989400	1.41281400	0.07319800
H	-1.22044200	-3.23919300	-0.00912100
H	-4.52458300	0.34983800	-0.05881800
H	-3.07981800	2.41426200	-0.09826500
H	1.21961000	-3.23950100	0.00963600
H	4.52466400	0.34870600	0.05865000
H	3.08042300	2.41349000	0.09812600
N	-1.33267300	1.35534000	-0.03492300

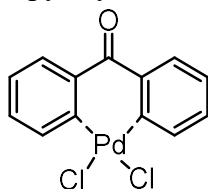
N	1.33300800	1.35500500	0.03495600
C	3.71786800	-2.21484700	-0.06072500
C	4.74577200	-2.38807700	0.87833700
C	3.55178300	-3.17410500	-1.07247500
C	5.57911000	-3.50322100	0.81637000
H	4.87485000	-1.65382200	1.66752400
C	4.39151500	-4.28421000	-1.13654100
H	2.78158700	-3.03210400	-1.82382000
C	5.40377100	-4.45394700	-0.19031400
H	6.36392800	-3.63013900	1.55542600
H	4.25995100	-5.01262400	-1.93056000
H	6.05502100	-5.32092800	-0.23978100
C	-3.71843200	-2.21391300	0.06074300
C	-3.55280500	-3.17310400	1.07263000
C	-4.74614100	-2.38700800	-0.87855600
C	-4.39280100	-4.28301400	1.13660300
H	-2.78275300	-3.03119900	1.82414300
C	-5.57974000	-3.50196300	-0.81668300
H	-4.87486100	-1.65280200	-1.66784700
C	-5.40486000	-4.45262500	0.19014200
H	-4.26159500	-5.01137800	1.93072800
H	-6.36440100	-3.62878400	-1.55592200
H	-6.05631300	-5.31945700	0.23953500
Pd	0.00036800	2.95235900	-0.00000800
Cl	-1.68976800	4.54765300	-0.05244000
Cl	1.69091100	4.54722400	0.05237700



C	-0.74440700	3.45526800	0.00016300
C	-1.99106700	2.84217200	0.00002400
C	-2.06218100	1.41624800	-0.00003300
C	-0.84122600	0.71558400	0.00004200
C	0.41527300	2.66547400	0.00020300
C	-3.29042800	0.68374400	-0.00015800
C	-0.84129600	-0.71550400	0.00003300
C	-2.06231900	-1.41604800	-0.00005100
C	-3.29049500	-0.68342500	-0.00016600
C	-1.99134600	-2.84197900	-0.00000500
C	-0.74474500	-3.45519800	0.00011900
C	0.41501200	-2.66551800	0.00016500
H	-4.22049400	1.23864800	-0.00024000

H	-0.63711700	4.53145900	0.00022700
H	1.41206500	3.09650900	0.00027100
H	-4.22061300	-1.23824000	-0.00025400
H	-0.63756100	-4.53139900	0.00016300
H	1.41176200	-3.09664800	0.00022400
N	0.37337600	1.33894800	0.00013500
N	0.37324500	-1.33898700	0.00011800
O	-3.17159500	3.48519700	-0.00006200
O	-3.17194000	-3.48488000	-0.00008700
C	-3.16818900	-4.91287400	0.00003500
H	-4.21583700	-5.21128600	-0.00015300
H	-2.67300900	-5.30313100	-0.89554400
H	-2.67337200	-5.30297100	0.89588300
C	-3.16766600	4.91318900	-0.00003800
H	-4.21527600	5.21172900	-0.00018900
H	-2.67274900	5.30328900	0.89575500
H	-2.67248300	5.30331800	-0.89567200
Pd	1.97113600	-0.00009500	0.00003200
Cl	3.56052300	1.69967500	-0.00013200
Cl	3.56034900	-1.70002700	-0.00013500

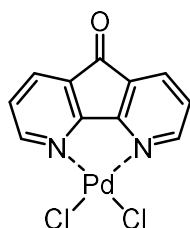
dipyridylketone



C	-3.70963500	0.90845900	0.93719400
C	-2.63814000	0.02238900	0.86410500
C	-1.31412500	1.61193600	-0.19407500
C	-2.36312100	2.53430800	-0.19089300
C	-3.57790500	2.18044800	0.38759200
H	-4.63233100	0.58532300	1.40541900
H	-2.71014900	-1.00068600	1.20876600
H	-2.19582300	3.50482800	-0.64037900
H	-4.40308300	2.88467000	0.40837300
C	0.00000300	2.09432400	-0.74656200
C	1.31412600	1.61193900	-0.19406000
C	2.36310900	2.53432600	-0.19082800
C	2.63815400	0.02236500	0.86406200
C	3.57789200	2.18045800	0.38765500
H	2.19580400	3.50486300	-0.64027700
C	3.70963700	0.90844400	0.93719600
H	2.71017200	-1.00072600	1.20867800
H	4.40305900	2.88469200	0.40847800
H	4.63233500	0.58530000	1.40541100

O	0.00000800	3.02543100	-1.53576600
N	1.46385500	0.37075100	0.30993700
N	-1.46384300	0.37076300	0.30996700
Pd	0.00000000	-1.08623700	-0.00860300
Cl	-1.65386200	-2.67741100	-0.39968000
Cl	1.65385600	-2.67740000	-0.39974800

diazafluorenone



C	0.28908100	-2.76295500	-0.00010900
C	1.55521100	-3.36317200	-0.00013300
C	2.73399000	-2.59354100	-0.00006200
C	2.58104500	-1.21174100	0.00010700
C	1.27987700	-0.72178700	0.00015400
H	-0.63719200	-3.32794500	-0.00021400
H	1.61416100	-4.44567100	-0.00024000
H	3.71248100	-3.06242700	-0.00014700
C	2.58102000	1.21177000	0.00011100
C	2.73393700	2.59357300	-0.00005200
C	1.55514200	3.36318000	-0.00012300
C	0.28902500	2.76293800	-0.00010600
C	1.27986200	0.72179000	0.00015500
H	3.71241900	3.06247900	-0.00013300
H	1.61407100	4.44568000	-0.00022500
H	-0.63726000	3.32790900	-0.00021300
C	3.51035400	0.00002400	0.00008600
O	4.71916000	0.00003700	0.00003500
N	0.15027400	1.42186100	-0.00002500
N	0.15030300	-1.42188100	-0.00002300
Pd	-1.48695700	-0.00000800	0.00000700
Cl	-3.03433200	1.71358600	0.00001200
Cl	-3.03432900	-1.71360400	0.00003100

1.5 References

1. Yamazaki, T.; Taguchi, T.; Ojima, I., Unique Properties of Fluorine and Their Relevance to Medicinal Chemistry and Chemical Biology. In *Fluorine in Medicinal Chemistry and Chemical Biology*, John Wiley & Sons, Ltd: 2009; pp 1-46.
2. Kirsch, P., *Modern Fluoroorganic Chemistry*. Wiley-VCH Verlag GmbH & Co. KGaA: Weinheim, Germany, 2013.
3. Kirk, K. L., Fluorination in Medicinal Chemistry: Methods, Strategies, and Recent Developments. *Organic Process Research & Development* **2008**, *12* (2), 305-321.
4. Wang, J.; Sánchez-Roselló, M.; Aceña, J. L.; del Pozo, C.; Sorochinsky, A. E.; Fustero, S.; Soloshonok, V. A.; Liu, H., Fluorine in Pharmaceutical Industry: Fluorine-Containing Drugs Introduced to the Market in the Last Decade (2001–2011). *Chemical Reviews* **2014**, *114* (4), 2432-2506.
5. Dong, C.; Huang, F.; Deng, H.; Schaffrath, C.; Spencer, J. B.; O'Hagan, D.; Naismith, J. H., Crystal Structure and Mechanism of a Bacterial Fluorinating Enzyme. *Nature* **2004**, *427* (6974), 561-565.
6. Harper, D. B.; O'Hagan, D., The Fluorinated Natural Products. *Natural Product Reports* **1994**, *11* (0), 123-133.
7. O'Hagan, D.; Schaffrath, C.; Cobb, S. L.; Hamilton, J. T. G.; Murphy, C. D., Biochemistry: Biosynthesis of an Organofluorine Molecule. *Nature* **2002**, *416* (6878), 279-279.
8. Gribble, G. W., The Diversity of Naturally Occurring Organobromine Compounds. *Chemical Society Reviews* **1999**, *28* (5), 335-346.
9. Baudoux, J.; Cahard, D., Electrophilic Fluorination with N–F Reagents. In *Organic Reactions*, John Wiley & Sons, Inc.: 2004.
10. Ma, J.-A.; Cahard, D., Update 1 of: Asymmetric Fluorination, Trifluoromethylation, and Perfluoroalkylation Reactions. *Chemical Reviews* **2008**, *108* (9), PR1-PR43.
11. Lectard, S.; Hamashima, Y.; Sodeoka, M., Recent Advances in Catalytic Enantioselective Fluorination Reactions. *Advanced Synthesis & Catalysis* **2010**, *352* (16), 2708-2732.
12. Valero, G.; Companyó, X.; Rios, R., Enantioselective Organocatalytic Synthesis of Fluorinated Molecules. *Chemistry – A European Journal* **2011**, *17* (7), 2018-2037.
13. Yang, X.; Wu, T.; Phipps, R. J.; Toste, F. D., Advances in Catalytic Enantioselective Fluorination, Mono-, Di-, and Trifluoromethylation, and Trifluoromethylthiolation Reactions. *Chemical Reviews* **2015**, *115* (2), 826-870.
14. Champagne, P. A.; Desroches, J.; Hamel, J.-D.; Vandamme, M.; Paquin, J.-F., Monofluorination of Organic Compounds: 10 Years of Innovation. *Chemical Reviews* **2015**, *115* (17), 9073-9174.
15. Thornbury, R.; Schäfer, G.; Toste, F. D., 9 - Catalytic Enantioselective Fluorination A2 - Grout, Henri. In *Modern Synthesis Processes and Reactivity of Fluorinated Compounds*, Leroux, F. R.; Tressaud, A., Eds. Elsevier: 2017; pp 223-263.
16. Chen, C.; Fu, L.; Chen, P.; Liu, G., Recent Advances and Perspectives of Transition Metal-Catalyzed Asymmetric Fluorination Reactions. *Chinese Journal of Chemistry* **2017**, *35* (12), 1781-1788.
17. In *Multicomponent Reactions*, Zhu, J. B., Hugues, Ed. Wiley-VCH Verlag GmbH & Co. KGaA: 2005.

18. Kalyani, D.; Sanford, M. S., Oxidatively Intercepting Heck Intermediates: Pd-Catalyzed 1,2- and 1,1-Arylhalogenation of Alkenes. *Journal of the American Chemical Society* **2008**, *130* (7), 2150-2151.
19. Urkalan, K. B.; Sigman, M. S., Palladium-Catalyzed Oxidative Intermolecular Difunctionalization of Terminal Alkenes with Organostannanes and Molecular Oxygen. *Angewandte Chemie International Edition* **2009**, *48* (17), 3146-3149.
20. Kalyani, D.; Satterfield, A. D.; Sanford, M. S., Palladium-Catalyzed Oxidative Arylhalogenation of Alkenes: Synthetic Scope and Mechanistic Insights. *Journal of the American Chemical Society* **2010**, *132* (24), 8419-8427.
21. Saini, V.; Liao, L.; Wang, Q.; Jana, R.; Sigman, M. S., Pd(0)-Catalyzed 1,1-Diarylation of Ethylene and Allylic Carbonates. *Organic Letters* **2013**, *15* (19), 5008-5011.
22. Talbot, E. P. A.; Fernandes, T. d. A.; McKenna, J. M.; Toste, F. D., Asymmetric Palladium-Catalyzed Directed Intermolecular Fluoroarylation of Styrenes. *Journal of the American Chemical Society* **2014**, *136* (11), 4101-4104.
23. Stokes, B. J.; Liao, L.; de Andrade, A. M.; Wang, Q.; Sigman, M. S., A Palladium-Catalyzed Three-Component-Coupling Strategy for the Differential Vicinal Diarylation of Terminal 1,3-Dienes. *Organic Letters* **2014**, *16* (17), 4666-4669.
24. Nelson, H. M.; Williams, B. D.; Miró, J.; Toste, F. D., Enantioselective 1,1-Arylborylation of Alkenes: Merging Chiral Anion Phase Transfer with Pd Catalysis. *Journal of the American Chemical Society* **2015**, *137* (9), 3213-3216.
25. He, Y.; Yang, Z.; Thornbury, R. T.; Toste, F. D., Palladium-Catalyzed Enantioselective 1,1-Fluoroarylation of Aminoalkenes. *Journal of the American Chemical Society* **2015**, *137* (38), 12207-12210.
26. McCammant, M. S.; Sigman, M. S., Development and Investigation of a Site Selective Palladium-catalyzed 1,4-Difunctionalization of Isoprene using Pyridine-Oxazoline Ligands. *Chemical Science* **2015**, *6* (2), 1355-1361.
27. Miró, J.; del Pozo, C.; Toste, F. D.; Fustero, S., Enantioselective Palladium-Catalyzed Oxidative β,β -Fluoroarylation of α,β -Unsaturated Carbonyl Derivatives. *Angewandte Chemie International Edition* **2016**, *55* (31), 9045-9049.
28. Yin, G.; Mu, X.; Liu, G., Palladium(II)-Catalyzed Oxidative Difunctionalization of Alkenes: Bond Forming at a High-Valent Palladium Center. *Accounts of Chemical Research* **2016**, *49* (11), 2413-2423.
29. Heck, R. F., Aromatic Haloethylation with Palladium and Copper Halides. *Journal of the American Chemical Society* **1968**, *90* (20), 5538-5542.
30. Tamaru, Y.; Hojo, M.; Higashimura, H.; Yoshida, Z.-i., PdII-Catalyzed Regioselective Arylchlorination and Oxyarylation of Unsaturated Alcohols. *Angewandte Chemie International Edition in English* **1986**, *25* (8), 735-737.
31. Tamaru, Y.; Hojo, M.; Kawamura, S.; Yoshida, Z., Synthesis of Five- and Six-membered Nitrogen Heterocycles via Palladium(II)-catalyzed Cyclization of Unsaturated Amides. *The Journal of Organic Chemistry* **1986**, *51* (21), 4089-4090.
32. Larhed, M.; Hallberg, A., Intermolecular Heck Reaction: Scope, Mechanism, and Other Fundamental Aspects of the Intermolecular Heck Reaction. In *Handbook of Organopalladium Chemistry for Organic Synthesis*, John Wiley & Sons, Inc.: 2003; pp 1133-1178.
33. Racowski, J. M.; Gary, J. B.; Sanford, M. S., Carbon(sp³)-Fluorine Bond-Forming Reductive Elimination from Palladium(IV) Complexes. *Angewandte Chemie International Edition* **2012**, *51* (14), 3414-3417.

34. Zhao, S.-B.; Becker, J. J.; Gagné, M. R., Steric Crowding Makes Challenging Csp³-F Reductive Eliminations Feasible. *Organometallics* **2011**, *30* (15), 3926-3929.
35. Mankad, N. P.; Toste, F. D., C(sp³)-F Reductive Elimination from Alkylgold(III) Fluoride Complexes. *Chemical Science* **2012**, *3* (1), 72-76.
36. Cochrane, N. A.; Nguyen, H.; Gagne, M. R., Catalytic Enantioselective Cyclization and C3-Fluorination of Polyenes. *Journal of the American Chemical Society* **2013**, *135* (2), 628-631.
37. Wang, H.; Guo, L.-N.; Duan, X.-H., Silver-catalyzed Decarboxylative Acylfluorination of Styrenes in Aqueous Media. *Chemical Communications* **2014**, *50* (55), 7382-7384.
38. Peng, H.; Liu, G., Palladium-Catalyzed Tandem Fluorination and Cyclization of Enynes. *Organic Letters* **2011**, *13* (4), 772-775.
39. Braun, M.-G.; Katcher, M. H.; Doyle, A. G., Carbofluorination via a Palladium-catalyzed Cascade Reaction. *Chemical Science* **2013**, *4* (3), 1216-1220.
40. Kindt, S.; Heinrich, M. R., Intermolecular Radical Carbofluorination of Non-activated Alkenes. *Chemistry – A European Journal* **2014**, *20* (47), 15344-15348.
41. Cahard, D.; Xu, X.; Couve-Bonnaire, S.; Pannecoucke, X., Fluorine & Chirality: How to Create a Nonracemic Stereogenic Carbon-Fluorine Centre? *Chemical Society Reviews* **2010**, *39* (2), 558-568.
42. Liang, T.; Neumann, C. N.; Ritter, T., Introduction of Fluorine and Fluorine-Containing Functional Groups. *Angewandte Chemie International Edition* **2013**, *52* (32), 8214-8264.
43. Mei, T.-S.; Werner, E. W.; Burckle, A. J.; Sigman, M. S., Enantioselective Redox-Relay Oxidative Heck Arylations of Acyclic Alkenyl Alcohols using Boronic Acids. *Journal of the American Chemical Society* **2013**, *135* (18), 6830-6833.
44. Patel, H. H.; Sigman, M. S., Palladium-Catalyzed Enantioselective Heck Alkenylation of Acyclic Alkenols Using a Redox-Relay Strategy. *Journal of the American Chemical Society* **2015**, *137* (10), 3462-3465.
45. Chen, Z.-M.; Hilton, M. J.; Sigman, M. S., Palladium-Catalyzed Enantioselective Redox-Relay Heck Arylation of 1,1-Disubstituted Homoallylic Alcohols. *Journal of the American Chemical Society* **2016**, *138* (36), 11461-11464.
46. Subburaj, K.; Katoch, R.; Muruges, M. G.; Trivedi, G. K., Regioselective Total Synthesis of (±) Neorautane, (±) Neorautanin and Their Analogs. Microwave Mediated Synthesis of 2H-Chromenes from Propargyl Phenyl Ethers. *Tetrahedron* **1997**, *53* (37), 12621-12628.
47. Oestreich, M., Directed Mizoroki–Heck Reactions. In *Directed Metallation*, Chatani, N., Ed. Springer Berlin Heidelberg: Berlin, Heidelberg, 2007; pp 169-192.
48. Yoo, K. S.; Park, C. P.; Yoon, C. H.; Sakaguchi, S.; O'Neil, J.; Jung, K. W., Asymmetric Intermolecular Heck-Type Reaction of Acyclic Alkenes via Oxidative Palladium(II) Catalysis. *Organic Letters* **2007**, *9* (20), 3933-3935.
49. Zeng, J.; Vedachalam, S.; Xiang, S.; Liu, X.-W., Direct C-Glycosylation of Organotrifluoroborates with Glycosyl Fluorides and Its Application to the Total Synthesis of (+)-Varitriol. *Organic Letters* **2011**, *13* (1), 42-45.
50. Li, J.; Yang, P.; Yao, M.; Deng, J.; Li, A., Total Synthesis of Rubrifloridilactone A. *Journal of the American Chemical Society* **2014**, *136* (47), 16477-16480.
51. Sigman, M. S.; Harper, K. C.; Bess, E. N.; Milo, A., The Development of Multidimensional Analysis Tools for Asymmetric Catalysis and Beyond. *Accounts of Chemical Research* **2016**, *49* (6), 1292-1301.
52. Reed, A. E.; Weinstock, R. B.; Weinhold, F., Natural Population Analysis. *The Journal of Chemical Physics* **1985**, *83* (2), 735-746.

53. Gross, K. C.; Seybold, P. G.; Hadad, C. M., Comparison of Different Atomic Charge Schemes for Predicting pKa Variations in Substituted Anilines and Phenols*. *International Journal of Quantum Chemistry* **2002**, *90* (1), 445-458.
54. Hollingsworth, C. A.; Seybold, P. G.; Hadad, C. M., Substituent Effects on the Electronic Structure and pKa of benzoic acid. *International Journal of Quantum Chemistry* **2002**, *90* (4-5), 1396-1403.
55. Glendening, E. D.; Landis, C. R.; Weinhold, F., NBO 6.0: Natural Bond Orbital Analysis Program. *Journal of Computational Chemistry* **2013**, *34* (16), 1429-1437.
56. White, P. B.; Jaworski, J. N.; Fry, C. G.; Dolinar, B. S.; Guzei, I. A.; Stahl, S. S., Structurally Diverse Diazafluorene-Ligated Palladium(II) Complexes and Their Implications for Aerobic Oxidation Reactions. *Journal of the American Chemical Society* **2016**, *138* (14), 4869-4880.
57. White, P. B.; Jaworski, J. N.; Zhu, G. H.; Stahl, S. S., Diazafluorenone-Promoted Oxidation Catalysis: Insights into the Role of Bidentate Ligands in Pd-Catalyzed Aerobic Aza-Wacker Reactions. *ACS Catalysis* **2016**, *6* (5), 3340-3348.
58. Jones, R. N.; Forbes, W. F.; Mueller, W. A., The Infrared Carbonyl Stretching Bands of Ring Substituted Acetophenones. *Canadian Journal of Chemistry* **1957**, *35* (5), 504-514.
59. Milo, A.; Bess, E. N.; Sigman, M. S., Interrogating Selectivity in Catalysis Using Molecular Vibrations. *Nature* **2014**, *507*, 210.
60. Hansch, C.; Leo, A.; Taft, R. W., A Survey of Hammett Substituent Constants and Resonance and Field Parameters. *Chemical Reviews* **1991**, *91* (2), 165-195.
61. Braun, M.-G.; Doyle, A. G., Palladium-Catalyzed Allylic C–H Fluorination. *Journal of the American Chemical Society* **2013**, *135* (35), 12990-12993.
62. Liron, F.; Oble, J.; Lorion, M. M.; Poli, G., Direct Allylic Functionalization Through Pd-Catalyzed C–H Activation. *European Journal of Organic Chemistry* **2014**, *2014* (27), 5863-5883.
63. Mei, T.-S.; Patel, H. H.; Sigman, M. S., Enantioselective Construction of Remote Quaternary Stereocentres. *Nature* **2014**, *508*, 340.
64. Hilton, M. J.; Xu, L.-P.; Norrby, P.-O.; Wu, Y.-D.; Wiest, O.; Sigman, M. S., Investigating the Nature of Palladium Chain-Walking in the Enantioselective Redox-Relay Heck Reaction of Alkenyl Alcohols. *The Journal of Organic Chemistry* **2014**, *79* (24), 11841-11850.
65. Daves, G. D.; Hallberg, A., 1,2-Additions to Heteroatom-substituted Olefins by Organopalladium Reagents. *Chemical Reviews* **1989**, *89* (7), 1433-1445.
66. Cabri, W.; Candiani, I.; Bedeschi, A.; Santi, R., Palladium-catalyzed Arylation of Unsymmetrical Olefins. Bidentate Phosphine Ligand Controlled Regioselectivity. *The Journal of Organic Chemistry* **1992**, *57* (13), 3558-3563.
67. Cabri, W.; Candiani, I.; Bedeschi, A.; Penco, S.; Santi, R., .alpha.-Regioselectivity in Palladium-catalyzed Arylation of Acyclic Enol Ethers. *The Journal of Organic Chemistry* **1992**, *57* (5), 1481-1486.
68. Cabri, W.; Candiani, I., Recent Developments and New Perspectives in the Heck Reaction. *Accounts of Chemical Research* **1995**, *28* (1), 2-7.
69. Cabri, W.; Candiani, I.; Bedeschi, A.; Santi, R., Ligand-controlled .alpha.-Regioselectivity in Palladium-catalyzed Arylation of Butyl Vinyl Ether. *The Journal of Organic Chemistry* **1990**, *55* (11), 3654-3655.
70. Ruan, J.; Xiao, J., From α -Arylation of Olefins to Acylation with Aldehydes: A Journey in Regiocontrol of the Heck Reaction. *Accounts of Chemical Research* **2011**, *44* (8), 614-626.

71. Ozawa, F.; Kubo, A.; Hayashi, T., Catalytic Asymmetric Arylation of 2,3-dihydrofuran with Aryl Triflates. *Journal of the American Chemical Society* **1991**, *113* (4), 1417-1419.
72. Werner, E. W.; Mei, T.-S.; Burckle, A. J.; Sigman, M. S., Enantioselective Heck Arylations of Acyclic Alkenyl Alcohols Using a Redox-Relay Strategy. *Science* **2012**, *338* (6113), 1455-1458.
73. Knowles, J. P.; Whiting, A., The Heck-Mizoroki Cross-coupling Reaction: a Mechanistic Perspective. *Organic & Biomolecular Chemistry* **2007**, *5* (1), 31-44.
74. Ishikawa, T. N., Keiko; Ohkubo, Naoko; Ishii, Hisashi, Cesium Fluoride-mediated Claisen Rearrangements of Phenyl Propargyl Ethers: Effect of a Substituent on the Phenyl Ring on the Rearrangement. *Heterocycles* 1994, *39* (1), 371-380.
75. Aissaoui, H. B., Christoph; Gude, Markus; Koberstein, Ralf; Lehmann, David; Sifferlen, Thierry; Trachsel, Daniel 3-Aza-bicyclo[3.1.0]hexane Derivatives. 2007.
76. Lykakis, I. N.; Efe, C.; Gryparis, C.; Stratakis, M., Ph3PAuNTf2 as a Superior Catalyst for the Selective Synthesis of 2H-Chromenes: Application to the Concise Synthesis of Benzopyran Natural Products. *European Journal of Organic Chemistry* **2011**, *2011* (12), 2334-2338.
77. Efe, C.; Lykakis, I. N.; Stratakis, M., Gold Nanoparticles Supported on TiO2 Catalyse the Cycloisomerisation/Oxidative Dimerisation of Aryl Propargyl Ethers. *Chemical Communications* **2011**, *47* (2), 803-805.
78. Nag, S.; Lehmann, L.; Ketschau, G.; Toth, M.; Heinrich, T.; Thiele, A.; Varrone, A.; Halldin, C., Development of a Novel Fluorine-18 Labeled Deuterated Fluororasagiline ([18F]fluororasagiline-D2) Radioligand for PET Studies of Monoamino Oxidase B (MAO-B). *Bioorganic & Medicinal Chemistry* **2013**, *21* (21), 6634-6641.
79. Frisch, M. J.; Trucks, G. W.; Schlegel, H. B.; Scuseria, G. E.; Robb, M. A.; Cheeseman, J. R.; Scalmani, G.; Barone, V.; Petersson, G. A.; Nakatsuji, H.; Li, X.; Caricato, M.; Marenich, A. V.; Bloino, J.; Janesko, B. G.; Gomperts, R.; Mennucci, B.; Hratchian, H. P.; Ortiz, J. V.; Izmaylov, A. F.; Sonnenberg, J. L.; Williams; Ding, F.; Lipparini, F.; Egidi, F.; Goings, J.; Peng, B.; Petrone, A.; Henderson, T.; Ranasinghe, D.; Zakrzewski, V. G.; Gao, J.; Rega, N.; Zheng, G.; Liang, W.; Hada, M.; Ehara, M.; Toyota, K.; Fukuda, R.; Hasegawa, J.; Ishida, M.; Nakajima, T.; Honda, Y.; Kitao, O.; Nakai, H.; Vreven, T.; Throssell, K.; Montgomery Jr., J. A.; Peralta, J. E.; Ogliaro, F.; Bearpark, M. J.; Heyd, J. J.; Brothers, E. N.; Kudin, K. N.; Staroverov, V. N.; Keith, T. A.; Kobayashi, R.; Normand, J.; Raghavachari, K.; Rendell, A. P.; Burant, J. C.; Iyengar, S. S.; Tomasi, J.; Cossi, M.; Millam, J. M.; Klene, M.; Adamo, C.; Cammi, R.; Ochterski, J. W.; Martin, R. L.; Morokuma, K.; Farkas, O.; Foresman, J. B.; Fox, D. J. *Gaussian 16 Rev. B.01*, Wallingford, CT, 2016.
80. Schäfer, A.; Huber, C.; Ahlrichs, R., Fully Optimized Contracted Gaussian Basis Sets of Triple Zeta Valence Quality for Atoms Li to Kr. *The Journal of Chemical Physics* **1994**, *100* (8), 5829-5835.
81. Seeman, J. I., The Curtin-Hammett Principle and the Winstein-Holness Equation: New Definition and Recent Extensions to Classical Concepts. *Journal of Chemical Education* **1986**, *63* (1), 42.

Chapter 2

Palladium-Catalyzed Functionalizations of Fluoroalkenes: A Defluorinative Coupling of 1-Aryl-2,2'-Dfluoroalkenes and Boronic Acids and the Enantioselective Aminofluorination 1-Aryl-2-Fluoroalkenes

Portions of this chapter have previously appeared in:

Thornbury, R. T.; Toste, F. D. *Angew. Chem. Int. Ed.* **2016**, *55*, 11629-11632.

2.1. Introduction

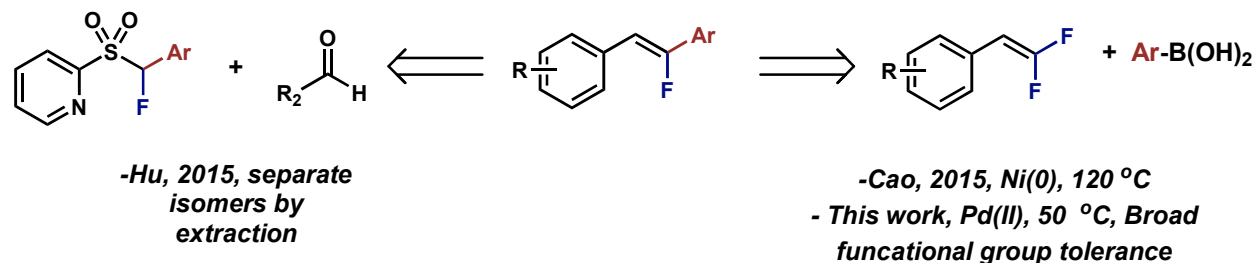
The use of bioisosteres, sometimes simply referred to as isosteres, has long attracted interest in the field of medicinal chemistry.¹⁻² Several definitions of a bioisostere can be found in the literature, but a useful definition offered by Alfred Burger states that a bioisosteric compounds are “compounds that poses near-equal molecular shapes and volumes, approximately the same distribution of electrons, and which exhibit similar physiochemical properties”.³ In short, these compounds have similar properties, despite having molecularly unique chemical structures. The utility of such compounds, however, is found in the subtle differences that remain between two bioisosteres. In an ideal scenario, the isostere would mimic the desirable properties of its molecular partner, while providing new or different properties that might be more desirable.

The amide bond is a ubiquitous structural motif found medicinal chemistry, and consequently much effort has been made to develop amide bond mimics.⁴ Monofluoroalkenes exhibit a similar steric and electronic profile to amides, and thus have been used frequently as amide isosteres.⁴⁻¹² In comparison to amides, monofluoroalkenes have some important orthogonal properties which could make them useful mimics in medicinal chemistry. Some of these include enhanced stability to peptidases, increased lipophilicity, conformational rigidity, and in some cases improved molecular recognition.⁴ Monofluoroalkenes could also serve as a low toxicity alternatives to anilides, which have a well-documented toxicity in medicinal chemistry.^{2, 13}

Monofluoroalkenes can be prepared via several types of transformations including elimination, olefination, cross-coupling, and cross metathesis reactions.¹⁴⁻¹⁵ Despite the variety of methods that have been developed to access different classes of monofluoroalkenes, challenges still remain. Amongst these challenges are the lack of syntheses that enable rapid diversification and methods that are highly stereoselective.¹⁴⁻¹⁵ The latter is of particular concern because traditional chromatographic techniques, including preparative HPLC, often fail to separate *E* and *Z* isomers of monofluoroalkenes, highlighting the importance of stereoselective methods.¹⁶

The independent works of Hu and Cao are representative examples of the successes and remaining challenges in monofluoroalkene synthesis. Hu and co-workers have recently developed Julia-Kocienski olefination procedure that utilizes a selective decomposition strategy of sulfinate intermediates to isolate the *E* and *Z* isomers by extraction (Scheme 2.1).¹⁶ While the procedure allows for isolation of both fluoroalkenes stereoisomers from the same reaction, this still leaves the issue of selective synthesis unsolved. Additionally, this protocol requires the synthesis of a new olefination reagent for each derivative, an impediment to modularity that is inherent to olefination strategies for monofluoroalkene synthesis.¹⁴⁻¹⁵ Cao and co-workers have recently reported a nickel-catalyzed Suzuki type coupling of boronic acids and difluorostyrenes that affords monofluoroalkenes stereoselectively (Scheme 2.1).¹⁷ It is proposed that reaction proceeds through oxidative addition into one of the vinyl C–F bond,¹⁸⁻²⁰ followed by cross-coupling with an aryl boronic acid. While a cross-coupling strategy provides the opportunity for more rapid diversification, the high temperature and reactive catalysts required for C–F bond activation led to limited functional group tolerance. In order to make a cross-coupling strategy with difluoroalkenes tolerant of functional groups relevant to pharmaceutical, agrochemical and material sciences, we believed a mechanistically distinct process would be required. Herein

we report the development of a palladium-catalyzed defluorinative coupling reaction to access single isomers of monofluorostilbenes under mild conditions (Scheme 2.1).

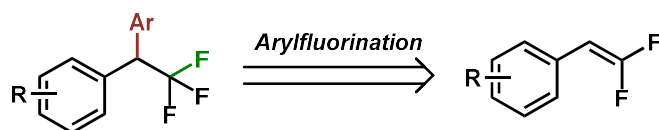


Scheme 2.1. Strategies for the synthesis of monofluorostilbenes

2.2. Results and Discussion

2.2.1. Defluorinative Coupling of Difluorostyrenes

As an extension of our arylfluorination chemistry,²¹⁻²³ we questioned whether we might be able to construct molecules with trifluoromethyl-containing stereocenters *via* a palladium-catalyzed difunctionalization of difluoroalkenes (Scheme 2.2).²⁴⁻²⁵ We hypothesized that this unconventional trifluoromethylation strategy could give us access to moieties not easily accessible by existing asymmetric trifluoromethylation methodologies.²⁶ It should also be noted that difluoroalkenes are a readily accessible class of substrates.²⁷⁻³⁰ While a variety of methods exist for their synthesis, perhaps the most notable is through a Julia-Kocienski olefination protocol utilizing commercially available difluoromethyl 2-pyridyl sulfone (Hu's reagent) and aldehydes or ketones, which we found to be useful for our purposes.

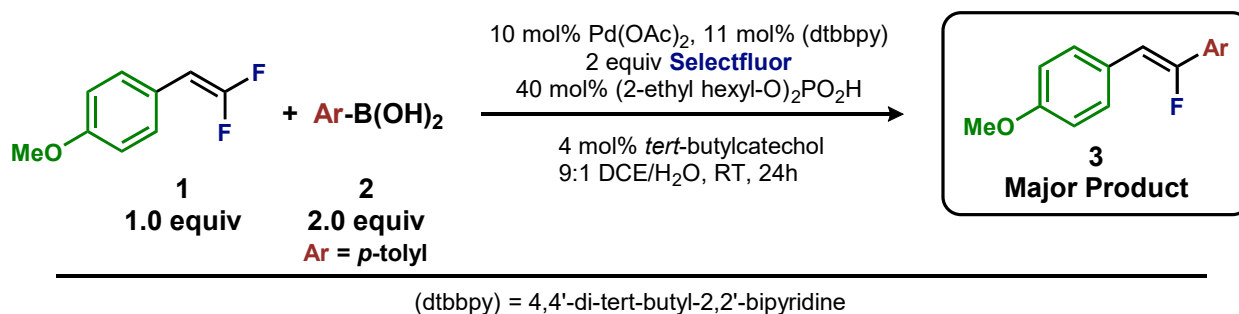


Scheme 2.2. Proposed retrosynthetic approach to trifluoromethyl functional group from difluoroalkene

During our studies on the arylfluorination of difluoroalkenes, we made some interesting observations. Under conditions similar to those employed in our arylfluorination reactions, we observed only traces of the desired trifluoromethyl-containing product (Scheme 2.3). Instead we observed monofluoroalkene **3** as the major product of the reaction. To rationalize this outcome, we envisioned a mechanistic scenario as outlined in Figure 2.2. Insertion of a difluoroalkene into a palladium-aryl bond of **A** would lead to the palladium alkyl intermediate, **B**. In an analogous fashion to beta-hydride elimination in the Heck reaction, β -fluoride elimination would lead to formation of the olefin product. The resulting palladium (II) species, **C**, could readily transmetallate with an aryl boronic acid to close the catalytic cycle. Importantly, such a process circumvents the generation of palladium(0) and is a redox neutral process, thus not requiring the use of external oxidants or added base. These aspects would be expected to help minimize issues with functional group compatibility. This serendipitous result led us to wonder if stereoselective

monofluoroalkene synthesis might be achieved *via* a defluorinative coupling reaction with difluoroalkenes.

Perhaps the most interesting aspect of this proposed mechanism is the β -fluoride elimination step. At the time of this report, β -fluoride elimination from organometallic intermediates was not without precedent; however, it was infrequently designed into catalytic transformations.³¹⁻³⁷ The most frequent application of this elementary step was in coupling reactions with trifluoromethyl-substituted alkenes.^{31, 33-34, 37} In recent years, several new reports of defluorinative coupling reactions with difluoroalkenes, including carbo-, boryl-, and hydrodefluorination, have begun to emerge, further demonstrating that difluoroalkenes are useful for constructing fluorinated building blocks.³⁸⁻⁴⁴



Scheme 2.3. Defluorinative coupling observed under arylfluorination conditions

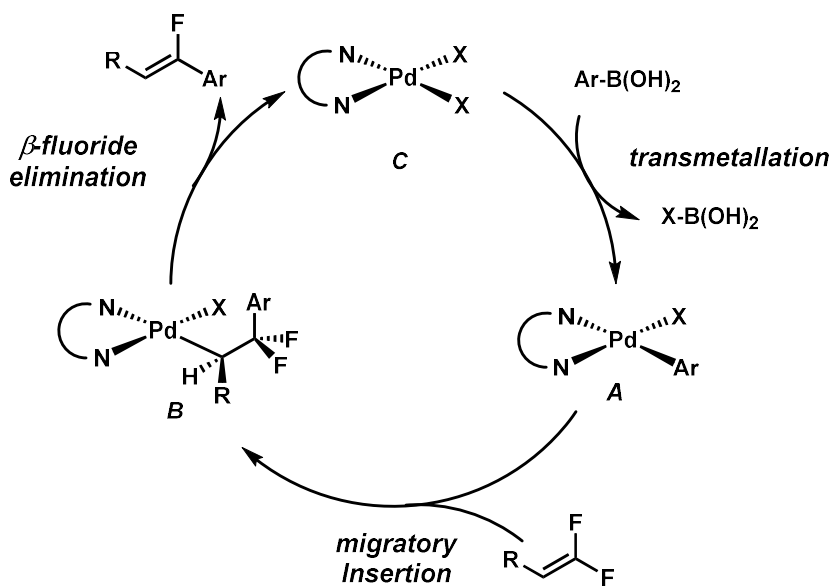
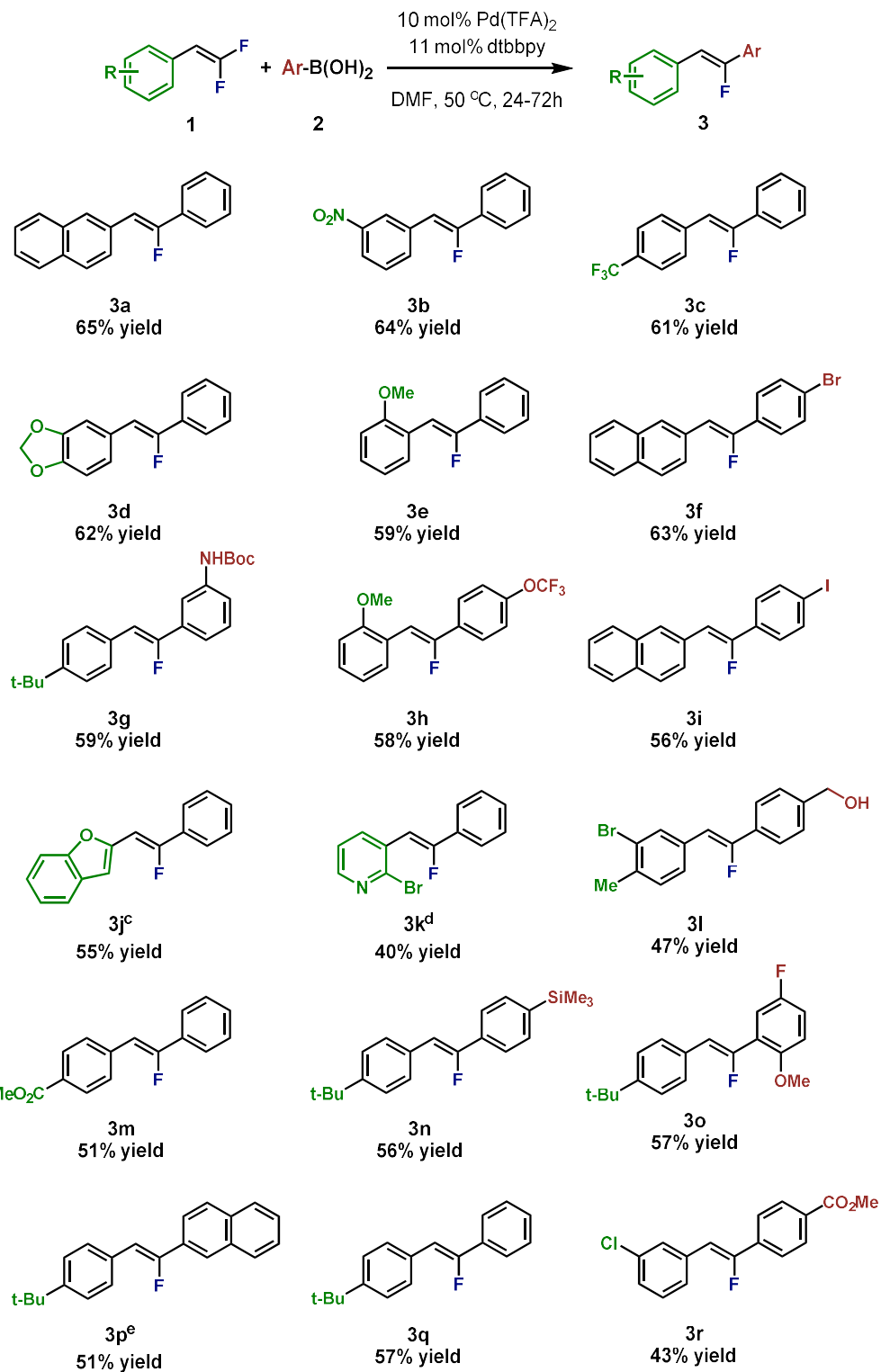


Figure 2.1. Proposed catalytic cycle for observed defluorinative coupling

With a variety of difluoroalkenes and boronic acids on hand we began to develop conditions for a palladium catalyzed defluorinative coupling (see supporting information). Our optimization efforts lead us to employ palladium(II) trifluoroacetate as a palladium source along with 4,4'-*tert*-butyl-2,2'-bipyridine as a ligand in dimethylformamide (DMF) solvent at 50 °C. We investigated the scope of this reaction (Table 2.1).



a.) standard reaction conditions: 0.2 mmol 1, 1.05-2.0 eq 2, 10 mol% Pd(TFA)₂, 11 mol% 4,4'-di-tert-butyl-2,2'-bipyridine (dtbbpy), 0.5 ml DMF, 50 °C; completion of reaction monitored by thin-layer chromatography. b.) Isolated yields c.) reaction run for 5 days. d.) reaction run at 85 °C for 4 days. e.) 47 % yield when corresponding potassium trifluoroborate salt is employed in place of boronic acid.

Table 2.1. Scope of defluorinative coupling^{a,b}

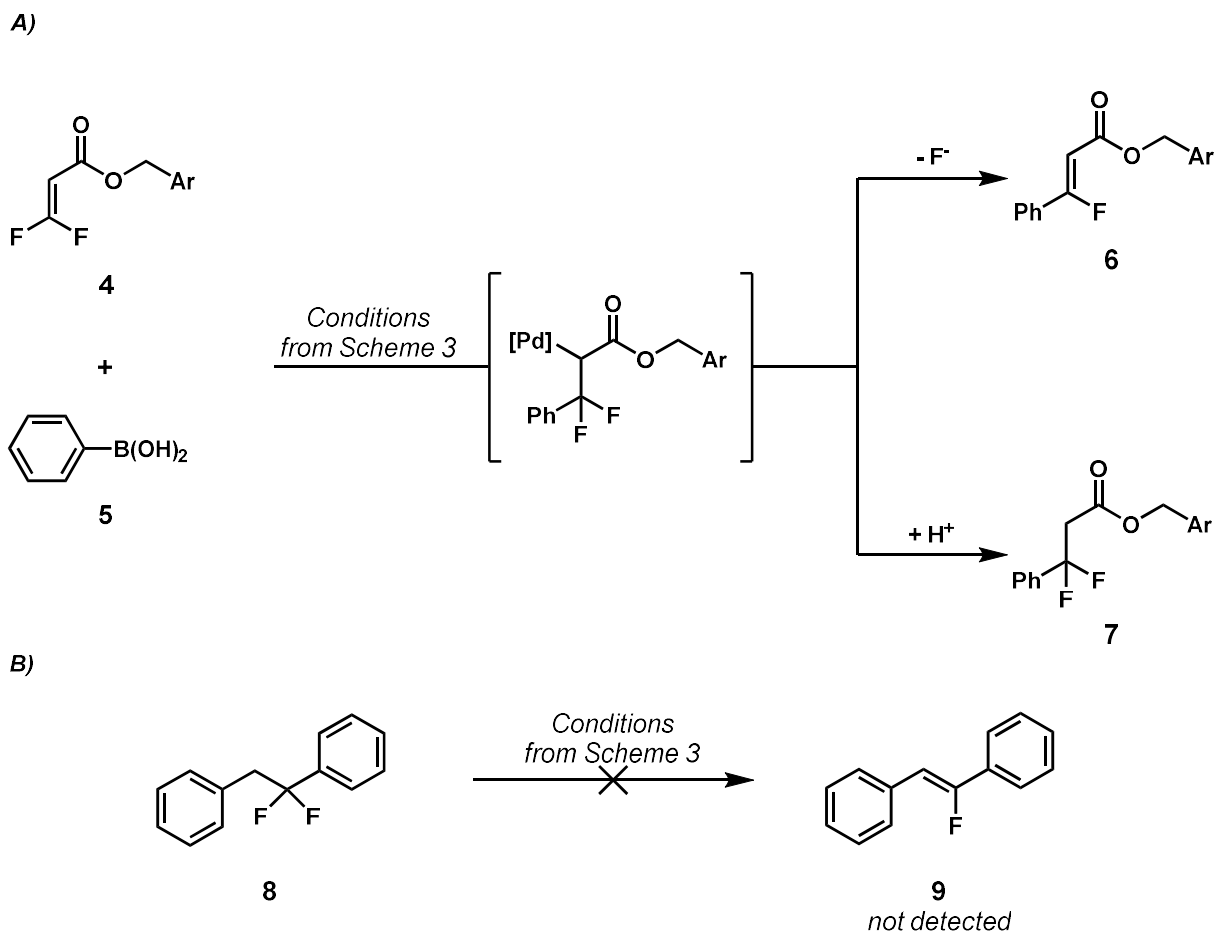
In all cases the monofluoroalkene products were formed in $\geq 50:1$ diastereomeric ratio. With respect to difluoroalkene, we found that a wide variety of functional groups were tolerated including alkyl, ester, nitro, trifluoromethyl, ether, and halogen substituents, as well as substitution at *ortho*-, *meta*-, and *para*- positions of the aromatic ring. The reaction also tolerates a variety of functional groups on the boronic acid coupling partner including halogens, esters, methoxy, trifluoromethoxy, trimethylsilyl, free alcohol, and protected amine substituents, as well as substitution at *ortho*-, *meta*-, and *para*- positions. Some heteroarene substituted difluoroalkenes are tolerated as well, although they require extended reaction times and/or elevated temperature (Table 2.1, footnotes c and d). Both benzofuran product **3j** and pyridine **3k** can be synthesized, increasing the diversity of molecules accessible by this method.

The reaction developed herein exhibits some interesting chemoselectivity and functional group tolerances worth further comment. First, in addition to being highly stereoselective, the reaction was also highly selective for mono-coupled products. Only in the case of **3m**, did we observe over-reaction side products. However, this could be easily remedied by reduction of boronic acid loading to near stoichiometric quantities, and **3m** was isolated in moderate yield.

Second, we have observed that the reaction conditions are uniquely suited to boron-based nucleophiles including boronic acids and potassium tetrafluoroborate salts (Table 2.1, footnote e), although boronic esters react sluggishly. Interestingly, we found that arylstannanes and arylsilanes were inert under our reaction conditions both with and without added equivalents of fluoride, affording the opportunity for orthogonal cross coupling.⁴⁵⁻⁴⁷

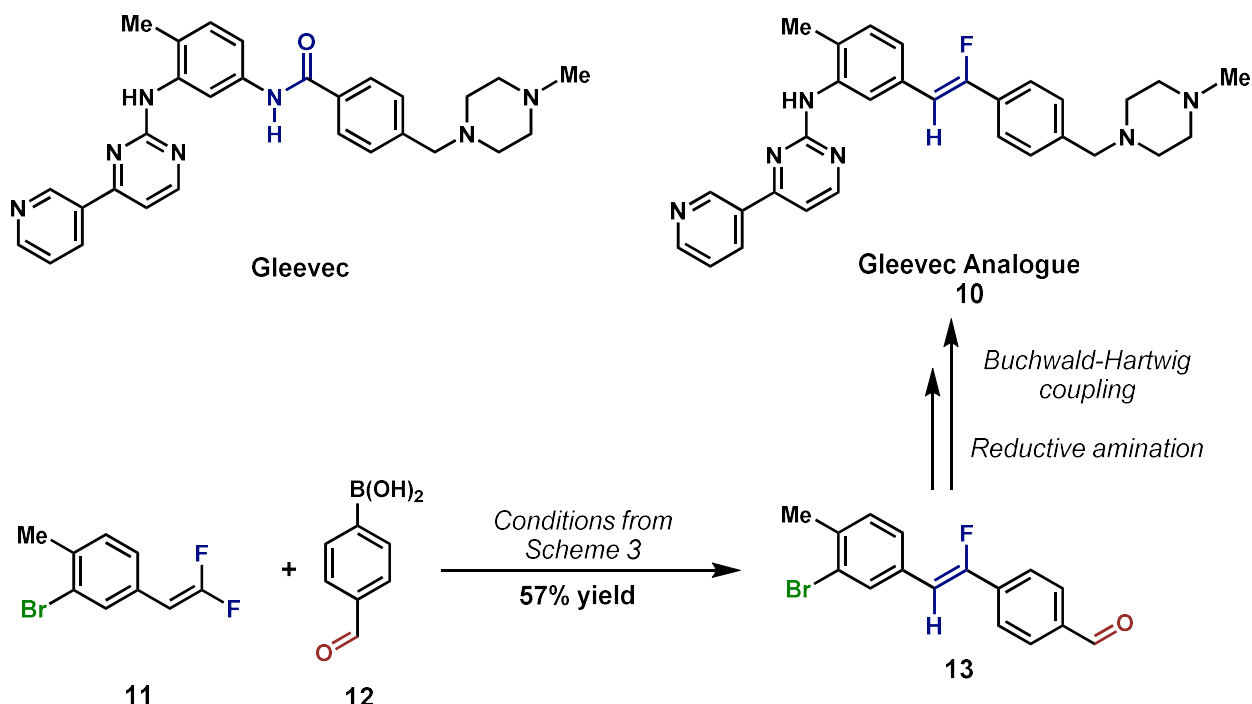
And finally, a variety of functional groups are tolerated that might be useful for further synthetic manipulations. Importantly, aryl halides are tolerated under these reaction conditions, including chlorides, bromides, and iodide. Even a substrate bearing a 2-bromopyridine is tolerated. In no case did we observe cross coupling with these functional groups, which stands in stark contrast to the nickel catalyzed procedure developed by Cao and co-workers who observe cross-coupling even with arylchlorides.⁵ These results together strongly suggest that our process does not involve formation of Pd(0), and supports our initial mechanistic hypothesis. We believe this distinct reactivity manifold enables significant expansion of functional group tolerance.

In an effort to lend support to our mechanistic hypothesis, we subjected a difluoroacrylate **4** to our reaction conditions. Analysis of the proton and fluorine NMR spectra revealed a mixture of defluorocoupled product **6**, and 1,4-conjugate addition product, **7** (Scheme 2.4A). Formation of **7** presumably proceeds through a palladium alkyl intermediate,⁴⁸ further supporting our proposal that the reaction proceeds through a migratory insertion, β -fluoride elimination pathway. Although we had never observed protonolysis products for the difluorostyrene substrates, observation of the protonolysis product, **7**, lead us to consider whether protonolysis followed by base catalyzed elimination might be responsible for the formation of the monofluoroalkenes. To test for this possibility, we subjected 1,1-difluoro-1,2-diphenylethane, **8**, to our standard reaction conditions (Scheme 2.4B). The corresponding monofluoroalkene, **9**, was not observed, thus suggesting the β -fluoride elimination is not simply base mediated and occurs from a palladium alkyl intermediate.



Scheme 2.4. Mechanistic investigations. Ar = *p*-Br-C₆H₄-. A) Difluoroacrylate as mechanistic probe. B) Stability of difluoromethylene under reaction conditions

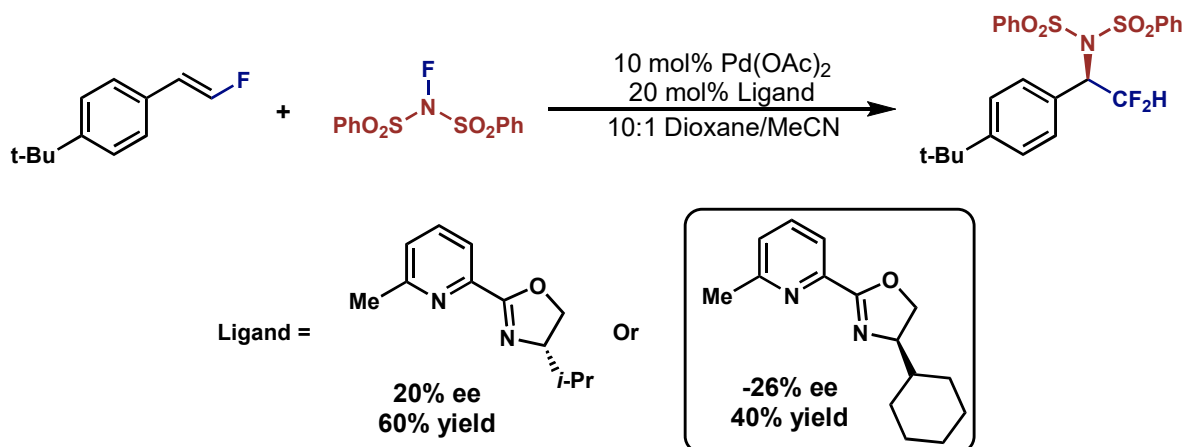
In order to demonstrate the utility of this palladium-catalyzed defluorinative coupling, we sought to apply our methodology to the synthesis of a Gleevec® isostere. Gleevec® is a tyrosine kinase inhibitor, and the first of its class to be approved for the treatment of a variety of cancers.⁴⁹⁻⁵⁰ Gleevec® contains a benzamide moiety, in its structure (Scheme 2.5), that we sought substitute with a monofluoroalkene moiety. Crystallographic studies suggest that the benzamide moiety adopts a *trans*- geometry in the enzyme binding site, making our stereoselective method particularly useful for accessing a conformationally locked analogue of Gleevec®.⁵¹ From commercially available 3-bromo-4-methyl-benzaldehyde, difluoroalkene **11** was synthesized using Hu's reagent, and then subjected to our reaction conditions in presence of 4-formylphenylboronic acid. Gratifyingly, the defluorocoupled product **13** was obtained in 57% yield. Reductive amination with 1-methylpiperazine followed by palladium-catalyzed Buchwald-Hartwig coupling with commercially available 4-(3-pyridinyl)-2-pyrimidine amine affords the monofluoroalkene derivative of Gleevec®, **10**, in 2 additional steps (See supporting information for details).⁵² Critical to the synthesis was the compatibility of functional groups such as the benzaldehyde moiety and the aryl bromide.



Scheme 2.5. Synthesis of Gleevec® Analogue 10

2.2.2. Aminofluorination of Fluoroalkenes

In addition to the arylfluorination of fluoroalkenes, we also investigated the aminofluorination of fluoroalkenes as a means to access trifluoromethyl and difluoromethyl containing products. Liu and co-workers reported the palladium-catalyzed aminofluorination of styrenes with *N*-fluorobenzenesulfonimide (NFSI), wherein the amino fragment is the bis-sulfonimide moiety from NFSI.⁵³ We questioned whether this strategy could be extended to difluoro- and monofluoroalkenes, and whether it might be possible to render the reaction asymmetric. We were pleased to find that indeed both monofluoro- and difluorostyrenes are competent in this reactions. We were further encouraged to find modest levels of enantioselectivity for the aminofluorination reaction, affording difluoromethyl-containing products (Scheme 2.6).



Scheme 2.6. Moderately enantioselective aminofluorination of monofluorostyrenes

Unfortunately, the maximum enantiomeric excess that was obtained was 26%. It should be noted that the presence of a non-hydrogen substituent (such as a methyl group) at the 6-position of the pyridine or a quinoline moiety in place of the pyridine was required on the ligand in order to obtain high yield (see supporting information for ligand screen data). The low enantiomeric excesses observed could conceivably be a function of these ligand requirements. Steric hindrance around the pyridine or quinoline nitrogen atom may encourage lability in the ligand.⁵⁴⁻⁵⁵ As shown in chapter 1 scheme 1.6 of this dissertation and in the literature, loss of rigidity in binding of the chiral ligand to palladium often results in poorer enantioselectivities.⁵⁶⁻⁵⁸ Future investigations should consider this possibility in addition to trying to identify other competent ligand classes.

2.3. Conclusion

In conclusion, we have developed the palladium catalyzed defluorinative coupling of 1-aryl-2,2-difluoroalkenes with boronic acids to afford a monofluoroalkenes with high diastereoselectivity. The relatively mild reaction conditions and distinct mechanistic manifold allow for the incorporation of variety of synthetically useful functional groups. The utility of this method and these monofluoroalkene building blocks was demonstrated by the synthesis of a Gleevec® amide isostere. Moreover, this method represents a promising general strategy to synthesize products that can serve as isosteres for anilides, which have known toxicity in a medicinal setting.

In addition, a moderately enantioselective aminofluorination of monofluorostyrenes has been developed. The unique ligand effects on reaction performance suggest that lability of the ligand may play an important role in catalyst performance and merits further study.

2.4. Supporting Information

2.4.1. General Information

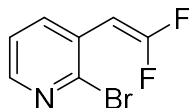
Unless otherwise noted, reagents were obtained from commercial sources and used without further purification. All reactions were carried out without rigorous exclusion of water and air and at room temperature (23 °C) except where otherwise indicated. All reactions were magnetically stirred and monitored by analytical thin layer chromatography (TLC) using Merck 60 pre-coated silica gel plates with F254 indicator. Visualization was accomplished by UV light (254 nm). Flash column chromatography was performed using ICN SiliTech 32-63 D 60Å silica gel. Commercial grade solvents were used without further purification except as indicated below. Tetrahydrofuran (THF), diethyl ether (Et₂O), dichloromethane (CH₂Cl₂), and, *N,N'*-dimethylformamide (DMF) were dried by passing commercially available pre-dried, oxygen-free formulations through activated alumina columns. ¹H NMR, ¹³C NMR, and ¹⁹F spectra were recorded on Bruker AMX-300, AVQ-400, AVB-400, DRX-500 and AV-600 spectrometers and referenced to CDCl₃ or CD₂Cl₂. Tetramethylsilane was used as an internal standard for ¹H NMR (δ: 0.0 ppm), and CDCl₃ or CD₂Cl₂ for ¹³C NMR (δ: 77.23 ppm and 53.84 respectively). Multiplicities are indicated by s (singlet), d (doublet), t (triplet), q (quartet), and m (multiplet). Mass spectral data were obtained from the QB3/Chemistry Mass Spectrometry Facility at the University of California, Berkeley.

2.4.2. Preparation and Characterization of Difluoroalkene Substrates

Unless otherwise noted, all difluoroalkene substrates were synthesized according to an adapted procedure of the method developed by Hu et al.¹⁶ A general procedure is provided below: To a flame dried 3-neck flask under N₂ difluoromethyl 2-pyridinyl sulfone (386 mg, 1.0 mmol, 1.0 eq) and the corresponding aldehyde (2.4 mmol, 1.2 eq) were added and dissolved in 4.0 mL of dry DMF. The contents of the flask were cooled to -50 °C on a dry ice acetone bath. Potassium *tert*-butoxide (404 mg, 3.6 mmol, 1.8 eq) was added dropwise as a solution in 4.0 mL of DMF. The solution was stirred, and allowed to slowly warm to -40 °C over the course of 45 minutes. The reaction mixture was then quenched with 4.0 mL of a saturated aqueous solution of NH₄Cl and 4.0 mL of 1 M aqueous HCl. The flask was allowed to warm to room temperature and stir for 2 hours. The contents of the flask were then transferred to a separatory funnel and diluted with H₂O and Et₂O. The aqueous layer was removed, and the organic layer was washed 3 times with a saturated aqueous NaCl solution. The organic layer was separated, dried over MgSO₄, filtered, and concentrated. The crude residue was purified by silica gel column chromatography (100 % hexanes to 90:10 hexanes ethyl acetate).

Spectra for compounds **1a-j**, **o**, **s** were in agreement with literature reports.^{16-17, 27, 59-60}

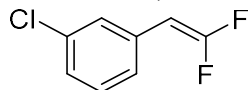
2-bromo-3-(2,2-difluorovinyl)pyridine **1k**:



Pale yellow oil :

- **¹H NMR** (400 MHz, CD₂Cl₂) δ 8.23 (dd, *J* = 4.5, 1.9 Hz, 1H), 7.80 (d, *J* = 7.7 Hz, 1H), 7.29 (dd, *J* = 7.8, 4.7 Hz, 1H), 5.67 (dd, *J* = 25.3, 3.1 Hz, 1H).
- **¹⁹F NMR** (377 MHz, CD₂Cl₂): δ -77.85 (dd, *J* = 21.3, 3.3 Hz), -80.46 (dd, *J* = 25.3, 21.2 Hz).
- **¹³C NMR** (126 MHz, CD₂Cl₂) δ 157.3 (dd, *J* = 299.9, 291.1 Hz), 148.7, 143.0 (d, *J* = 6.3 Hz), 137.2 (d, *J* = 8.8 Hz), 128.5 (d, *J* = 7.6 Hz), 123.3, 80.8 (dd, *J* = 34.0, 12.6 Hz).
- **HRMS** (EI): M⁺ found 218.9496; C₇H₅BrF₂N requires 218.9495

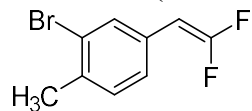
1-chloro-3-(2,2-difluorovinyl)benzene **1r**:



Colorless oil :

- **¹H NMR** (500 MHz, CD₂Cl₂) δ 7.34 (d, *J* = 2.1 Hz, 1H), 7.31 – 7.17 (m, 3H), 5.28 (dd, *J* = 26.0, 3.7 Hz, 1H).
- **¹⁹F NMR** (377 MHz, CD₂Cl₂) δ -80.45 (dd, *J* = 28.5, 25.9 Hz), -82.54 (dd, *J* = 28.8, 3.5 Hz).
- **¹³C NMR** (126 MHz, CD₂Cl₂) δ 157.0 (dd, *J* = 299.9, 289.8 Hz), 134.8, 132.6 (m), 130.4, 127.8 (dd, *J* = 7.6, 3.8 Hz), 127.5, 126.2 (dd, *J* = 6.3, 3.8 Hz), 81.8 (dd, *J* = 30.2, 13.9 Hz).
- **HRMS** (EI): M⁺ found 174.0050; C₈H₅ClF₂ requires 174.0048

2-bromo-4-(2,2-difluorovinyl)-1-methylbenzene11:



Colorless oil :

- **¹H NMR** (500 MHz, CD₂Cl₂) δ 7.52 (d, *J* = 1.8 Hz, 1H), 7.28 – 7.11 (m, 2H), 5.25 (dd, *J* = 26.2, 3.7 Hz, 1H), 2.37 (s, 3H).
- **¹⁹F NMR** (377 MHz, CD₂Cl₂): δ -81.33 (dd, *J* = 30.7, 26.0 Hz), -83.53 (dd, *J* = 31.3, 3.8 Hz).
- **¹³C NMR** (126 MHz, CD₂Cl₂) δ ¹³C NMR (126 MHz, CDCl₃) δ 156.7 (dd, *J* = 299.3, 289.2 Hz), 137.2, 131.4 (dd, *J* = 7.6, 3.8 Hz), 131.3, 130.0 (m), 126.8 (dd, *J* = 6.3, 3.8 Hz), 125.4, 81.4 (dd, *J* = 29.0, 12.6 Hz), 22.7.
- **HRMS** (EI): M+H⁺ found 231.9700; C₉H₇BrF₂ requires 231.9699

2.4.3. Optimization, Preparation, and Characterization of Defluoro-coupling Products

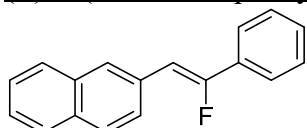
Selected Optimization on Substrate 3a:

Entry	Pd Source	Ligand	Solvent	Temp.	Yield
1	Pd(TFA) ₂	dtbbpy	DMF	50 °C	65% ^{isolated}
2	Pd(TFA) ₂	dtbbpy	MeCN	50 °C	< 10%
3	Pd(TFA) ₂	dtbbpy	Dioxane	50 °C	30%
4	Pd(OAc) ₂	dtbbpy	Dioxane	100 °C	37%
5	Pd(OAc) ₂	dtbbpy	THF	50 °C	25%
6	Pd(OAc) ₂	Phenanthroline	Dioxane	50 °C	13%
7	(MeCN) ₂ PdCl ₂	dtbbpy	Dioxane	50 °C	0%
8	Pd(OAc) ₂	dtbbpy	Dioxane	50 °C	24%
9	(dppp)PdCl ₂	N/A	Dioxane	50 °C	0%

General Defluoro-coupling procedure:

To an oven dried septum capped vial, palladium (II) trifluoroacetate (6.6 mg, 0.020 mmol, 0.10 eq.) was added in a N₂ atmosphere glovebox. The vial was removed from the glovebox, and 4,4'-di-*tert*-butyl-2,2'-dipyridyl (6.0 mg, 0.022 mmol, 0.11 eq.). The solids were suspended in 0.25 mL of DMF and stirred for 30 minutes. Difluoroalkene substrate (0.200 mmol, 1.0 eq.) was added as a solution in 0.25 mL of DMF. Aryl boronic acid (0.400 mmol, 2.00 eq.) was added as a solid. The vial was capped and the vial was placed in a 50 °C oil bath. The contents of the vial were stirred and the progress of the reaction was monitored by TLC. After complete consumption of the starting material, the solution was cooled to room temperature and diluted with EtOAc and transferred to a separatory funnel. The organic layer was washed 3 times with a saturated aqueous NaCl solution. The organic layer was separated, dried over MgSO₄, and concentrated. The crude residue was purified by silica gel chromatography (hexanes/ethyl acetate mixtures).

(Z)-2-(2-fluoro-2-phenylvinyl)naphthalene 3a:

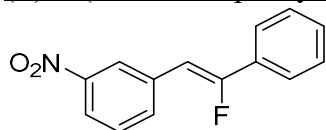


White solid:

Spectra were in agreement with literature report.¹⁶

- ¹H NMR (400 MHz, CD₂Cl₂) δ 8.10 (d, *J* = 1.6 Hz, 1H), 7.92 – 7.80 (m, 4H), 7.77 – 7.69 (m, 2H), 7.58 – 7.36 (m, 6H), 6.54 (d, *J* = 40.0 Hz, 1H).
- ¹⁹F NMR (376 MHz, CD₂Cl₂): δ -113.61 (d, *J* = 40.0 Hz).
- ¹³C NMR (126 MHz, CD₂Cl₂) δ 157.9 (d, *J* = 259.6 Hz), 133.9, 133.1 (d, *J* = 27.7 Hz), 132.9, 131.6 (d, *J* = 2.5 Hz), 129.5, 129.1, 129.0, 128.4, 128.4, 127.9, 127.1 (d, *J* = 7.6 Hz), 126.6, 126.5, 124.6 (d, *J* = 7.6 Hz), 106.3 (d, *J* = 10.1 Hz).

(Z)-1-(2-fluoro-2-phenylvinyl)-3-nitrobenzene 3b:

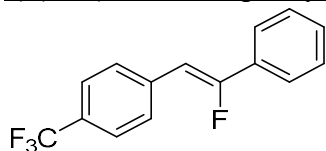


White solid:

Spectra were in agreement with literature report.¹⁶

- **¹H NMR** (400 MHz, CDCl₃) δ 8.50 (s, 1H), 8.16 – 8.06 (m, 1H), 7.95 (d, *J* = 7.8 Hz, 1H), 7.68 (dd, *J* = 7.9, 1.8 Hz, 2H), 7.55 (t, *J* = 8.0 Hz, 1H), 7.45 (d, *J* = 7.1 Hz, 3H), 6.38 (d, *J* = 37.9 Hz, 1H).
- **¹⁹F NMR** (376 MHz, CDCl₃): δ -109.45 (d, *J* = 38.0 Hz).
- **¹³C NMR** (126 MHz, CD₂Cl₂) δ 159.4 (d, *J* = 262.1 Hz), 148.9, 135.7 (d, *J* = 2.5 Hz), 134.9 (d, *J* = 8.8 Hz), 132.2 (d, *J* = 27.7 Hz), 130.2, 129.9, 129.1 (d, *J* = 1.3 Hz), 124.9 (d, *J* = 7.6 Hz), 123.6 (d, *J* = 8.8 Hz), 122.1 (d, *J* = 1.3 Hz), 104.2 (d, *J* = 10.1 Hz).

(Z)-1-(2-fluoro-2-phenylvinyl)-4-(trifluoromethyl)benzene 3c:

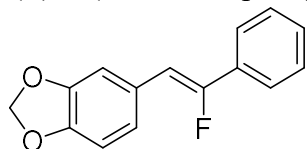


White solid:

Spectra were in agreement with literature report.¹⁶

- **¹H NMR** (400 MHz, CDCl₃) δ 7.74 (d, *J* = 8.2 Hz, 2H), 7.67 (dd, *J* = 7.9, 1.8 Hz, 2H), 7.62 (d, *J* = 8.2 Hz, 2H), 7.51 – 7.37 (m, 3H), 6.35 (d, *J* = 38.6 Hz, 1H).
- **¹⁹F NMR** (376 MHz, CDCl₃): δ -61.76, -110.26 (d, *J* = 38.6 Hz).
- **¹³C NMR** (126 MHz, CD₂Cl₂) δ 159.1 (d, *J* = 262.1 Hz), 137.7, 132.5 (d, *J* = 27.7 Hz), 130.1, 129.4 (d, *J* = 8.8 Hz), 129.1 (d, *J* = 2.5 Hz), 125.8 (q, *J* = 3.8 Hz), 124.9 (d, *J* = 7.6 Hz), 124.7 (q, *J* = 272.2 Hz), 104.9 (d, *J* = 10.1 Hz). The resonance for the aromatic carbon *ipso*- to the trifluoromethyl substituent could not be resolved. This is in agreement with the previous literature report.¹⁶

(Z)-5-(2-fluoro-2-phenylvinyl)benzo[d][1,3]dioxole 3d:

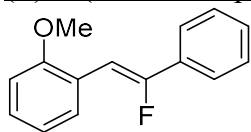


White solid:

Spectra were in agreement with literature report.¹⁷

- **¹H NMR** (400 MHz, CDCl₃) δ 7.65 – 7.58 (m, 2H), 7.44 – 7.32 (m, 3H), 7.29 (d, *J* = 1.8 Hz, 1H), 7.03 (dd, *J* = 8.1, 1.7 Hz, 1H), 6.82 (d, *J* = 8.1 Hz, 1H), 6.24 (d, *J* = 39.2 Hz, 1H), 5.99 (s, 2H).
- **¹⁹F NMR** (377 MHz, CDCl₃): δ -115.4 (d, *J* = 39.2 Hz).
- **¹³C NMR** (151 MHz, CDCl₃): δ 156.3 (d, *J* = 256.7 Hz), 148.0, 147.0 (d, *J* = 3.0 Hz), 133.1 (d, *J* = 27.2 Hz), 128.9, 128.7 (d, *J* = 1.5 Hz), 128.0 (d, *J* = 23.0 Hz), 124.2 (d, *J* = 7.6 Hz), 123.4 (d, *J* = 6.0 Hz), 109.1 (d, *J* = 10.6 Hz), 108.5, 105.8 (d, *J* = 10.6 Hz), 101.3.

(Z)-1-(2-fluoro-2-phenylvinyl)-2-methoxybenzene 3e:

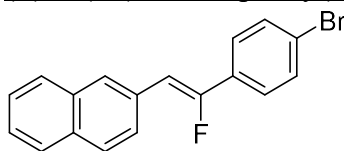


White solid:

Spectra were in agreement with literature report.¹⁶

- **¹H NMR** (400 MHz, CDCl₃) δ 7.95 (dd, *J* = 7.8, 1.7 Hz, 1H), 7.73 – 7.61 (m, 2H), 7.47 – 7.23 (m, 4H), 7.00 (t, *J* = 7.6 Hz, 1H), 6.91 (dd, *J* = 8.2, 1.1 Hz, 1H), 6.79 (d, *J* = 40.8 Hz, 1H), 3.88 (s, 3H).
- **¹⁹F NMR** (377 MHz, CDCl₃): -115.2 (d, *J* = 41.3 Hz)
- **¹³C NMR** (126 MHz, CD₂Cl₂) ¹³C NMR (126 MHz, CDCl₃) δ 157.4 (d, *J* = 257.0 Hz), 157.0, 133.65 (d, *J* = 27.7 Hz), 130.1 (d, *J* = 13.9 Hz), 129.2, 128.9, 128.9, 124.5 (d, *J* = 7.6 Hz), 122.6, 121.0, 110.9, 99.7 (d, *J* = 8.8 Hz), 55.9.

(Z)-2-(2-(4-bromophenyl)-2-fluorovinyl)naphthalene 3f:

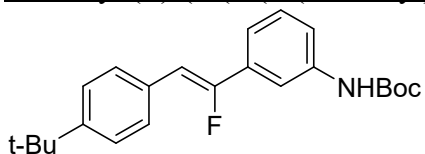


White solid:

Spectra were in agreement with literature report.¹⁶

- **¹H NMR** (400 MHz, CDCl₃) δ 8.07 (s, 1H), 7.88 – 7.76 (m, 4H), 7.56 (s, 4H), 7.52 – 7.44 (m, 2H), 6.48 (d, *J* = 39.3 Hz, 1H).
- **¹⁹F NMR** (377 MHz, CDCl₃): δ -113.61 (d, *J* = 39.3 Hz).
- **¹³C NMR** (126 MHz, CD₂Cl₂) δ 156.9 (d, *J* = 258.3 Hz), 133.9, 133.0, 132.2 (d, *J* = 27.7 Hz), 132.2 (d, *J* = 2.5 Hz), 131.3 (d, *J* = 3.8 Hz), 128.6 (d, *J* = 8.8 Hz), 128.5 (d, *J* = 3.8 Hz), 127.9, 127.0 (d, *J* = 7.6 Hz), 126.7, 126.7, 126.2, 126.1, 123.5, 106.9 (d, *J* = 10.1 Hz).

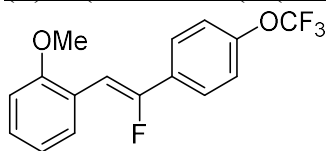
tert-butyl (Z)-(3-(2-(4-(tert-butyl)phenyl)-1-fluorovinyl)phenyl)carbamate 3g:



White solid :

- **¹H NMR** (500 MHz, CD₂Cl₂) δ ¹H NMR (500 MHz, Chloroform-*d*) δ 7.72 (s, 1H), 7.59 (d, *J* = 8.0 Hz, 2H), 7.42 (d, *J* = 8.0 Hz, 2H), 7.39 – 7.29 (m, 3H), 6.75 (s, 1H), 6.35 (d, *J* = 40.2 Hz, 1H), 1.54 (s, 9H), 1.34 (s, 9H).
- **¹⁹F NMR** (377 MHz, CD₂Cl₂): δ -114.87 (d, *J* = 40.6 Hz).
- **¹³C NMR** (126 MHz, CD₂Cl₂) δ 156.8 (d, *J* = 257.0 Hz) 153.0, 151.0 (d, *J* = 2.5 Hz), 139.5 (d, *J* = 2.5 Hz), 134.0 (d, *J* = 27.7 Hz), 131.1 (d, *J* = 2.5 Hz), 129.6 (d, *J* = 2.5 Hz), 129.1 (d, *J* = 7.6 Hz), 125.9, 119.1, 119.0 (d, *J* = 7.6 Hz), 114.2 (d, *J* = 8.8 Hz), 106.3 (d, *J* = 10.1 Hz), 80.9, 34.9, 31.4, 28.4.
- **HRMS** (ESI): M+Na⁺ found 392.1995; C₂₃H₂₈FNO₂Na requires 392.1996

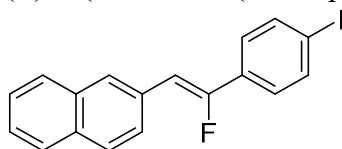
(Z)-1-(2-fluoro-2-(4-(trifluoromethoxy)phenyl)vinyl)-2-methoxybenzene 3h:



Colorless oil :

- **¹H NMR** (400 MHz, CDCl₃) δ 7.93 (dd, *J* = 7.7, 1.7 Hz, 1H), 7.69 (d, *J* = 8.9 Hz, 2H), 7.34 – 7.20 (m, 3H), 7.01 (t, *J* = 7.6 Hz, 1H), 6.91 (dd, *J* = 8.3, 1.1 Hz, 1H), 6.78 (d, *J* = 40.6 Hz, 1H), 3.88 (s, 3H).
- **¹⁹F NMR** (377 MHz, CDCl₃): δ -57.00 , -115.36 (d, *J* = 40.6 Hz).
- **¹³C NMR** (126 MHz, CD₂Cl₂) δ 157.0, 156.2 (d, *J* = 257.0 Hz), 149.68, 132.4 (d, *J* = 29.0 Hz), 130.1 (d, *J* = 13.7 Hz), 129.3 (d, *J* = 2.5 Hz), 126.2 (d, *J* = 7.6 Hz), 122.3 (d, *J* = 3.8 Hz), 121.4, 121.0, 120.9 (q, *J* = 258.3 Hz), 110.9, 100.6 (d, *J* = 8.8 Hz), 55.9.
- **HRMS** (EI): M⁺ found 312.0773; C₁₆H₁₂F₄O₂ requires 312.0773

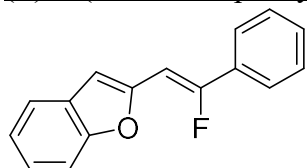
(Z)-2-(2-fluoro-2-(4-iodophenyl)vinyl)naphthalene 3i:



Off white solid :

- **¹H NMR** (400 MHz, CD₂Cl₂) δ 8.09 (s, 1H), 7.91 – 7.76 (m, 6H), 7.53 – 7.47 (m, 2H), 7.45 (d, *J* = 8.6 Hz, 2H), 6.55 (d, *J* = 39.7 Hz, 1H).
- **¹⁹F NMR** (377 MHz, CD₂Cl₂): δ -114.62 (d, *J* = 39.9 Hz).
- **¹³C NMR** (151 MHz, CD₂Cl₂) δ 157.1(d, *J* = 258.2 Hz), 138.3 (d, *J* = 3.0 Hz), 134.0, 133.1 (d, *J* = 3.0 Hz), 132.8 (d, *J* = 28.7 Hz), 131.4 (d, *J* = 4.5 Hz), 128.7 (d, *J* = 7.6 Hz), 128.5, 128.5, 128.0, 127.1 (d, *J* = 9.1 Hz), 126.8, 126.7, 126.3 (d, *J* = 7.6 Hz), 107.1 (d, *J* = 9.1 Hz), 95.2.
- **HRMS** (EI): M⁺ found 373.9975; C₁₈H₁₂FI requires 373.9968

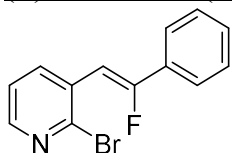
(Z)-2-(2-fluoro-2-phenylvinyl)benzofuran 3j:



White solid:

- **¹H NMR** (600 MHz, CD₂Cl₂) δ 7.71 – 7.66 (m, 2H), 7.63 – 7.57 (m, 1H), 7.51 – 7.39 (m, 4H), 7.29 (td, *J* = 8.2, 7.7, 1.4 Hz, 1H), 7.24 (td, *J* = 7.5, 1.1 Hz, 1H), 7.07 (s, 1H), 6.56 (d, *J* = 38.0 Hz, 1H).
- **¹⁹F NMR** (377 MHz, CDCl₃): δ -106.98 (d, *J* = 38.2 Hz).
- **¹³C NMR** (151 MHz, CD₂Cl₂) δ 158.9 (d, *J* = 261.2 Hz), 154.7 (d, *J* = 1.5 Hz), 151.5 (d, *J* = 3.0 Hz), 132.0 (d, *J* = 27.2 Hz), 130.1, 129.7, 129.2 (d, *J* = 3.0 Hz), 124.9, 124.7 (d, *J* = 7.6 Hz), 123.5, 121.4, 111.3, 106.9 (d, *J* = 12.1 Hz), 96.6 (d, *J* = 13.6 Hz).
- **HRMS** (EI): M⁺ found 238.0797; C₁₆H₁₁FO requires 238.0794

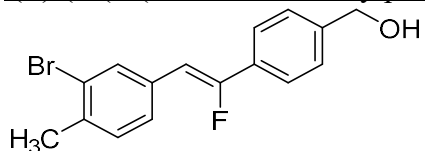
(Z)-2-bromo-3-(2-fluoro-2-phenylvinyl)pyridine 3k:



White solid :

- **¹H NMR** (600 MHz, CDCl₃) δ 8.30 – 8.18 (m, 2H), 7.69 (dd, *J* = 7.7, 1.8 Hz, 2H), 7.45 (m, 3H), 7.30 (dd, *J* = 7.8, 4.6 Hz, 1H), 6.66 (d, *J* = 37.7 Hz, 1H).
- **¹⁹F NMR** (377 MHz, CDCl₃): δ -111.58 (d, *J* = 37.7 Hz)
- **¹³C NMR** (151 MHz, CDCl₃) δ 159.7 (d, *J* = 262.7 Hz), 148.2 (d, *J* = 3.0 Hz), 143.3, 138.3 (d, *J* = 13.6 Hz), 132.0 (d, *J* = 27.2 Hz), 131.1 (d, *J* = 1.5 Hz), 130.2, 128.9 (d, *J* = 3.0 Hz), 124.9 (d, *J* = 7.6 Hz), 123.0, 102.7 (d, *J* = 7.6 Hz).
- **HRMS** (EI): M⁺ found 276.9902; C₁₃H₉BrFN requires 276.9902

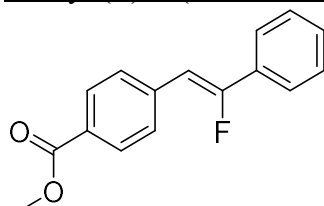
(Z)-4-(2-(3-bromo-4-methylphenyl)-1-fluorovinyl)phenyl)methanol 3l:



White solid :

- **¹H NMR** (400 MHz, CD₂Cl₂) δ 7.84 (d, *J* = 1.8 Hz, 1H), 7.63 (d, *J* = 8.3 Hz, 2H), 7.48 (dd, *J* = 7.9, 1.8 Hz, 1H), 7.42 (d, *J* = 8.0 Hz, 2H), 7.25 (d, *J* = 7.9 Hz, 1H), 6.27 (d, *J* = 39.5 Hz, 1H), 4.81 – 4.62 (m, 2H), 2.40 (s, 3H).
- **¹⁹F NMR** (377 MHz, CD₂Cl₂): δ -112.98 (d, *J* = 39.4 Hz).
- **¹³C NMR** (151 MHz, CDCl₃) ¹³C NMR (151 MHz, CD₂Cl₂) δ 157.9 (d, *J* = 258.2 Hz), 142.9, 137.4 (d, *J* = 3.0 Hz), 133.5 (d, *J* = 3.0 Hz), 132.7 (d, *J* = 9.1 Hz), 132.0 (d, *J* = 28.7 Hz), 131.3, 128.2 (d, *J* = 7.6 Hz), 127.4 (d, *J* = 3.0 Hz), 125.4, 124.8 (d, *J* = 7.6 Hz), 104.7 (d, *J* = 10.6 Hz), 65.0, 22.9.
- **HRMS** (EI): M⁺ found 320.0211; C₁₆H₁₄BrFO requires 320.0212

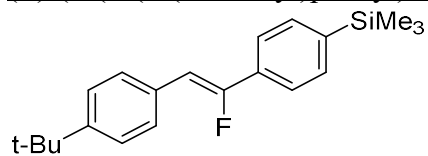
methyl (Z)-4-(2-fluoro-2-phenylvinyl)benzoate 3m:



White solid :

- **¹H NMR** (600 MHz, CDCl₃) δ 8.04 (d, *J* = 8.4 Hz, 2H), 7.74 – 7.63 (m, 4H), 7.49 – 7.35 (m, 3H), 6.36 (d, *J* = 38.9 Hz, 1H), 3.93 (s, 3H).
- **¹⁹F NMR** (565 MHz, CDCl₃): δ -111.46 (d, *J* = 39.0 Hz).
- **¹³C NMR** (151 MHz, CDCl₃) δ 167.0, 158.9 (d, *J* = 262.7 Hz), 138.4 (d, *J* = 3.0 Hz), 132.5 (d, *J* = 27.2 Hz), 130.0, 129.7, 128.9, 128.8, 128.7 (d, *J* = 3.0 Hz), 124.7, 105.2 (d, *J* = 9.1 Hz), 52.2.
- **HRMS** (EI): M⁺ found 256.0906; C₁₆H₁₃FO₂ requires 256.0900

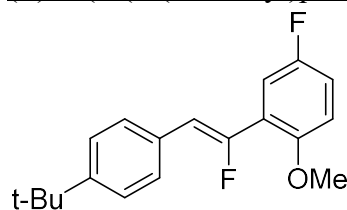
(Z)-2-(2-(4-(tert-butyl)phenyl)-1-fluorovinyl)phenyl)trimethylsilane 3n:



White solid :

- **¹H NMR** (600 MHz, CDCl₃) δ 7.61 (m, 4H), 7.56 (d, *J* = 7.8 Hz, 2H), 7.41 (d, *J* = 8.1 Hz, 2H), 6.33 (d, *J* = 39.8 Hz, 1H), 1.35 (s, 9H), 0.29 (s, 9H).
- **¹⁹F NMR** (377 MHz, CDCl₃): δ -114.80 (d, *J* = 39.8 Hz).
- **¹³C NMR** (151 MHz, CDCl₃) δ 157.0 (d, *J* = 258.2 Hz), 150.6 (d, *J* = 3.0 Hz), 141.8, 133.7 (d, *J* = 3.0 Hz), 133.5 (d, *J* = 27.2 Hz), 131.0 (d, *J* = 3.0 Hz), 128.9 (d, *J* = 7.6 Hz), 125.7, 123.4 (d, *J* = 7.6 Hz), 105.9 (d, *J* = 10.6 Hz), 34.8, 31.4, -1.0.
- **HRMS** (EI): M⁺ found 326.1870; C₂₁H₂₇FSi requires 326.1866

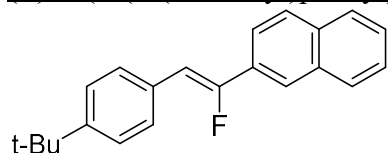
(Z)-2-(2-(4-(tert-butyl)phenyl)-1-fluorovinyl)-4-fluoro-1-methoxybenzene 3o:



Viscous colorless oil:

- **¹H NMR** (400 MHz, CD₂Cl₂) δ 7.57 (d, *J* = 8.5 Hz, 2H), 7.41 (d, *J* = 8.5 Hz, 2H), 7.34 (dd, *J* = 9.8, 3.1 Hz, 1H), 7.03 (ddd, *J* = 9.1, 7.5, 3.1 Hz, 1H), 6.94 (ddd, *J* = 9.1, 4.5, 1.2 Hz, 1H), 6.84 (d, *J* = 43.4 Hz, 1H), 3.93 (s, 3H), 1.34 (s, 9H).
- **¹⁹F NMR** (377 MHz, CDCl₃): δ -108.51 (d, *J* = 43.4 Hz), -123.53 (m).
- **¹³C NMR** (126 MHz, CD₂Cl₂) δ 157.2 (d, *J* = 238.1 Hz), 152.9 (d, *J* = 253.3 Hz), 153.2 (d, *J* = 5.0 Hz), 151.0 (d, *J* = 3.0 Hz), 131.5, 129.4 (d, *J* = 7.6 Hz), 125.9, 123.1 (dd, *J* = 20.2, 8.8 Hz), 115.9 (d, *J* = 22.7 Hz), 113.8 (dd, *J* = 25.2, 12.6 Hz), 112.8 (dd, *J* = 5.0, 2.5 Hz), 112.0 (d, *J* = 8.8 Hz), 56.5, 34.9, 31.4.
- **HRMS** (EI): M⁺ found 302.1483; C₁₉H₂₀F₂O requires 302.1482

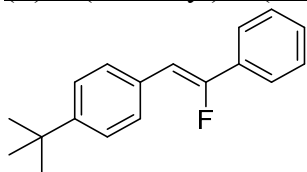
(Z)-2-(2-(4-(tert-butyl)phenyl)-1-fluorovinyl)naphthalene 3p:



White solid:

- **¹H NMR** (500 MHz, CD₂Cl₂) δ 8.14 (s, 1H), 7.96 – 7.82 (m, 3H), 7.74 (d, *J* = 8.6 Hz, 1H), 7.65 (d, *J* = 8.2 Hz, 2H), 7.53 (m, 2H), 7.45 (d, *J* = 8.1 Hz, 2H), 6.50 (d, *J* = 40.4 Hz, 1H), 1.36 (s, 9H).
- **¹⁹F NMR** (377 MHz, CD₂Cl₂): δ -115.38 (d, *J* = 40.5 Hz).
- **¹³C NMR** (126 MHz, CD₂Cl₂) δ ¹³C NMR (126 MHz, CDCl₃) δ 157.2 (d, *J* = 257.0 Hz), 151.1 (d, *J* = 2.5 Hz), 133.7, 133.5, 131.2 (d, *J* = 2.5 Hz), 130.5 (d, *J* = 27.7 Hz), 129.1, 129.1, 128.8, 128.7 (d, *J* = 2.5 Hz), 128.0, 127.1, 126.0, 123.6 (d, *J* = 8.8 Hz), 122.0 (d, *J* = 6.3 Hz), 106.6 (d, *J* = 10.1 Hz), 34.9, 31.4.
- **HRMS** (EI): M⁺ found 304.1640; C₂₂H₂₁F requires 304.1627

(Z)-1-(tert-butyl)-4-(2-fluoro-2-phenylvinyl)benzene 3q:

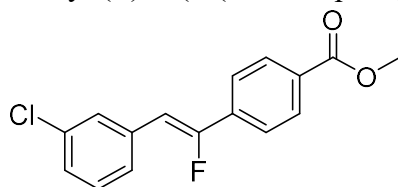


White solid:

Spectra were in agreement with literature report.¹⁶

- **¹H NMR** (400 MHz, CDCl₃) δ 7.64 (d, *J* = 7.0 Hz, 1H), 7.59 (d, *J* = 8.5 Hz, 2H), 7.46 – 7.31 (m, 5H), 6.31 (d, *J* = 39.8 Hz, 1H), 1.34 (s, 9H).
- **¹⁹F NMR** (376 MHz, CDCl₃) δ -114.42 (d, *J* = 39.8 Hz).
- **¹³C NMR** (126 MHz, CD₂Cl₂) δ 157.1 (d, *J* = 257.0 Hz), 151.0 (d, *J* = 2.5 Hz), 133.3 (d, *J* = 27.7 Hz), 131.1 (d, *J* = 2.5 Hz), 129.3, 129.0, 129.0, 125.9, 124.4 (d, *J* = 7.6 Hz), 106.0 (d, *J* = 11.3 Hz), 34.9, 31.4.

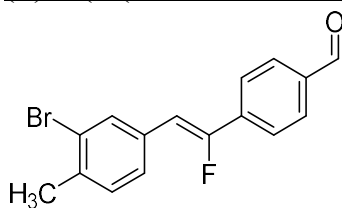
methyl (Z)-4-(2-(3-chlorophenyl)-1-fluorovinyl)benzoate 3r:



White solid :

- **¹H NMR** (400 MHz, CD₂Cl₂) δ 8.08 (d, *J* = 8.2 Hz, 2H), 7.78 – 7.66 (m, 3H), 7.54 (d, *J* = 7.7 Hz, 1H), 7.35 (t, *J* = 7.9 Hz, 1H), 7.29 (d, *J* = 8.1 Hz, 1H), 6.44 (d, *J* = 38.7 Hz, 1H), 3.91 (s, 3H).
- **¹⁹F NMR** (377 MHz, CD₂Cl₂): δ -112.78 (d, *J* = 38.8 Hz).
- **¹³C NMR** (126 MHz, CD₂Cl₂) δ 166.6, 157.4 (d, *J* = 259.6 Hz), 136.7 (d, *J* = 27.7 Hz), 135.3 (d, *J* = 3.8 Hz), 134.8, 131.2, 130.3, 130.2 (d, *J* = 2.5 Hz), 129.2 (d, *J* = 8.8 Hz), 128.2 (d, *J* = 2.5 Hz), 127.8 (d, *J* = 7.6 Hz), 124.6 (d, *J* = 7.6 Hz), 107.1 (d, *J* = 10.1 Hz), 52.5.
- **HRMS** (EI): M⁺ found 290.0512; C₁₆H₁₂ClFO₂ requires 290.0510

(Z)-4-(2-(3-bromo-4-methylphenyl)-1-fluorovinyl)benzaldehyde 13:

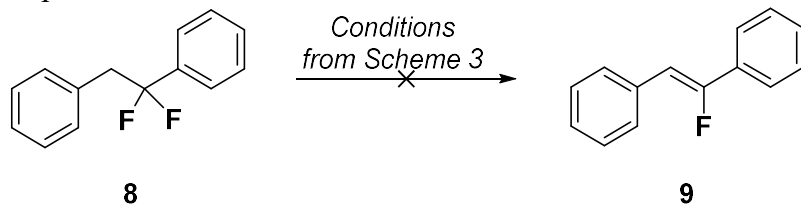


White solid :

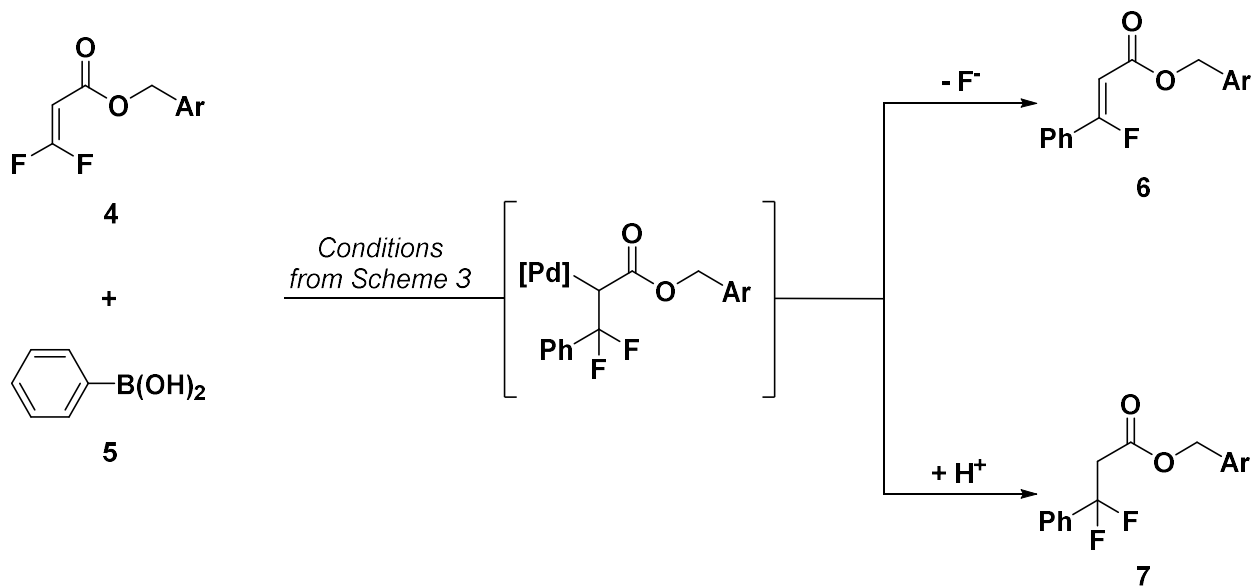
- **¹H NMR** (400 MHz, CD₂Cl₂) δ 10.02 (s, 1H), 7.92 (d, *J* = 8.0 Hz, 2H), 7.87 (s, 1H), 7.79 (d, *J* = 8.1 Hz, 2H), 7.52 (d, *J* = 8.0 Hz, 1H), 7.28 (d, *J* = 7.9 Hz, 1H), 6.44 (d, *J* = 39.0 Hz, 1H), 2.41 (s, 3H).
- **¹⁹F NMR** (377 MHz, CD₂Cl₂): δ -114.03 (d, *J* = 38.9 Hz).
- **¹³C NMR** (126 MHz, CDCl₃) δ 191.7, 156.6 (d, *J* = 259.6 Hz), 138.3 (d, *J* = 1.3 Hz), 138.1 (d, *J* = 27.7 Hz), 136.8, 132.9 (d, *J* = 8.8 Hz), 132.8 (d, *J* = 2.5 Hz), 131.3, 130.2 (d, *J* = 2.5 Hz), 128.5 (d, *J* = 8.8 Hz), 125.4, 124.9 (d, *J* = 7.6 Hz), 107.7 (d, *J* = 10.1 Hz), 23.0.
- **HRMS** (EI): M⁺ found 318.0059; C₁₆H₁₂BrFO requires 318.0056

2.4.4. Mechanistic Experiments

Experimental :



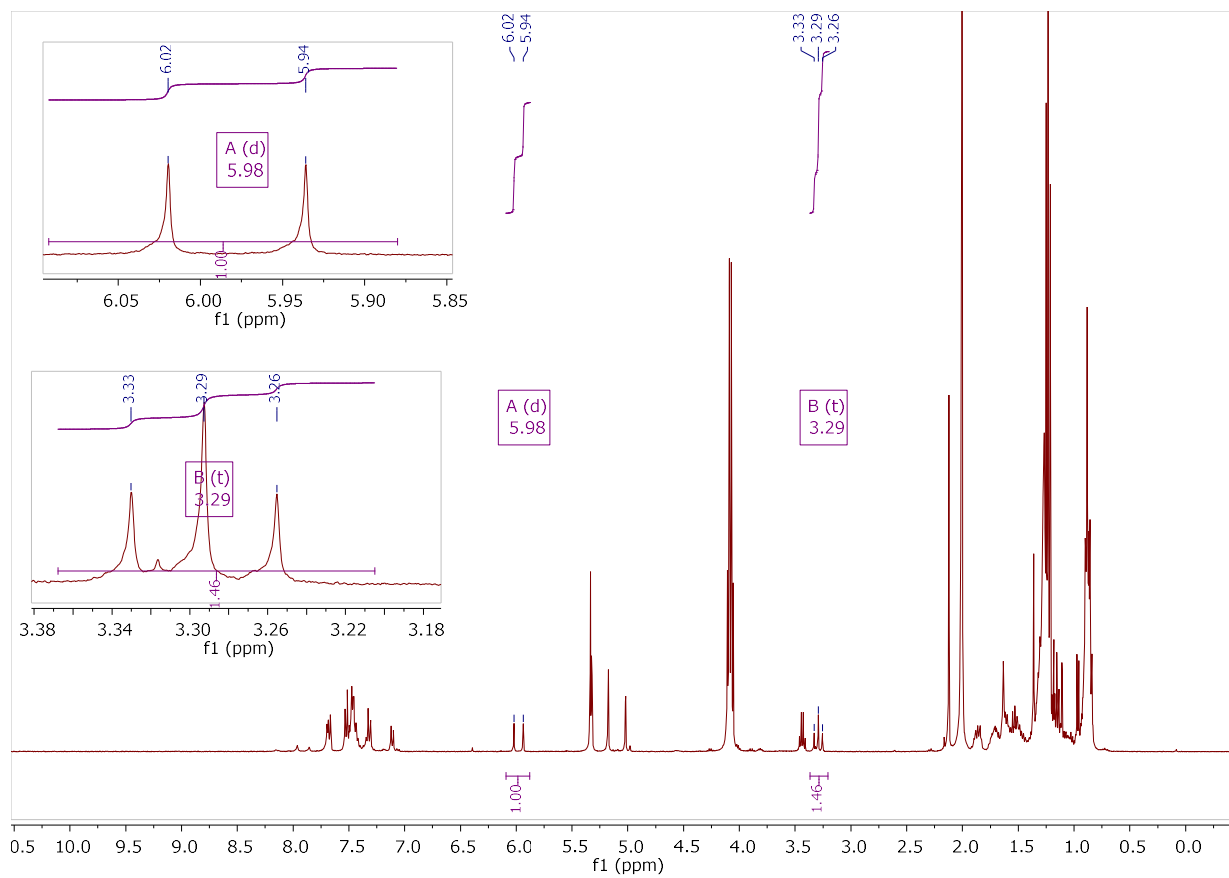
8 was prepared according to literature procedure⁶¹ and subjected to the reaction conditions detailed in section 3 with phenylboronic acid as the arylboronic acid. No monofluoroalkene product was observed.

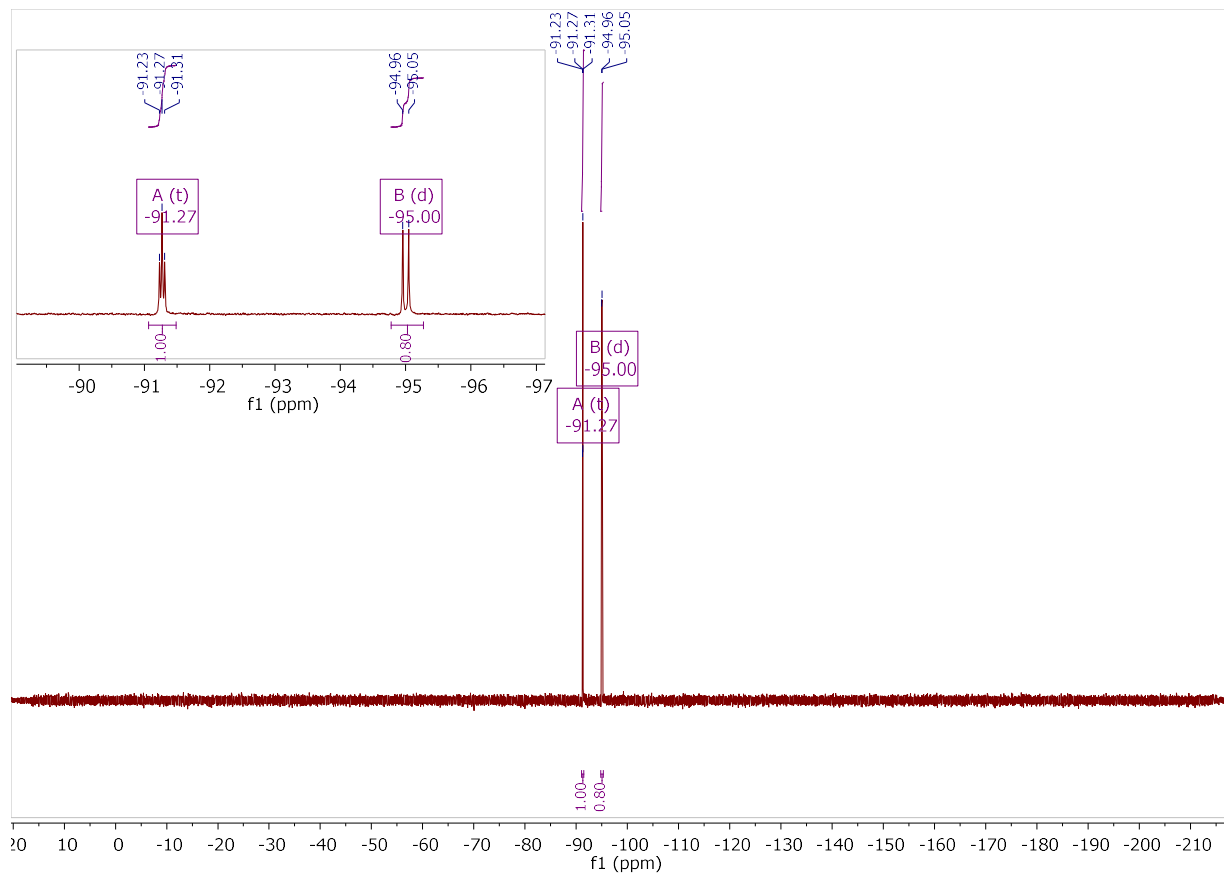


Difluoroacrylate **4** was prepared⁶² and subjected to same reaction conditions detailed in section 3. Products **6** and **7** were identified in the crude reaction mixture by ¹H and ¹⁹F NMR spectroscopy. Co-polarity of **6** and **7** precluded their isolation from each other however, diagnostic signals were in agreement with related reports from the literature.⁶³⁻⁶⁴ Crude spectra are provided below :

Diagnostic resonances:

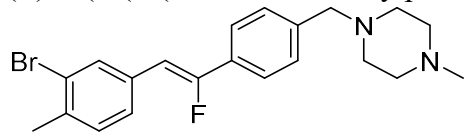
- ¹H NMR (400 MHz, CD₂Cl₂) For compound **6**: δ 5.98 (d, *J* = 33.5 Hz, 1H), For compound **7**: δ 3.29 (t, *J* = 15.0 Hz).
- ¹⁹F NMR (377 MHz, CD₂Cl₂): For compound **7**: δ -91.27 (t, *J* = 14.9 Hz), For compound **6**: δ -95.00 (d, *J* = 33.7 Hz).





2.4.5. Synthesis of Gleevec Derivative

(Z)-1-(4-(2-(3-bromo-4-methylphenyl)-1-fluorovinyl)benzyl)-4-methylpiperazine **14**



Compound **12** was synthesized as described above.

To a flame dried Schlenk flask under N₂ **12** (79.8 mg, 0.25 mmol, 1.0 eq) was added in 2.0 mL of 1,2-dichloroethane (used as received). To the flask, 1-methylpiperazine (138.0 μL, 1.25 mmol, 5.0 eq) was added via syringe. Contents of flask were stirred for 20 minutes resulting in a slightly yellow solution. Sodium cyanoborohydride (31.4 mg, 0.5 mmol, 2.0 eq) was added as a solid, and the contents of the flask were stirred. The reaction progress was monitored by thin-layer chromatography. After 12 hours, the reaction was incomplete. At this time an additional portion of sodium cyanoborohydride (equivalent to first portion) was added. After 18 hours of total reaction time the reaction was complete. The contents of the flask were diluted with water and DCM. The aqueous layer was washed twice with DCM. The combined organic layers were dried over MgSO₄, filtered, and concentrated. Crude NMR analysis indicated that **3m** was formed as a side product (2.5 : 1 **13/3m**). The crude solid was purified by silica gel chromatography (99.5 : 0.5 : 0 to 98.5 : 0.5 : 1.0 DCM/TEA/MeOH) to afford **13** (45 mg, 45%, *Z/E* = 50 : 1) as a white solid.

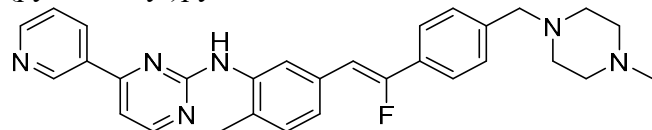
• ¹H NMR (400 MHz, CD₂Cl₂) δ 7.83 (d, *J* = 1.7 Hz, 1H), 7.58 (d, *J* = 8.4 Hz, 2H), 7.48 (dd, *J* = 7.9, 1.8 Hz, 1H), 7.37 (d, *J* = 8.1 Hz, 2H), 7.29 – 7.19 (m, 1H), 6.25 (d, *J* = 39.5 Hz, 1H), 3.52 (s, 2H), 2.44 (m, 11H), 2.28 (s, 3H).

• ¹⁹F NMR (377 MHz, CD₂Cl₂): δ -112.82 (d, *J* = 39.6 Hz).

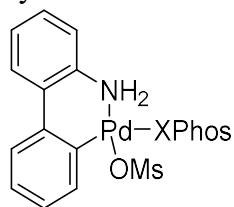
• ¹³C NMR (126 MHz, CDCl₃) δ 157.6 (d, *J* = 259.6 Hz), 140.2, 136.9 (d, *J* = 2.5 Hz), 133.2 (d, *J* = 2.5 Hz), 132.2 (d, *J* = 8.8 Hz), 131.1 (d, *J* = 27.7 Hz), 130.8, 129.3, 127.7 (d, *J* = 8.8 Hz), 124.9, 124.1 (d, *J* = 7.6 Hz), 104.0 (d, *J* = 10.1 Hz), 62.3, 53.1, 45.6, 22.5.

• HRMS (ESI): M+H⁺ found 403.1173; C₂₁H₂₅BrFN₂ requires 403.1180

(Z)-N-(5-(2-fluoro-2-(4-((4-methylpiperazin-1-yl)methyl)phenyl)vinyl)-2-methylphenyl)-4-(pyridin-3-yl)pyrimidin-2-amine **10**



A procedure was adapted from Buchwald et al.⁵² The following palladium pre-catalyst was synthesized according to literature report.⁶⁵



To a flame 2 dram vial equipped with a stir bar, **14** (40.3 mg, 0.100 mmol, 1.0 eq), XPhos pre-catalyst (4.2 mg, 0.005 mmol, 5 mol%), Xphos (2.4 mg, 0.005 mmol, 5 mol%), 4-(pyridin-3-yl)pyrimidin-2-amine (20.7 mg, 0.120 mmol, 1.2 eq), and potassium carbonate (30.4 mg, 0.220

mmol, 2.2 eq) were added as solids. The vial was evacuated and back-filled 4 times with N₂. The contents of the vial were dissolved in 0.5 mL of dry degassed *tert*-butanol. The solution was heated to 110 °C for 6 hours, after which the reaction the starting material was completely consumed. The contents of the flask were cooled to room temperature and were diluted with EtOAc and H₂O. The organic layer was washed once with H₂O and once with brine. The organic layer was separated and dried over MgSO₄, filtered, and concentrated. The crude solid was purified by silica gel chromatography (99.5 :0.5 :0 to 98.5 :0.5 :1.0 DCM/TEA/MeOH) to afford a white solid. The solid was taken up in DCM and washed with H₂O to remove triethylammonium salts. The DCM layer was dried over Na₂SO₄ filtered and concentrated to afford 9 (16 mg, 34%, *Z/E* = 12:1) as a white solid.

• **¹H NMR** (600 MHz, CD₂Cl₂) δ 9.26 (s, 1H), 8.69 (d, *J* = 4.7 Hz, 1H), 8.51 (d, *J* = 5.1 Hz, 1H), 8.48 – 8.37 (m, 2H), 7.60 (d, *J* = 8.3 Hz, 2H), 7.47 – 7.40 (m, 1H), 7.38 (d, *J* = 8.1 Hz, 2H), 7.32 (dd, *J* = 7.8, 1.8 Hz, 1H), 7.26 (d, *J* = 7.9 Hz, 1H), 7.22 (d, *J* = 5.1 Hz, 1H), 7.05 (s, 1H), 6.36 (d, *J* = 40.2 Hz, 1H), 3.51 (s, 2H), 2.37 (br, piperazine protons), 2.23 (s, 3H).

• **¹⁹F NMR** (377 MHz, CD₂Cl₂): δ -95.91 (d, *J* = 22.0 Hz, minor *E* diastereomer), -114.03 (d, *J* = 40.1 Hz).

• **¹³C NMR** (151 MHz, CD₂Cl₂) δ 162.6, 160.9, 159.1, 156.9 (d, *J* = 256.7 Hz), 151.4, 148.5, 139.9, 137.7, 134.3, 132.6, 132.0, 131.5 (d, *J* = 28.7 Hz), 130.5, 129.2 (d, *J* = 1.5 Hz), 128.5, 124.4 (d, *J* = 7.6 Hz), 123.9 (d, *J* = 7.6 Hz), 123.5, 122.2 (d, *J* = 7.6 Hz), 108.2, 105.4 (d, *J* = 10.6 Hz), 62.4, 55.1, 45.7, 17.7. (One carbon resonance corresponding to the piperazine moiety under the CD₂Cl₂ peak)

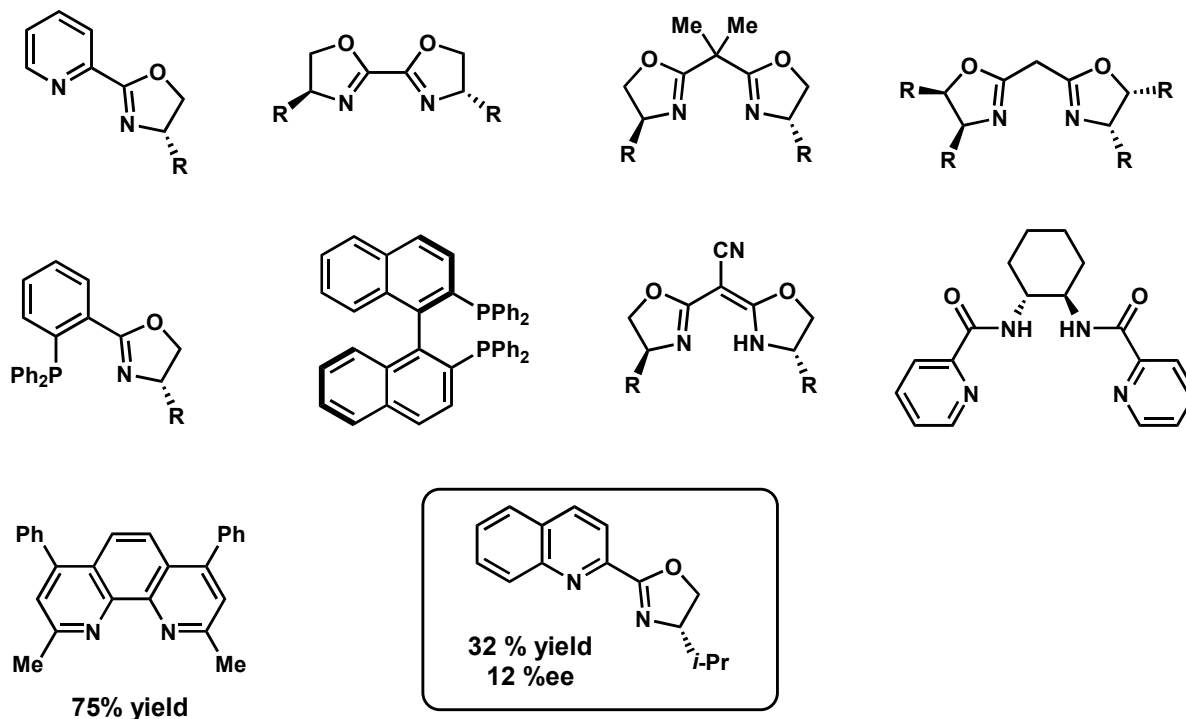
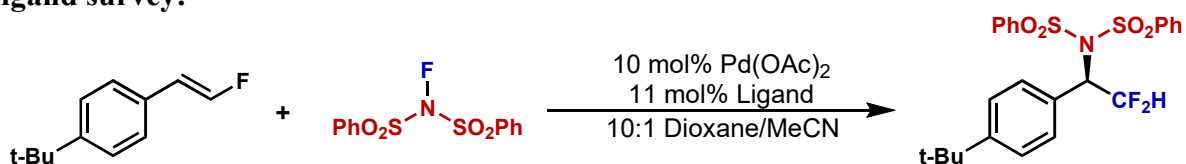
• **HRMS** (ESI): M+H⁺ found 495.2654; C₃₀H₃₂FN₆ requires 495.2667

2.4.6. Data for aminofluorination of monofluorostyrenes

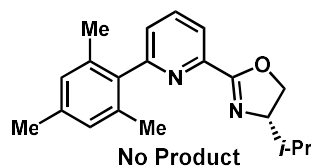
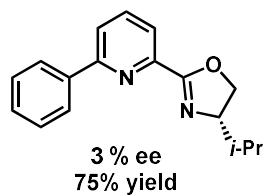
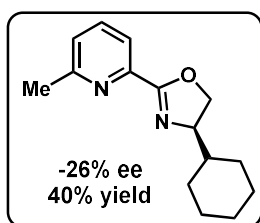
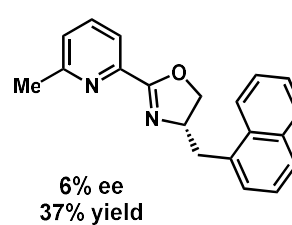
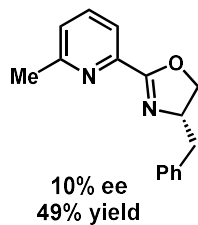
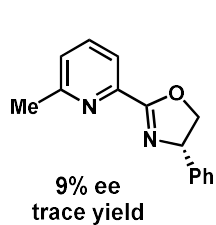
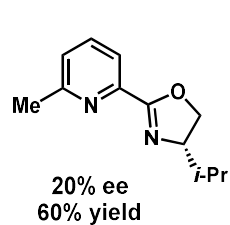
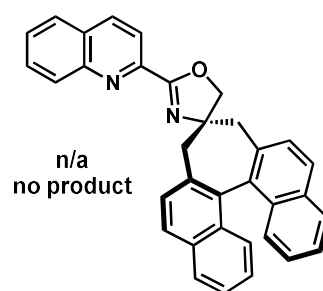
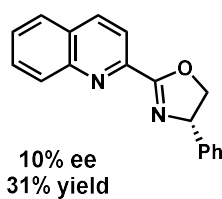
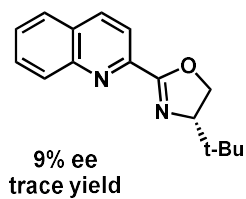
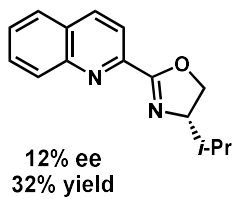
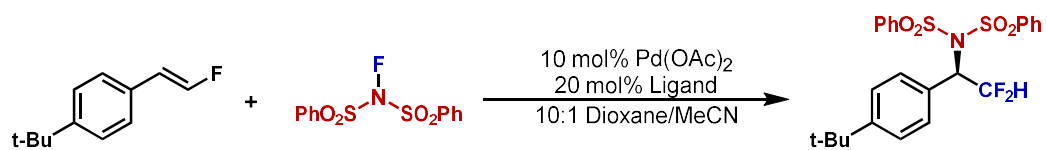
Procedure for asymmetric aminofluorination of fluoroalkenes:

To a 1 dram vial, Pd(OAc)₂ (.02 mmol, 0.1 eq) and chiral ligand (0.04 mmol, 0.2 eq) were added and suspended in 0.5 mL of bench top dioxane. The contents of the vial were stirred for 15 minutes. The substrate (0.2 mmol, 1.0 eq) was added as a solution in 0.5 mL of dioxane. NFSI (0.3 mmol, 1.5 eq) was added as a solid followed by 0.1 mL of acetonitrile. The reaction mixture was stirred at room temperature and monitored by TLC (10:1 Hex/EA) (18-36 hours). After completion, the reaction mixture was concentrated and immediately purified by silica gel chromatography (20:1 Hex/EA). The spectral data for the product was consistent with literature reports.⁵³ Yields refer to isolated yields. Enantiomeric excess determined by Chiral HPLC analysis (AD-H, 95:5 hexanes/IPA, 1.0 mL/min).

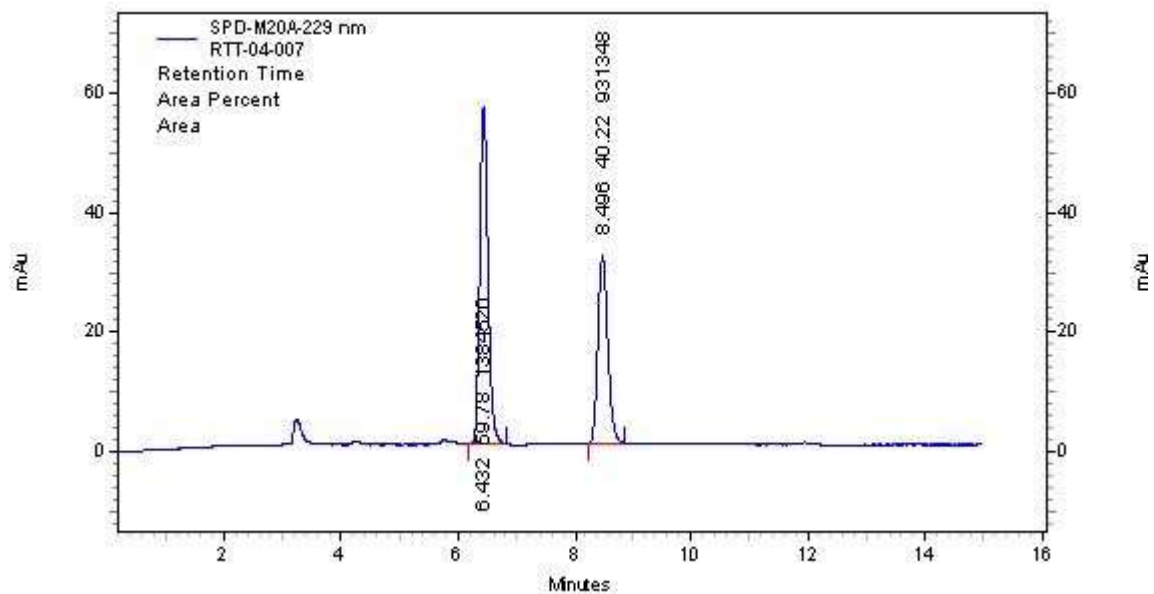
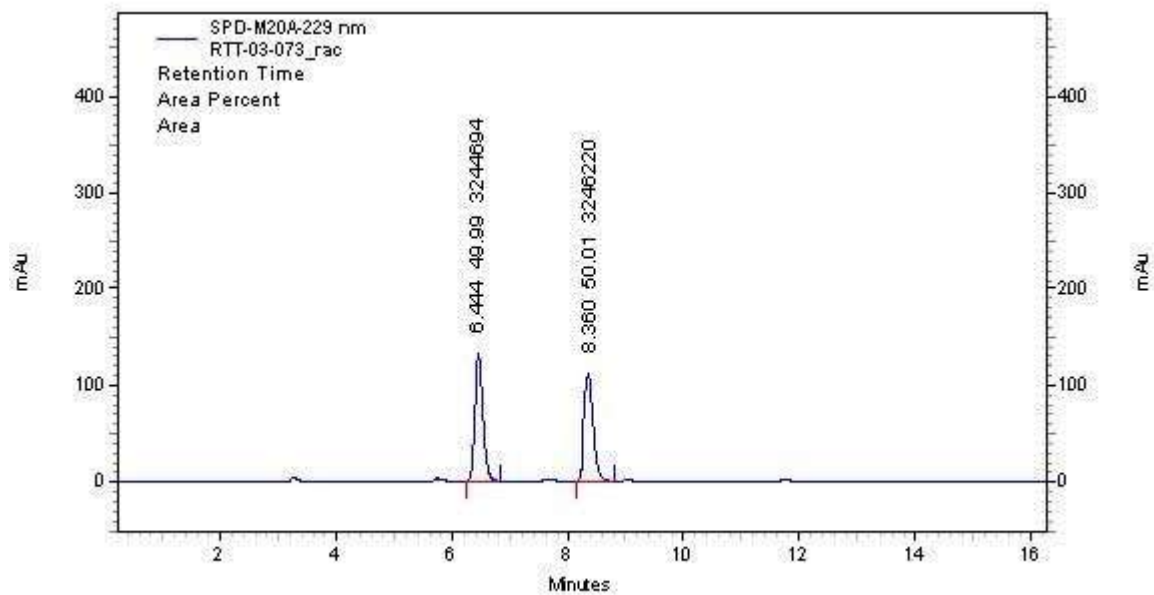
Ligand survey:



Trace or no product observed where yield is not indicated.

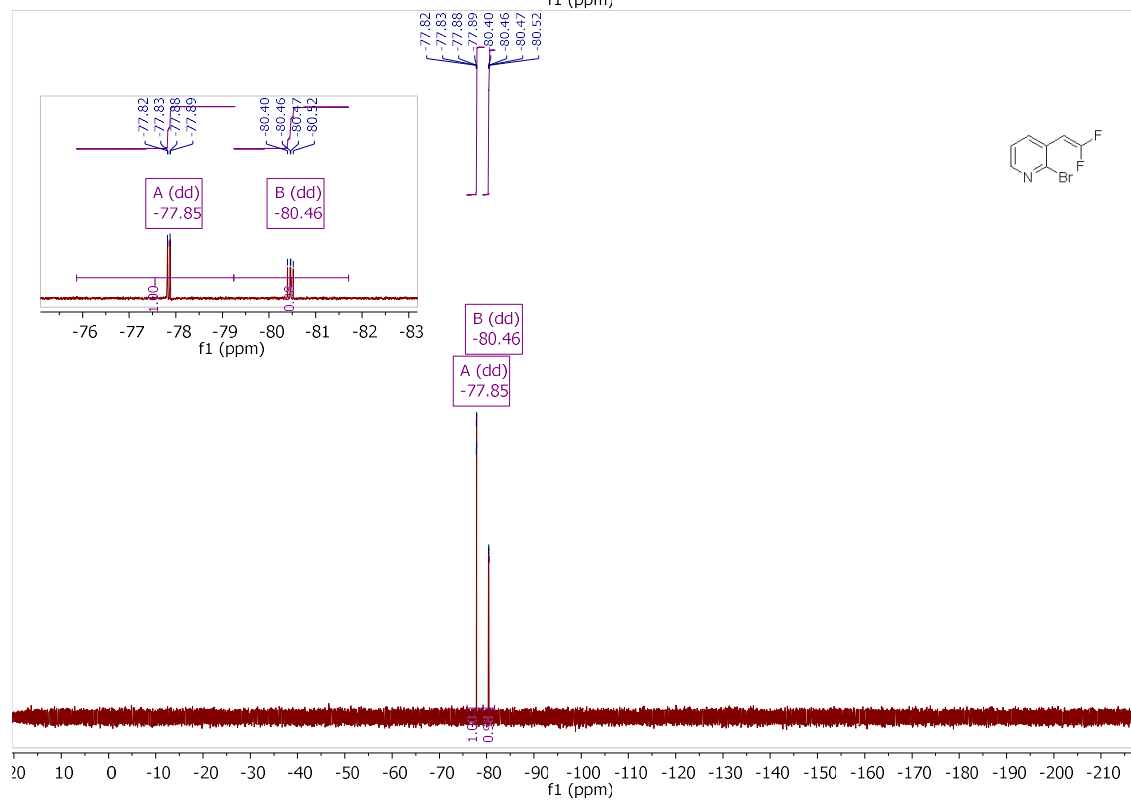
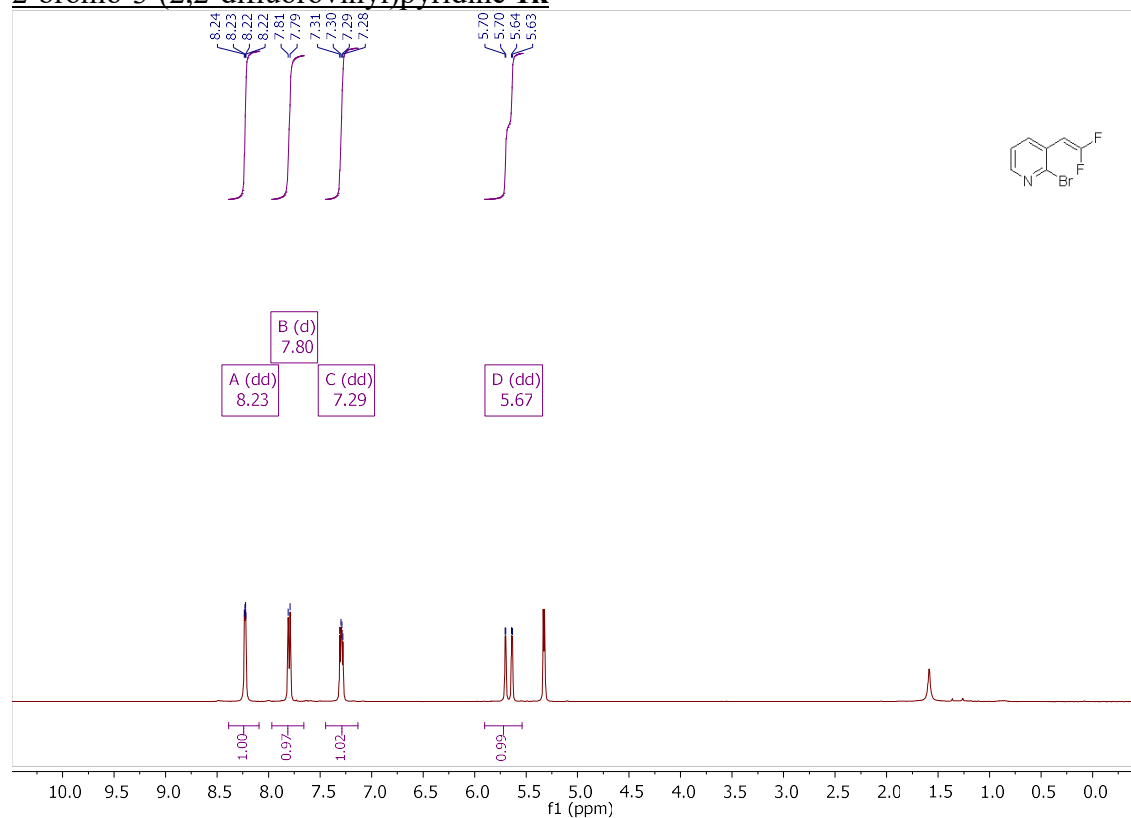


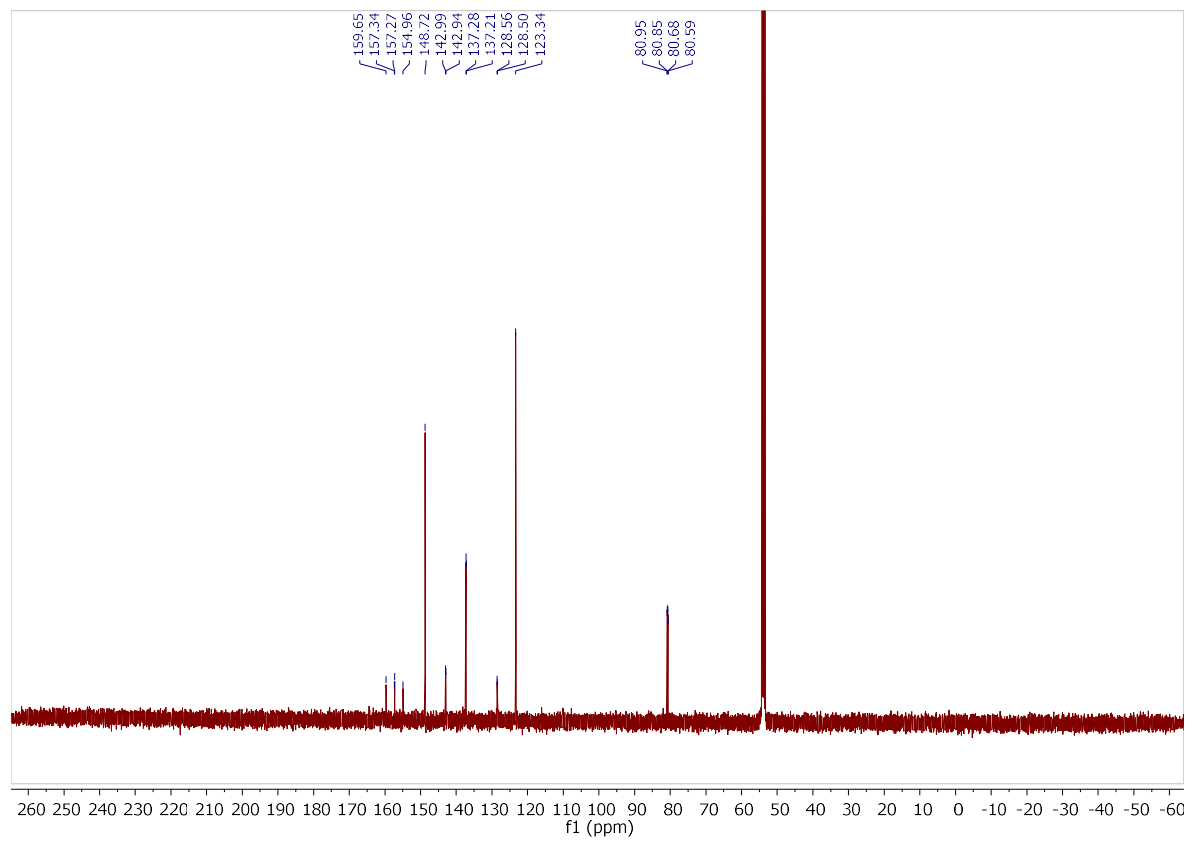
HPLC data for fluoroamination product:



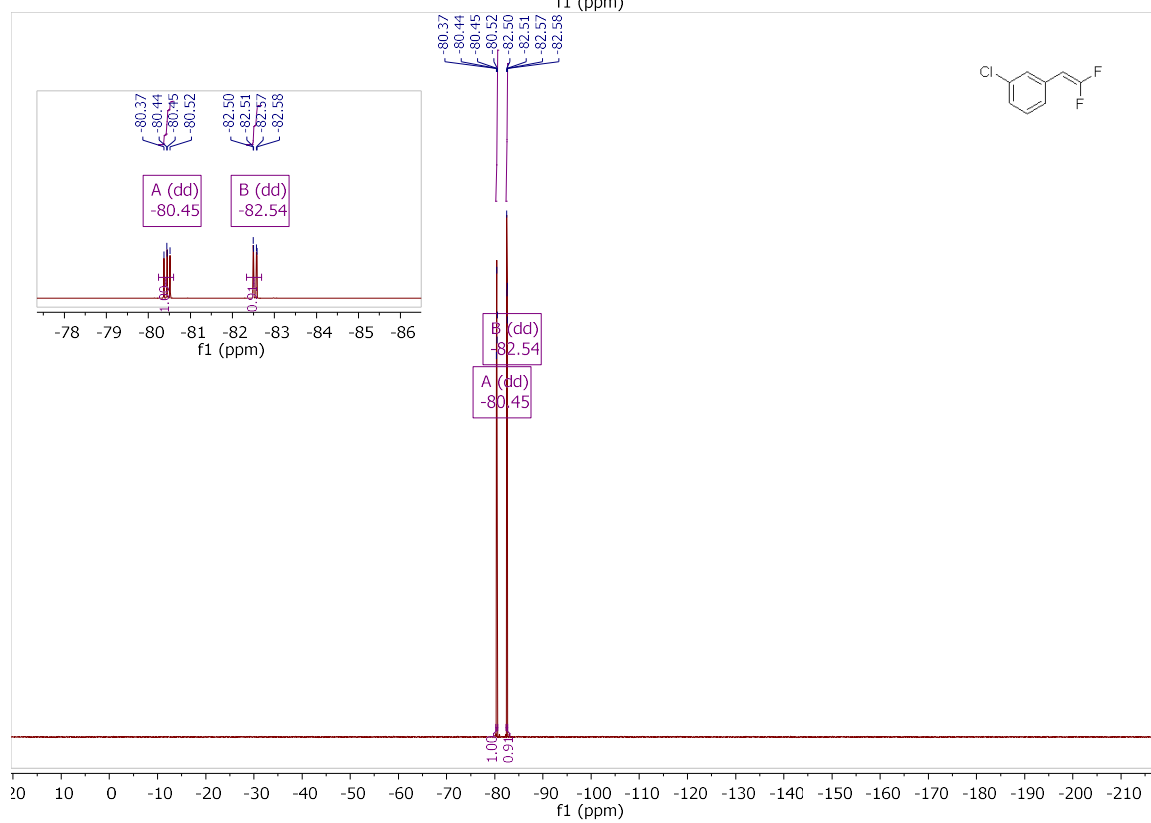
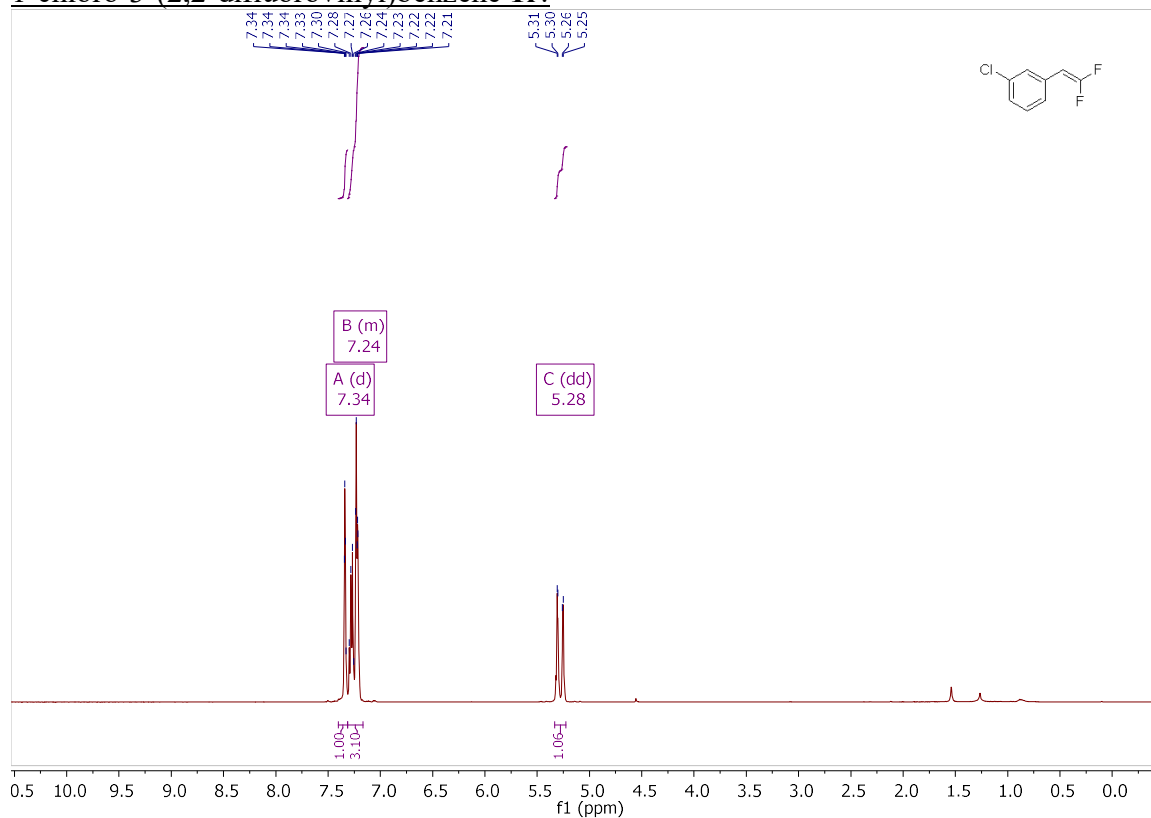
2.4.7. Spectral Data

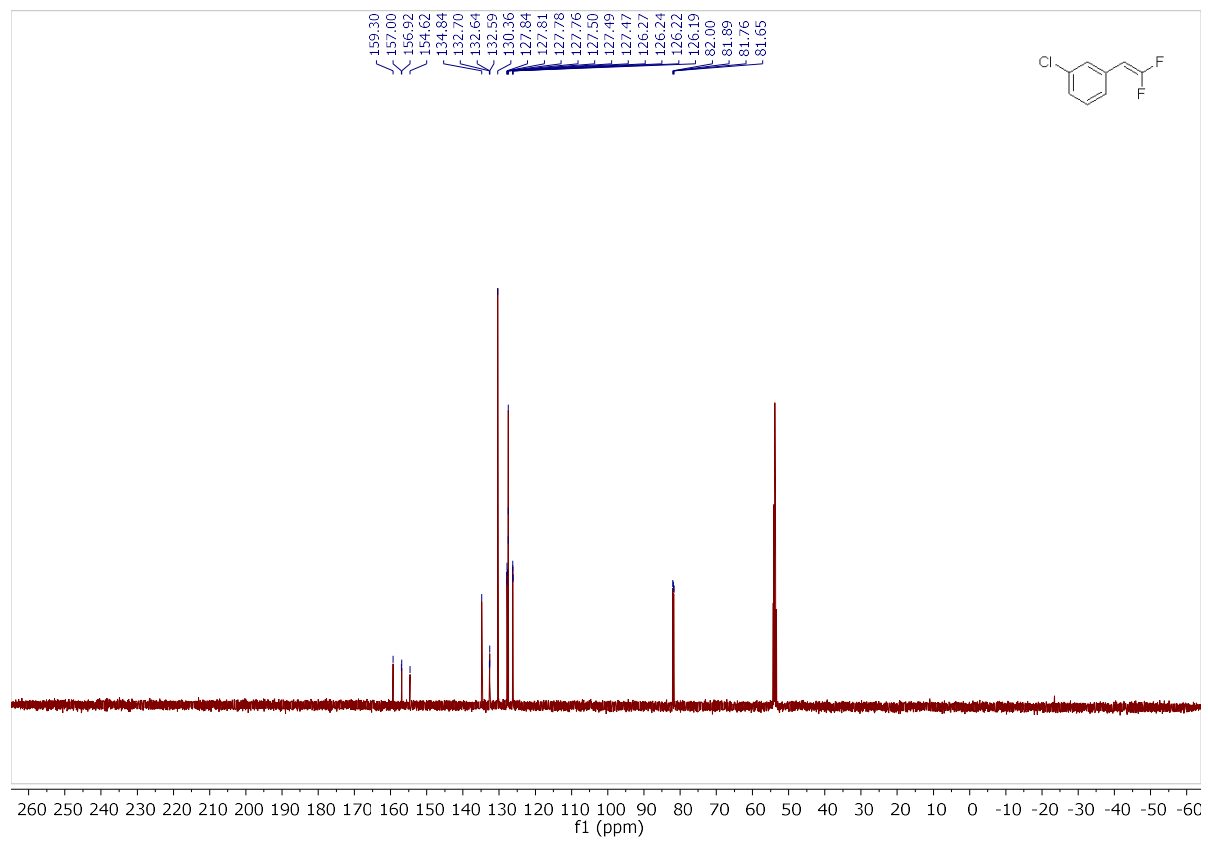
2-bromo-3-(2,2-difluorovinyl)pyridine **1k**



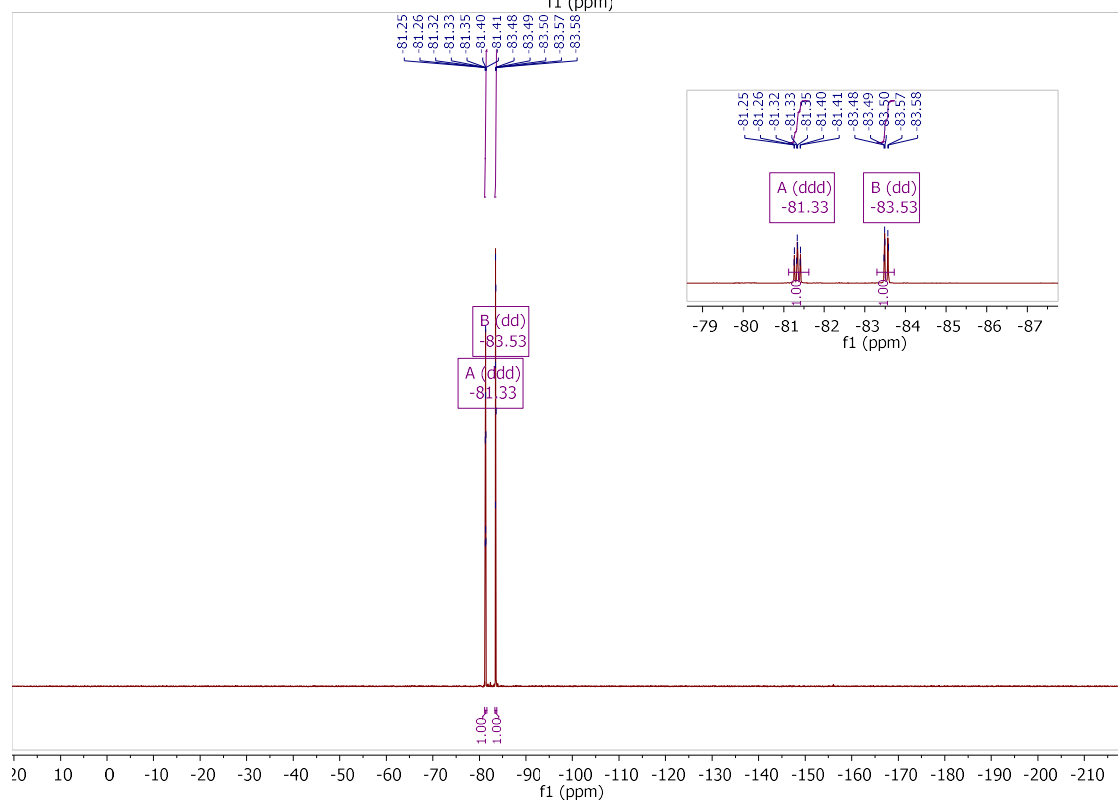
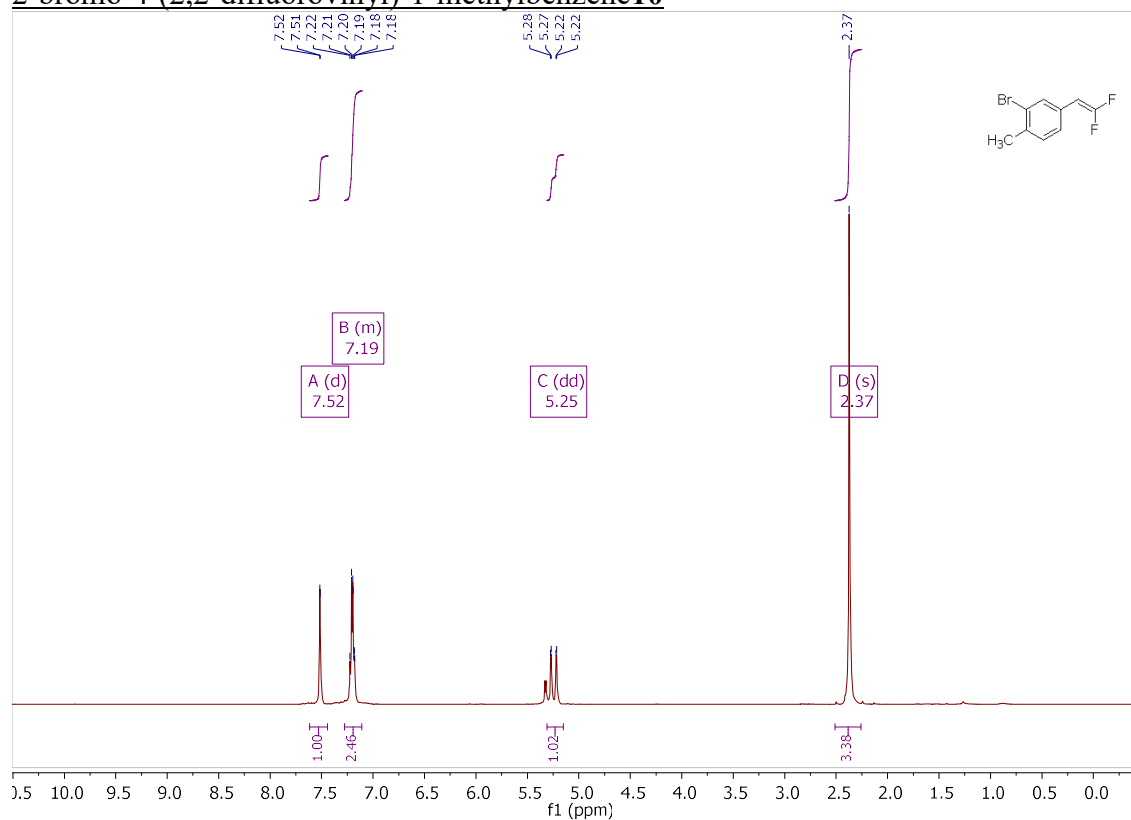


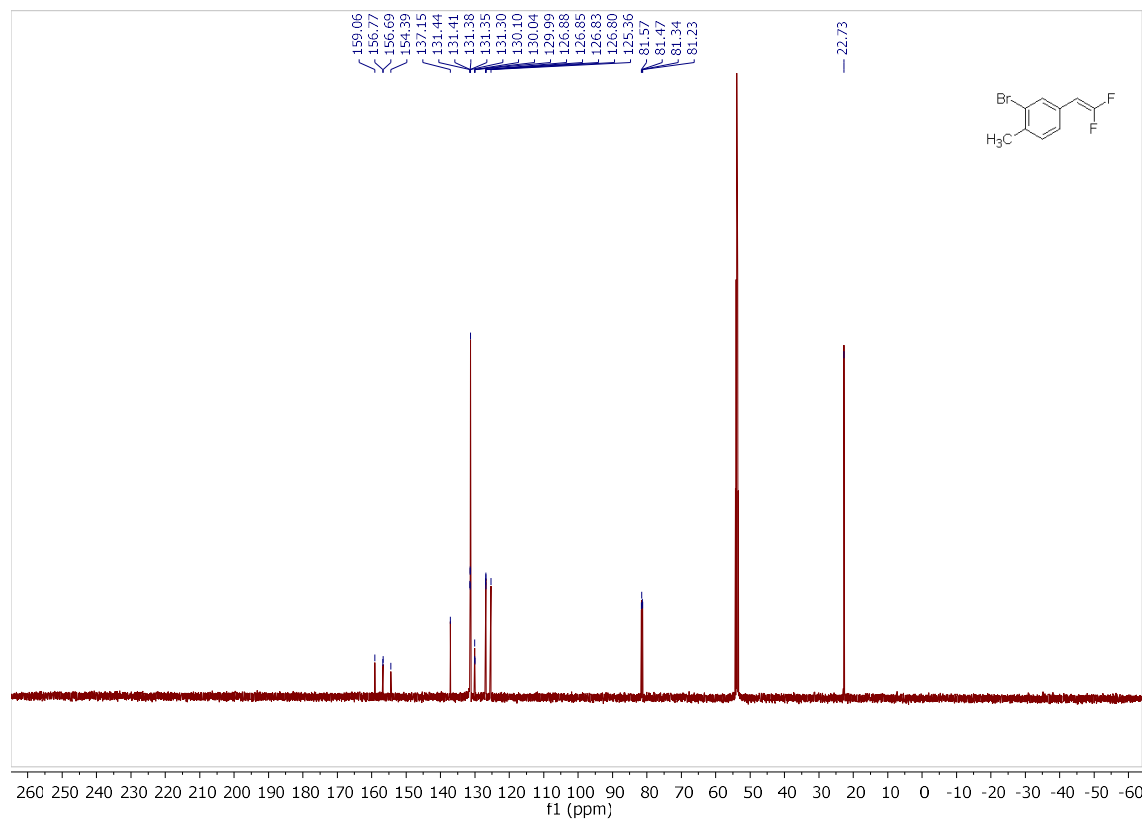
1-chloro-3-(2,2-difluorovinyl)benzene **1r**:



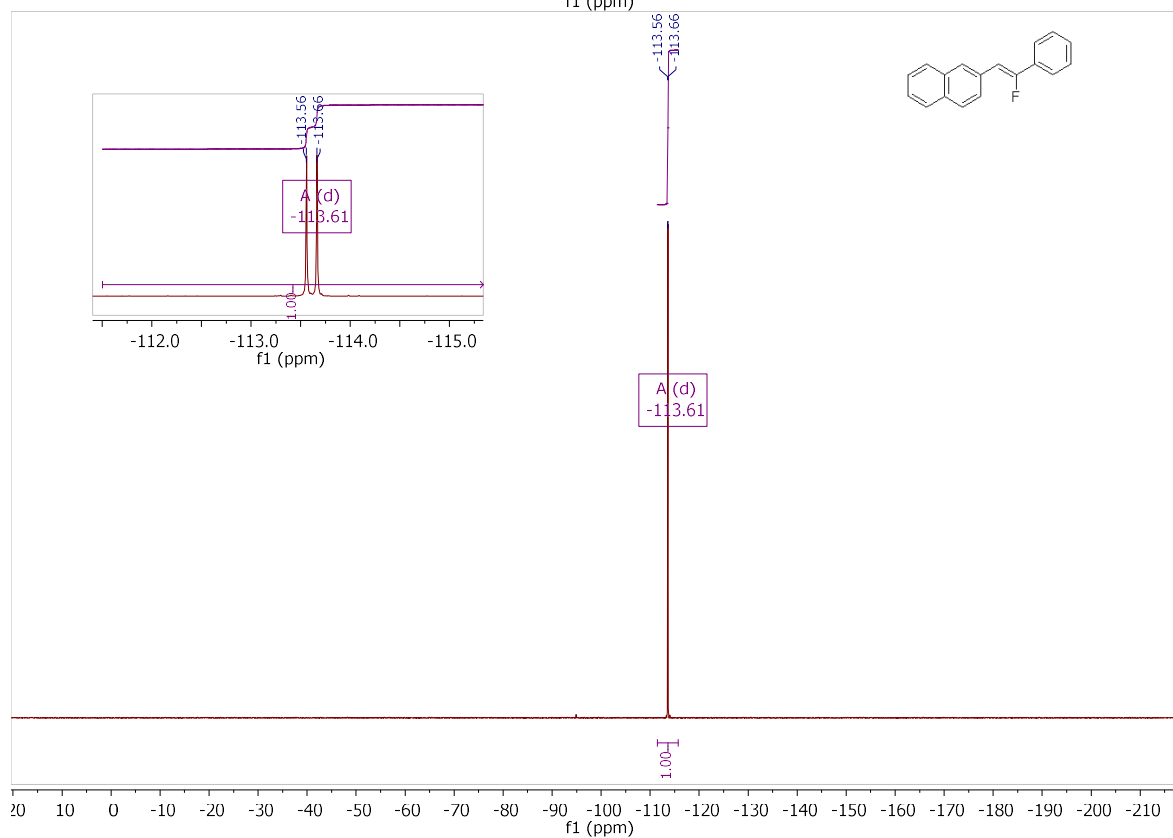
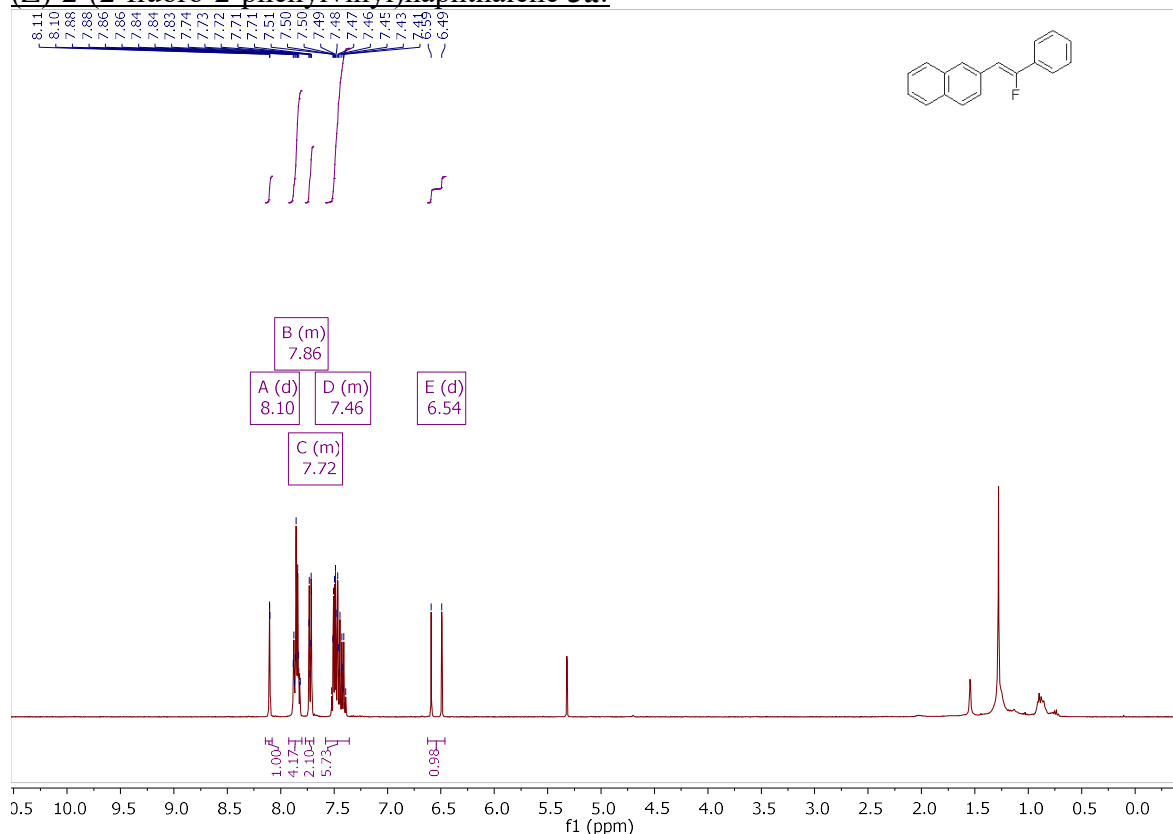


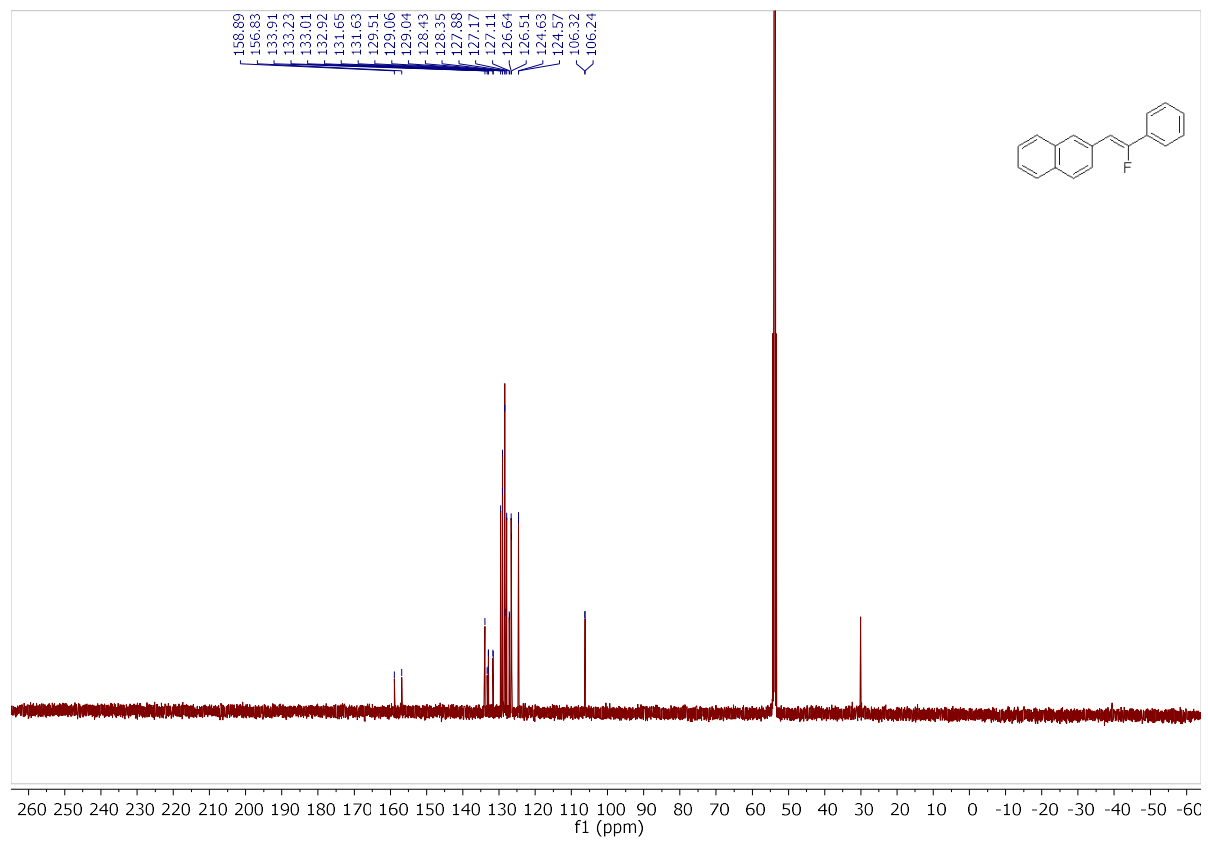
2-bromo-4-(2,2-difluorovinyl)-1-methylbenzene¹⁰



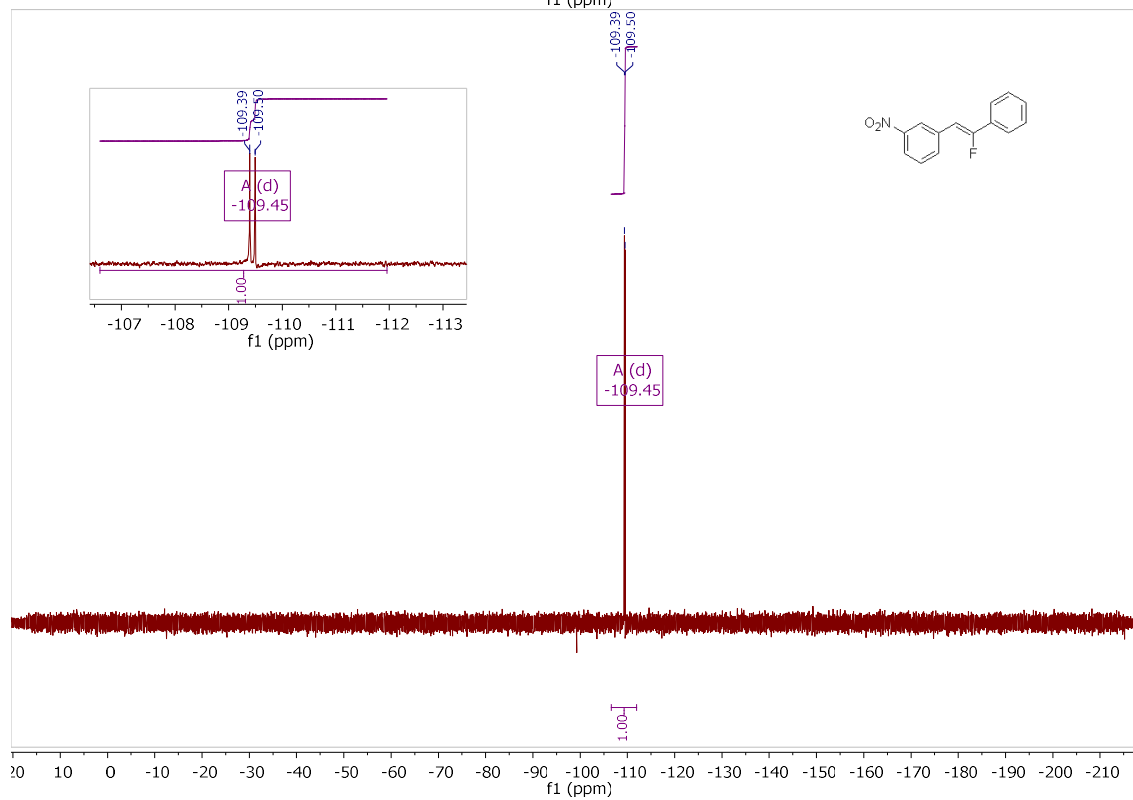
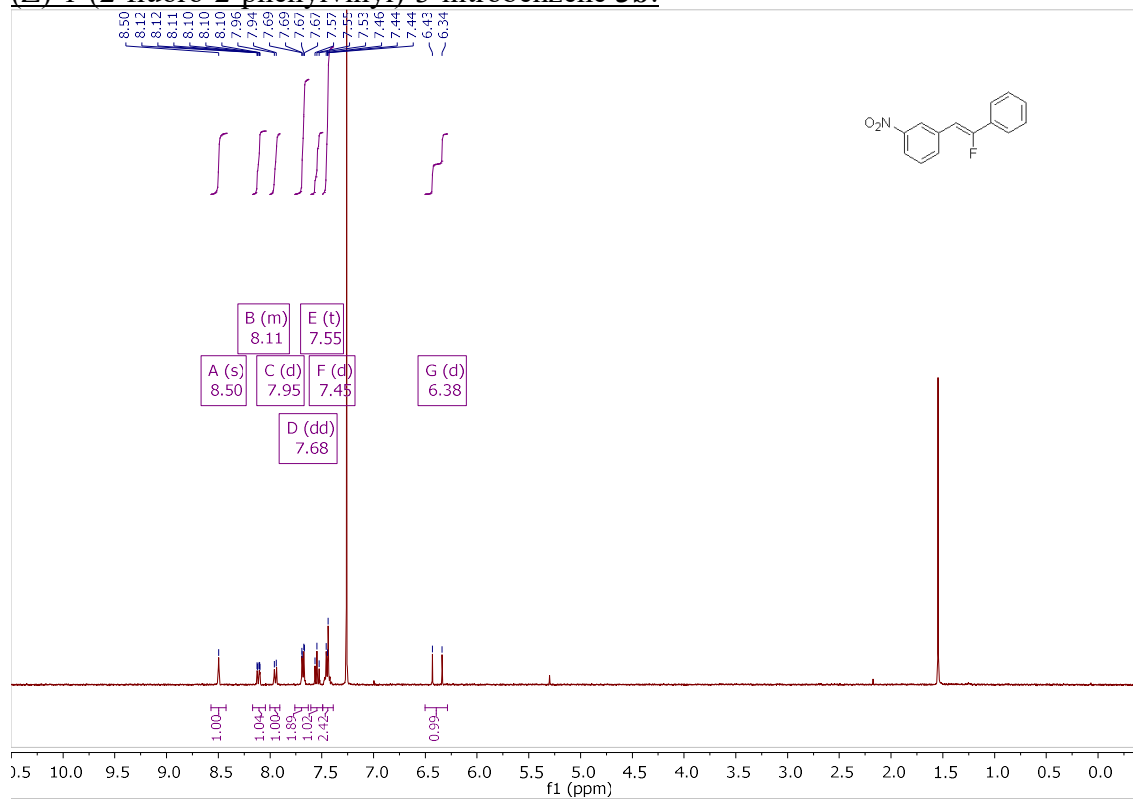


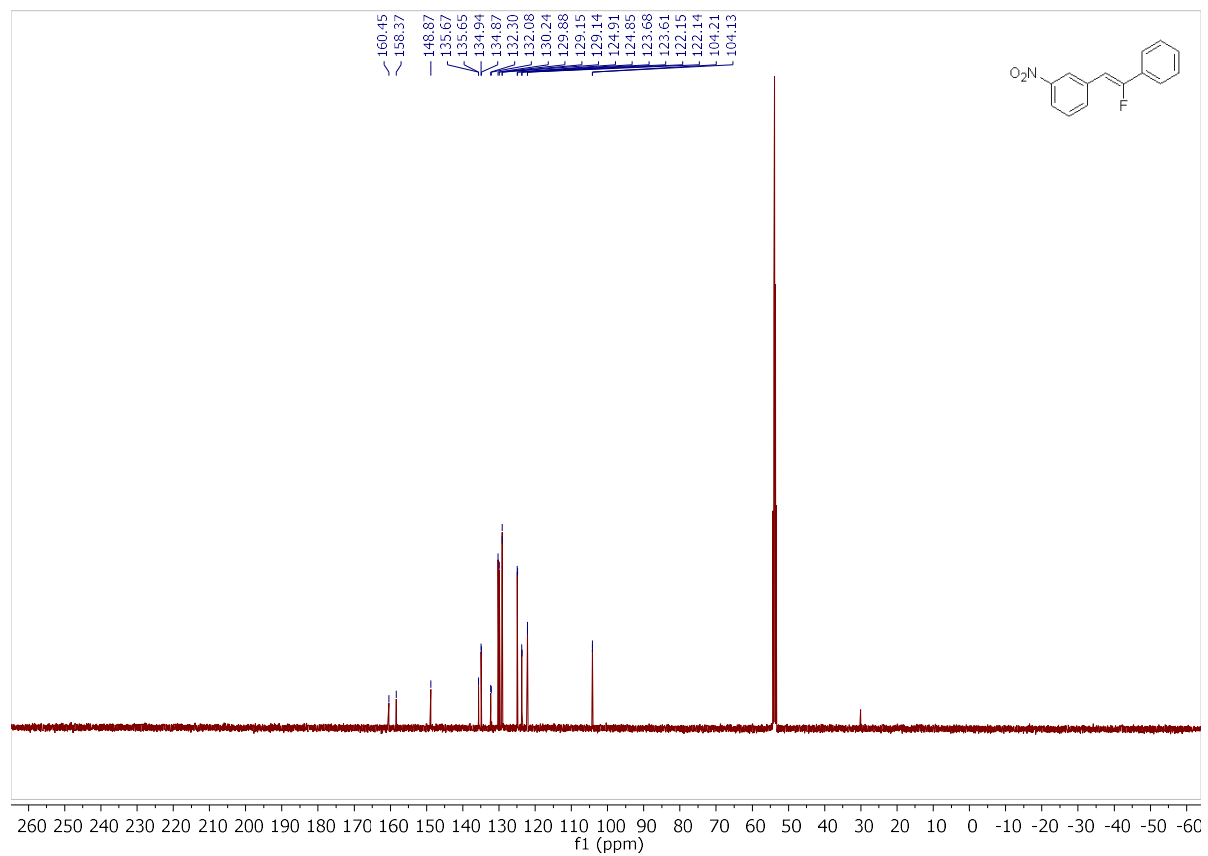
(Z)-2-(2-fluoro-2-phenylvinyl)naphthalene 3a:



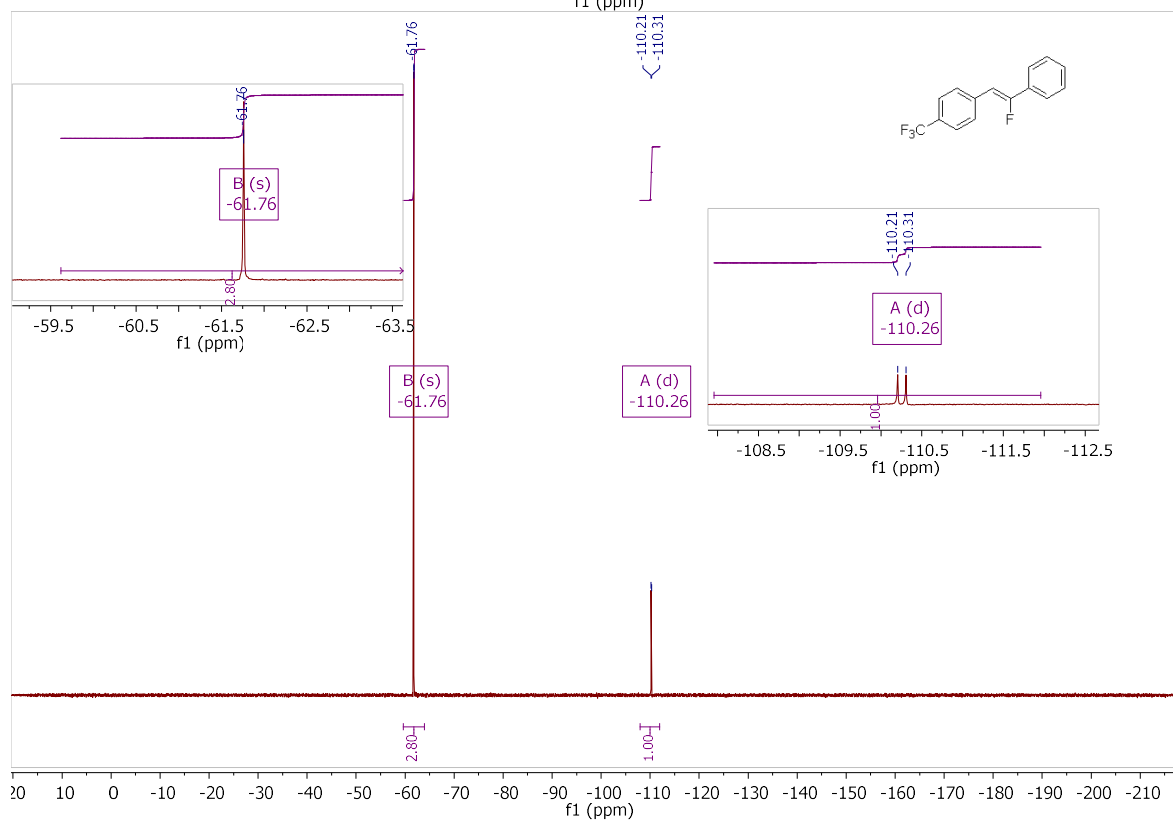
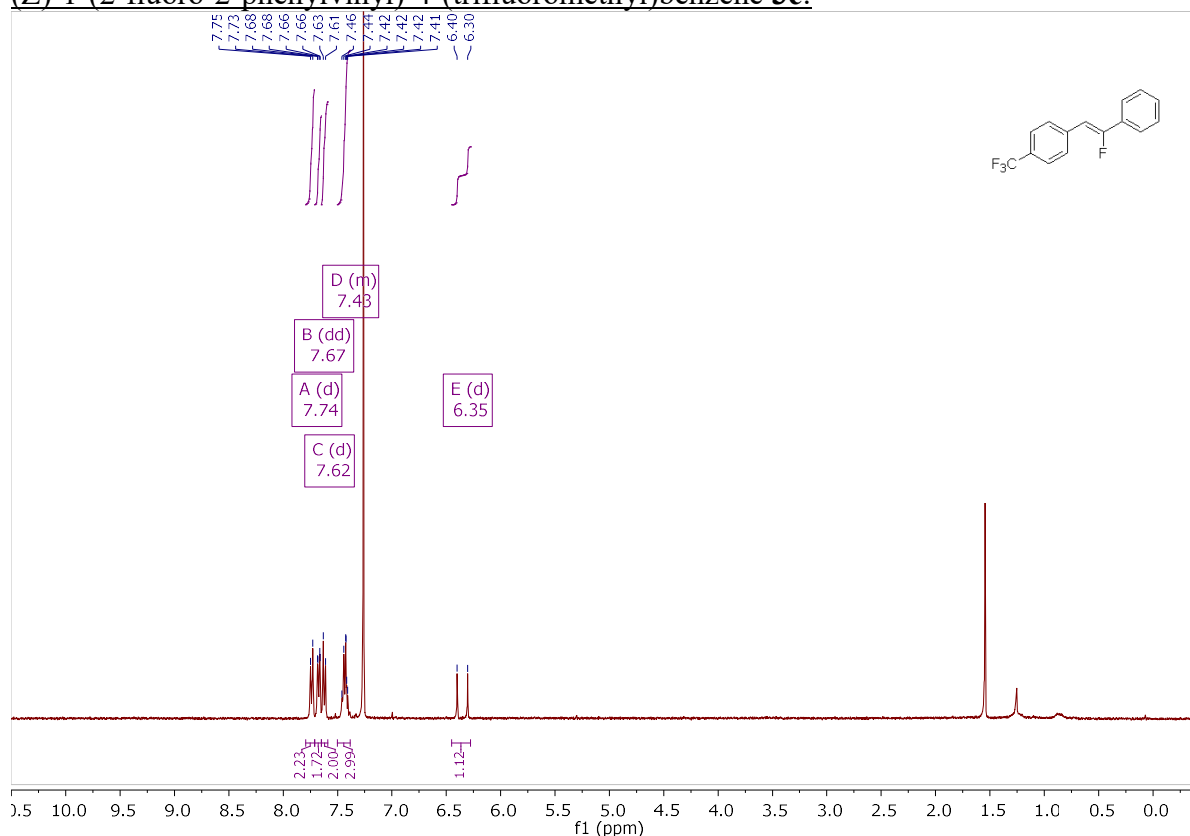


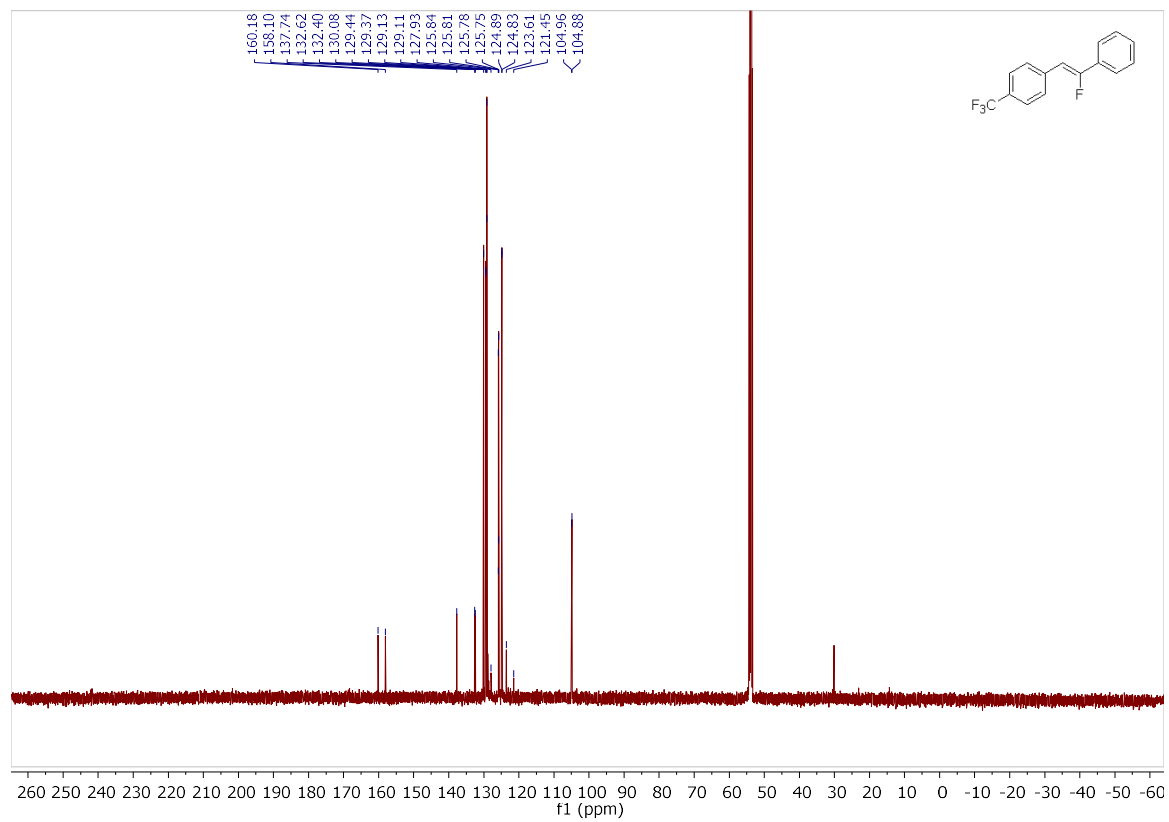
(Z)-1-(2-fluoro-2-phenylvinyl)-3-nitrobenzene 3b:



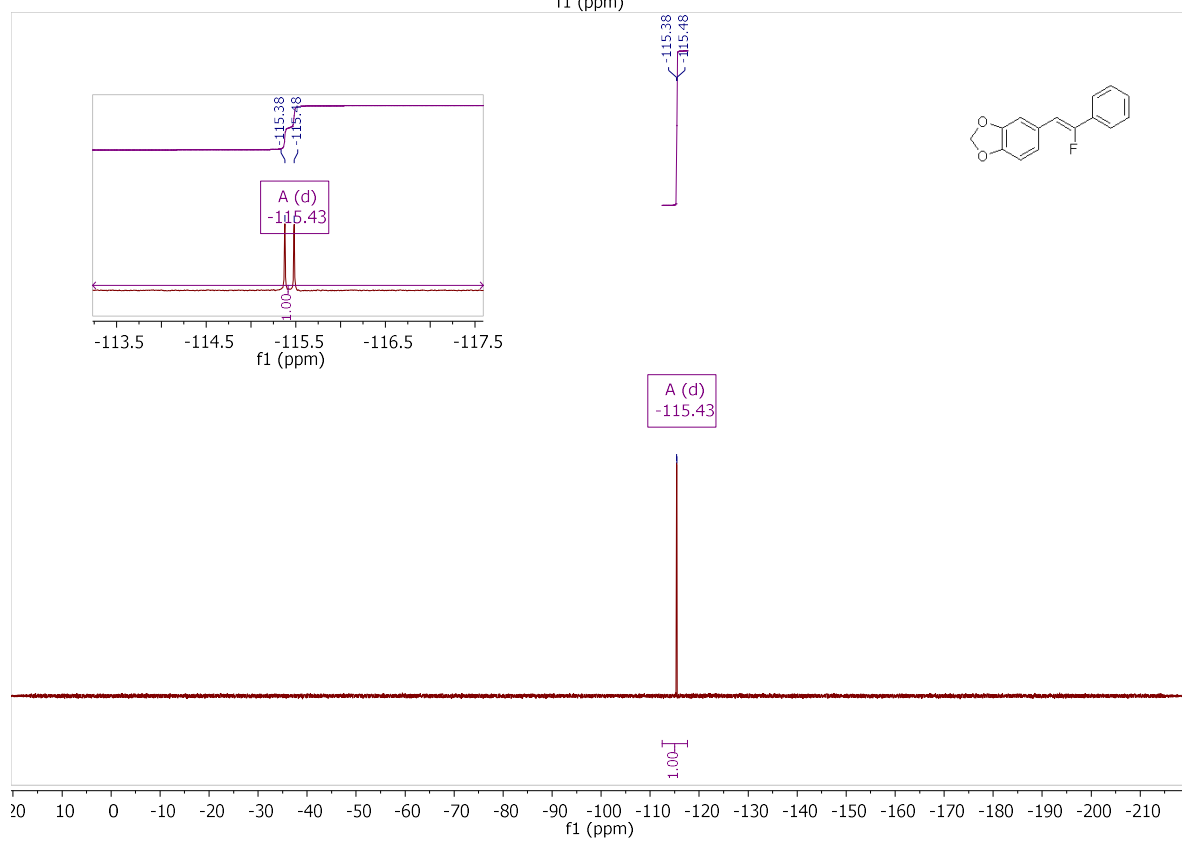
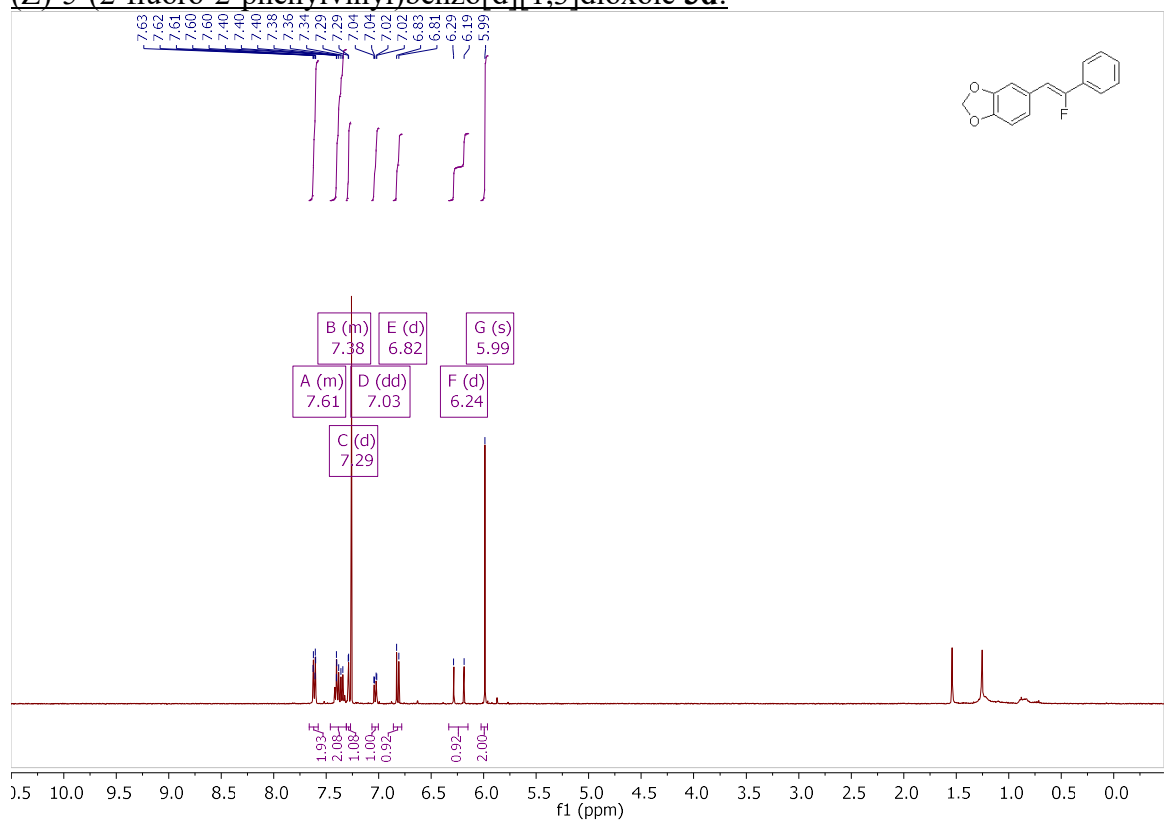


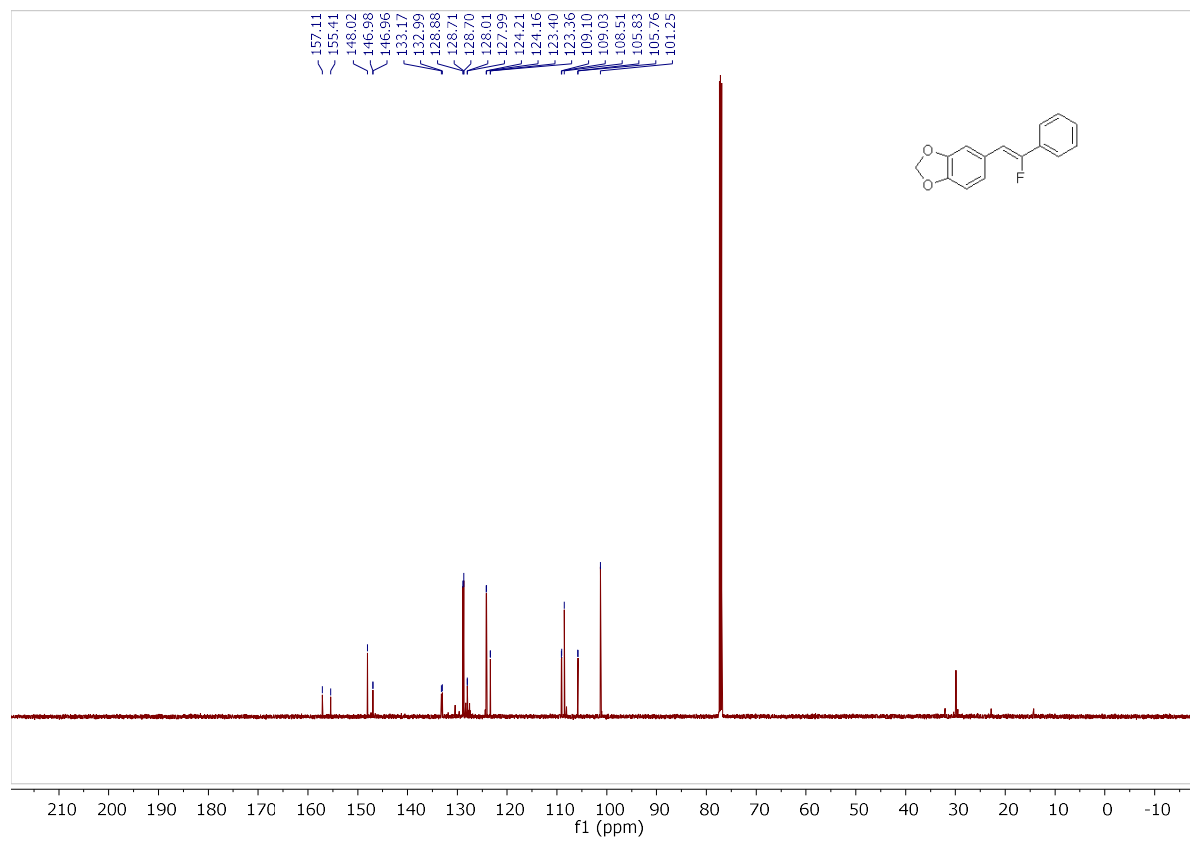
(Z)-1-(2-fluoro-2-phenylvinyl)-4-(trifluoromethyl)benzene 3c:



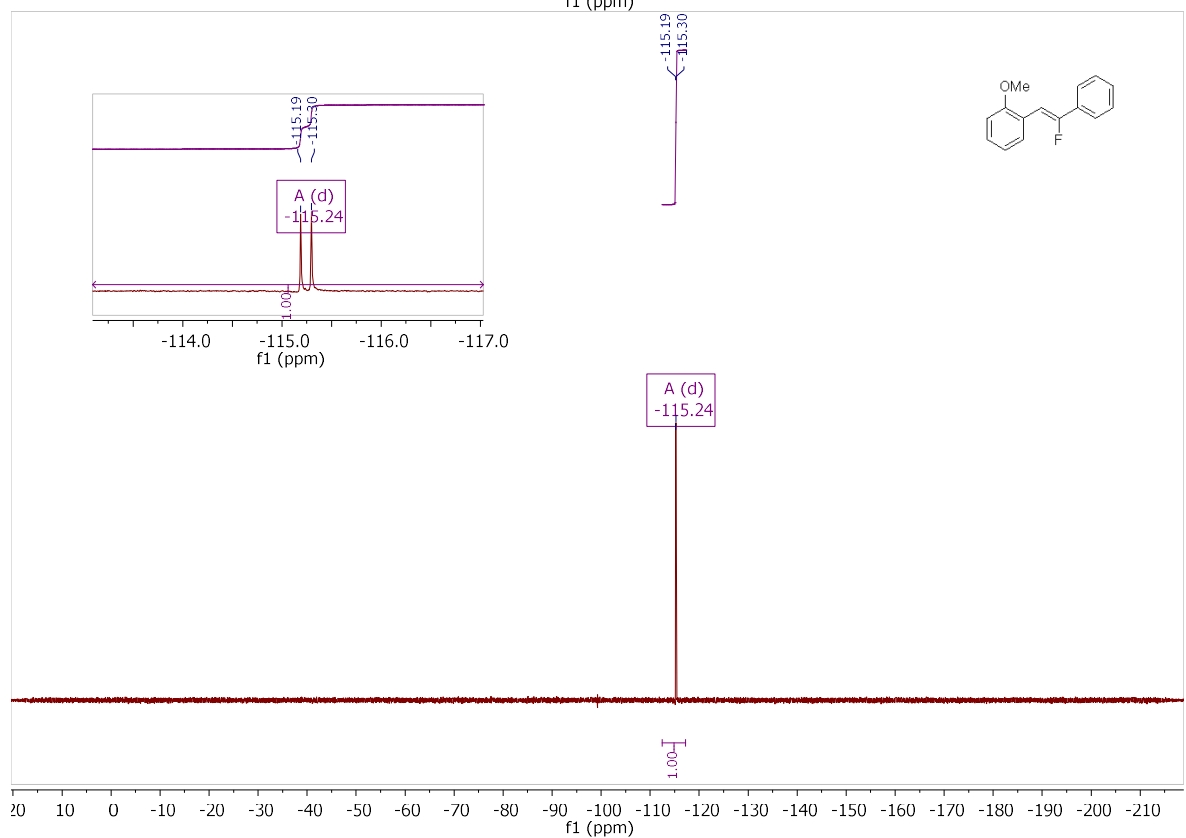
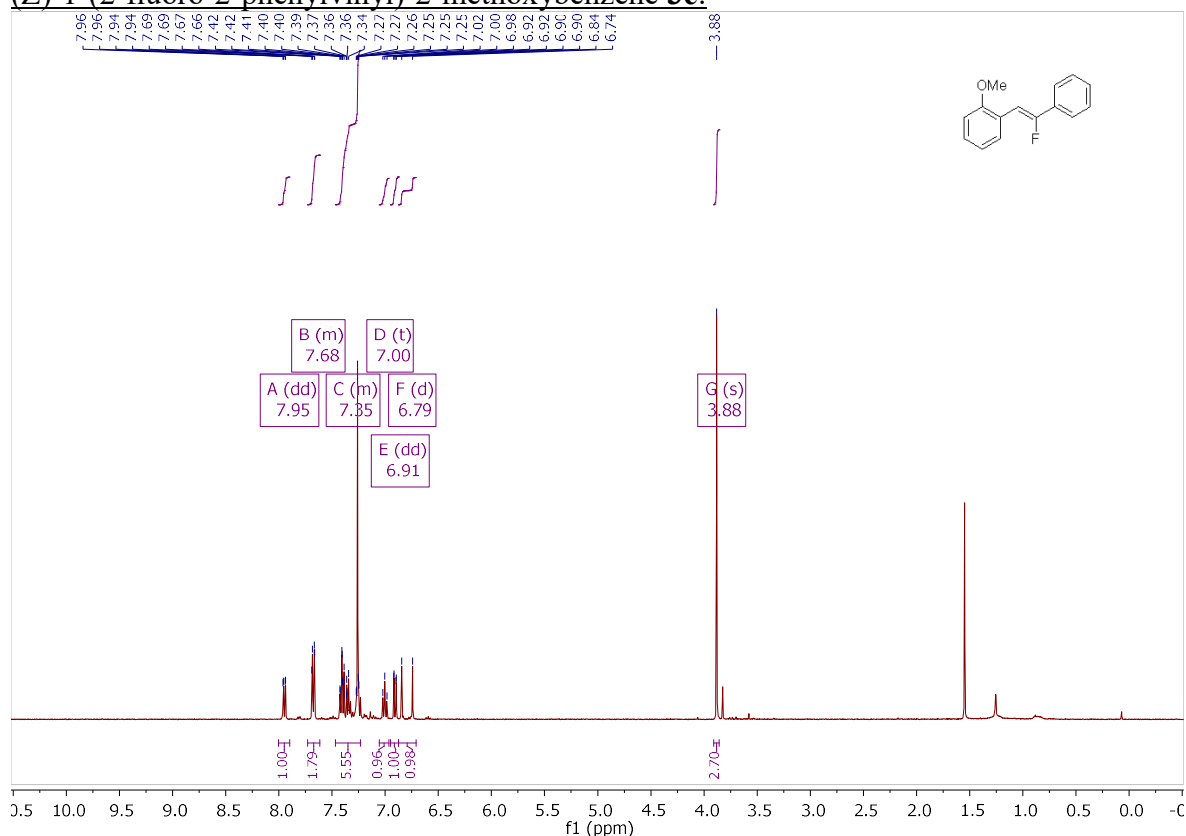


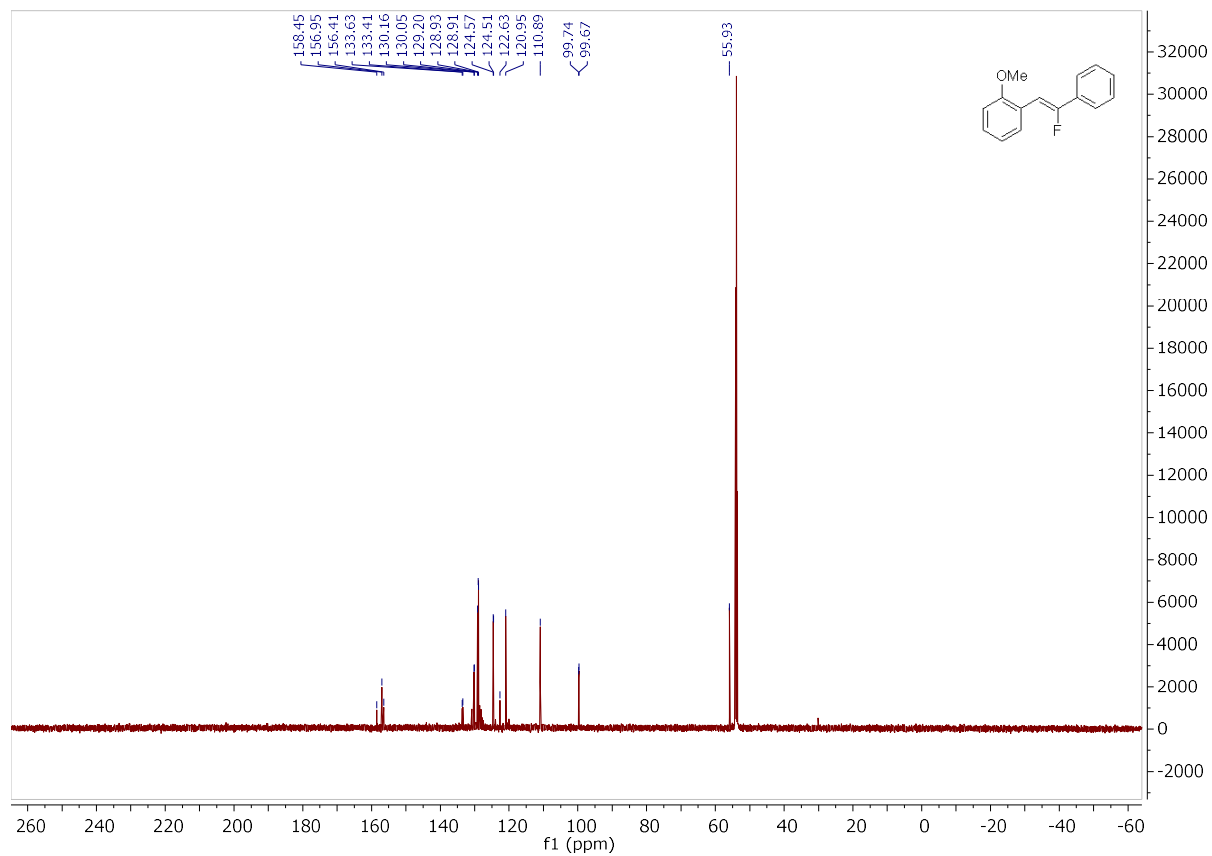
(Z)-5-(2-fluoro-2-phenylvinyl)benzo[d][1,3]dioxole 3d:



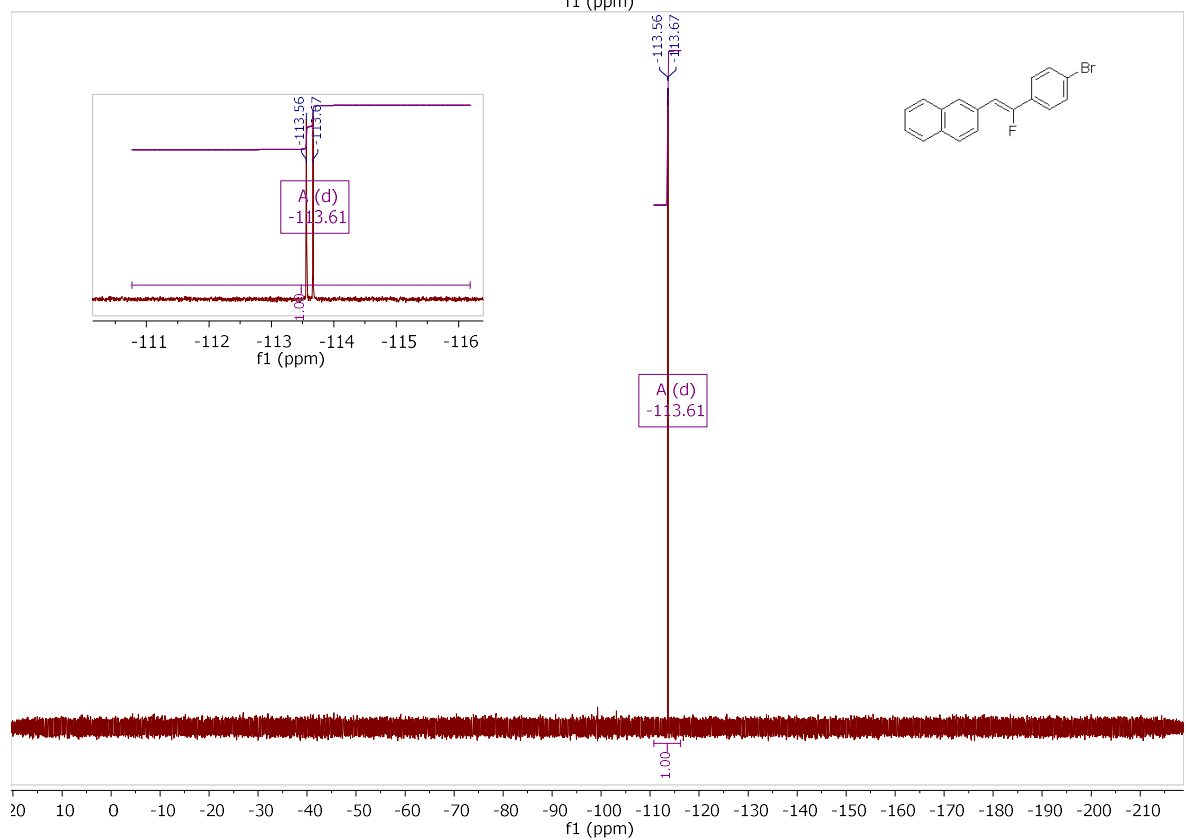
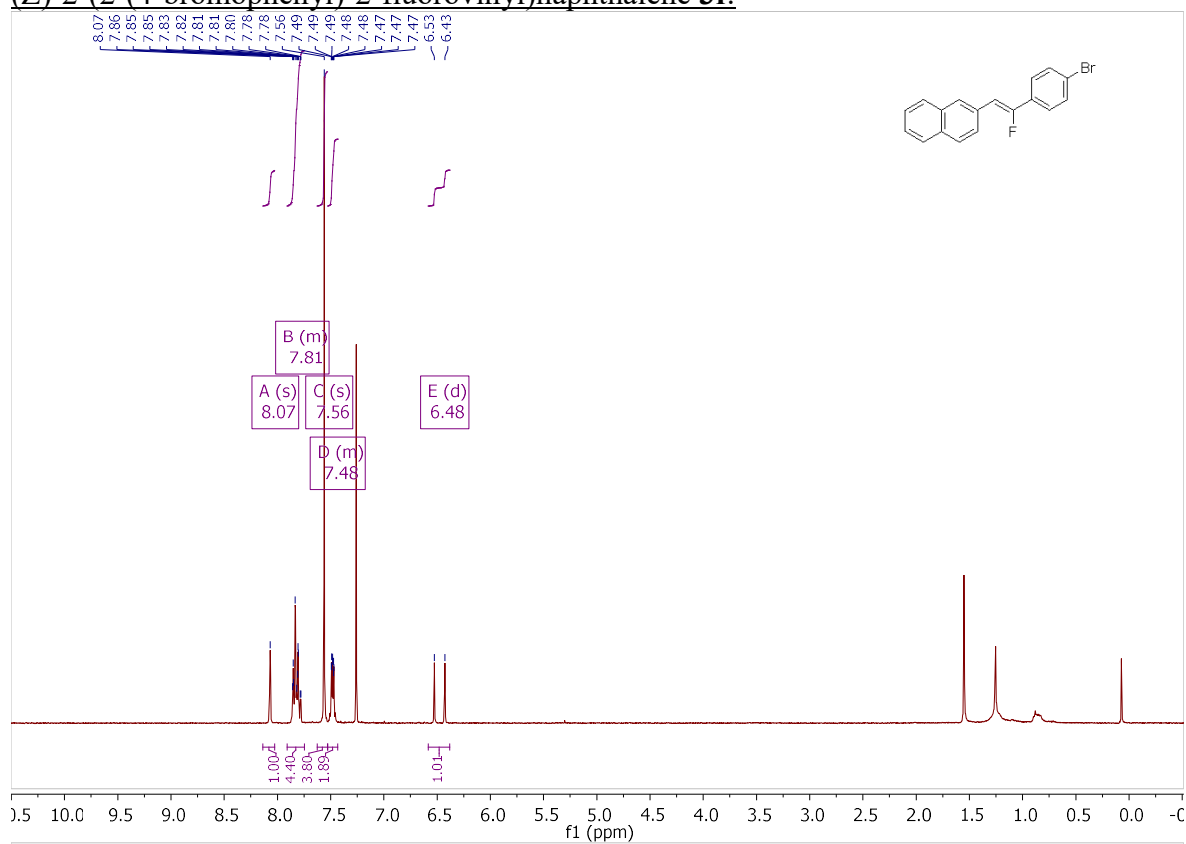


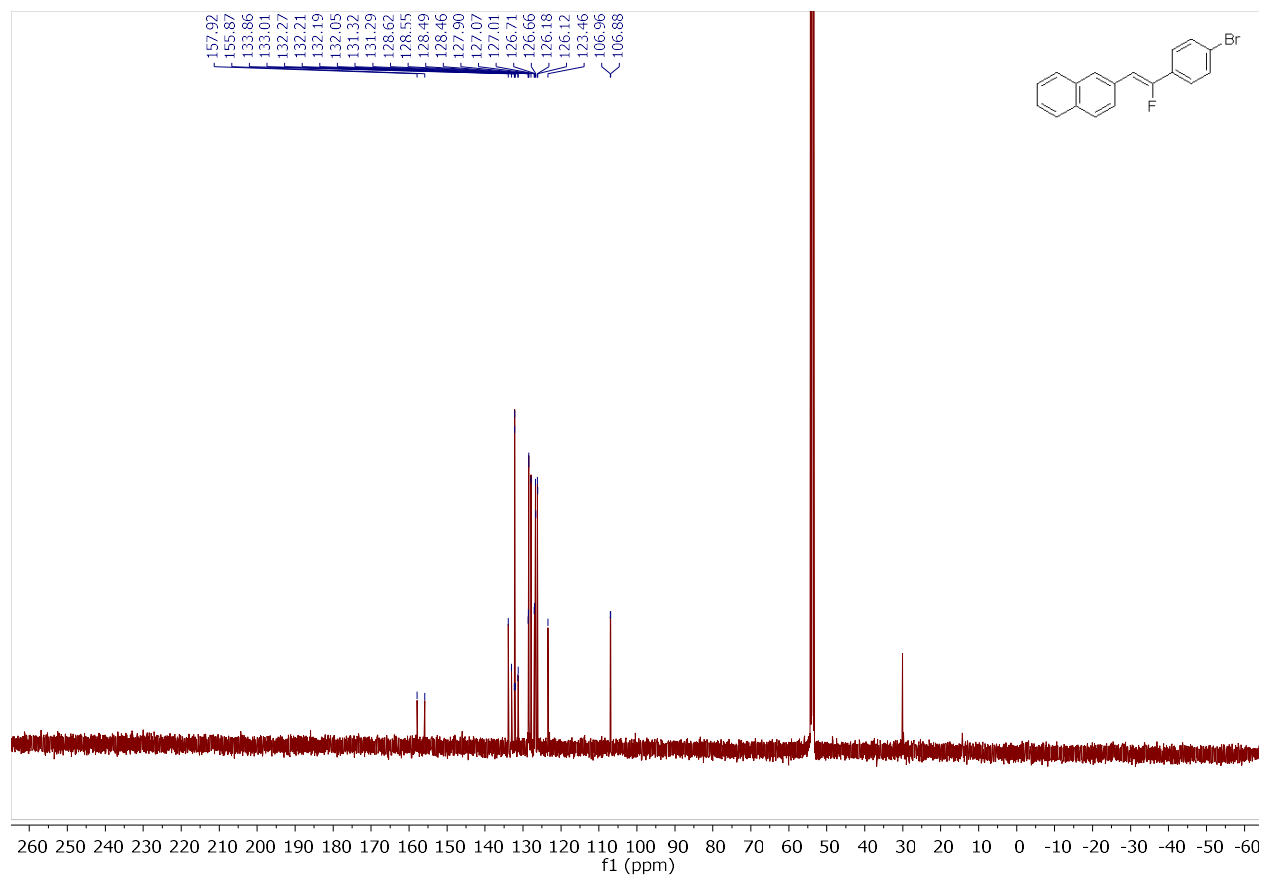
(Z)-1-(2-fluoro-2-phenylvinyl)-2-methoxybenzene 3e:



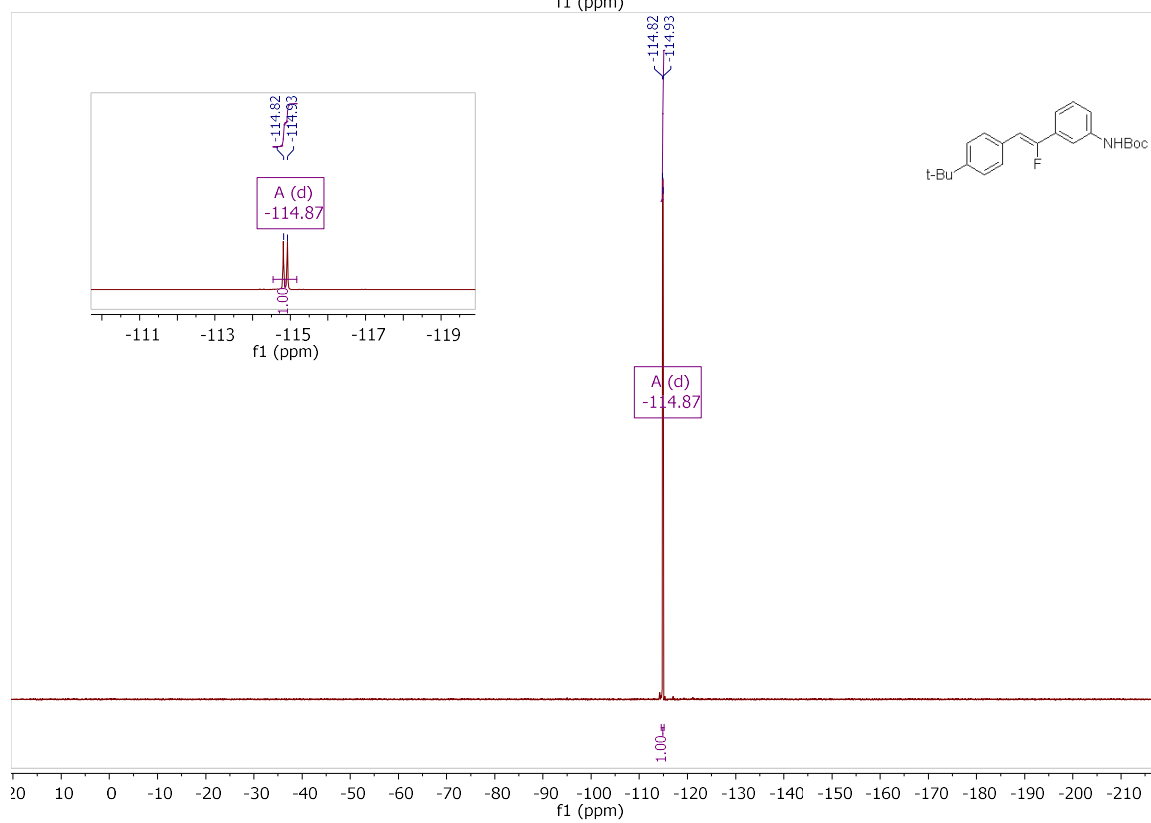
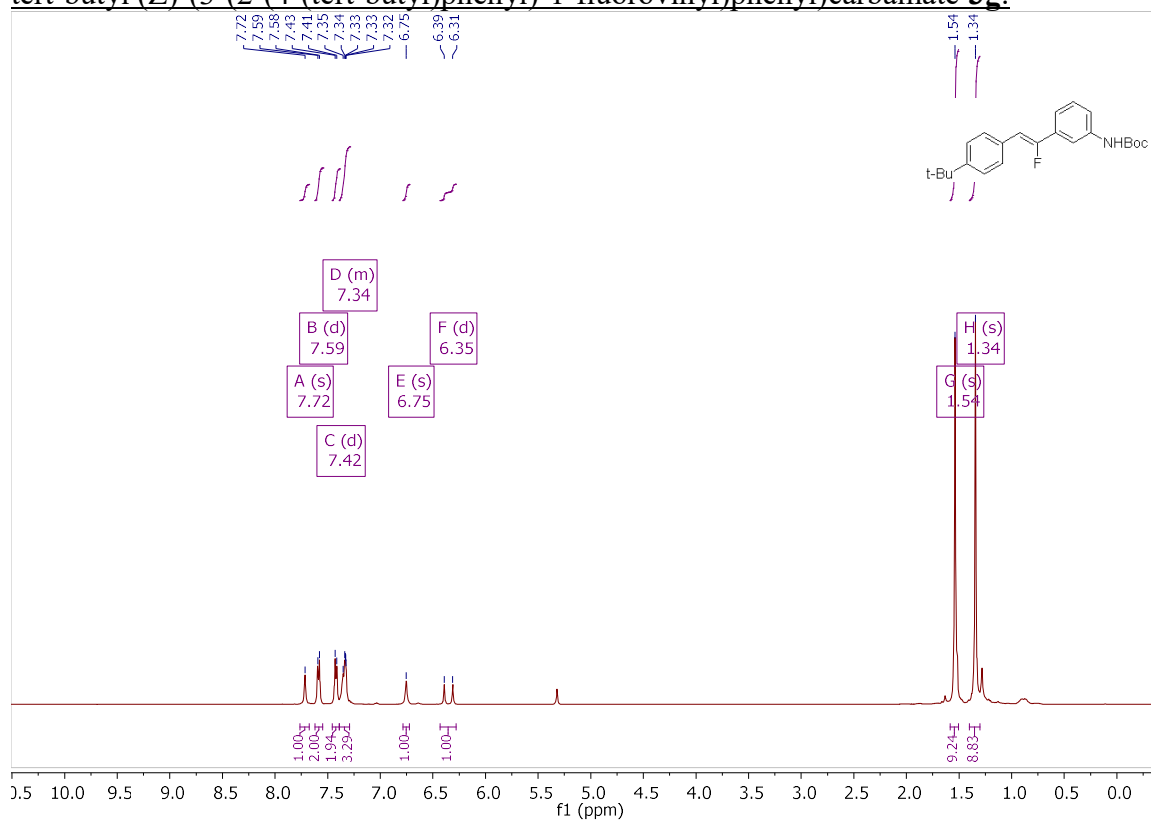


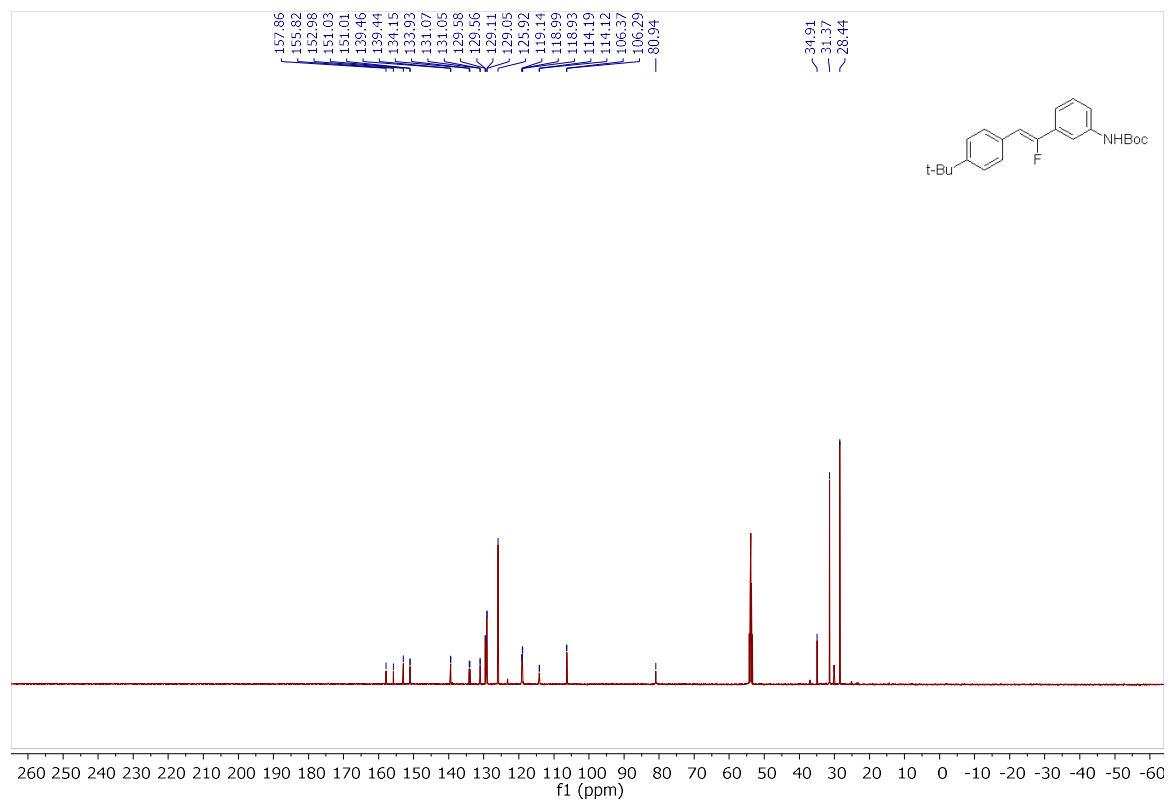
(Z)-2-(2-(4-bromophenyl)-2-fluorovinyl)naphthalene 3f:



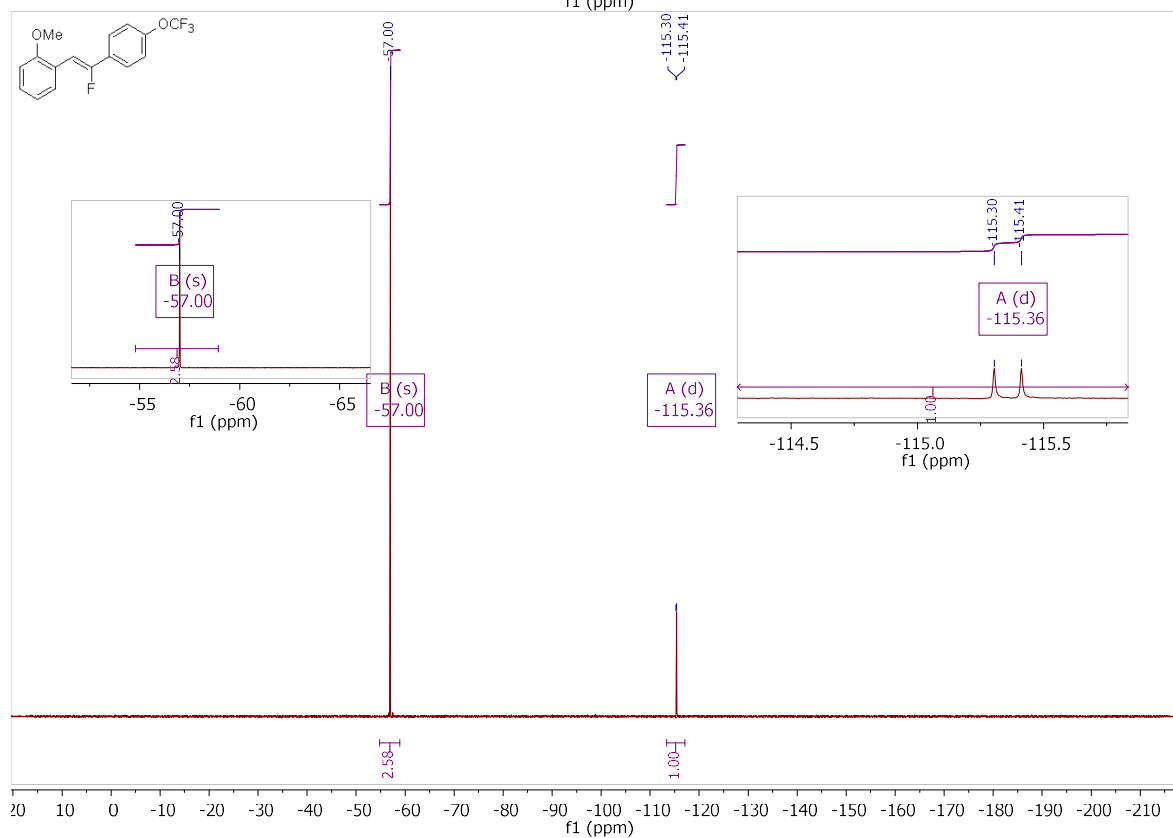
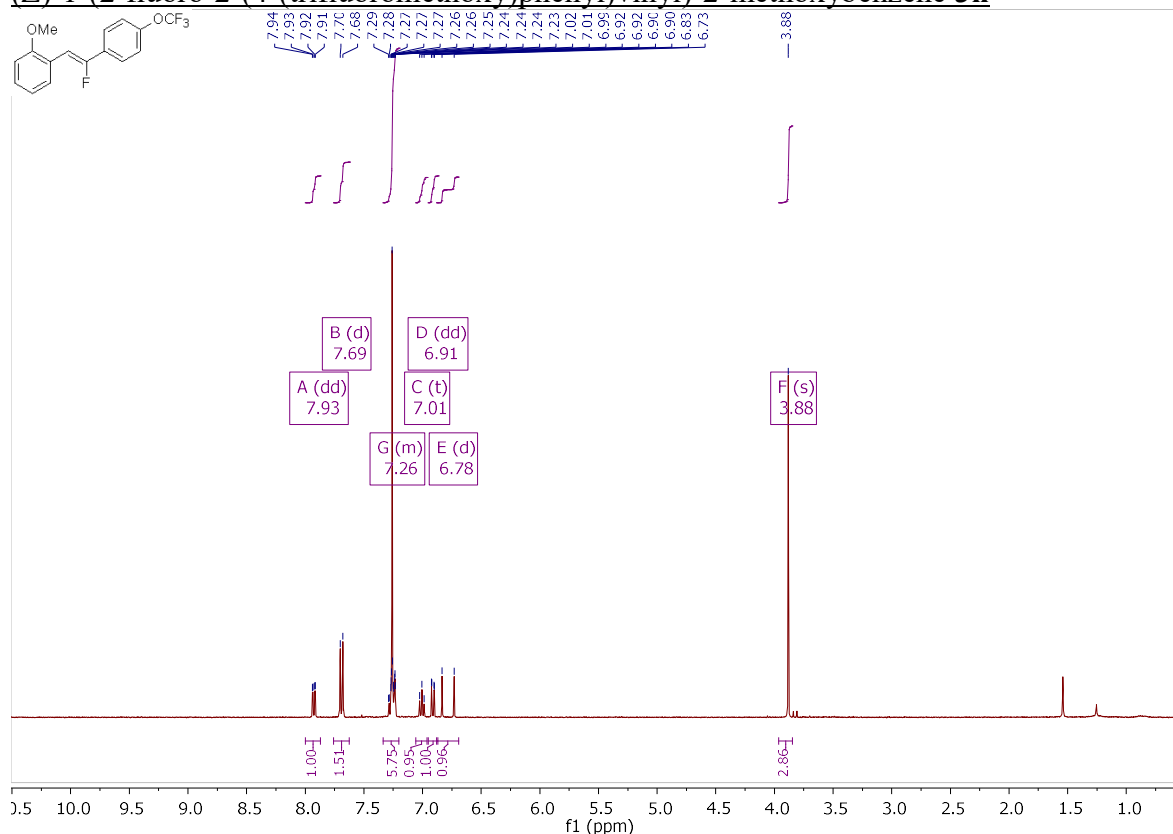


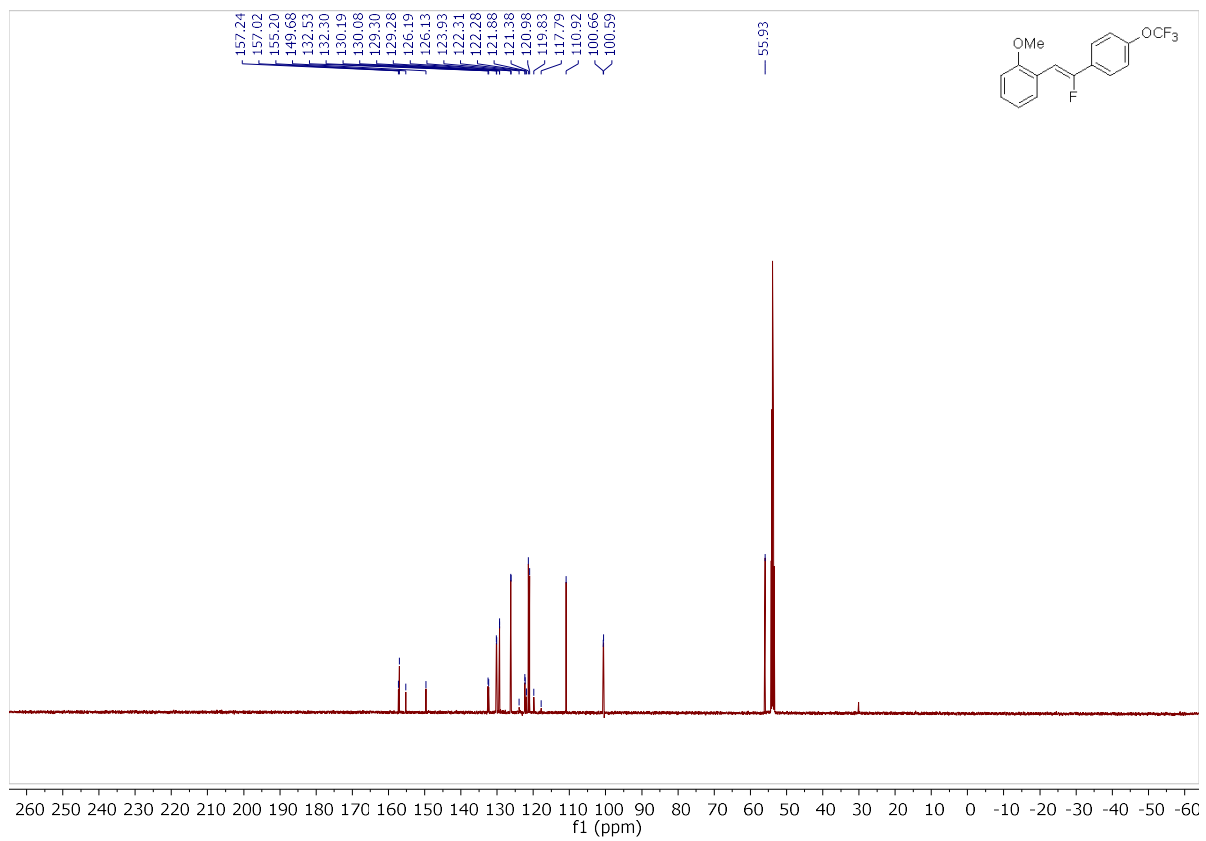
tert-butyl (Z)-3-(2-(4-(tert-butyl)phenyl)-1-fluorovinyl)phenyl)carbamate **3g**:



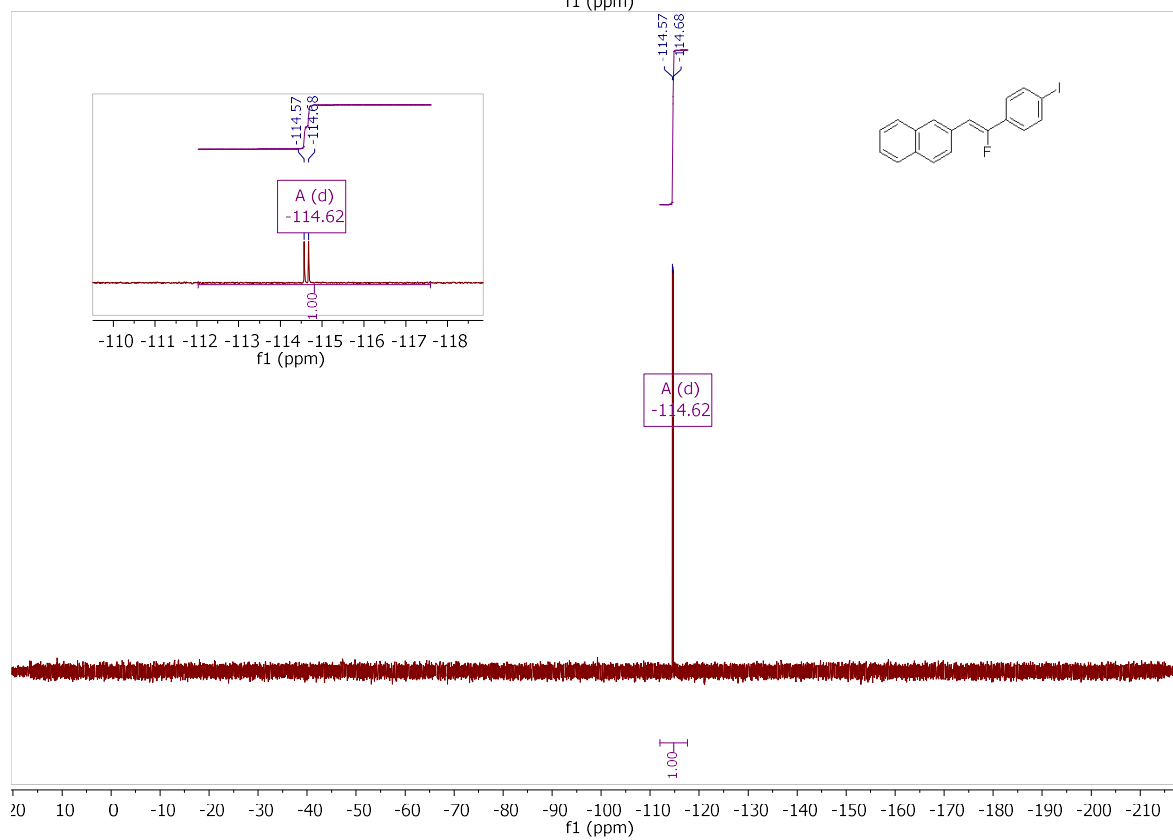
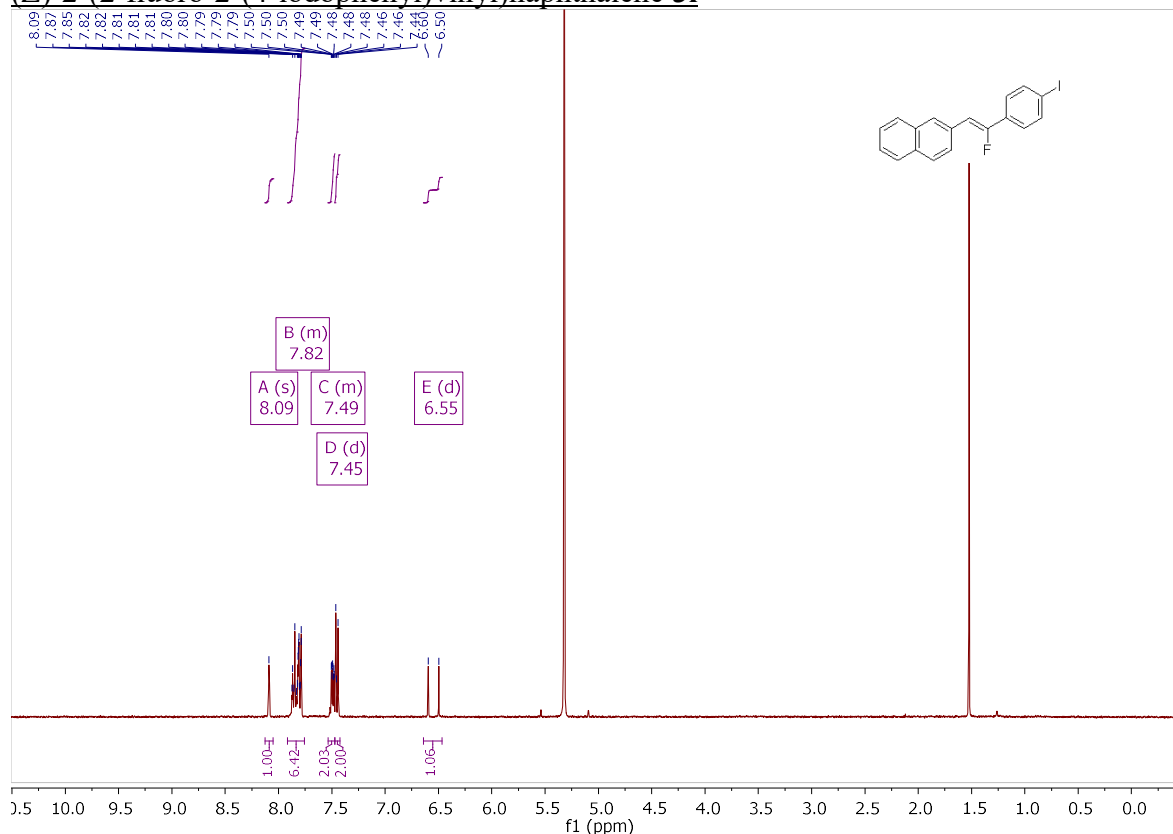


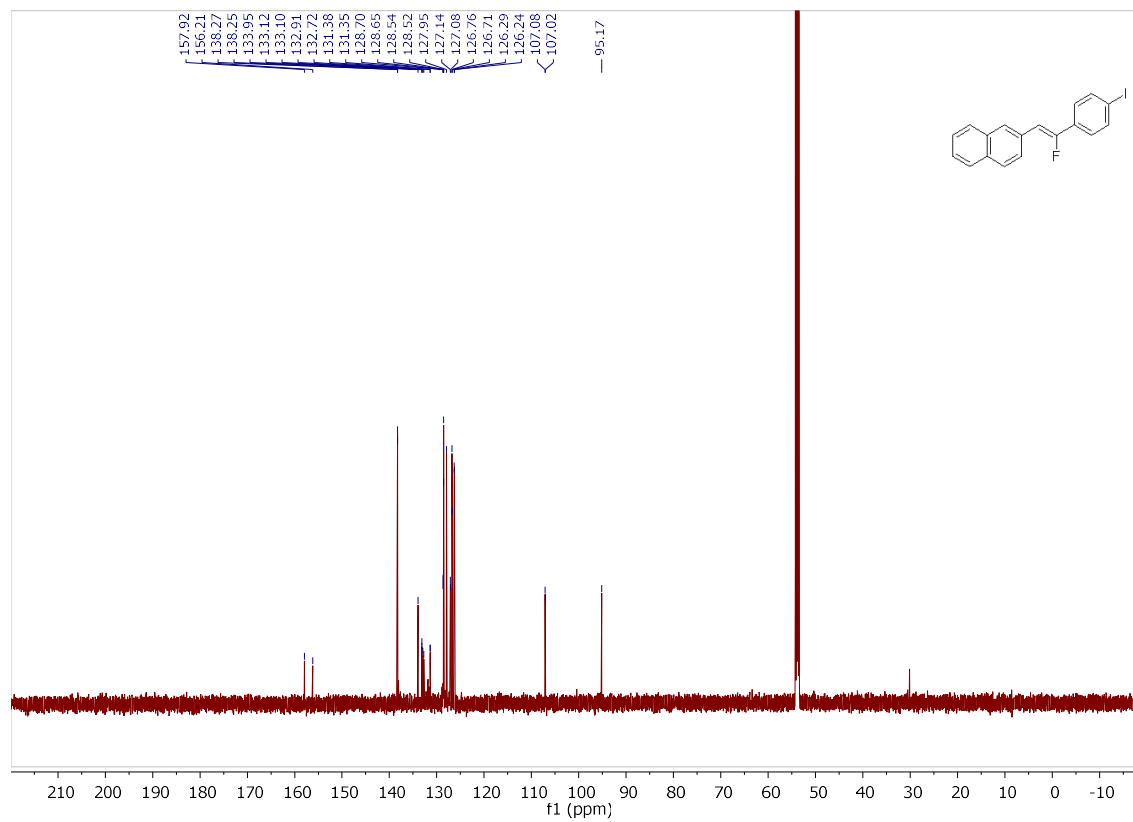
(Z)-1-(2-fluoro-2-(4-(trifluoromethoxy)phenyl)vinyl)-2-methoxybenzene 3h



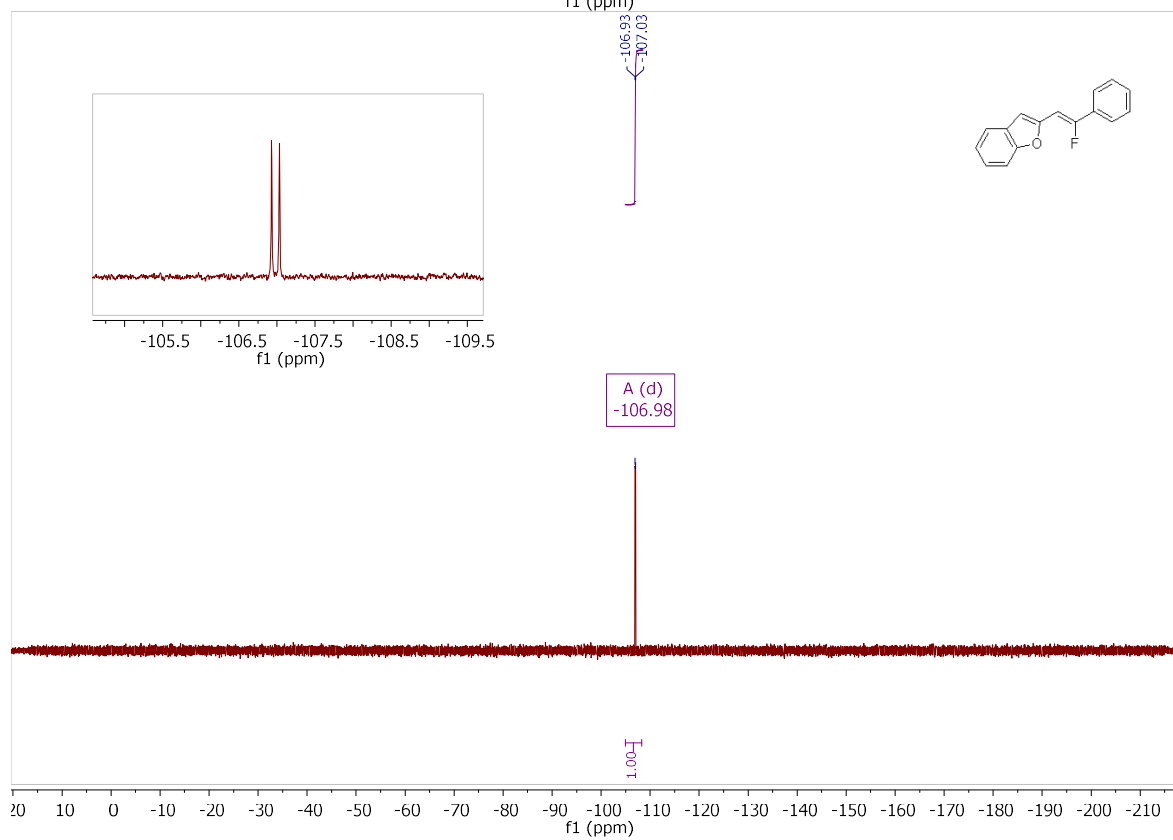
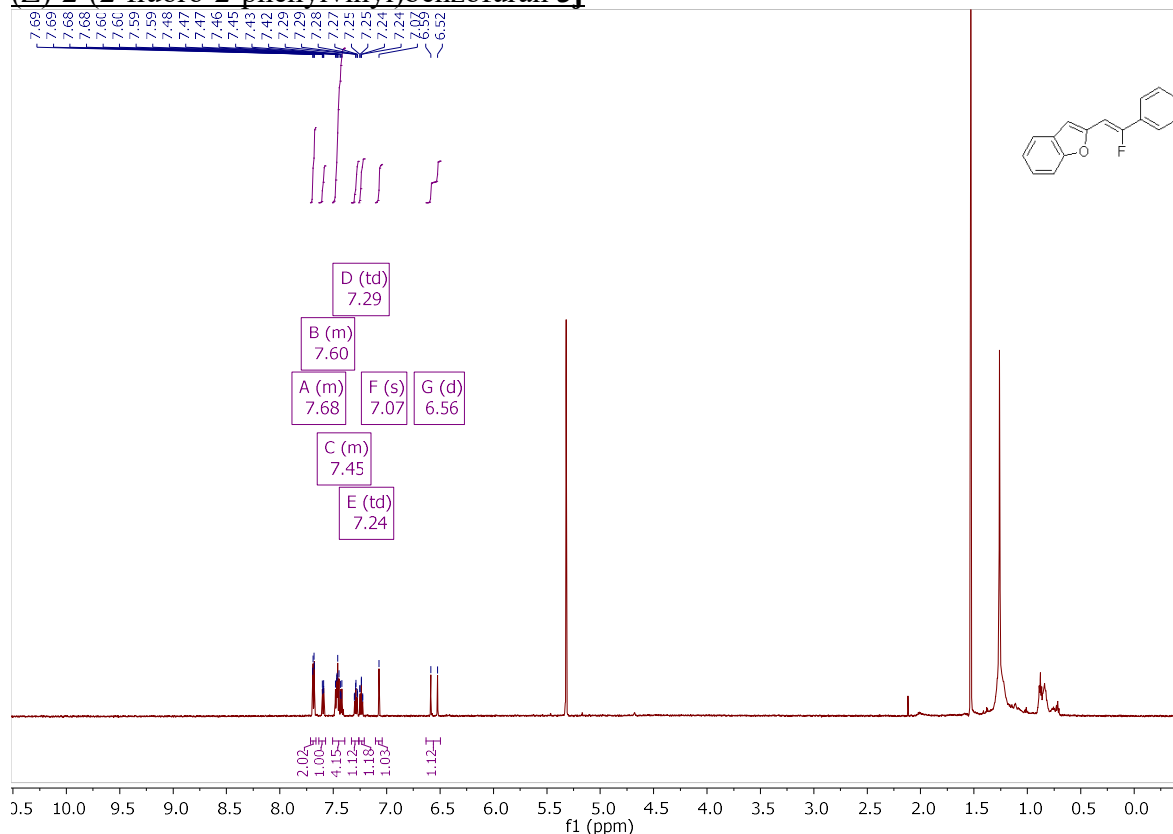


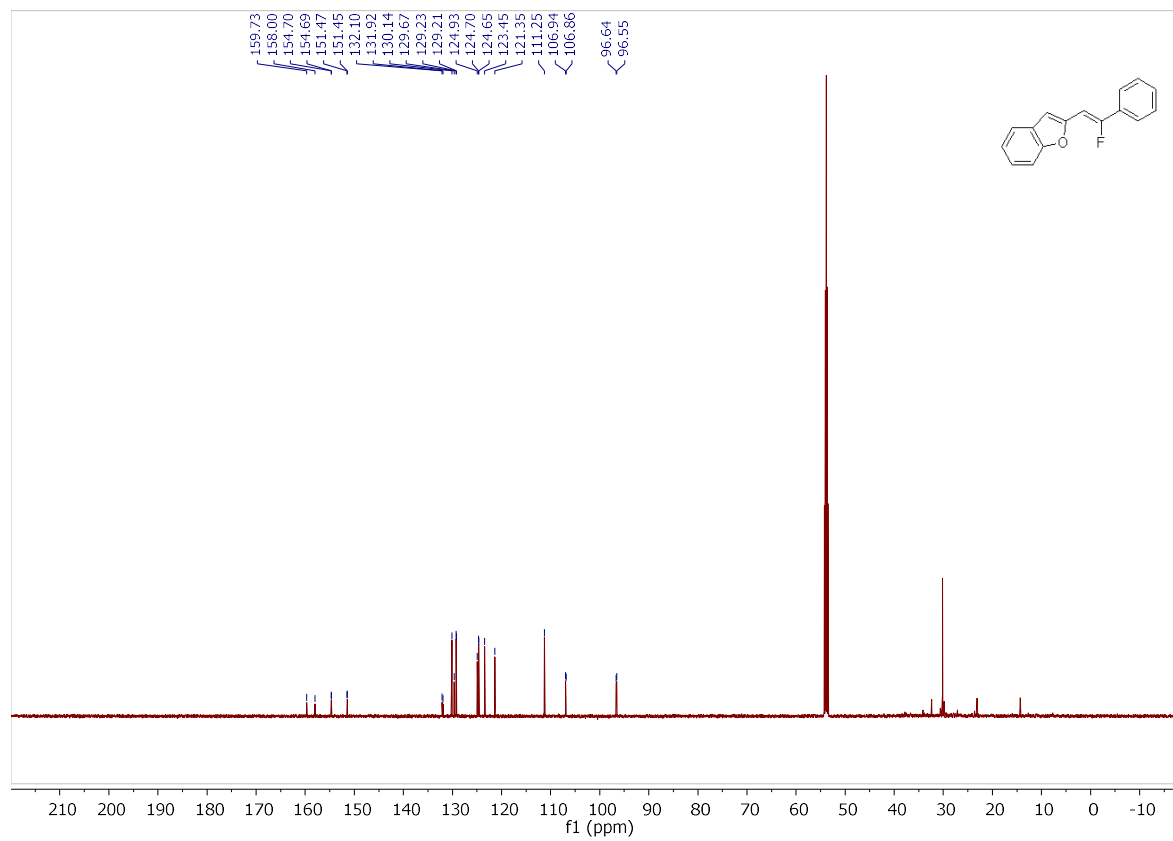
(Z)-2-(2-fluoro-2-(4-iodophenyl)vinyl)naphthalene 3i



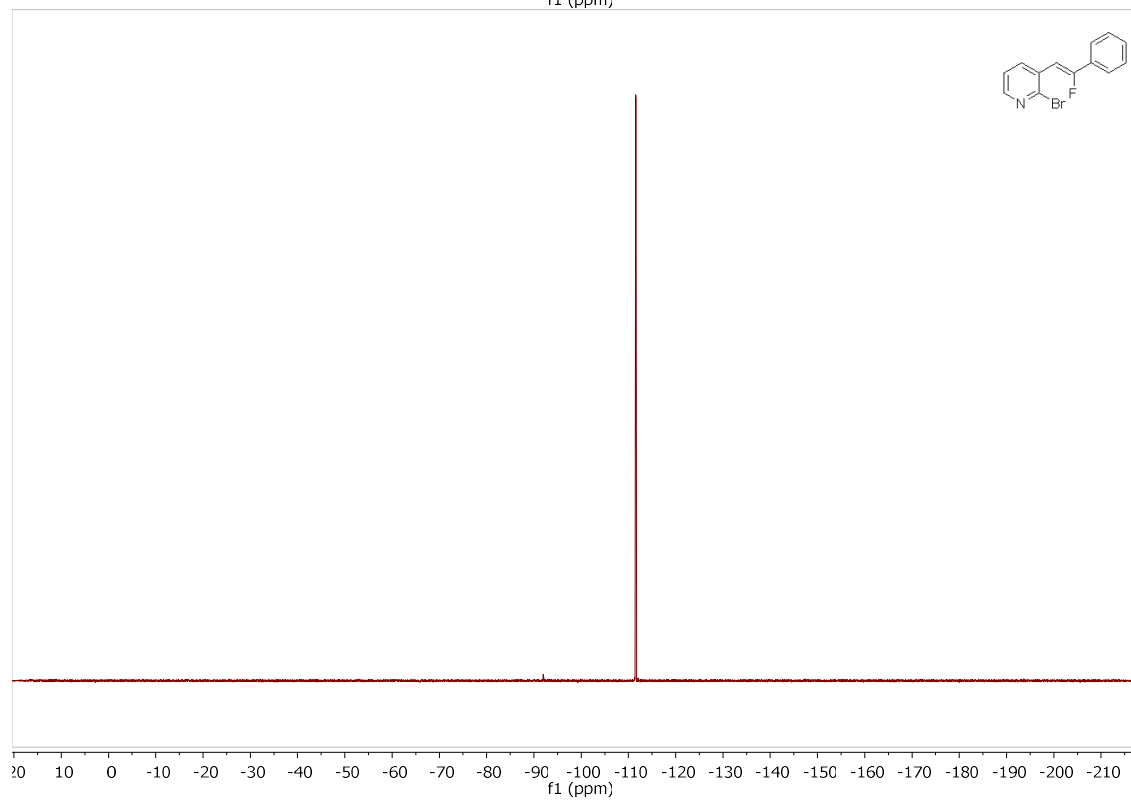
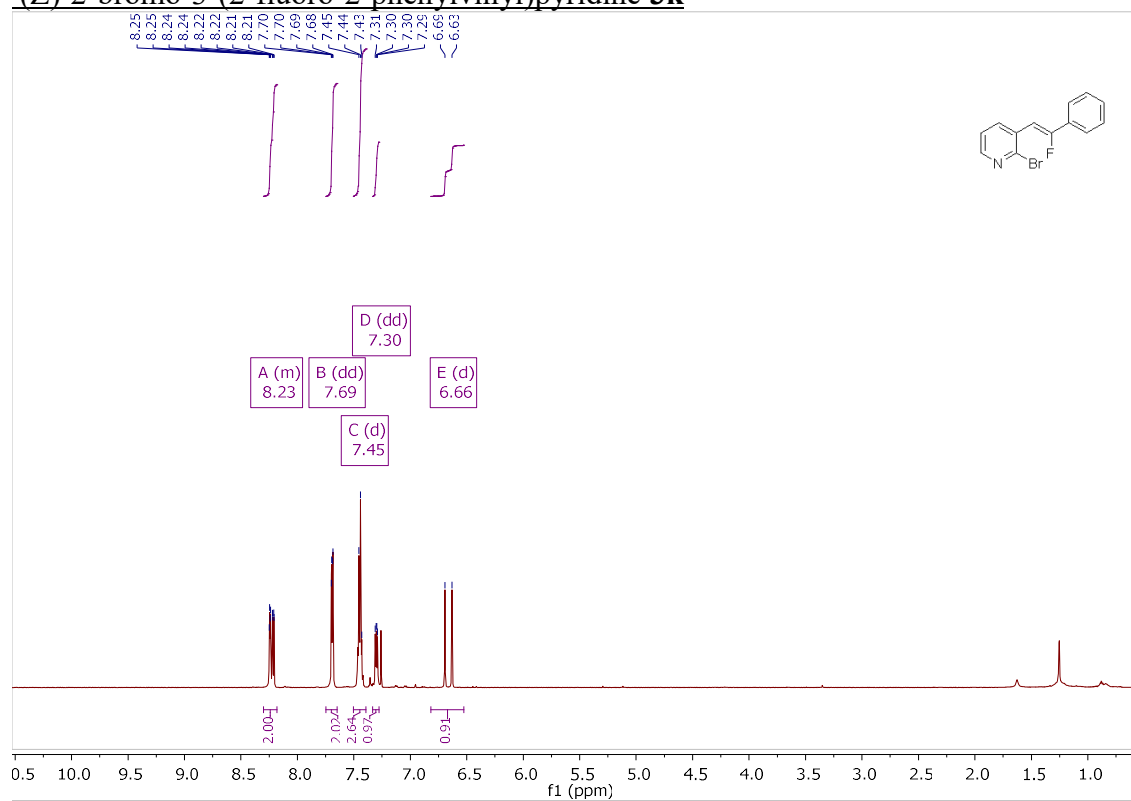


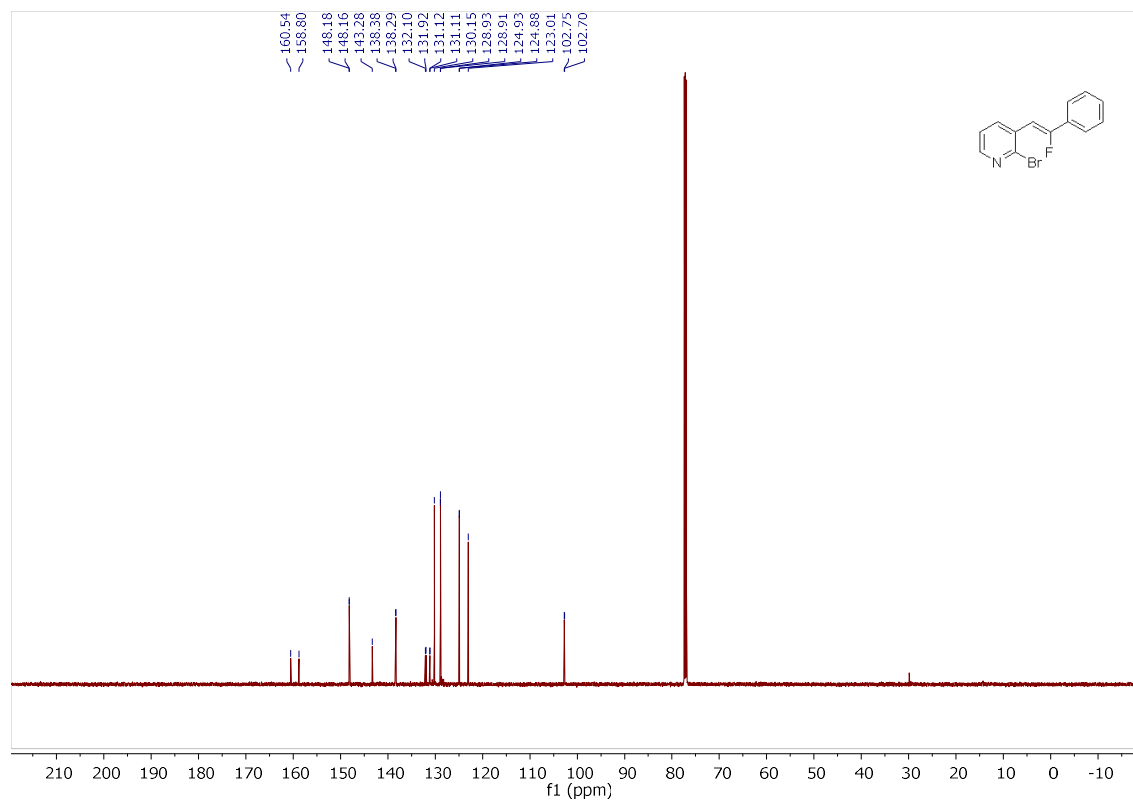
(Z)-2-(2-fluoro-2-phenylvinyl)benzofuran 3j



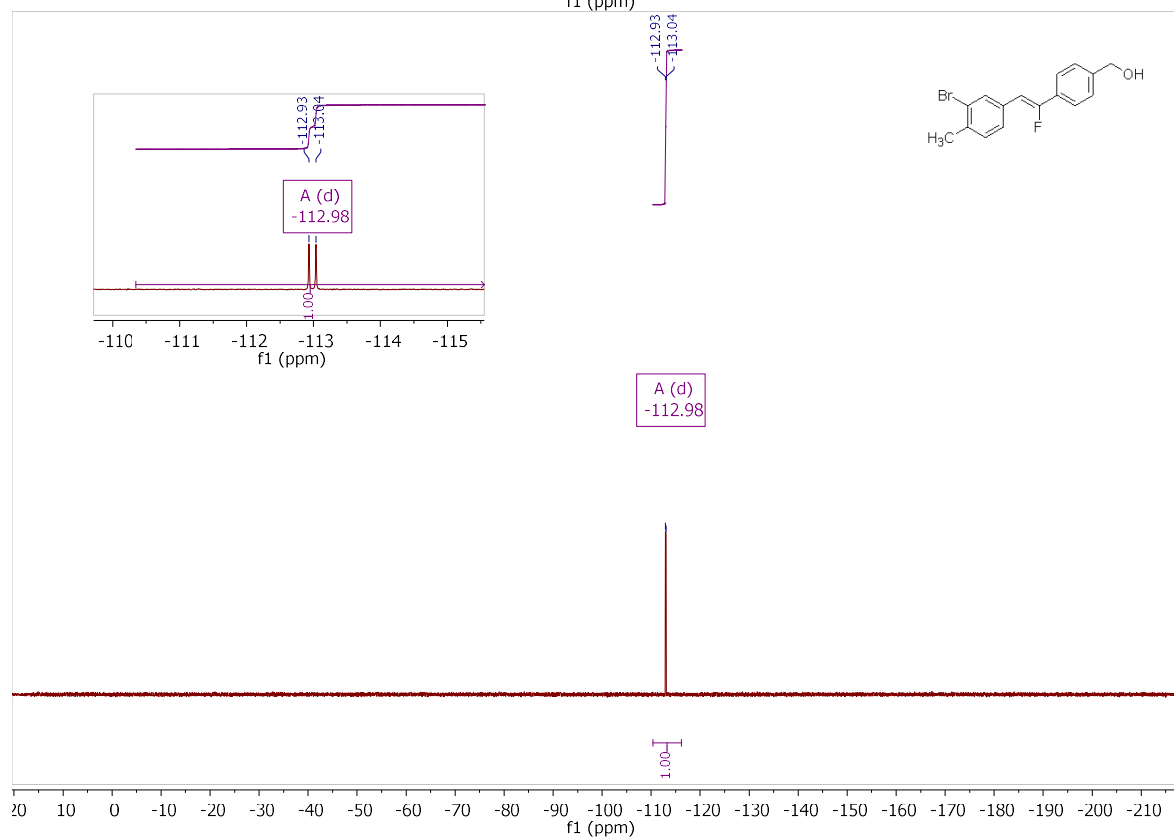
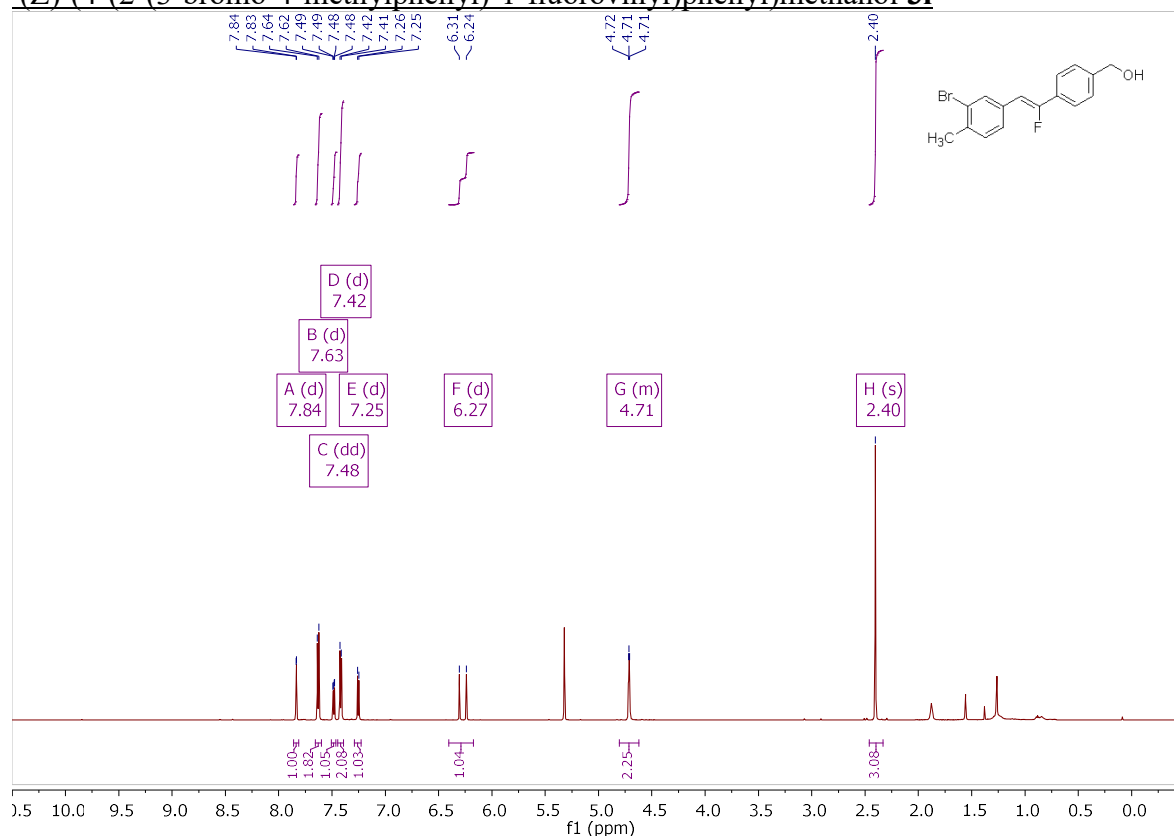


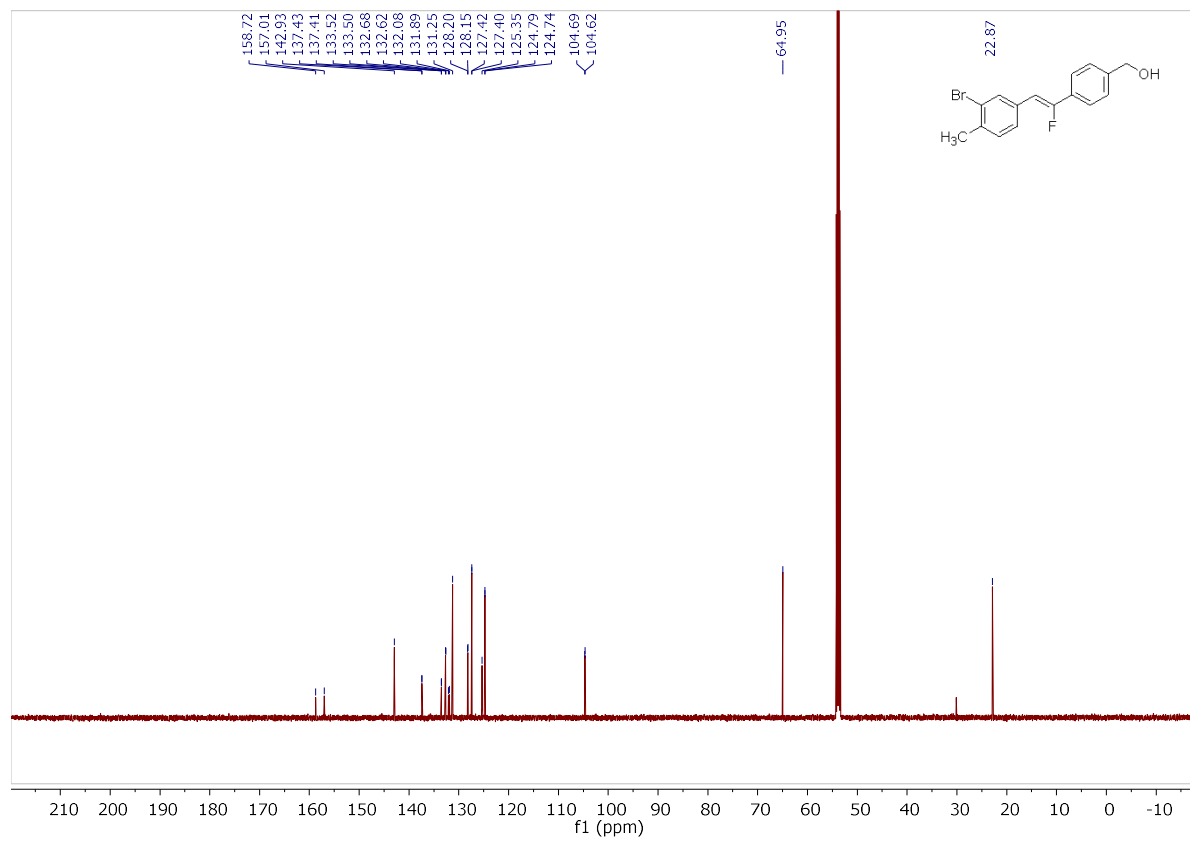
(Z)-2-bromo-3-(2-fluoro-2-phenylvinyl)pyridine 3k



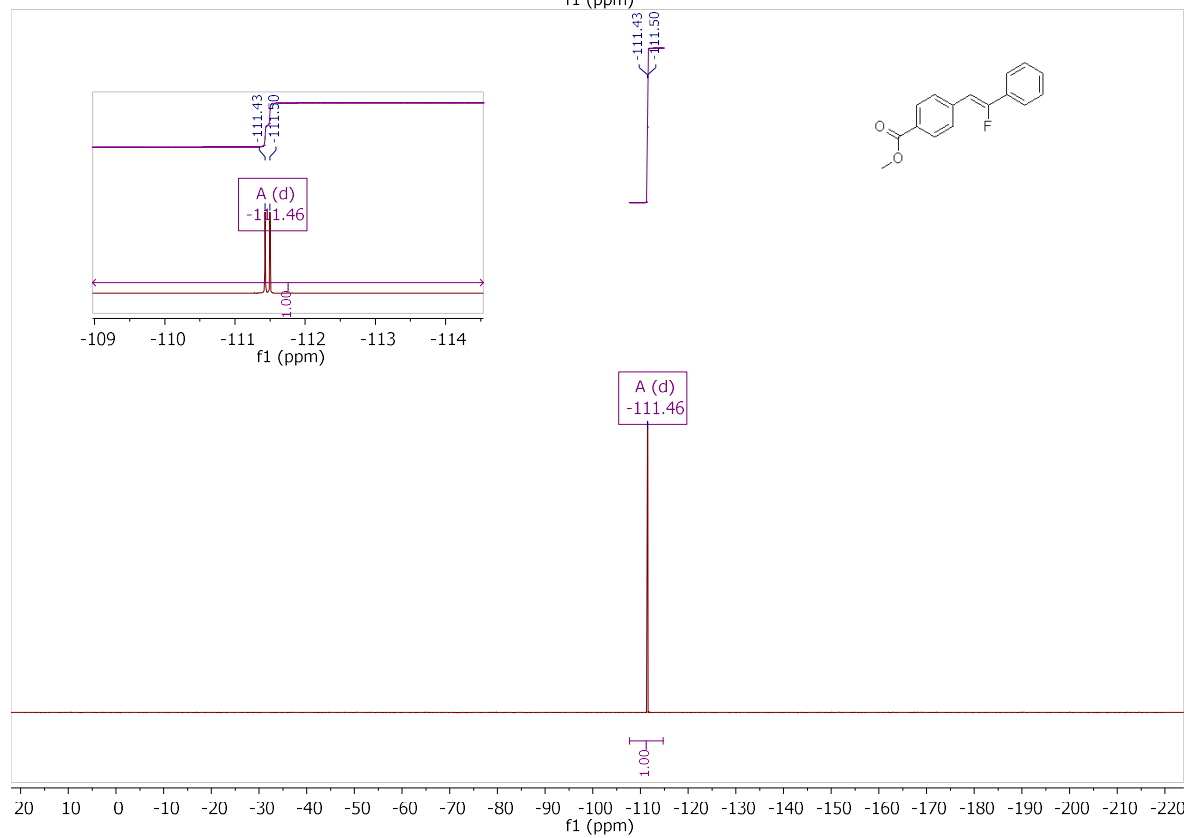
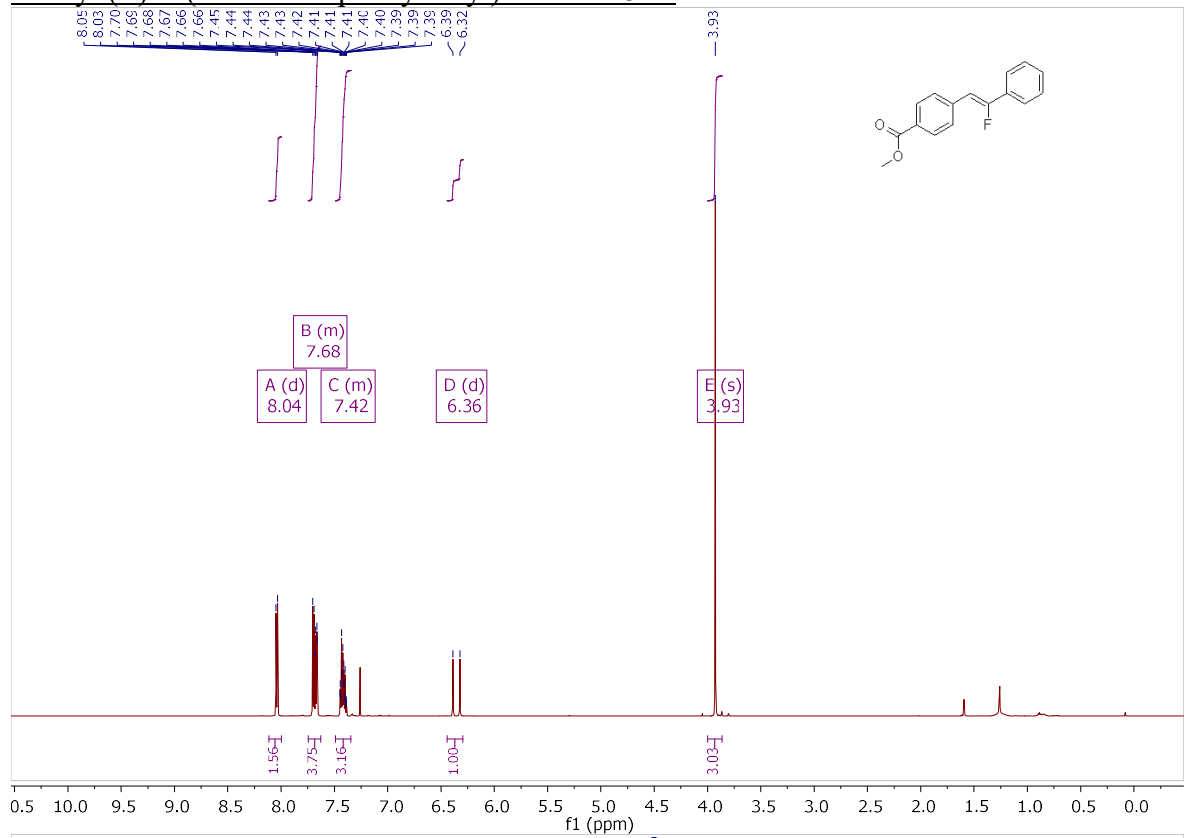


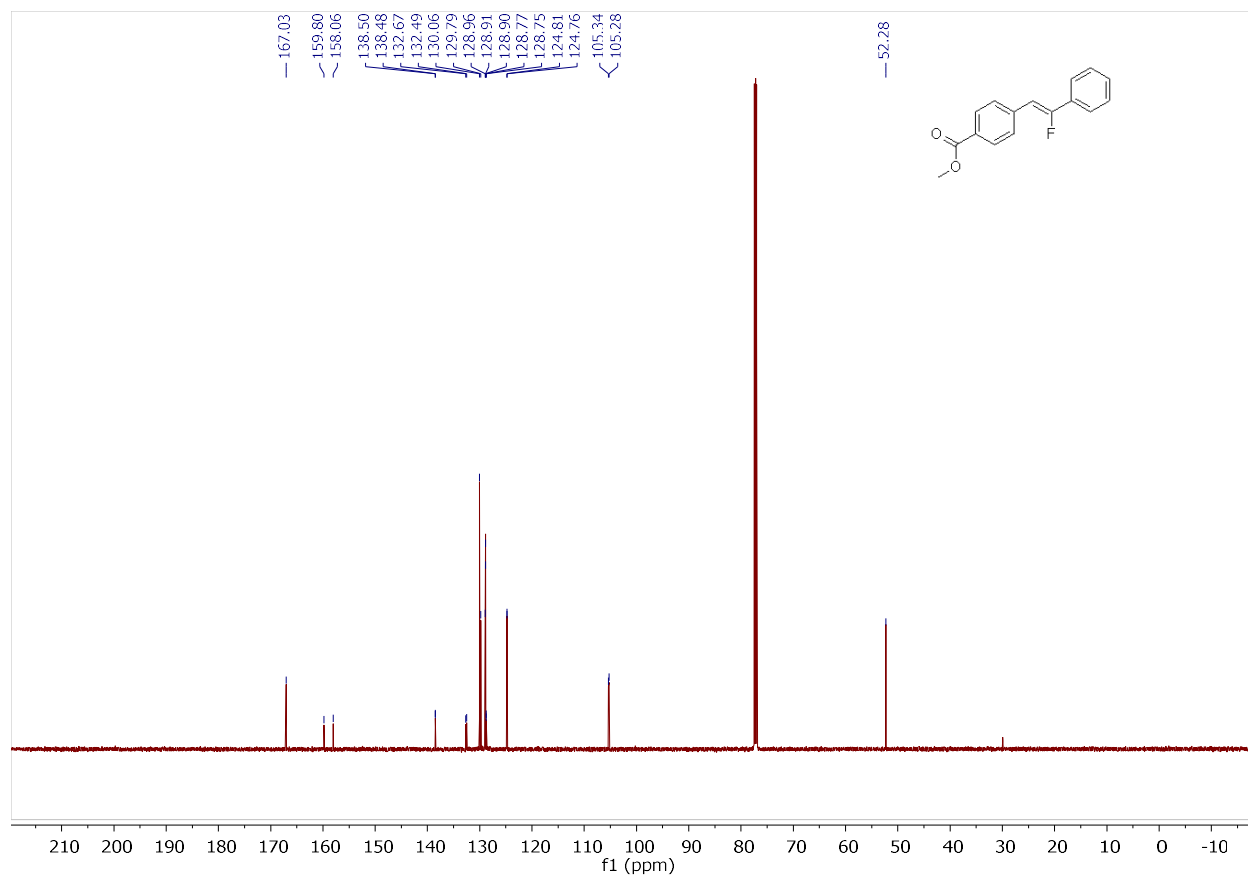
(Z)-4-(2-(3-bromo-4-methylphenyl)-1-fluorovinyl)phenylmethanol 31



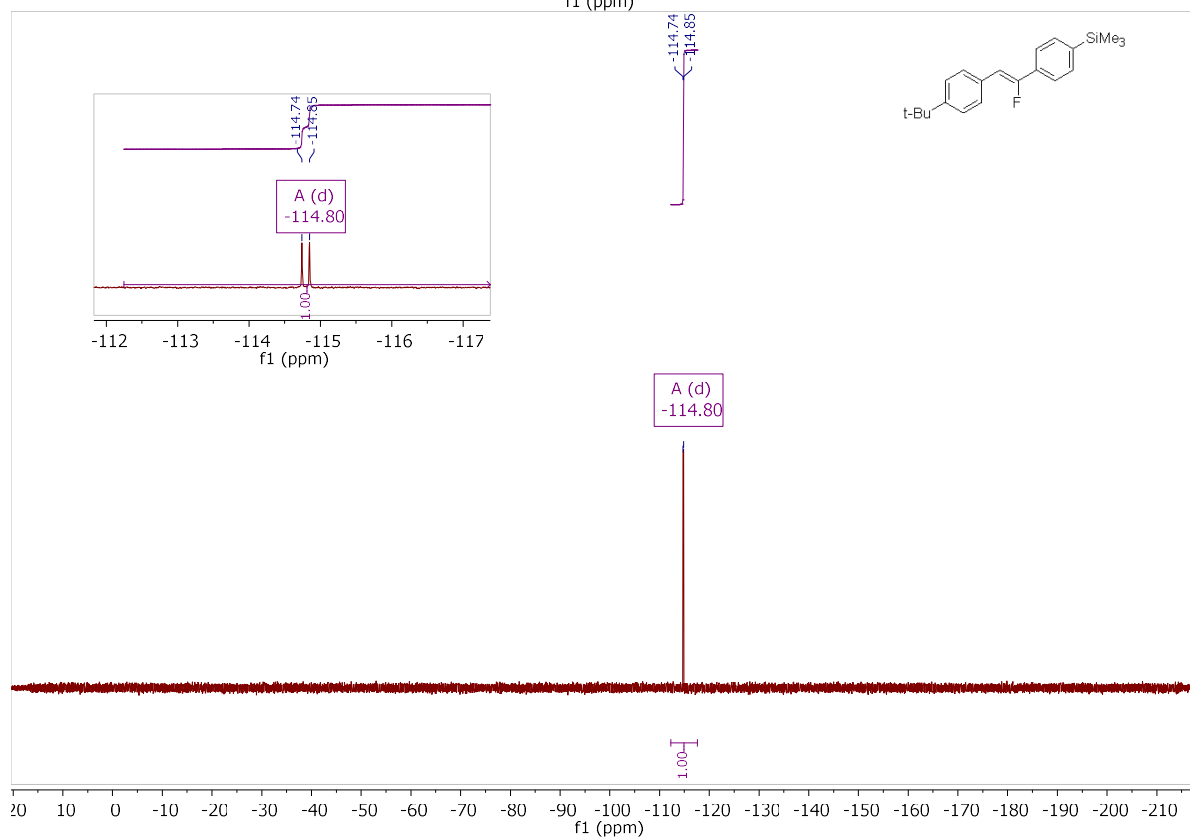
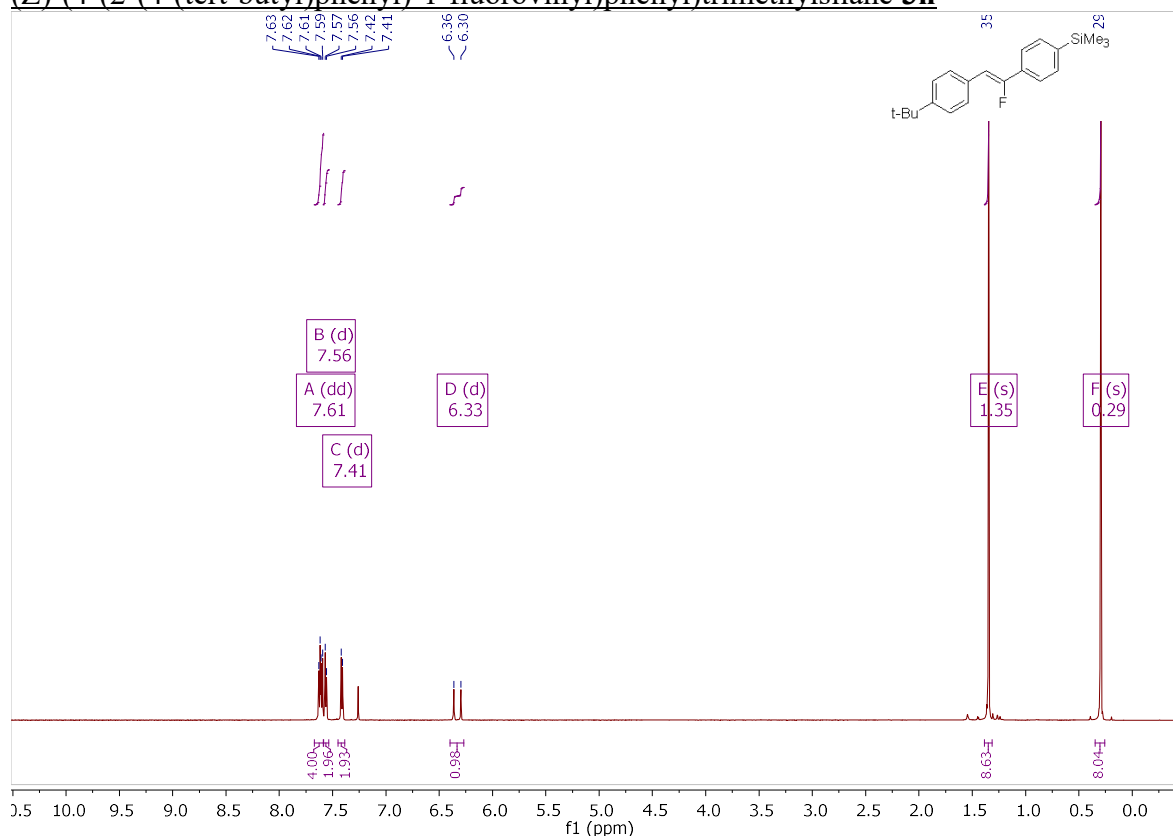


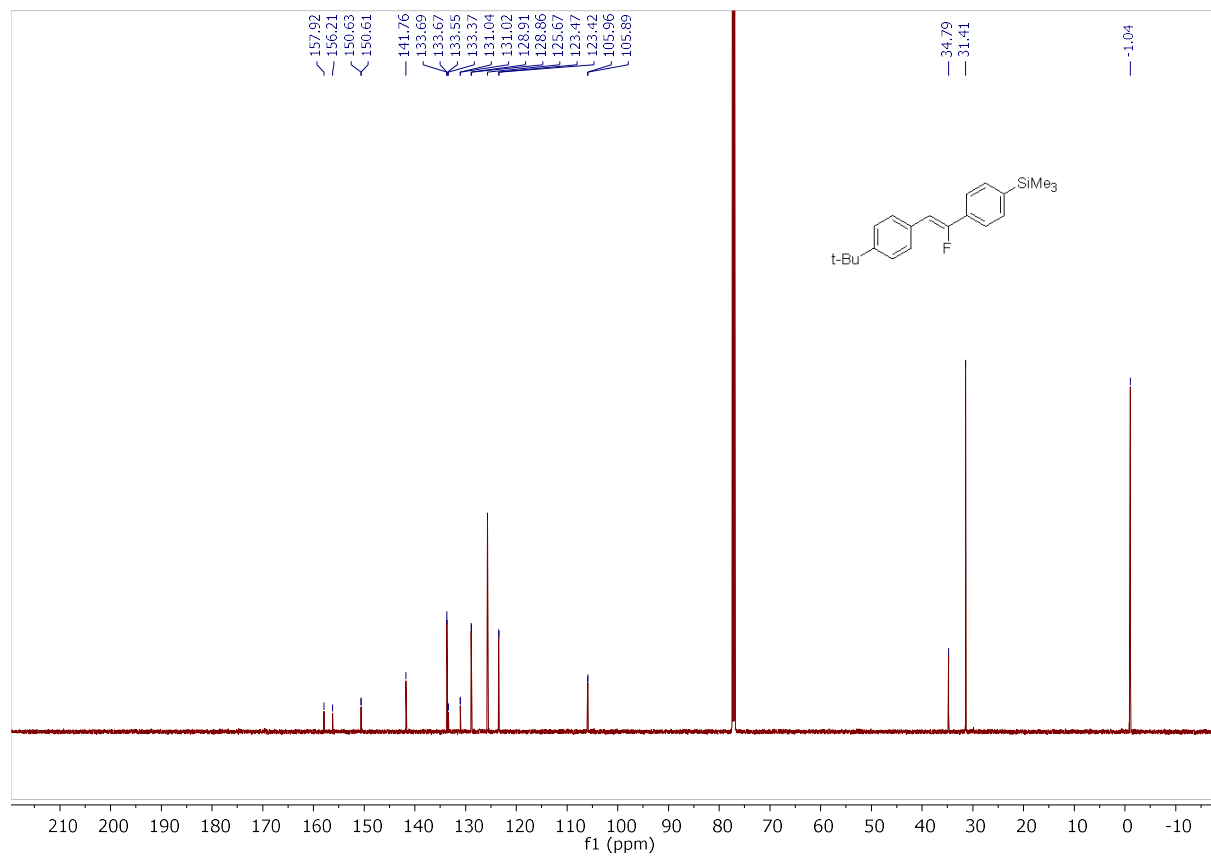
methyl (Z)-4-(2-fluoro-2-phenylvinyl)benzoate 3m:



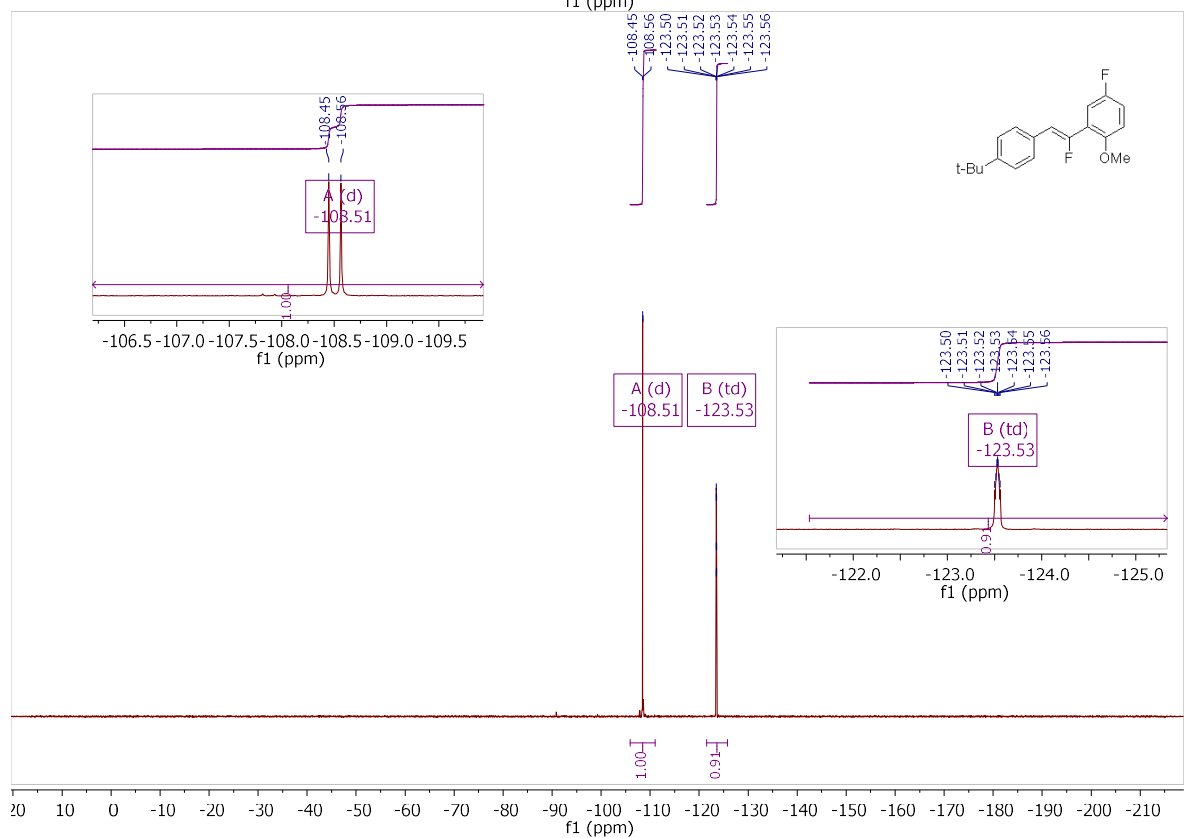
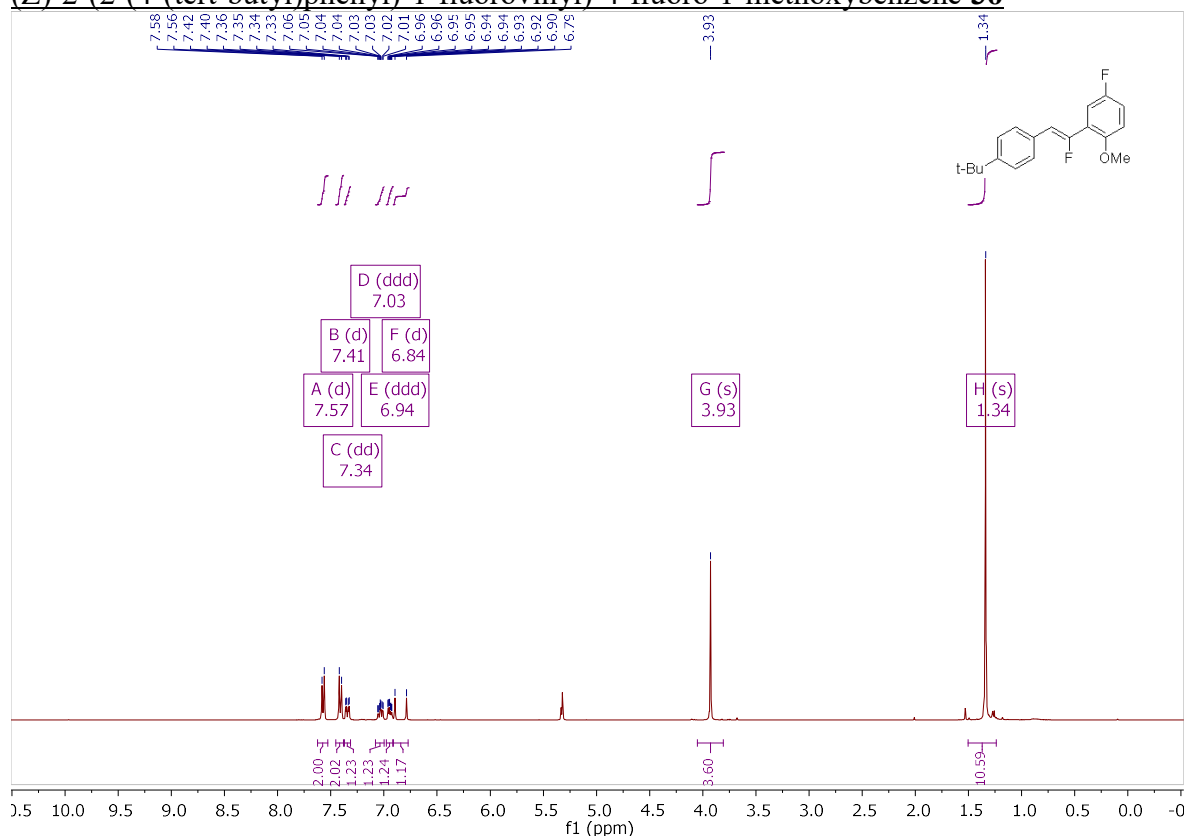


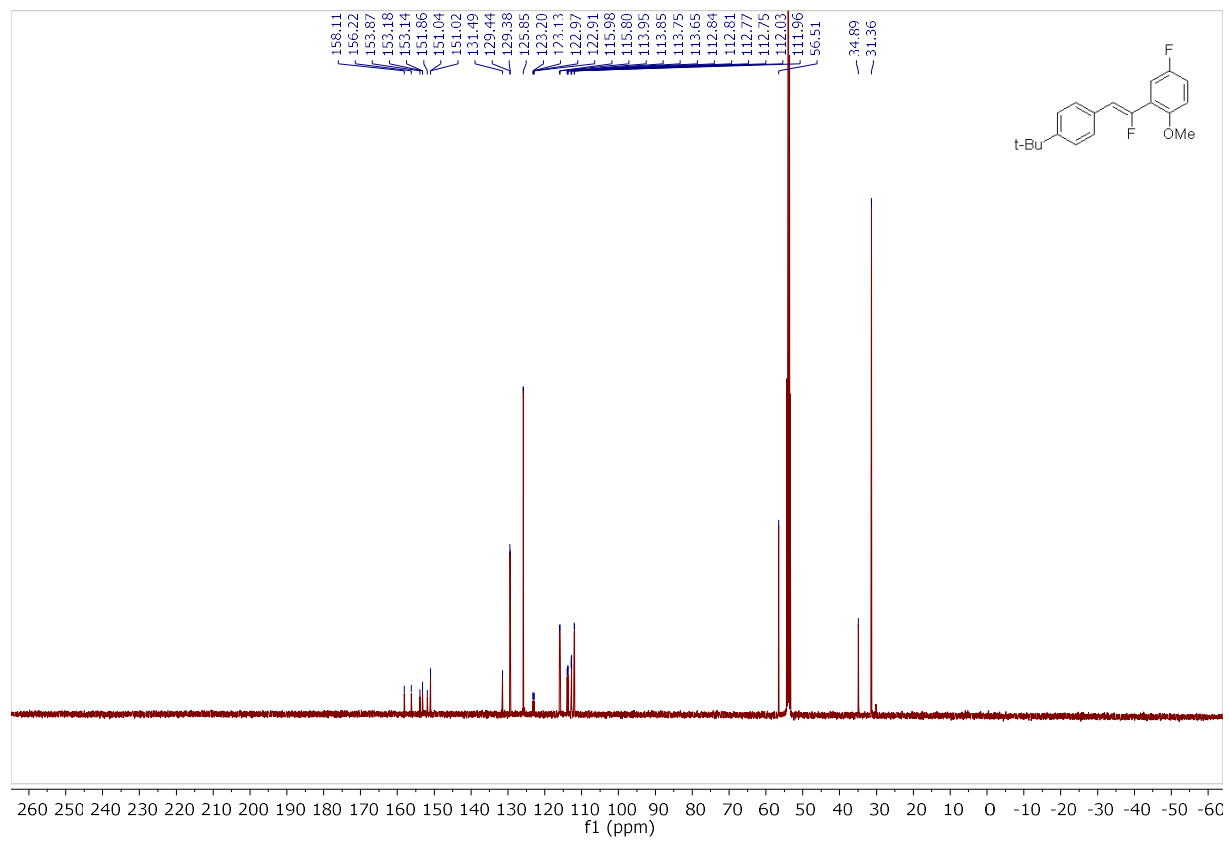
(Z)-4-(2-(4-(tert-butyl)phenyl)-1-fluorovinyl)phenyltrimethylsilane 3n



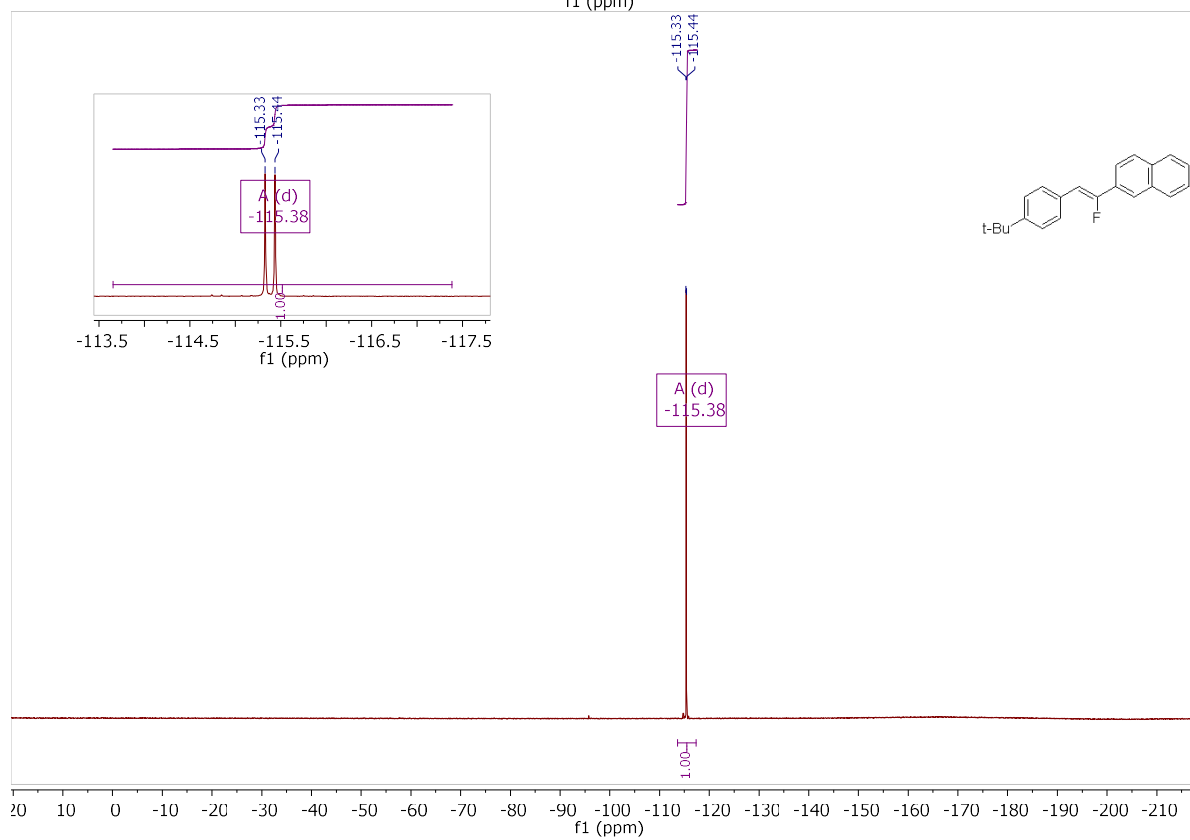
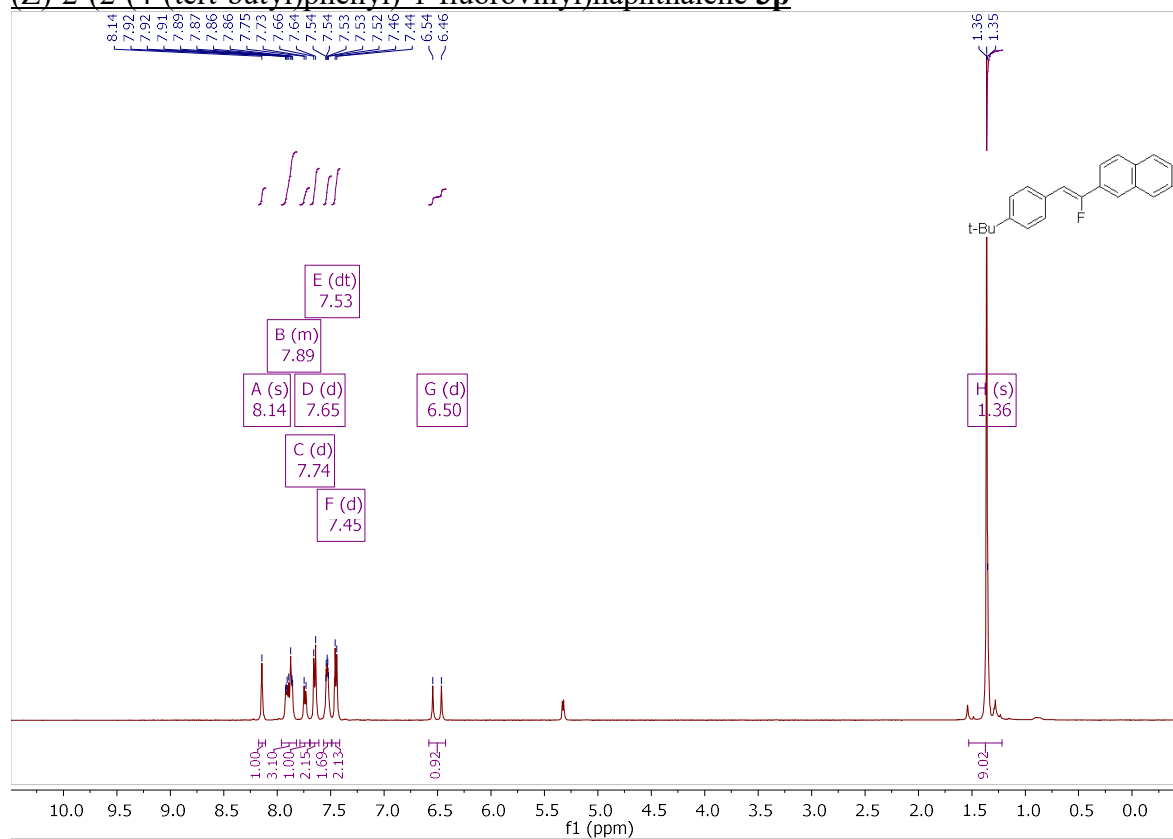


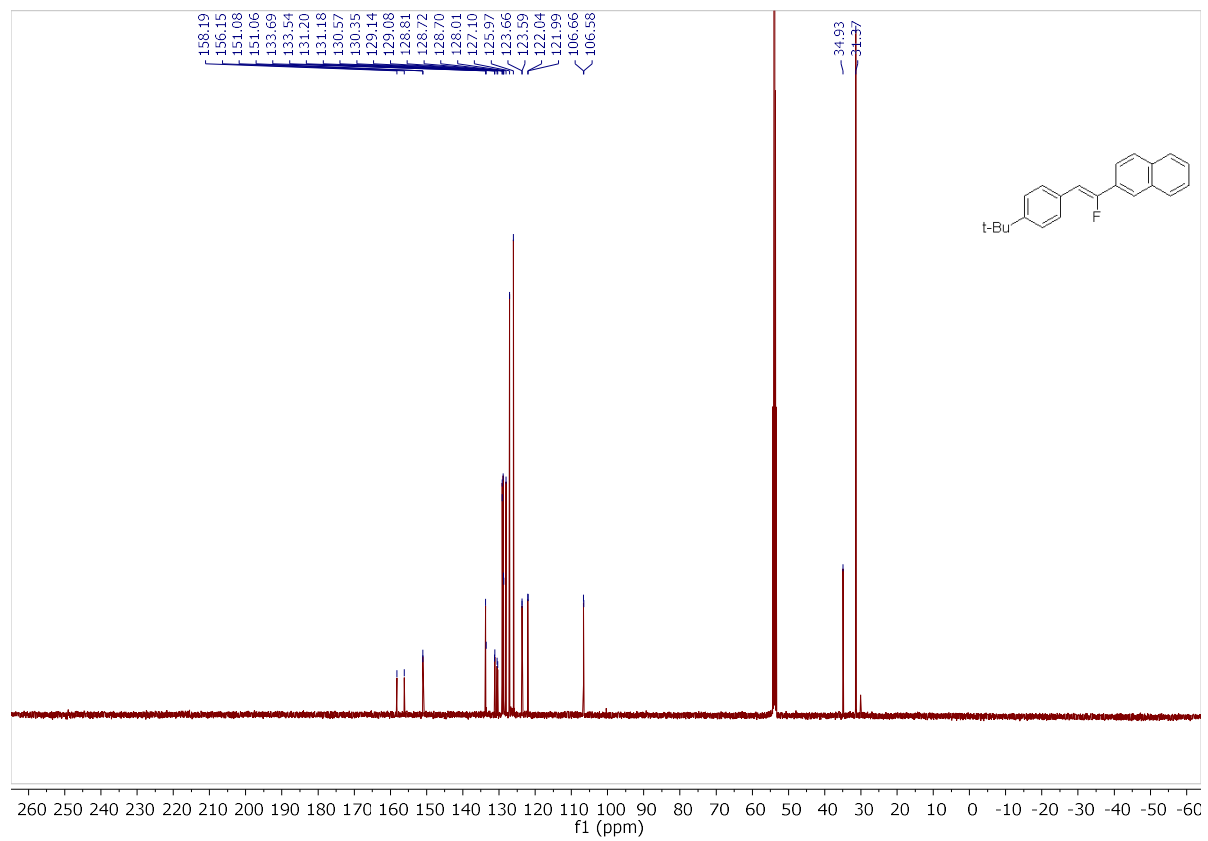
(Z)-2-(2-(4-(tert-butyl)phenyl)-1-fluorovinyl)-4-fluoro-1-methoxybenzene 3o



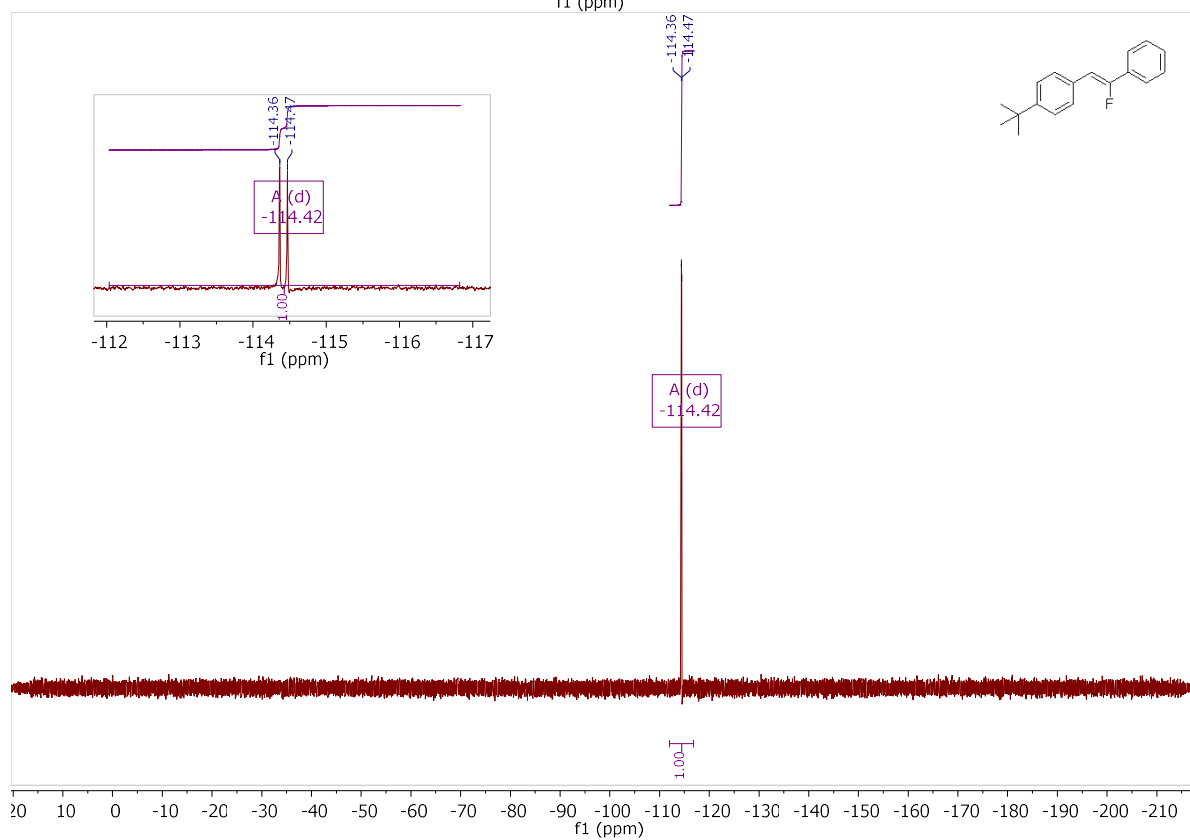
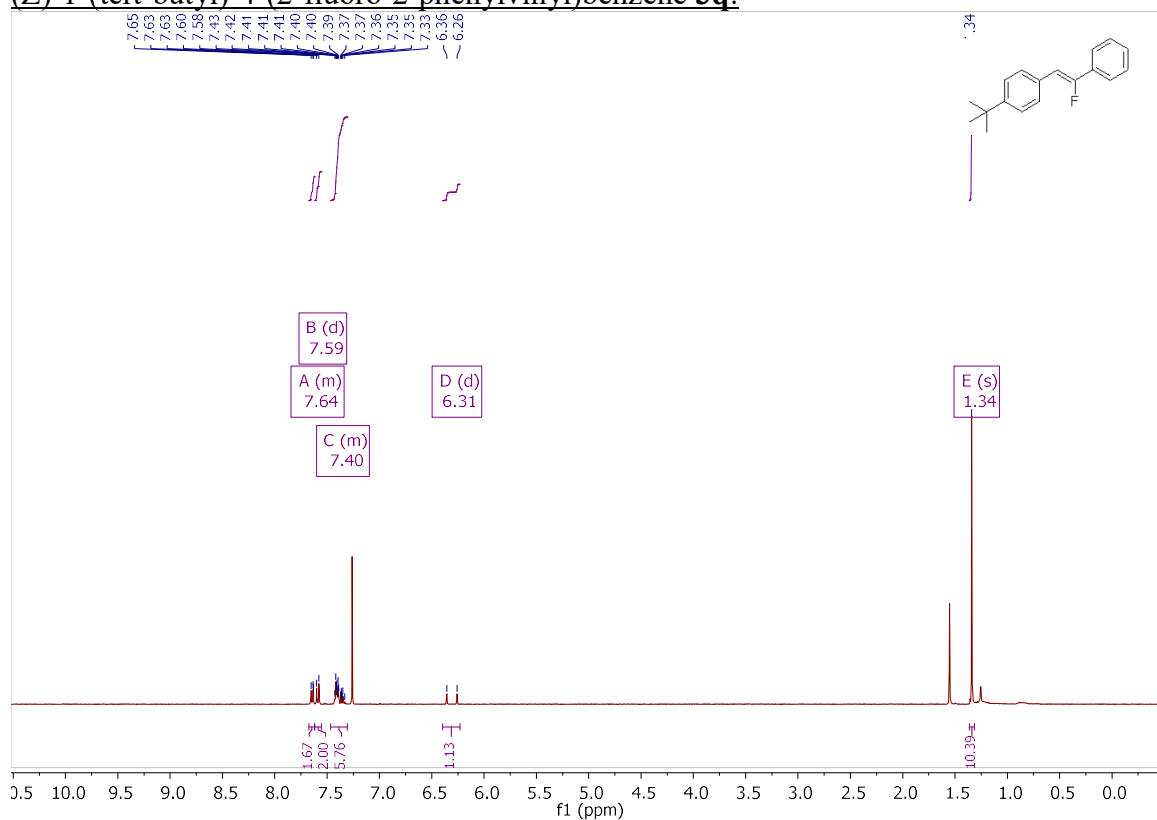


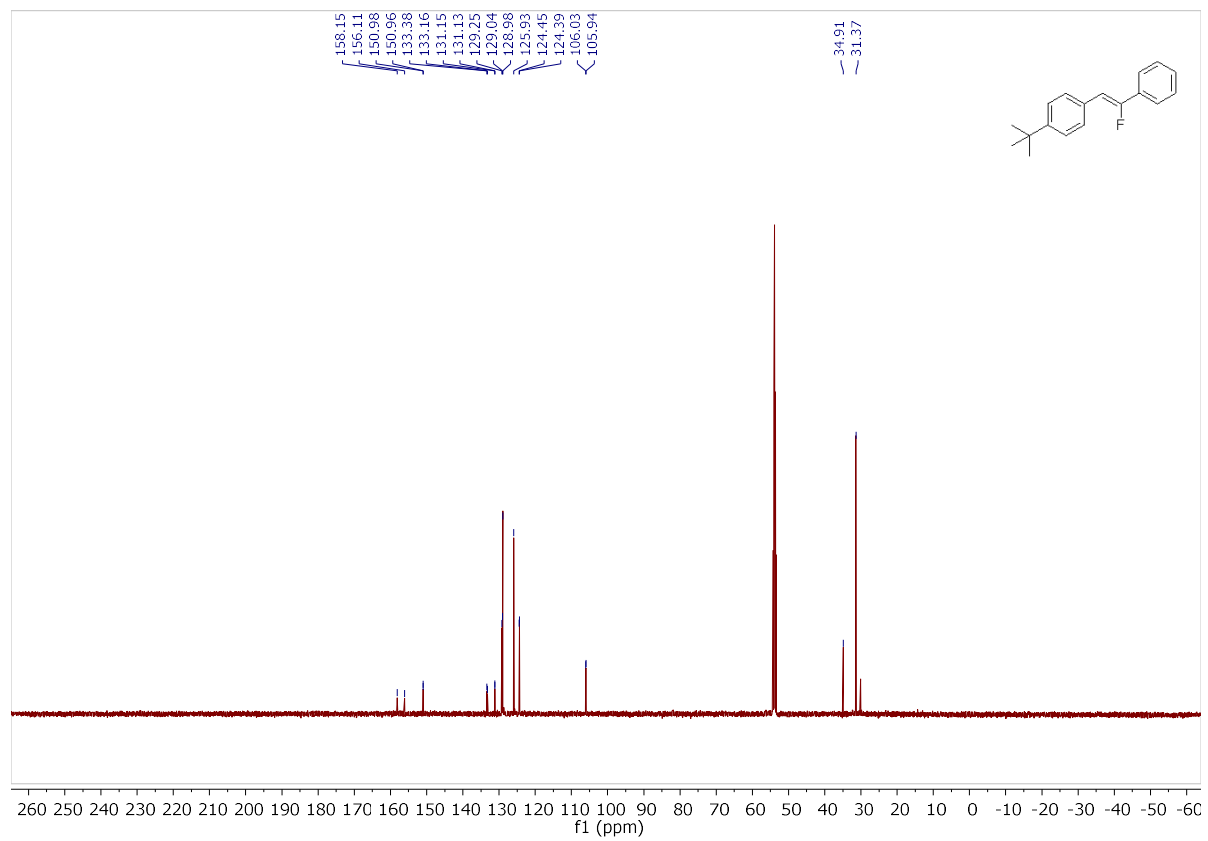
(Z)-2-(2-(4-(tert-butyl)phenyl)-1-fluorovinyl)naphthalene 3p



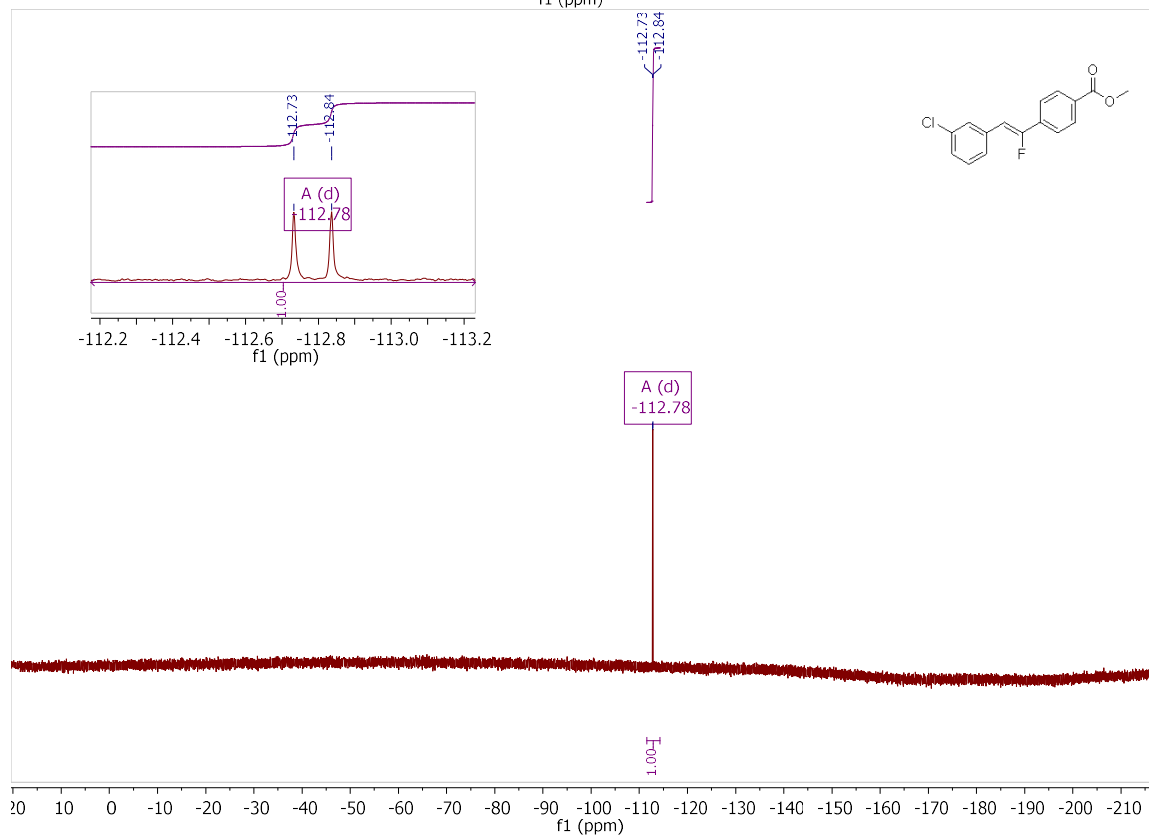
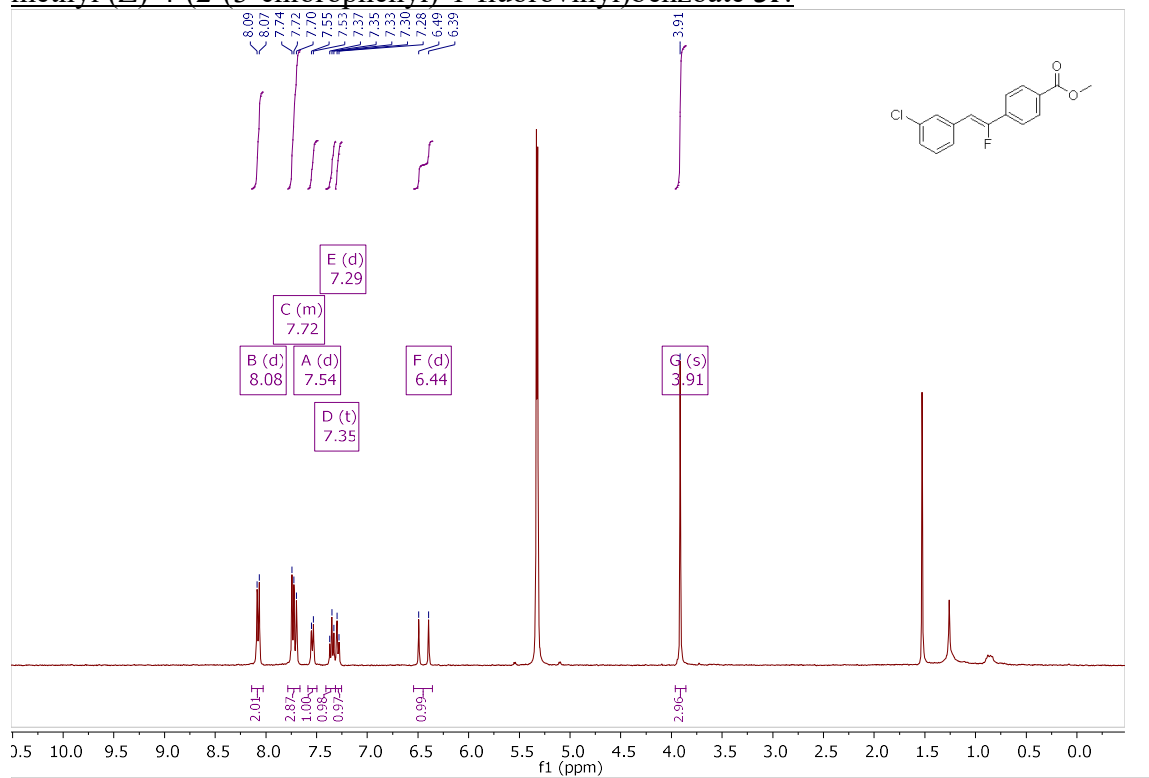


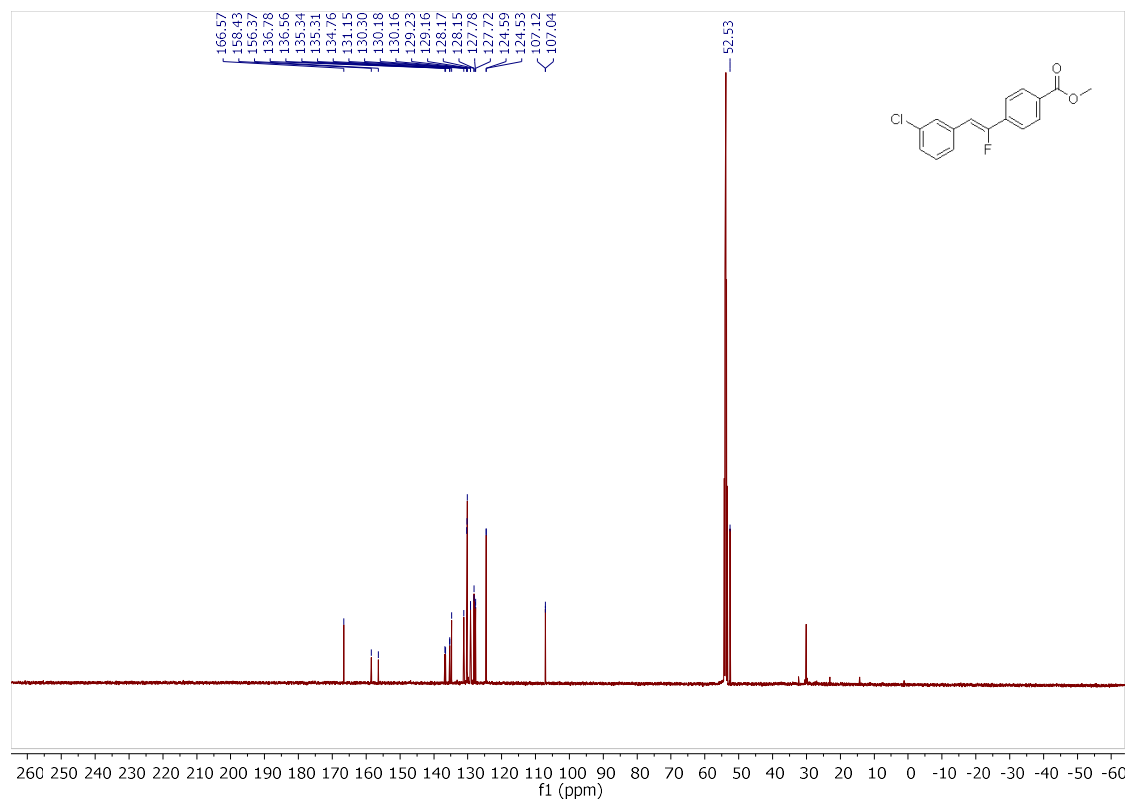
(Z)-1-(tert-butyl)-4-(2-fluoro-2-phenylvinyl)benzene 3q:



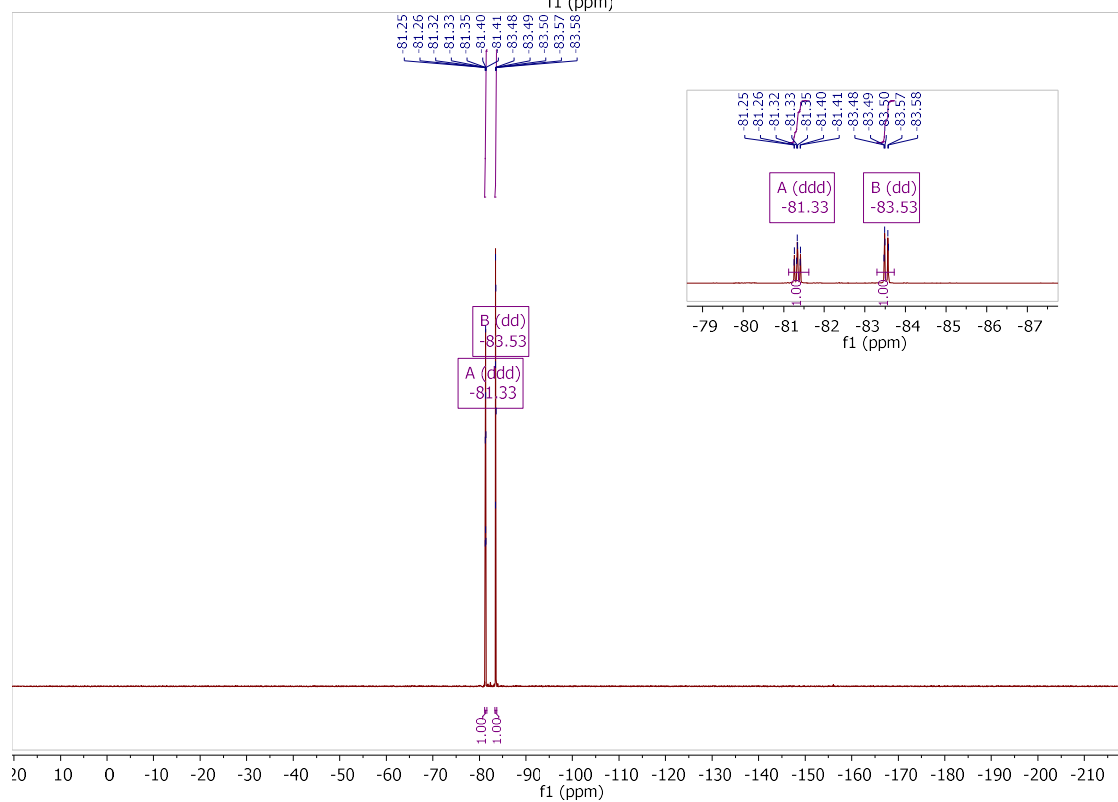
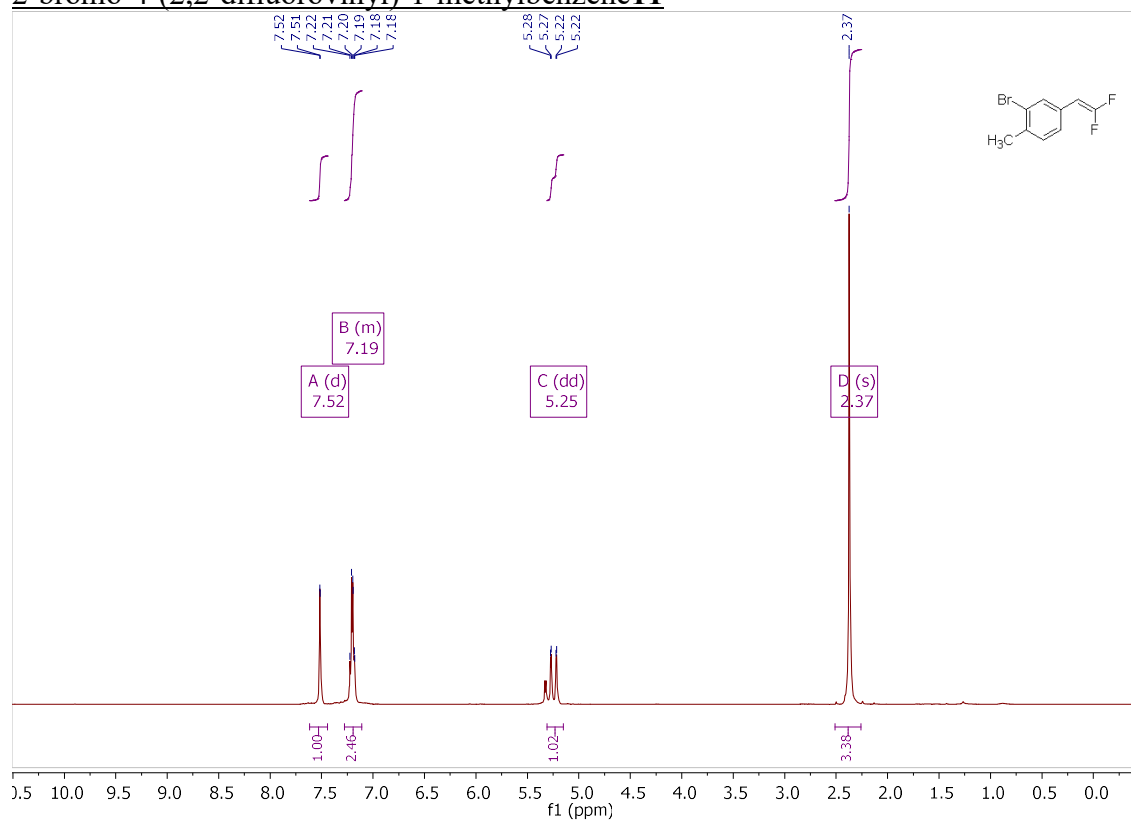


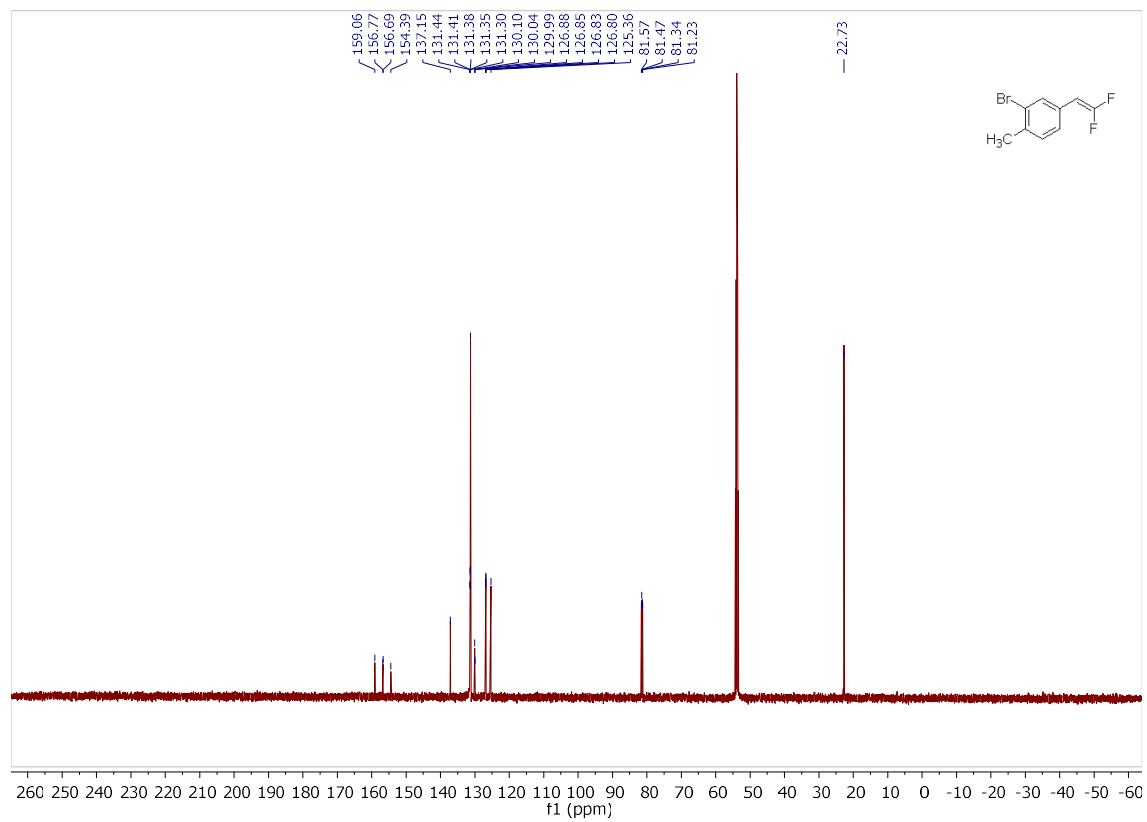
methyl (Z)-4-(2-(3-chlorophenyl)-1-fluorovinyl)benzoate **3r**:



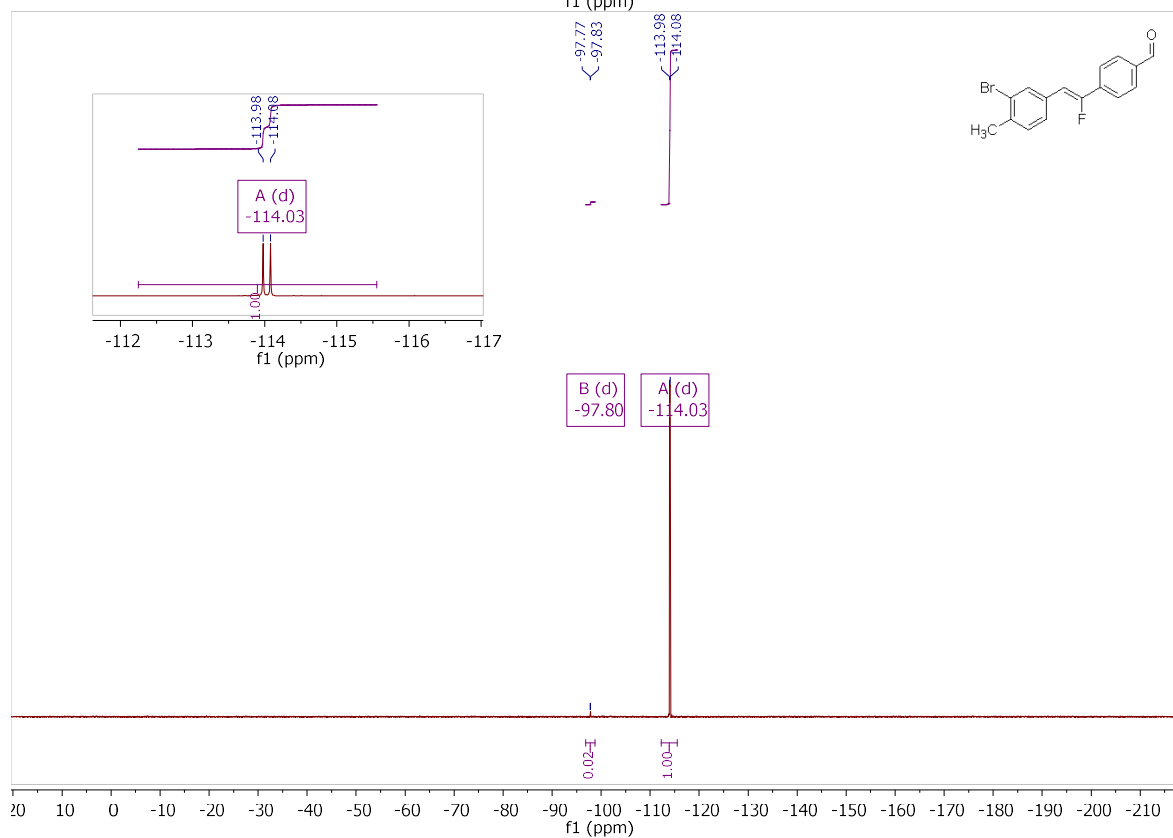
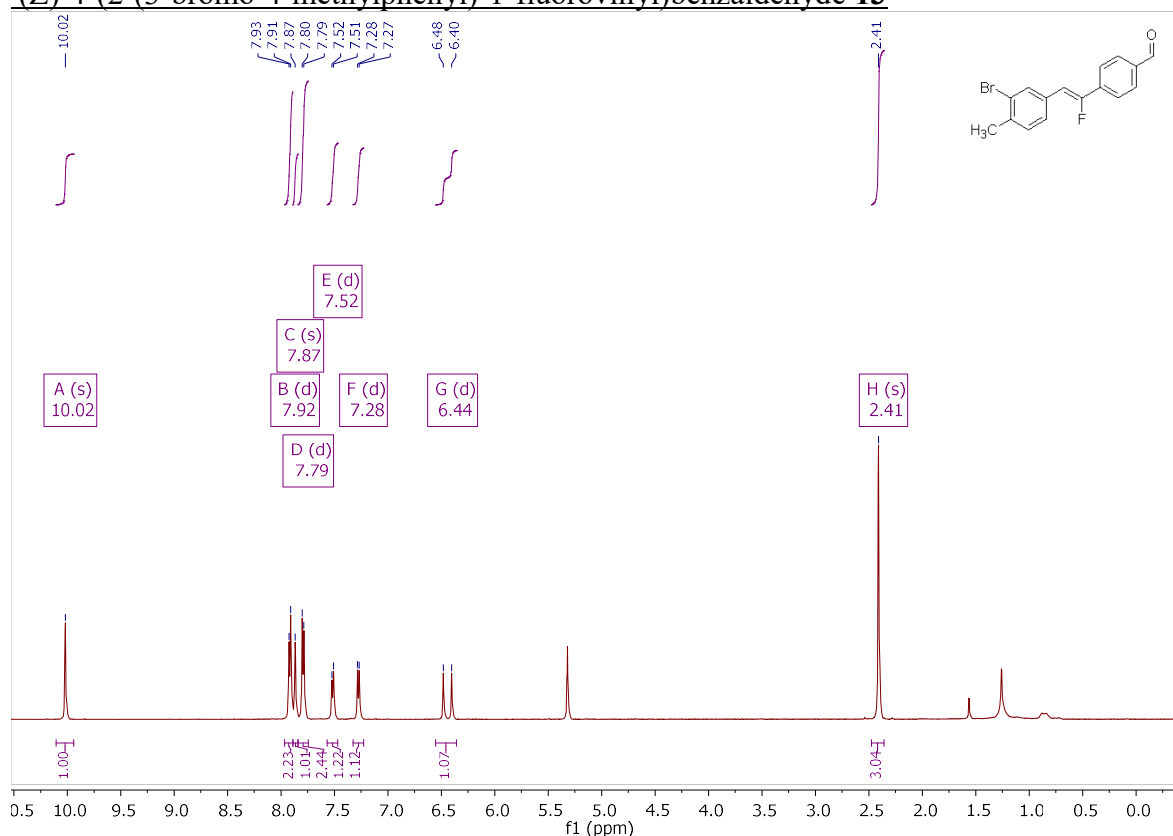


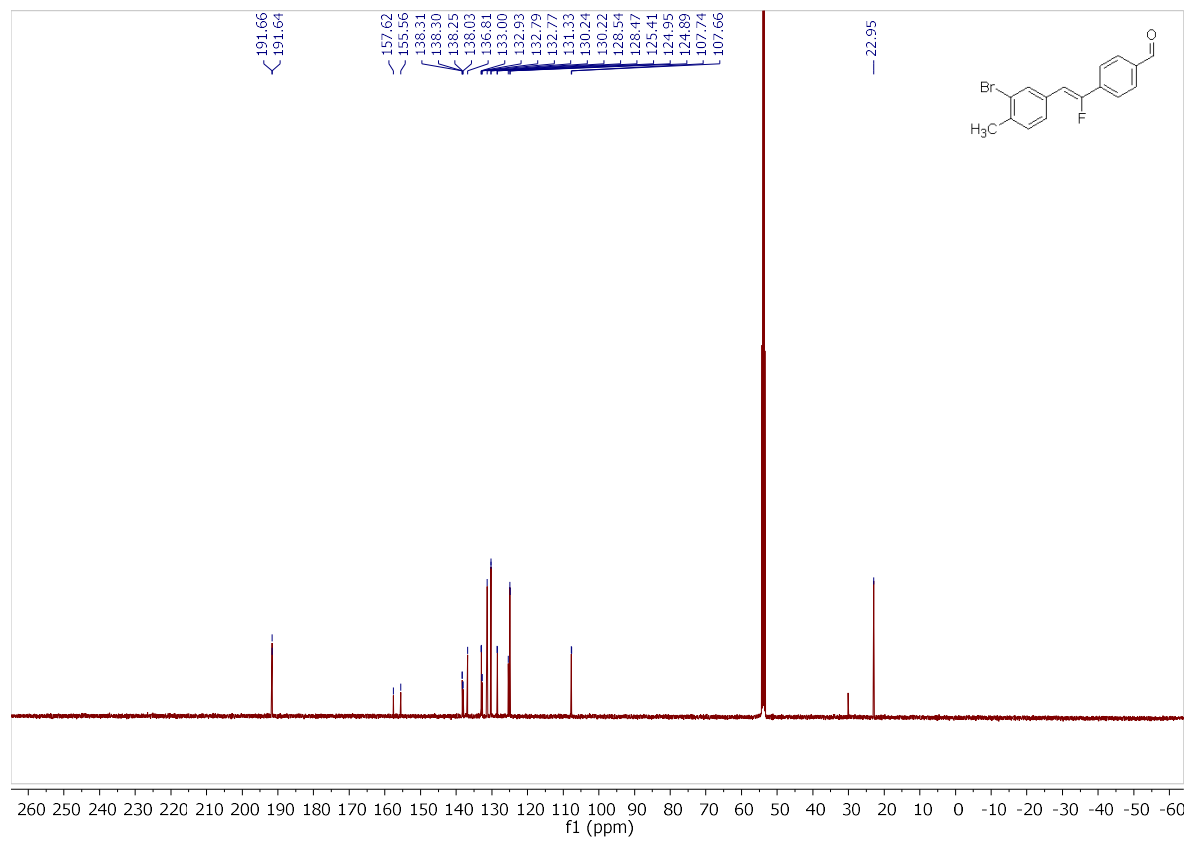
2-bromo-4-(2,2-difluorovinyl)-1-methylbenzene11



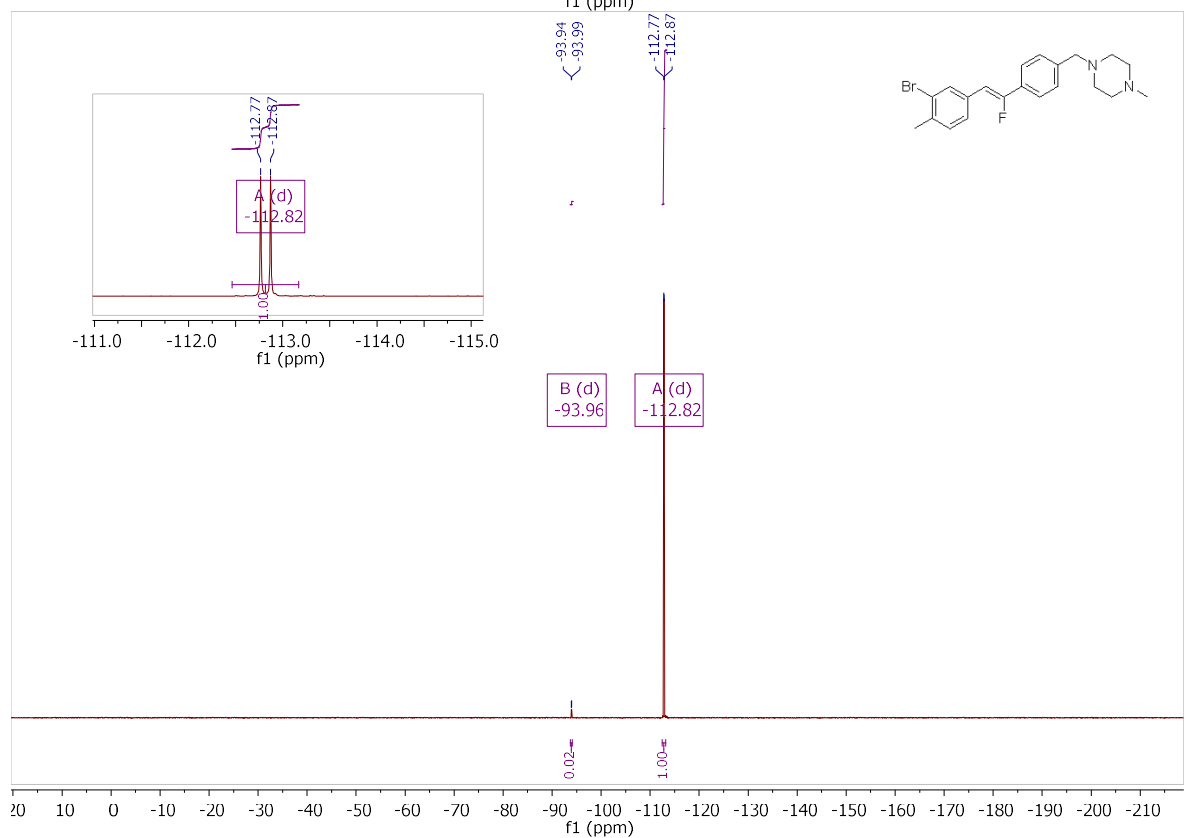
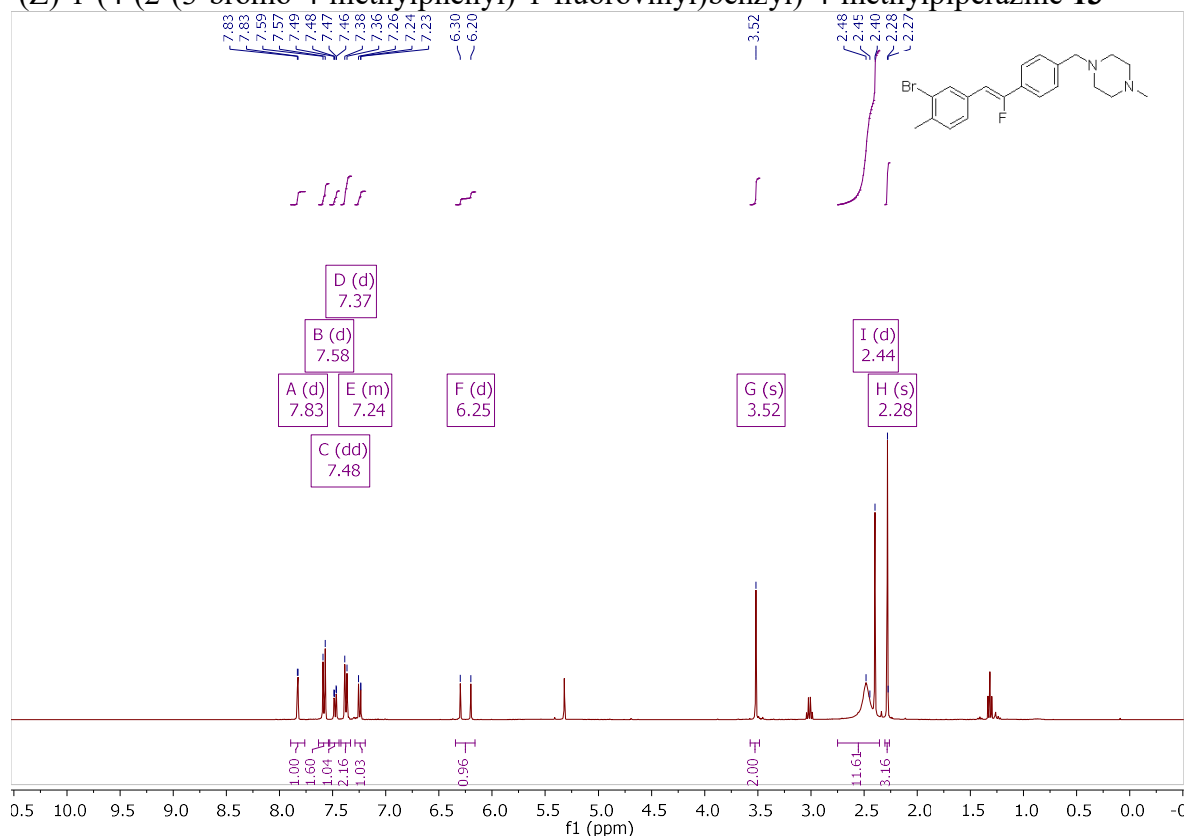


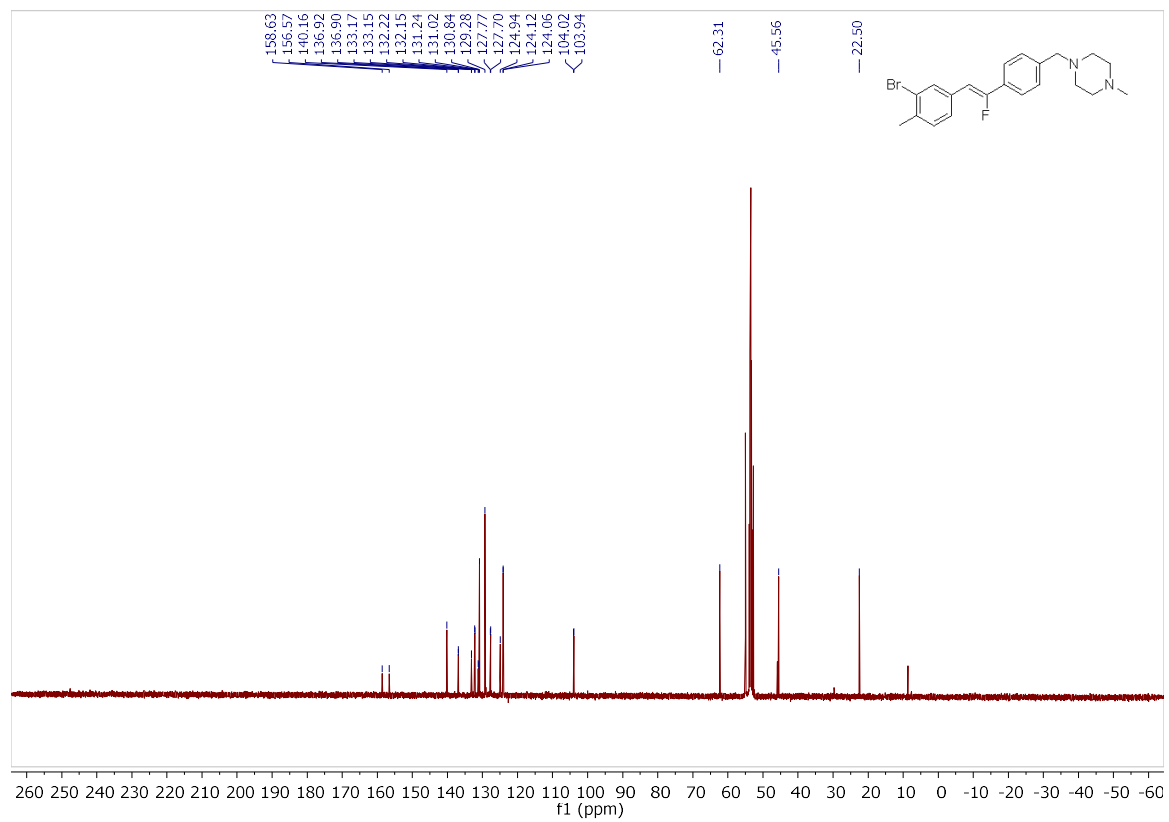
(Z)-4-(2-(3-bromo-4-methylphenyl)-1-fluorovinyl)benzaldehyde 13



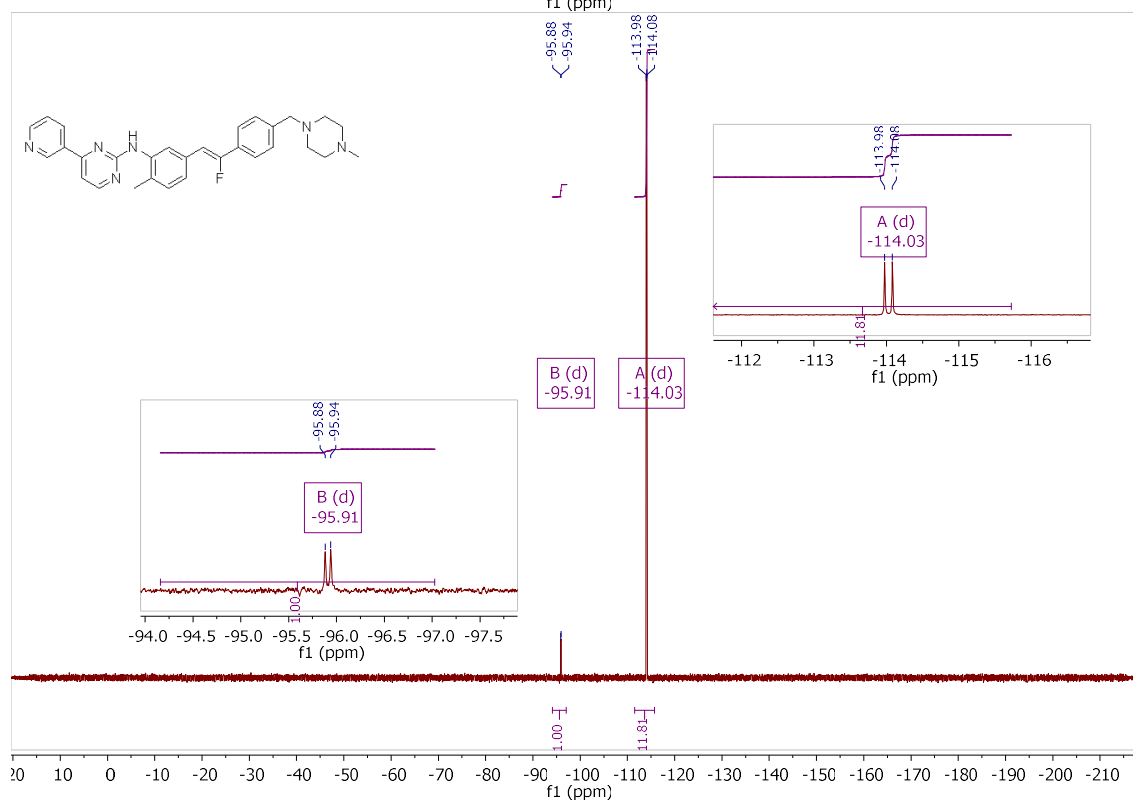
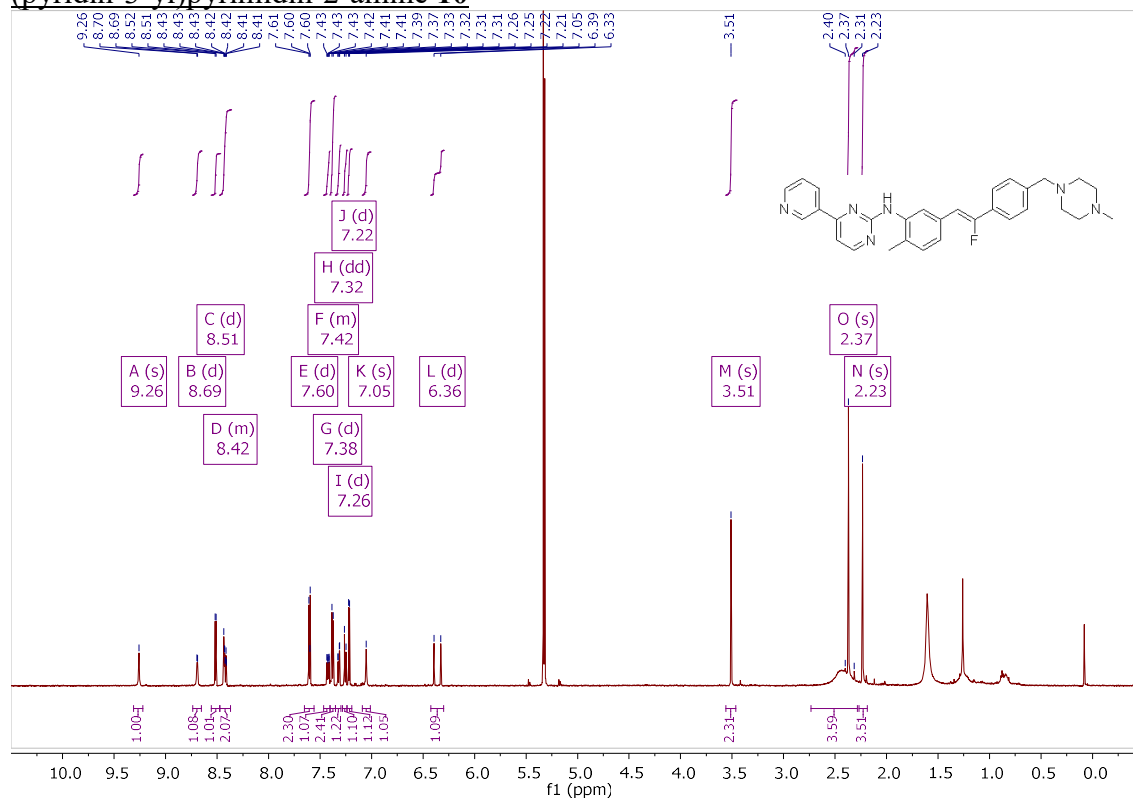


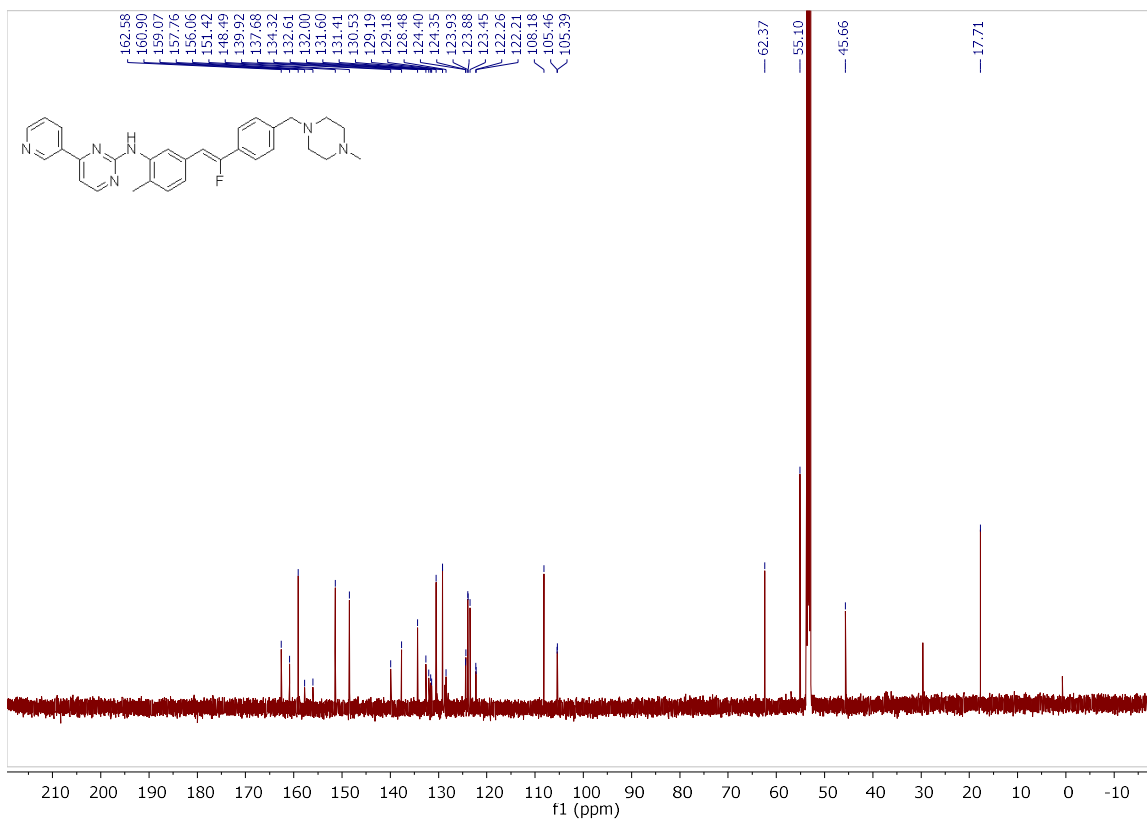
(Z)-1-(4-(2-(3-bromo-4-methylphenyl)-1-fluorovinyl)benzyl)-4-methylpiperazine **13**





(Z)-N-(5-(2-fluoro-2-(4-((4-methylpiperazin-1-yl)methyl)phenyl)vinyl)pyridin-3-yl)pyrimidin-2-amine **10**





2.5 References

1. Brown, N., *Bioisosterism in Medicinal Chemistry*. Wiley-VCH Verlag & Co.: Weinheim, Germany, 2012.
2. Meanwell, N. A., Fluorine and Fluorinated Motifs in the Design and Application of Bioisosteres for Drug Design. *Journal of Medicinal Chemistry* **2018**.
3. Burger, A., Isosterism and Bioisosterism in Drug Design. In *Progress in Drug Research / Fortschritte der Arzneimittelforschung / Progrès des recherches pharmaceutiques*, Jucker, E., Ed. Birkhäuser Basel: Basel, 1991; pp 287-371.
4. Taguchi, T. Y., Hikaru, Fluorinated Moieties for Replacement of Amide and Peptide Bonds. In *Fluorine in Medicinal Chemistry and Chemical Biology*, Ojima, I., Ed. 2009; pp 257-290.
5. Sciotti, R. J.; Pliushchev, M.; Wiedeman, P. E.; Balli, D.; Flamm, R.; Nilus, A. M.; Marsh, K.; Stolarik, D.; Jolly, R.; Ulrich, R.; Djuric, S. W., The Synthesis and Biological Evaluation of a Novel Series of Antimicrobials of the Oxazolidinone Class. *Bioorganic & Medicinal Chemistry Letters* **2002**, *12* (16), 2121-2123.
6. Asahina, Y.; Iwase, K.; Iinuma, F.; Hosaka, M.; Ishizaki, T., Synthesis and Antibacterial Activity of 1-(2-Fluorovinyl)-7-substituted-4-quinolone-3-carboxylic Acid Derivatives, Conformationally Restricted Analogues of Fleroxacin. *Journal of Medicinal Chemistry* **2005**, *48* (9), 3194-3202.
7. Couve-Bonnaire, S.; Cahard, D.; Pannecoucke, X., Chiral Dipeptide Mimics Possessing a Fluoroolefin Moiety: A Relevant Tool for Conformational and Medicinal Studies. *Organic & Biomolecular Chemistry* **2007**, *5* (8), 1151-1157.
8. Edmondson, S. D.; Wei, L.; Xu, J.; Shang, J.; Xu, S.; Pang, J.; Chaudhary, A.; Dean, D. C.; He, H.; Leiting, B.; Lyons, K. A.; Patel, R. A.; Patel, S. B.; Scapin, G.; Wu, J. K.; Beconi, M. G.; Thornberry, N. A.; Weber, A. E., Fluoroolefins as Amide Bond Mimics in Dipeptidyl Peptidase IV Inhibitors. *Bioorganic & Medicinal Chemistry Letters* **2008**, *18* (7), 2409-2413.
9. Oishi, S.; Kamitani, H.; Koderu, Y.; Watanabe, K.; Kobayashi, K.; Narumi, T.; Tomita, K.; Ohno, H.; Naito, T.; Kodama, E.; Matsuoka, M.; Fujii, N., Peptide Bond Mimicry by (E)-Alkene and (Z)-Fluoroalkene Peptide Isosteres: Synthesis and Bioevaluation of α -Helical Anti-HIV Peptide Analogues. *Organic & Biomolecular Chemistry* **2009**, *7* (14), 2872-2877.
10. McKinney, B. E.; Urban, J. J., Fluoroolefins as Peptide Mimetics. 2. A Computational Study of the Conformational Ramifications of Peptide Bond Replacement. *The Journal of Physical Chemistry A* **2010**, *114* (2), 1123-1133.
11. Jakobsche, C. E.; Choudhary, A.; Miller, S. J.; Raines, R. T., $n \rightarrow \pi^*$ Interaction and $n(\pi)$ Pauli Repulsion Are Antagonistic for Protein Stability. *Journal of the American Chemical Society* **2010**, *132* (19), 6651-6653.
12. Osada, S.; Sano, S.; Ueyama, M.; Chuman, Y.; Kodama, H.; Sakaguchi, K., Fluoroalkene Modification of Mercaptoacetamide-based Histone Deacetylase Inhibitors. *Bioorganic & Medicinal Chemistry* **2010**, *18* (2), 605-611.
13. Stepan, A. F.; Walker, D. P.; Bauman, J.; Price, D. A.; Baillie, T. A.; Kalgutkar, A. S.; Aleo, M. D., Structural Alert/Reactive Metabolite Concept as Applied in Medicinal Chemistry to Mitigate the Risk of Idiosyncratic Drug Toxicity: A Perspective Based on the Critical Examination of Trends in the Top 200 Drugs Marketed in the United States. *Chemical Research in Toxicology* **2011**, *24* (9), 1345-1410.

14. Landelle, G.; Bergeron, M.; Turcotte-Savard, M.-O.; Paquin, J.-F., Synthetic Approaches to Monofluoroalkenes. *Chemical Society Reviews* **2011**, *40* (5), 2867-2908.
15. Yanai, H.; Taguchi, T., Synthetic Methods for Fluorinated Olefins. *European Journal of Organic Chemistry* **2011**, *2011* (30), 5939-5954.
16. Zhao, Y.; Jiang, F.; Hu, J., Spontaneous Resolution of Julia-Kocienski Intermediates Facilitates Phase Separation to Produce Z- and E-Monofluoroalkenes. *Journal of the American Chemical Society* **2015**, *137* (15), 5199-5203.
17. Xiong, Y.; Huang, T.; Ji, X.; Wu, J.; Cao, S., Nickel-catalyzed Suzuki-Miyaura Type Cross-coupling Reactions of (2,2-Difluorovinyl)benzene Derivatives with Arylboronic Acids. *Organic & Biomolecular Chemistry* **2015**, *13* (27), 7389-7392.
18. Amii, H.; Uneyama, K., C-F Bond Activation in Organic Synthesis. *Chemical Reviews* **2009**, *109* (5), 2119-2183.
19. Ahrens, T.; Kohlmann, J.; Ahrens, M.; Braun, T., Functionalization of Fluorinated Molecules by Transition-Metal-Mediated C-F Bond Activation To Access Fluorinated Building Blocks. *Chemical Reviews* **2015**, *115* (2), 931-972.
20. Ohashi, M.; Saijo, H.; Shibata, M.; Ogoshi, S., Palladium-Catalyzed Base-Free Suzuki-Miyaura Coupling Reactions of Fluorinated Alkenes and Arenes via a Palladium Fluoride Key Intermediate. *European Journal of Organic Chemistry* **2013**, *2013* (3), 443-447.
21. Talbot, E. P. A.; Fernandes, T. d. A.; McKenna, J. M.; Toste, F. D., Asymmetric Palladium-Catalyzed Directed Intermolecular Fluoroarylation of Styrenes. *Journal of the American Chemical Society* **2014**, *136* (11), 4101-4104.
22. He, Y.; Yang, Z.; Thornbury, R. T.; Toste, F. D., Palladium-Catalyzed Enantioselective 1,1-Fluoroarylation of Aminoalkenes. *Journal of the American Chemical Society* **2015**, *137* (38), 12207-12210.
23. Miró, J.; del Pozo, C.; Toste, F. D.; Fustero, S., Enantioselective Palladium-Catalyzed Oxidative β,β -Fluoroarylation of α,β -Unsaturated Carbonyl Derivatives. *Angewandte Chemie International Edition* **2016**, *55* (31), 9045-9049.
24. Tang, H. J.; Lin, L. Z.; Feng, C.; Loh, T. P., Palladium-Catalyzed Fluoroarylation of gem-Difluoroalkenes. *Angewandte Chemie International Edition* **2017**, *56* (33), 9872-9876.
25. Gao, B.; Zhao, Y.; Ni, C.; Hu, J., AgF-Mediated Fluorinative Homocoupling of gem-Difluoroalkenes. *Organic Letters* **2014**, *16* (1), 102-105.
26. Yang, X.; Wu, T.; Phipps, R. J.; Toste, F. D., Advances in Catalytic Enantioselective Fluorination, Mono-, Di-, and Trifluoromethylation, and Trifluoromethylthiolation Reactions. *Chemical Reviews* **2015**, *115* (2), 826-870.
27. Zhao, Y.; Huang, W.; Zhu, L.; Hu, J., Difluoromethyl 2-Pyridyl Sulfone: A New gem-Difluoroolefination Reagent for Aldehydes and Ketones. *Organic Letters* **2010**, *12* (7), 1444-1447.
28. Chelucci, G., Synthesis and Metal-Catalyzed Reactions of gem-Dihalovinyl Systems. *Chemical Reviews* **2012**, *112* (3), 1344-1462.
29. Gao, B.; Zhao, Y.; Hu, M.; Ni, C.; Hu, J., gem-Difluoroolefination of Diaryl Ketones and Enolizable Aldehydes with Difluoromethyl 2-Pyridyl Sulfone: New Insights into the Julia-Kocienski Reaction. *Chemistry – A European Journal* **2014**, *20* (25), 7803-7810.
30. Hu, M.; Ni, C.; Li, L.; Han, Y.; Hu, J., gem-Difluoroolefination of Diazo Compounds with TMSCF₃ or TMSCF₂Br: Transition-Metal-Free Cross-Coupling of Two Carbene Precursors. *Journal of the American Chemical Society* **2015**, *137* (45), 14496-14501.
31. Tomoya, M.; Yoshiteru, I.; Masahiro, M., Synthesis of gem-Difluoroalkenes via β -Fluoride Elimination of Organorhodium(I). *Chemistry Letters* **2008**, *37* (9), 1006-1007.

32. Tian, P.; Feng, C.; Loh, T.-P., Rhodium-catalysed C(sp²)–C(sp²) Bond Formation via C–H/C–F activation. *Nature Communications* **2015**, *6*, 7472.
33. Ichitsuka, T.; Fujita, T.; Arita, T.; Ichikawa, J., Double C–F Bond Activation Through β -Fluorine Elimination: Nickel-Mediated [3+2] Cycloaddition of 2-Trifluoromethyl-1-alkenes with Alkynes. *Angewandte Chemie International Edition* **2014**, *53* (29), 7564-7568.
34. Ichitsuka, T.; Fujita, T.; Ichikawa, J., Nickel-Catalyzed Allylic C(sp³)–F Bond Activation of Trifluoromethyl Groups via β -Fluorine Elimination: Synthesis of Difluoro-1,4-dienes. *ACS Catalysis* **2015**, *5* (10), 5947-5950.
35. Heitz, W.; Knebelkamp, A., Synthesis of Fluorostyrenes via Palladium-catalyzed Reactions of Aromatic Halides with Fluoroolefins. *Die Makromolekulare Chemie, Rapid Communications* **1991**, *12* (2), 69-75.
36. Saeki, T.; Takashima, Y.; Tamao, K., Nickel- and Palladium-Catalyzed Cross-Coupling Reaction of Polyfluorinated Arenes and Alkenes with Grignard Reagents. *Synlett* **2005**, *2005* (11), 1771-1774.
37. Ichikawa, J.; Nadano, R.; Ito, N., 5-endo Heck-type Cyclization of 2-(Trifluoromethyl)allyl Ketone Oximes: Synthesis of 4-Difluoromethylene-substituted 1-Pyrrolines. *Chemical Communications* **2006**, (42), 4425-4427.
38. Kong, L.; Zhou, X.; Li, X., Cobalt(III)-Catalyzed Regio- and Stereoselective α -Fluoroalkenylation of Arenes with gem-Difluorostyrenes. *Organic Letters* **2016**, *18* (24), 6320-6323.
39. Hu, J.; Han, X.; Yuan, Y.; Shi, Z., Stereoselective Synthesis of Z Fluoroalkenes through Copper-Catalyzed Hydrodefluorination of gem-Difluoroalkenes with Water. *Angewandte Chemie International Edition* **2017**, *56* (43), 13342-13346.
40. Cai, S.-H.; Ye, L.; Wang, D.-X.; Wang, Y.-Q.; Lai, L.-J.; Zhu, C.; Feng, C.; Loh, T.-P., Manganese-catalyzed Synthesis of Monofluoroalkenes via C-H Activation and C-F Cleavage. *Chemical Communications* **2017**, *53* (62), 8731-8734.
41. Kong, L.; Liu, B.; Zhou, X.; Wang, F.; Li, X., Rhodium(iii)-catalyzed Regio- and Stereoselective Benzylic α -Fluoroalkenylation with gem-Difluorostyrenes. *Chemical Communications* **2017**, *53* (74), 10326-10329.
42. Zhang, J.; Dai, W.; Liu, Q.; Cao, S., Cu-Catalyzed Stereoselective Borylation of gem-Difluoroalkenes with B₂pin₂. *Organic Letters* **2017**, *19* (12), 3283-3286.
43. Kojima, R.; Kubota, K.; Ito, H., Stereodivergent Hydrodefluorination of gem-Difluoroalkenes: Selective Synthesis of (Z)- and (E)-monofluoroalkenes. *Chemical Communications* **2017**, *53* (77), 10688-10691.
44. Tan, D. H.; Lin, E.; Ji, W. W.; Zeng, Y. F.; Fan, W. X.; Li, Q.; Gao, H.; Wang, H., Copper-Catalyzed Stereoselective Defluorinative Borylation and Silylation of gem-Difluoroalkenes. *Advanced Synthesis & Catalysis* **2018**, *360* (5), 1032-1037.
45. Cordovilla, C.; Bartolomé, C.; Martínez-Illarduya, J. M.; Espinet, P., The Stille Reaction, 38 Years Later. *ACS Catalysis* **2015**, *5* (5), 3040-3053.
46. Sore, H. F.; Galloway, W. R. J. D.; Spring, D. R., Palladium-catalysed Cross-coupling of Organosilicon Reagents. *Chemical Society Reviews* **2012**, *41* (5), 1845-1866.
47. Denmark, S. E.; Ambrosi, A., Why You Really Should Consider Using Palladium-Catalyzed Cross-Coupling of Silanols and Silanolates. *Organic Process Research & Development* **2015**, *19* (8), 982-994.
48. Kikushima, K.; Holder, J. C.; Gatti, M.; Stoltz, B. M., Palladium-Catalyzed Asymmetric Conjugate Addition of Arylboronic Acids to Five-, Six-, and Seven-Membered β -Substituted

Cyclic Enones: Enantioselective Construction of All-Carbon Quaternary Stereocenters. *Journal of the American Chemical Society* **2011**, *133* (18), 6902-6905.

49. Capdeville, R.; Buchdunger, E.; Zimmermann, J.; Matter, A., Glivec (STI571, imatinib), a Rationally Developed, Targeted Anticancer Drug. *Nature Reviews Drug Discovery* **2002**, *1*, 493.

50. Deininger, M.; Buchdunger, E.; Druker, B. J., The Development of Imatinib as a Therapeutic Agent for Chronic Myeloid Leukemia. *Blood* **2005**, *105* (7), 2640-2653.

51. Schindler, T.; Bornmann, W.; Pellicena, P.; Miller, W. T.; Clarkson, B.; Kuriyan, J., Structural Mechanism for STI-571 Inhibition of Abelson Tyrosine Kinase. *Science* **2000**, *289* (5486), 1938-1942.

52. Maiti, D.; Fors, B. P.; Henderson, J. L.; Nakamura, Y.; Buchwald, S. L., Palladium-Catalyzed Coupling of Functionalized Primary and Secondary Amines with Aryl and Heteroaryl Halides: Two Ligands Suffice in Most Cases. *Chemical Science* **2011**, *2* (1), 57-68.

53. Qiu, S.; Xu, T.; Zhou, J.; Guo, Y.; Liu, G., Palladium-Catalyzed Intermolecular Aminofluorination of Styrenes. *Journal of the American Chemical Society* **2010**, *132* (9), 2856-2857.

54. White, P. B.; Jaworski, J. N.; Fry, C. G.; Dolinar, B. S.; Guzei, I. A.; Stahl, S. S., Structurally Diverse Diazafluorene-Ligated Palladium(II) Complexes and Their Implications for Aerobic Oxidation Reactions. *Journal of the American Chemical Society* **2016**, *138* (14), 4869-4880.

55. White, P. B.; Jaworski, J. N.; Zhu, G. H.; Stahl, S. S., Diazafluorenone-Promoted Oxidation Catalysis: Insights into the Role of Bidentate Ligands in Pd-Catalyzed Aerobic Aza-Wacker Reactions. *ACS Catalysis* **2016**, *6* (5), 3340-3348.

56. Ozawa, F.; Kubo, A.; Hayashi, T., Catalytic Asymmetric Arylation of 2,3-Dihydrofuran with Aryl Triflates. *Journal of the American Chemical Society* **1991**, *113* (4), 1417-1419.

57. Werner, E. W.; Mei, T.-S.; Burckle, A. J.; Sigman, M. S., Enantioselective Heck Arylations of Acyclic Alkenyl Alcohols Using a Redox-Relay Strategy. *Science* **2012**, *338* (6113), 1455-1458.

58. Knowles, J. P.; Whiting, A., The Heck-Mizoroki Cross-coupling Reaction: a Mechanistic Perspective. *Organic & Biomolecular Chemistry* **2007**, *5* (1), 31-44.

59. Wu, G.; Deng, Y.; Wu, C.; Wang, X.; Zhang, Y.; Wang, J., Switchable 2,2,2-Trifluoroethylation and gem-Difluorovinylolation of Organoboronic Acids with 2,2,2-Trifluorodiazethane. *European Journal of Organic Chemistry* **2014**, *2014* (21), 4477-4481.

60. Wang, X. P.; Lin, J. H.; Xiao, J. C.; Zheng, X., Decarboxylative Julia-Kocienski gem-Difluoro-Olefination of 2-Pyridinyl Sulfonyldifluoroacetate. *European Journal of Organic Chemistry* **2014**, *2014* (5), 928-932.

61. Kitamura, T.; Muta, K.; Oyamada, J., Hypervalent Iodine-Mediated Fluorination of Styrene Derivatives: Stoichiometric and Catalytic Transformation to 2,2-Difluoroethylarenes. *The Journal of Organic Chemistry* **2015**, *80* (21), 10431-10436.

62. McAlpine, I.; Tran-Dubé, M.; Wang, F.; Scales, S.; Matthews, J.; Collins, M. R.; Nair, S. K.; Nguyen, M.; Bian, J.; Alsina, L. M.; Sun, J.; Zhong, J.; Warmus, J. S.; O'Neill, B. T., Synthesis of Small 3-Fluoro- and 3,3-Difluoropyrrolidines Using Azomethine Ylide Chemistry. *The Journal of Organic Chemistry* **2015**, *80* (14), 7266-7274.

63. Hamman, S.; Beguin, C. G., Hydrofluorination and Bromofluorination of Halogeno-Substituted Ethyl Cinnamates and Related Compounds. *Journal of Fluorine Chemistry* **1979**, *13* (2), 163-174.

64. Lecea, M.; Grassin, A.; Ferreiro-Mederos, L.; Choppin, S.; Urbano, A.; Carreño, M. C.; Colobert, F., One-Step Stereoselective Synthesis of Trisubstituted Monofluoroalkenes from 3,3,3-Trifluoropropionates. *European Journal of Organic Chemistry* **2013**, 2013 (21), 4486-4489.
65. Bruno, N. C.; Tudge, M. T.; Buchwald, S. L., Design and Preparation of New Palladium Precatalysts for C-C and C-N Cross-coupling Reactions. *Chemical Science* **2013**, 4 (3), 916-920.